

# IEEE Standard for Digitizing Waveform Recorders

IEEE Instrumentation Society

Sponsored by the  
Waveform Generation, Testing, and Measurement Committee

---

IEEE  
3 Park Avenue  
New York, NY 10016-5997  
USA

**IEEE Std 1057™-2017**  
(Revision of IEEE Std 1057-2007)

# **IEEE Standard for Digitizing Waveform Recorders**

Sponsor

**Waveform Generation, Testing, and Measurement Committee  
of the  
IEEE Instrumentation Society**

Approved 28 September 2017

**IEEE-SA Standards Board**

**Abstract:** Terminology and test methods for describing the performance of waveform recorders are presented in this standard.

**Keywords:** effective number of bits, frequency response, noise, IEEE 1057™, sine fitting, step pulse response, total harmonic distortion, transitions levels, waveform recorders

---

The Institute of Electrical and Electronics Engineers, Inc.  
3 Park Avenue, New York, NY 10016-5997, USA

Copyright © 2018 by The Institute of Electrical and Electronics Engineers, Inc.  
All rights reserved. Published 26 January 2018. Printed in the United States of America.

IEEE is a registered trademark in the U.S. Patent & Trademark Office, owned by The Institute of Electrical and Electronics Engineers, Incorporated.

PDF: ISBN 978-1-5044-4301-2 STD22763  
Print: ISBN 978-1-5044-4302-9 STDPD22763

*IEEE prohibits discrimination, harassment, and bullying.  
For more information, visit <http://www.ieee.org/web/aboutus/whatis/policies/p9-26.html>.  
No part of this publication may be reproduced in any form, in an electronic retrieval system or otherwise, without the prior written permission of the publisher.*

## **Important Notices and Disclaimers Concerning IEEE Standards Documents**

IEEE documents are made available for use subject to important notices and legal disclaimers. These notices and disclaimers, or a reference to this page, appear in all standards and may be found under the heading "Important Notices and Disclaimers Concerning IEEE Standards Documents." They can also be obtained on request from IEEE or viewed at <http://standards.ieee.org/IPR/disclaimers.html>.

### **Notice and Disclaimer of Liability Concerning the Use of IEEE Standards Documents**

IEEE Standards documents (standards, recommended practices, and guides), both full-use and trial-use, are developed within IEEE Societies and the Standards Coordinating Committees of the IEEE Standards Association ("IEEE-SA") Standards Board. IEEE ("the Institute") develops its standards through a consensus development process, approved by the American National Standards Institute ("ANSI"), which brings together volunteers representing varied viewpoints and interests to achieve the final product. IEEE Standards are documents developed through scientific, academic, and industry-based technical working groups. Volunteers in IEEE working groups are not necessarily members of the Institute and participate without compensation from IEEE. While IEEE administers the process and establishes rules to promote fairness in the consensus development process, IEEE does not independently evaluate, test, or verify the accuracy of any of the information or the soundness of any judgments contained in its standards.

IEEE Standards do not guarantee or ensure safety, security, health, or environmental protection, or ensure against interference with or from other devices or networks. Implementers and users of IEEE Standards documents are responsible for determining and complying with all appropriate safety, security, environmental, health, and interference protection practices and all applicable laws and regulations.

IEEE does not warrant or represent the accuracy or content of the material contained in its standards, and expressly disclaims all warranties (express, implied and statutory) not included in this or any other document relating to the standard, including, but not limited to, the warranties of: merchantability; fitness for a particular purpose; non-infringement; and quality, accuracy, effectiveness, currency, or completeness of material. In addition, IEEE disclaims any and all conditions relating to: results; and workmanlike effort. IEEE standards documents are supplied "AS IS" and "WITH ALL FAULTS."

Use of an IEEE standard is wholly voluntary. The existence of an IEEE standard does not imply that there are no other ways to produce, test, measure, purchase, market, or provide other goods and services related to the scope of the IEEE standard. Furthermore, the viewpoint expressed at the time a standard is approved and issued is subject to change brought about through developments in the state of the art and comments received from users of the standard.

In publishing and making its standards available, IEEE is not suggesting or rendering professional or other services for, or on behalf of, any person or entity nor is IEEE undertaking to perform any duty owed by any other person or entity to another. Any person utilizing any IEEE Standards document, should rely upon his or her own independent judgment in the exercise of reasonable care in any given circumstances or, as appropriate, seek the advice of a competent professional in determining the appropriateness of a given IEEE standard.

IN NO EVENT SHALL IEEE BE LIABLE FOR ANY DIRECT, INDIRECT, INCIDENTAL, SPECIAL, EXEMPLARY, OR CONSEQUENTIAL DAMAGES (INCLUDING, BUT NOT LIMITED TO: PROCUREMENT OF SUBSTITUTE GOODS OR SERVICES; LOSS OF USE, DATA, OR PROFITS; OR BUSINESS INTERRUPTION) HOWEVER CAUSED AND ON ANY THEORY OF LIABILITY, WHETHER IN CONTRACT, STRICT LIABILITY, OR TORT (INCLUDING NEGLIGENCE OR OTHERWISE) ARISING IN ANY WAY OUT OF THE PUBLICATION, USE OF, OR RELIANCE UPON ANY STANDARD, EVEN IF ADVISED OF THE POSSIBILITY OF SUCH DAMAGE AND REGARDLESS OF WHETHER SUCH DAMAGE WAS FORESEEABLE.

## **Translations**

The IEEE consensus development process involves the review of documents in English only. In the event that an IEEE standard is translated, only the English version published by IEEE should be considered the approved IEEE standard.

## **Official statements**

A statement, written or oral, that is not processed in accordance with the IEEE-SA Standards Board Operations Manual shall not be considered or inferred to be the official position of IEEE or any of its committees and shall not be considered to be, or be relied upon as, a formal position of IEEE. At lectures, symposia, seminars, or educational courses, an individual presenting information on IEEE standards shall make it clear that his or her views should be considered the personal views of that individual rather than the formal position of IEEE.

## **Comments on standards**

Comments for revision of IEEE Standards documents are welcome from any interested party, regardless of membership affiliation with IEEE. However, IEEE does not provide consulting information or advice pertaining to IEEE Standards documents. Suggestions for changes in documents should be in the form of a proposed change of text, together with appropriate supporting comments. Since IEEE standards represent a consensus of concerned interests, it is important that any responses to comments and questions also receive the concurrence of a balance of interests. For this reason, IEEE and the members of its societies and Standards Coordinating Committees are not able to provide an instant response to comments or questions except in those cases where the matter has previously been addressed. For the same reason, IEEE does not respond to interpretation requests. Any person who would like to participate in revisions to an IEEE standard is welcome to join the relevant IEEE working group.

Comments on standards should be submitted to the following address:

Secretary, IEEE-SA Standards Board  
445 Hoes Lane  
Piscataway, NJ 08854 USA

## **Laws and regulations**

Users of IEEE Standards documents should consult all applicable laws and regulations. Compliance with the provisions of any IEEE Standards document does not imply compliance to any applicable regulatory requirements. Implementers of the standard are responsible for observing or referring to the applicable regulatory requirements. IEEE does not, by the publication of its standards, intend to urge action that is not in compliance with applicable laws, and these documents may not be construed as doing so.

## **Copyrights**

IEEE draft and approved standards are copyrighted by IEEE under US and international copyright laws. They are made available by IEEE and are adopted for a wide variety of both public and private uses. These include both use, by reference, in laws and regulations, and use in private self-regulation, standardization, and the promotion of engineering practices and methods. By making these documents available for use and adoption by public authorities and private users, IEEE does not waive any rights in copyright to the documents.

## **Photocopies**

Subject to payment of the appropriate fee, IEEE will grant users a limited, non-exclusive license to photocopy portions of any individual standard for company or organizational internal use or individual, non-commercial use only. To arrange for payment of licensing fees, please contact Copyright Clearance Center, Customer Service, 222 Rosewood Drive, Danvers, MA 01923 USA; +1 978 750 8400. Permission to photocopy portions of any individual standard for educational classroom use can also be obtained through the Copyright Clearance Center.

## **Updating of IEEE Standards documents**

Users of IEEE Standards documents should be aware that these documents may be superseded at any time by the issuance of new editions or may be amended from time to time through the issuance of amendments, corrigenda, or errata. An official IEEE document at any point in time consists of the current edition of the document together with any amendments, corrigenda, or errata then in effect.

Every IEEE standard is subjected to review at least every 10 years. When a document is more than 10 years old and has not undergone a revision process, it is reasonable to conclude that its contents, although still of some value, do not wholly reflect the present state of the art. Users are cautioned to check to determine that they have the latest edition of any IEEE standard.

In order to determine whether a given document is the current edition and whether it has been amended through the issuance of amendments, corrigenda, or errata, visit the IEEE Xplore at <http://ieeexplore.ieee.org/> or contact IEEE at the address listed previously. For more information about the IEEE-SA or IEEE's standards development process, visit the IEEE-SA Website at <http://standards.ieee.org>.

## **Errata**

Errata, if any, for all IEEE standards can be accessed on the IEEE-SA Website at the following URL: <http://standards.ieee.org/findstds/errata/index.html>. Users are encouraged to check this URL for errata periodically.

## **Patents**

Attention is called to the possibility that implementation of this standard may require use of subject matter covered by patent rights. By publication of this standard, no position is taken by the IEEE with respect to the existence or validity of any patent rights in connection therewith. If a patent holder or patent applicant has filed a statement of assurance via an Accepted Letter of Assurance, then the statement is listed on the IEEE-SA Website at <http://standards.ieee.org/about/sasb/patcom/patents.html>. Letters of Assurance may indicate whether the Submitter is willing or unwilling to grant licenses under patent rights without compensation or under reasonable rates, with reasonable terms and conditions that are demonstrably free of any unfair discrimination to applicants desiring to obtain such licenses.

Essential Patent Claims may exist for which a Letter of Assurance has not been received. The IEEE is not responsible for identifying Essential Patent Claims for which a license may be required, for conducting inquiries into the legal validity or scope of Patents Claims, or determining whether any licensing terms or conditions provided in connection with submission of a Letter of Assurance, if any, or in any licensing agreements are reasonable or non-discriminatory. Users of this standard are expressly advised that determination of the validity of any patent rights, and the risk of infringement of such rights, is entirely their own responsibility. Further information may be obtained from the IEEE Standards Association.

## Participants

At the time this IEEE standard was completed, the Waveform Recorder Working Group had the following membership:

### **William B. Boyer, Chair**

Francisco Alegria  
Eualia Balestrieri  
Niclas Bjorsell  
Jerome Blair  
Andrea Cataldo  
Lorenzo Ciani  
Dominique Dallet

Pasquale Daponte  
Egidio De Benedetto  
Luca De Vito  
Izzet Kale  
Donald Larson  
Dennis Lia

Thomas Linnenbrink  
Sol Max  
Kruno Miličević  
Antonio Moschitta  
Sergio Rapuano  
Steve Tilden

The following members of the balloting committee voted on this standard. Balloters may have voted for approval, disapproval, or abstention.

Ali Al Awazi  
Charles Barest  
Niclas Bjorsell  
Jerome Blair  
William Boyer  
Demetrio Bucaneg Jr.  
Andrea Cataldo  
Luca De Vito  
Sourav Dutta

Gearold O. H. Eidhin  
Randall Groves  
Werner Hoelzl  
Ronald Jarrett  
Donald Larson  
Dennis Lia  
Thomas Linnenbrink  
Sol Max  
Edward McCall

Kruno Miličević  
R. Murphy  
Sergio Rapuano  
Jeremy Smith  
Joseph Stanco  
Walter Struppler  
Steven Tilden  
Lisa Ward  
Jian Yu

When the IEEE-SA Standards Board approved this standard on 28 September 2017, it had the following membership:

### **Jean-Philippe Faure, Chair** **Gary Hoffman, Vice Chair** **John D. Kulick, Past Chair** **Konstantinos Karachalios, Secretary**

Chuck Adams  
Masayuki Ariyoshi  
Ted Burse  
Stephen Dukes  
Doug Edwards  
J. Travis Griffith  
Michael Janezic

Thomas Koshy  
Joseph L. Koepfinger\*  
Kevin Lu  
Daleep Mohla  
Damir Novosel  
Ronald C. Petersen  
Annette D. Reilly

Robby Robson  
Dorothy Stanley  
Adrian Stephens  
Mehmet Ulema  
Phil Wennblom  
Howard Wolfman  
Yu Yuan

\*Member Emeritus

## Introduction

This introduction is not part of IEEE Std 1057-2017, IEEE Standard for Digitizing Waveform Recorders.

This standard is a revision and modernization of the previous standard, IEEE Std 1057-2007. It presents methods for the test and evaluations of digitizing waveform recorders approved by the balloting committee.

## Contents

|  |     |
|--|-----|
| 1. Overview.....   | 15  |
| 1.1 Scope.....   | 15  |
| 1.2 Waveform recorder background .....                                 | 15  |
| 2. Normative references .....  | 16  |
| 3. Definitions.....  | 17  |
| 3.1 Definitions.....   | 17  |
| 3.2 Symbols and acronyms.....  | 24  |
| 4. Test parameters and methods.....                                    | 28  |
| 4.1 Manufacturer supplied information.....                             | 28  |
| 4.2 Test selection .....   | 31  |
| 4.3 Test setup .....   | 32  |
| 4.4 Equivalent-time sampling.....                                      | 39  |
| 4.5 Discrete Fourier transform (DFT) .....                             | 43  |
| 4.6 Sine wave testing and fitting .....                                | 52  |
| 4.7 Locating code transition levels .....                              | 59  |
| 4.8 Step function response measurements .....                          | 77  |
| 4.9 Tests using a dc input .....                                       | 80  |
| 5. Input impedance .....   | 81  |
| 5.1 Test method .....  | 81  |
| 5.2 Alternate test method using a time domain reflectometer (TDR)..... | 81  |
| 5.3 Input impedance for out-of-range signals .....                     | 81  |
| 6. Static gain and offset.....   | 83  |
| 6.1 Independently based gain and offset .....                          | 83  |
| 6.2 Terminal-based gain and offset .....                               | 85  |
| 7. Linearity .....   | 85  |
| 7.1 Integral nonlinearity (INL) .....                                  | 85  |
| 7.2 Maximum static error (MSE).....                                    | 86  |
| 7.3 Differential nonlinearity (DNL) and missing codes .....            | 86  |
| 7.4 Example INL and DNL data .....                                     | 87  |
| 7.5 Monotonicity .....   | 89  |
| 7.6 Hysteresis .....   | 90  |
| 7.7 Total harmonic distortion (THD).....                               | 91  |
| 7.8 Intermodulation distortion (IMD).....                              | 96  |
| 7.9 Noise power ratio (NPR) .....                                      | 98  |
| 8. Noise <sup>7</sup> .....  | 104 |
| 8.1 Comments on noise .....  | 105 |
| 8.2 Ratio of signal to noise and distortion (SINAD).....               | 105 |
| 8.3 Signal to noise ratio (SNR).....                                   | 106 |
| 8.4 Comments on SINAD and SNR .....                                    | 106 |
| 8.5 Effective number of bits (ENOB) .....                              | 107 |
| 8.6 Random noise .....   | 110 |
| 8.7 Spurious components .....  | 111 |
| 8.8 Spurious-free dynamic range (SFDR) .....                           | 112 |

|   |     |
|---|-----|
| 9.2 Transition duration of the step response.....   | 117 |
| 9.3 Slew rate limit.....  | 119 |
| 9.4 Overshoot and precursors .....  | 119 |
| 9.5 Aperture duration.....  | 119 |
| 9.6 Limitations on the use of step responses .....  | 124 |
| <br>10. Frequency response parameters.....  | 127 |
| 10.1 Analog bandwidth .....   | 127 |
| 10.2 Gain error (gain flatness) .....   | 127 |
| 10.3 Frequency response and gain from step response .....                                     | 128 |
| <br>11. Interchannel parameters .....   | 133 |
| 11.1 Crosstalk.....   | 133 |
| 11.2 Multiple input reverse coupling.....   | 133 |
| <br>12. Time base parameters .....  | 134 |
| 12.1 Fixed error in sample time .....   | 134 |
| 12.2 Aperture uncertainty.....  | 134 |
| 12.3 Long-term stability .....  | 136 |
| <br>13. Out-of-range recovery .....   | 137 |
| 13.1 Test method for absolute out-of-range voltage recovery.....                              | 138 |
| 13.2 Test method for relative out-of-range voltage recovery .....                             | 138 |
| 13.3 Comments on test method .....  | 138 |
| <br>14. Word error rate .....   | 138 |
| 14.1 Test method for word error rate.....   | 138 |
| 14.2 Comment on the number of samples required for word error rate.....                       | 139 |
| 14.3 Comments on test equipment and making measurements.....                                  | 139 |
| <br>15. Differential input specifications.....  | 139 |
| 15.1 Differential input impedance to ground .....   | 139 |
| 15.2 Common-mode rejection ratio (CMRR) and maximum common-mode signal level .....            | 140 |
| 15.3 Maximum operating common-mode signal.....  | 140 |
| 15.4 Common-mode out-of-range signal recovery time.....                                       | 141 |
| <br>16. Cycle time .....  | 141 |
| 16.1 Test method .....  | 141 |
| 16.2 Comment.....   | 142 |
| <br>17. Triggering.....   | 142 |
| 17.1 Trigger delay and trigger jitter .....   | 142 |
| 17.2 Trigger sensitivity.....   | 143 |
| 17.3 Trigger minimum rate of change .....   | 144 |
| 17.4 Trigger coupling to signal .....   | 145 |
| <br>Annex A (informative) Sine fitting algorithms .....                                       | 146 |
| <br>Annex B (informative) Phase noise.....  | 150 |
| <br>Annex C (informative) Comment on errors associated with word-error-rate measurement ..... | 159 |
| <br>Annex D (informative) Measurement of random noise below the quantization level.....       | 161 |
| <br>Annex E (informative) Software consideration .....  | 164 |

|  |     |
|--|-----|
| Annex F (informative) Excitation with precision source with ramp verneir: determination of the test parameters ..... | 165 |
| Annex G (informative) Presentation of sine wave data .....   | 168 |
| Annex H (informative) Bibliography .....   | 177 |

## List of Figures

|   |    |
|---|----|
| Figure 1—Block diagram of a common waveform recorder .....  | 16 |
| Figure 2—Definitions pertaining to input quantization .....   | 18 |
| Figure 3—Block diagram of waveform recorder “ground” nodes.....   | 35 |
| Figure 4—Generic waveform recorder with features that facilitate testing .....  | 37 |
| Figure 5—General sine wave test setup.....  | 38 |
| Figure 6—General setup for test using an arbitrary signal generator.....  | 38 |
| Figure 7—General setup for pulse and step signal testing .....  | 39 |
| Figure 8—Equivalent-time sampling extraction example .....  | 40 |
| Figure 9—Example DFT spectrum using positive and negative frequencies .....   | 44 |
| Figure 10—Example DFT showing the negative frequencies mapped up to the frequencies between<br>the Nyquist frequency and twice the Nyquist frequency .....  | 44 |
| Figure 11—Plot of DFT detected frequencies versus input frequency for a waveform recorder .....   | 45 |
| Figure 12—Plot showing how negative DFT frequencies are mapped up to the frequencies between<br>the Nyquist frequency and twice the Nyquist frequency .....   | 46 |
| Figure 13—Fourier transform of the Hann and the rectangular windows.....  | 47 |
| Figure 14—Fourier transform of the Hann and the Blackman windows .....  | 48 |
| Figure 15—Plot of signals and samples that generate the spectrum shown in <a href="#">Figure 9</a> .....  | 51 |
| Figure 16—Spectrum analyzer display of signal with DFT results shown in <a href="#">Figure 9</a> .....  | 52 |
| Figure 17—Block diagram of feedback technique for determining waveform recorder code thresholds.....  | 61 |
| Figure 18—Plot of perfect waveform recorder-computed transition level deviations using sine wave<br>histogram with additive harmonic distortion (Effect of 2nd, 3rd, 4th, 5th harmonics on transition<br>levels are shown. The harmonic amplitude is 1 LSB, sine and cosine components.)..... | 68 |
| Figure 19—Plot of acceptable ramp test input signals.....   | 69 |
| Figure 20—Plot of transition uncertainty .....  | 71 |
| Figure 21—Ramp vernier test signals applied to waveform recorder.....   | 72 |
| Figure 22—Test procedure for excitation using a high-precision dc source with ramp vernier .....  | 74 |
| Figure 23—Representation of the cumulative histograms computed in each step in the case of a 5-bit<br>converter and a test with four steps.....   | 75 |
| Figure 24—Example data for limited accuracy triangle wave measurement of code transition levels<br>(Data are for an input voltage of 5.2 V, $Q = 1 \text{ V/count}$ , and a noise level of $1 \text{ V}_{\text{rms}}$ .....   | 76 |
| Figure 25—Setup for a simple step response measurement.....   | 79 |

|  |     |
|--|-----|
| Figure 26—Test setup for measuring input impedance for out-of-range signals by time domain reflectometry .....   | 82  |
| Figure 27—Example of calculated INL from a terminal-based calibrated 12-bit device.....  | 88  |
| Figure 28—DNL from a terminal-based calibrated 12-bit device .....   | 89  |
| Figure 29—Block diagram of hysteresis and alternation.....   | 91  |
| Figure 30—Plot of distribution of calculated values of fundamental and harmonic amplitudes for noncoherent sampling with random phase between the 2nd harmonic and the fundamental.....  | 95  |
| Figure 31—THD deviation from true value as a function of number of cycles in the record.....   | 96  |
| Figure 32—Test setup for measuring NPR .....   | 99  |
| Figure 33—Spectrum of NPR test signal.....   | 100 |
| Figure 34—Time domain representation of NPR test signal .....  | 101 |
| Figure 35—Plot of ideal and measured NPR for a Gaussian noise input from <a href="#">Equation (71)</a> .....   | 103 |
| Figure 36—Plot of ideal and measured NPR for a uniform noise input from <a href="#">Equation (72)</a> .....  | 103 |
| Figure 37—Frequency domain AWG generated NPR test input to the waveform recorder.....  | 104 |
| Figure 38—Histogram from 16 K sample set .....   | 104 |
| Figure 39—Illustration of the use of the histogram to remove the sine wave peaks .....   | 108 |
| Figure 40—Example of potential errors in measuring the final value of a step pulse response waveform when a final time shorter than 1 s is used (In the plot, $\varepsilon_1$ is the short-term settling error, and $\varepsilon_2$ is settling error. In this case, the final value at 1 s is 0.0 V.) ..... | 115 |
| Figure 41—Impulse response of a sample-and-hold amplifier while in the sample mode .....   | 120 |
| Figure 42—The step response corresponding to the impulse response of <a href="#">Figure 41</a> .....   | 121 |
| Figure 43—View of start of transition duration for $p = 99.9\%$ .....  | 121 |
| Figure 44—Aperture duration for $p = 50\%$ and $p = 80\%$ .....  | 122 |
| Figure 45—Evaluation of aperture-duration stop time for $p = 99.9\%$ .....   | 122 |
| Figure 46—Ringing impulse response .....   | 123 |
| Figure 47—Ringing step response .....  | 123 |
| Figure 48—Zoomed ringing transition.....   | 124 |
| Figure 49—Example of noise reduction using an expanding-window moving-average filter on step data for different values of $R$ (The waveform contains two time constants separated by a factor of 10).....  | 131 |
| Figure 50—Example of a network for simultaneously applying a normal-mode signal and a common-mode signal for measuring maximum operating common-mode signal level.....   | 141 |
| Figure 51—Trigger sensitivity parameters.....  | 144 |
| Figure B.1—Phase noise plot .....  | 151 |
| Figure B.2—Two examples of phase noise as displayed on a spectrum analyzer .....   | 151 |

|   |     |
|---|-----|
| Figure B.3—Mathematica program to compute phase noise integral.....   | 153 |
| Figure B.4—Function $D(f)$ with record length $T_R = 1$ s .....   | 155 |
| Figure B.5—Mathematica program to compute frequency deviation integral .....  | 155 |
| Figure G.1—Example plot of ENOB versus frequency for a two-channel waveform recorder.....   | 168 |
| Figure G.2—Example plots of sine fit residuals (the left side shows a modulo time plot, and the right side shows a PSD. Both represent the same data) ..... | 169 |
| Figure G.3—Same as <a href="#">Figure G.2</a> , but for channel 1 of the recorder (this figure shows the interleaving error) .....                          | 171 |
| Figure G.4—Plot of 1024-point record containing 7 cycles of the fundamental from a 10-bit data recorder   | 172 |
| Figure G.5—Plot of the magnitude of the spectrum of the signal shown in <a href="#">Figure G.4</a> .....  | 173 |
| Figure G.6—Plot of the residual signal .....  | 174 |
| Figure G.7—Plot of unwound data (original record is reordered) .....  | 175 |
| Figure G.8—Plot of unfolded residual .....  | 176 |

## List of Tables

|  |     |
|--|-----|
| Table 1—Critical waveform recorder parameters .....  | 30  |
| Table 2—Properties of various data windows .....   | 50  |
| Table 3—Uncertainty of estimates of code transition level .....  | 62  |
| Table 4—Values of $Z_{u/2}$ and $Z_{N,u/2}$ .....  | 66  |
| Table 5—Step response parameters.....  | 78  |
| Table 6—Maximum NPR for Gaussian and uniform noise sources .....   | 101 |
| Table 7—Maximum effective bits versus normalized jitter (fraction of sine wave period) .....                             | 110 |
| Table 8—Worst-case aliasing error in transition duration .....   | 127 |
| Table 9—Worst-case aliasing error in frequency response magnitude and phase.....   | 130 |
| Table B.1—Frequency tolerance and deviation as a function of record length.....  | 156 |
| Table B.2—Noise level .....  | 157 |
| Table B.3—Step response time jitter results for various upper limits of integration.....                                 | 157 |
| Table C.1—Examples of the number of standard deviations covered by confidence $\Phi[k]$ in a Gaussian distribution ..... | 159 |

# IEEE Standard for Digitizing Waveform Recorders

## 1. Overview

### 1.1 Scope

This standard defines specifications and describes test methods for measuring the performance of electronic digitizing waveform recorders, waveform analyzers, and digitizing oscilloscopes with digital outputs. The standard is directed toward, but not restricted to, general-purpose waveform recorders and analyzers.

Special applications can require additional manufacturer information and verification tests not covered in this standard.

IEEE Std 1057<sup>TM</sup> has many similarities to IEEE Std 1241<sup>TM</sup>-2010 [B24], which applies to analog-to-digital converters (ADCs).<sup>1</sup> However, IEEE Std 1057 shall be used for waveform recorders, and IEEE Std 1241-2010 shall be used for ADCs.

### 1.2 Waveform recorder background

A waveform recorder is a device for capturing an amplitude versus time portion of a possibly time-varying signal, such as a voltage, by digitizing it and storing the results in an internal memory. The data capture is normally done in real time and in the time domain. Non-real time sampling recorders and frequency domain data recorders do also exist but are not specifically covered in this standard.

A generic waveform recorder is shown in [Figure 1](#).

---

<sup>1</sup>The numbers in brackets correspond to those of the bibliography in [Annex H](#).

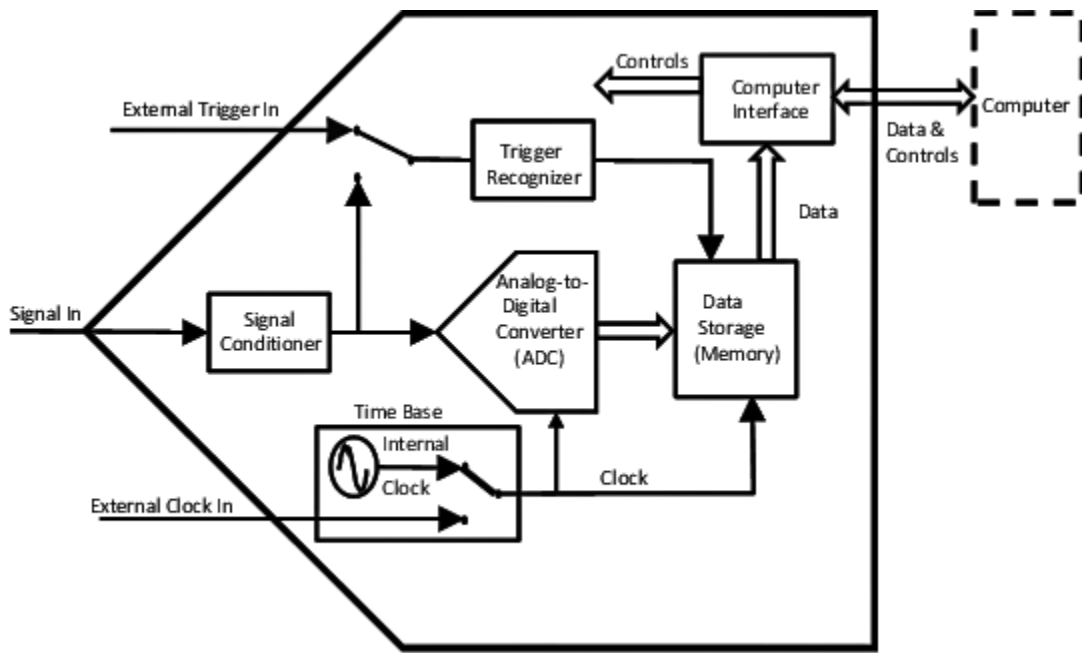


**Figure 1—Block diagram of a common waveform recorder**

Some key components of common waveform recorders are:

- Signal conditioner – provides impedance matching, gain/attenuation, filtering, etc. for the Signal In.
- Analog-to-digital convertor – samples the input and converts each sample to a digital word. The ADC can consist of multiple interleaved ADCs.
- Time base – controls the digitizing sample times.
- Trigger recognizer – determines the start of the digitized epoch.
- Data storage (memory) – stores the digitized waveform.
- Computer interface – provides for computer control of various recorder functions and for the readout of the digitized waveform data.

## 2. Normative references

The following referenced documents are indispensable for the application of this document (i.e., they must be understood and used, so each referenced document is cited in text and its relationship to this document is explained). For dated references, only the edition cited applies. For undated references, the latest edition of the referenced document (including any amendments or corrigenda) applies.

IEEE Std 181™-2011, IEEE Standard on Transitions, Pulses, and Related Waveforms.<sup>2,3</sup>

<sup>2</sup>The IEEE standards or products referred to in Clause 2 are trademarks owned by the Institute of Electrical and Electronics Engineers, Incorporated.

<sup>3</sup>IEEE publications are available from the Institute of Electrical and Electronics Engineers (<http://standards.ieee.org/>).

### 3. Definitions

For the purposes of this document, the following terms and definitions apply. The *IEEE Standards Dictionary Online* should be consulted for terms not defined in this clause.<sup>4</sup>

#### 3.1 Definitions

**ac coupled recorder:** A recorder whose input circuitry does not pass dc. Such recorders use either a series capacitance or a transformer at the input.

**aliasing:** The phenomenon in sampled data systems whereby signal components at input frequencies greater than half the sampling frequency are converted to frequencies at less than half the sampling frequency in the output data record.

**analog bandwidth (BW):** Unless otherwise specified, the difference between the upper and lower frequency at which the amplitude response as seen in the data record is 0.707 (–3 dB) of the response as seen in the data record at the specified reference frequency.

**aperture:** The interval during which the input to the waveform recorder affects the output or the weighting function that determines the sampled output from the input signal.

**aperture duration ( $p\%$ ):** The  $[50 - (p/2)]\%$  to  $[50 + (p/2)]\%$  transition duration of the step response of the ADC. If ringing of the step response causes multiple crossings of either of the levels, the  $p\%$  aperture duration is the time from the first crossing of the first level to the last crossing of the second level.

NOTE—The significance is that the output of the waveform recorder’s ADC is determined, with an error of  $(100 - p)\%$  or less, by the input signal in an interval of this duration. Common values of  $p$  are 50, 80, and 99.9. For  $p = 80$ , this is the 10% to 90% transition duration of the step response.

**aperture uncertainty:** The standard deviation of the sample instant in time. *Syn:* **short-term timing instability; timing jitter; timing phase noise.**

**code bin  $k$ :** A digital output that is designed to correspond to a particular set of input values.

NOTE—See [Equation \(1\)](#) in **code bin width  $W[k]$  definition.<sup>5</sup>**

**code bin width  $W[k]$ :** The difference of the code transition levels that delimit the bin.

$$W[k] = T[k+1] - T[k] \quad \text{for } 1 \leq k \leq 2^N - 2 \tag{1}$$

**code transition level:** The boundary between two adjacent code bins.

**code transition level  $T[k]$ :** The value of the recorder input parameter at the transition point between two given, adjacent code bins. The transition point is defined as the input value that causes 50% of the output codes to be greater than or equal to the upper code of the transition, and 50% to be less than the upper code of the transition. The transition level  $T[k]$  lies between code bin  $k-1$  and code bin  $k$ .  $N$  is the number of digitized bits in a recorder data word. *See:* **transition point.**

<sup>4</sup>*IEEE Standards Dictionary Online* is available at: <http://dictionary.ieee.org>.

<sup>5</sup>Notes in text, tables, and figures of a standard are given for information only and do not contain requirements needed to implement this standard.

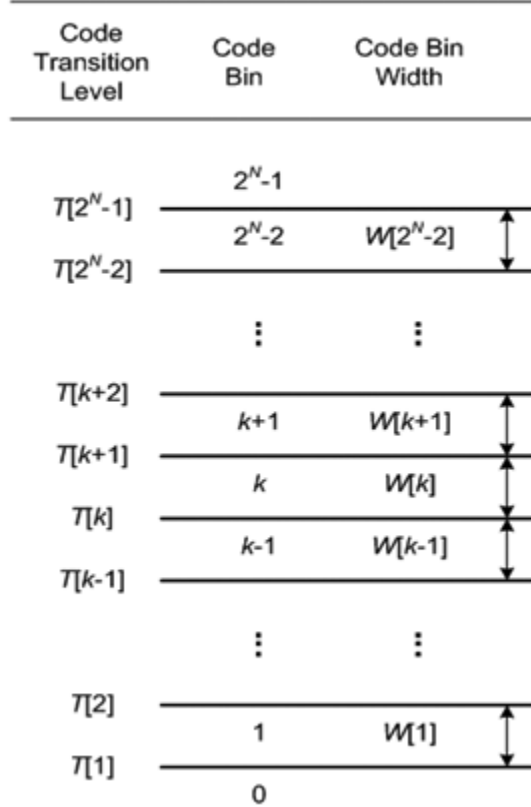


**Figure 2—Definitions pertaining to input quantization**

**coherent sampling:** Sampling of a periodic waveform in which there is an integer number of cycles in the data record.

**common-mode maximum operating signal:** The largest common-mode signal for which a waveform recorder with differential inputs will meet its recording specifications while recording a normal-mode signal.

**common-mode maximum signal level:** For recorders with differential inputs, the maximum level of the common-mode signal at which the common-mode rejection ratio (CMRR) is still valid.

**common-mode out-of-range:** A signal level whose magnitude is less than the specified maximum safe common-mode signal but greater than the maximum operating common-mode signal.

**common-mode out-of-range recovery time:** The time required for the recorder to return to its specified characteristics after the end of a common-mode overvoltage signal.

**common-mode rejection ratio (CMRR):** The ratio of the input common-mode signal to the effect produced at the output of the recorder in units of the input.

**common-mode signal:** The average value of the signals at the positive input and the negative input of a differential-input analog-to-digital converter. If the signal at the positive input is designated  $V_+$ , and the signal at the negative input is designated  $V_-$ , then the common-mode signal  $V_{cm}$  is given in [Equation \(2\)](#):

$$V_{cm} = \frac{V_+ + V_-}{2} \quad (2)$$

**crosstalk (multichannel):** The ratio (usually expressed in decibels) of the signal induced in one channel to a common signal applied to all other channels.

**cumulative distribution function (cdf):** For a continuous random variable, the function  $F_X(x)$ , which is the probability that the random variable,  $X$ , is less than or equal to  $x$ . This function is positive and nondecreasing.

**cycle time:** The real time elapsed (with a recorder continually taking records of data) between the beginning of two successive records.

**data window:** A set of coefficients by which corresponding samples in the data record are multiplied to more accurately estimate certain properties of the signal, particularly frequency domain properties. Generally, the coefficient values increase smoothly and symmetrically toward a maximum at the center of the record.

**dc coupled recorder:** A recorder whose input circuitry passes dc.

**decibels full scale (dBFS):** The root-mean-square (rms) amplitude of any signal in decibels relative to a sine wave that spans the entire input range of the recorder.

**differential input impedance:** For a differential-input waveform recorder, the impedance between the positive input and the negative input with grounds and shields terminated as specified.

**differential input recorder:** A waveform recorder with differential inputs, which produces output codes that are a function of the difference between two input signals. The two input signals are typically called positive (or plus) and negative (or minus). If the signal at the positive input is designated  $V_+$ , and the signal at the negative input is designated  $V_-$ , then the differential signal ( $V_{dm}$ ) is given in [Equation \(3\)](#):

$$V_{dm} = V_+ - V_- \quad (3)$$

**differential nonlinearity (DNL):** The difference between a specified code bin width and the average code bin width, divided by the average code bin width.

**discrete Fourier transform (DFT):** A mathematical operation that converts sampled data from the time domain to the frequency domain. *Contrast: inverse discrete Fourier transform (IDFT).*

**distortion:** Aberrations in the output of the waveform recorder caused by nonlinearities. Distortion effects appear as harmonics and intermodulation products of the input signal frequencies in the frequency domain of the output signal.

**dynamic range:** *See: effective number of bits (ENOB), ratio of signal to noise and distortion (SINAD), signal-to-noise ratio (SNR), spurious free dynamic range (SFDR).*

NOTE—The term *dynamic range* has a number of meanings depending on the application. It is not used by itself in this standard.

**effective number of bits (ENOB):** For an input sine wave of specified frequency and amplitude, the number of bits of an ideal waveform recorder for which the rms quantization error is equal to the rms noise and distortion of the waveform recorder under test.

**equivalent-time sampling:** A process by which consecutive samples of a repetitive waveform are acquired and assembled from multiple repetitions of the waveform, to produce a record of samples representing a single repetition of the waveform sampled at a higher rate.

**fixed error in sample time:** A nonrandom error in the instant of sampling. A fixed error in sample time can be fixed with respect to the data samples acquired or correlated with an event that is detected by the sampling process. Unless otherwise specified, the term is usually taken to mean the maximum systematic fixed error that can be observed.

**frequency response:** The complex gain (magnitude and phase) as a function of input frequency, or the Fourier transform of the impulse response.

**full-scale [input] range (FSR):** The difference between the maximum and the minimum recordable input values as specified by the manufacturer exclusive of quantization limitations.

**full-scale signal:** A signal whose peak-to-peak amplitude spans the entire range of input values recordable by the analog-to-digital converter under test.

**gain error: (A) (dynamic):** The difference between the dynamic gain,  $G(f)$ , of the waveform recorder at a given frequency and its gain at a specified reference frequency divided by its gain at the reference frequency. **(B) (static):** The difference between the actual gain and the nominal gain.

**gain flatness:** Variation of gain over a specified frequency range, usually expressed in decibels.

**harmonic distortion:** For a pure sine wave input, output components at frequencies that are an integer multiple of the applied sine wave frequency.

**hysteresis:** The maximum systematic difference in values for a digitizer code transition level when the transition level is approached from either side of the transition with a specified limit on the slew rate of the input signal.

**ideal code bin width ( $Q$ ):** The full-scale input range divided by the total number of code bins.

**input impedance:** The impedance between a signal input terminal and a specified reference terminal.

**integral nonlinearity (INL):** The maximum systematic difference between the ideal and actual code transition levels after correcting for gain and offset.

**intermodulation distortion (IMD):** When there is an input signal with multiple frequencies at the input to the recorder, the generation of distortion signals at the sum and difference frequencies of the inputs due to nonlinearities in the waveform recorder response.

**inverse discrete Fourier transform (IDFT):** A mathematical operation that converts sampled data from the frequency domain to the time domain. *Contrast:* **discrete Fourier transform (DFT).**

**$k^{\text{th}}$  code transition level  $T[k]$ :** The input value corresponding to the transition between codes  $k-1$  and  $k$ .

NOTE—See [Figure 2](#).

**large signal:** A signal whose peak-to-peak amplitude (including noise) is as large as can be practically recorded by the instrument within, but not including, the maximum and minimum amplitude data codes. As a minimum, the signal shall span at least  $-1$  dBFS ( $\sim 89\%$ ) of the waveform recorder range.

**least significant bit (LSB):** One integer count in the digitized output of the waveform recorder. (If the recorder outputs data in a floating point format, e.g., input units, the data can be converted to LSBs using the manufacturer's instructions.) The nominal value associated with an LSB is the ideal code bin width,  $Q$ .

**long-term settling error:** The absolute difference between the final value specified for short-term transition settling duration, and the value 1 s after the beginning of the step, expressed as a percentage of the step amplitude.

**long-term time base stability:** The change in time base frequency (usually given in parts in  $10^6$ ) over a specified period of time at a specified sampling rate.

**maximum static error:** The maximum difference between any code transition level and its ideal value.

**mod( $x, m$ ):** A function that gives the remainder when  $x$  is divided by  $m$ , e.g.,  $\text{mod}(8.1, 2.5) = 0.6$ . The sign of the result is the same as the sign of  $m$ .

**monotonic recorder:** A recorder that has output codes that do not systematically decrease (increase) for a uniformly increasing (decreasing) input signal.

**noise:** Any deviation between the output signal (converted to input units) and the input signal except deviations caused by linear time invariant system response (gain and phase shift), a dc level shift, total harmonic distortion (THD), or an error in the sample rate.

NOTE—Noise has historically been an ambiguous term. In this standard, noise is defined as indicated above.

**noise and distortion (NAD):** The sum of the effects of noise and total harmonic distortion (THD).

**noise floor:** Maximum power level over a given frequency band in the frequency domain of components that are not due to the applied signal, harmonics, or spurious signals. The level could be absolute (expressed in decibels with respect to a milliwatt per unit of bandwidth) or relative to the waveform recorder input full scale (expressed in decibels with respect to full scale per unit of bandwidth).

**noise power ratio (NPR):** The ratio of the average out-of-notch to the average in-notch power spectral density magnitudes for the discrete Fourier transform (DFT) spectrum of the waveform recorder output sample set measured using a notch-filtered broadband white-noise generator as the input to the waveform recorder under test.

**noncoherent sampling:** Sampling of a periodic waveform where there is no integer number of cycles in the data.

**normalized noise power gain (NNPG):** Sum of squares of the values of a data window function divided by the number of samples.

**normalized signal-to-noise (SNR1Hz):** Signal-to-noise ratio (SNR) normalized to a reference bandwidth of 1 Hz. *Syn:* **noise spectral density.**

**normal-mode signal (or differential signal):** The difference between the signal at the positive input and the negative input of a differential input waveform recorder.

**Nyquist frequency:** Frequency equal to one-half the sampling frequency.

**offset:** *See:* **static gain and offset.**

**out of range (overvoltage):** Any voltage whose magnitude is less than the maximum safe input voltage of the recorder but greater than the full-scale value for the selected range.

**overshoot:** The maximum amount by which the step response is above the high state for a positive-going transition or is below the low state for a negative-going transition, specified as a percentage of (recorded) pulse amplitude.

NOTE—See IEEE Std 181-2011 for more information on low and high states.<sup>6</sup>

**Parseval relationship:** The relationship where the sum (or integral) of the square of a function is equal to the sum (or integral) of the square of its Fourier transform.

**passband:** The band of input signal frequencies that the waveform recorder is intended to digitize with nominally constant gain.

**phase nonlinearity:** The deviation in phase response from a perfectly linear-phase response as a function of frequency.

**precursor:** Any deviations from the low state for a positive-going transition or from the high state for a negative-going transition prior to the step transition.

NOTE—See IEEE Std 181-2011 for more information on low and high states.

**probability density function (pdf):** For a continuous random variable, the function  $f_X(x)$ , which has the interpretation that  $f_X(x)dx$  is the probability that the random variable,  $X$ , lies in the interval  $(x, x+dx)$ .

**quantization:** A process in which the continuous range of values of an input signal is divided into subranges, and to each subrange a discrete value of the output is uniquely assigned. In the ideal case, these subranges are nonoverlapping and equal in size. Whenever the signal value falls within a given subrange, the ideal output has the corresponding discrete value.

**quantization error:** The error caused by conversion of a variable having a continuous range of values to a quantized form having only discrete values, as in analog-to-digital conversion. The error is the difference between the original (analog) value and its quantized (digital) representation translated into input units.

**quantization noise:** Equivalent noise produced during the quantization of a continuous range variable. A quantization process of step size  $Q$  produces a root-mean-square (rms) quantization noise of  $Q/\sqrt{12}$  when the continuous variable range is much larger than  $Q$ .

**random noise:** A nondeterministic fluctuation in the output of a waveform recorder, usually described by its frequency spectrum and its amplitude statistical properties.

**ratio of signal to noise and distortion (SINAD):** For a pure sine wave input of specified amplitude and frequency, the ratio of root-mean-square (rms) signal to rms noise and distortion (NAD).

**record of data:** A sequential collection of samples acquired by the waveform recorder.

**relatively prime:** A descriptor of two integers when their greatest common divisor is 1.

**residuals:** For least squares curve fitting of data to a mathematically defined function, the differences between the recorded data and the fitted function. The mathematically defined function is often a sine wave.

**reverse coupling:** The ratio of the spurious signal generated by a signal at some other input to the recorder and the signal recorded at the specified input of the recorder.

---

<sup>6</sup>Information on references can be found in Clause 2.

**root-mean-square (rms):** For a given set of data, the square root of the arithmetic mean of the squared values of each of the data.

**sampling:** The process of extracting values at discrete time instants from a continuous input signal.

**short-term settling error:** The maximum absolute difference between the waveform and the final value at all times between a specified time measured from the 50% reference level instant of the waveform and the end of the data record expressed as a percentage of step amplitude. The final value is defined to occur 1 s (unless otherwise specified) after the beginning of the step.

**short-term timing instability:** See: **aperture uncertainty**.

**short-term transition settling duration:** Measured from the 50% reference level of the output, the time at which the step response enters and subsequently remains within a specified error band around the final value. The final value is defined to occur at 1 s after the beginning of the step unless otherwise specified.

**signal-to-noise ratio (SNR):** The ratio of a signal to the noise where noise is any deviation between the output signal (converted to input units) and the input signal except deviations caused by linear time invariant system response (gain and phase shift), a dc level shift, total harmonic distortion (THD), or an error in the sample rate.

**sine wave histogram:** A histogram where each bin contains the total number of occurrences of each digitized level of an input sine wave signal.

**single-ended recorder:** A recorder that measures the voltage difference between a single input connection and ground.

**slew rate limit:** The value of rate of change of output codes (referenced to the input) for which an increased amplitude input step causes no change.

**spectral leakage:** Spectral lines adjacent to the input line produced by the discrete Fourier transform (DFT) when the input is a pure sine wave whose frequency does not satisfy the coherent sampling condition and thus is not at the center of a DFT frequency bin.

**spurious components:** Persistent sine waves at any frequencies other than the input or harmonic frequencies.

**spurious free dynamic range:** The frequency domain difference in decibels between the full-scale signal level and the largest spurious component (including harmonics) for a large, pure sine wave signal input.

**static (parameter, error, or test):** A static test is a test in which the input signal is essentially constant, meaning the signal is varying slowly enough that the results are the same as that obtained by a constant signal. A static parameter or error is the value obtained when measured with a static test.

**static gain and offset: (A)** (*independently based*). The values by which the transition levels are multiplied and then to which the transition levels are added, respectively, to minimize the mean squared deviation from the ideal transition levels. **(B)** (*terminal-based*). The values by which the transition levels are multiplied and then to which the transition levels are added, respectively, to cause the deviations from the ideal transition levels to be zero at the terminal points, that is, at the first and last code transitions.

**step response:** The recorded output response for an ideal input step with designated low state and high state.

NOTE—See IEEE Std 181-2011 for more information on low and high states.

**timing jitter:** See: **aperture uncertainty**.

**timing phase noise:** See: **aperture uncertainty.**

**total harmonic distortion (THD):** The scaled square root of the sum of squares of a specified set of harmonic distortion components including their aliases for a pure sine wave input of specified amplitude and frequency.

**transfer curve:** The representation of the average digital output code of a waveform recorder as a function of the input signal value.

**transition duration of the step response:** The duration between the instants corresponding to two reference levels. Unless otherwise specified, the two reference levels are the 10% and 90% reference levels.

**transition level:** The input value that causes 50% of the output codes to be greater than or equal to the upper code of the transition, and 50% to be less than the upper code of the transition.

**transition settling duration:** The time at which the step response enters and subsequently remains within a specified error band around the final value, measured from the 50% point of the response.

**trigger delay:** The elapsed time from the occurrence of a trigger pulse at the trigger input connector, to the time at which the first or a specified data sample is recorded.

**trigger jitter:** The standard deviation in the trigger delay time over multiple records.

**trigger minimum rate of change:** The slowest rate of change of the transition duration of a pulse of a specified level that will consistently trigger the recorder.

**trigger signal coupling:** The ratio of the spurious signal level (that is recorded by an input to the recorder) to the trigger signal level.

**waveform:** A manifestation or representation (e.g., graph, plot, oscilloscope presentation, discrete time series, equations, table of coordinates, or statistical data) or a visualization of a signal.

**waveform epoch:** An interval to which consideration of a waveform is restricted for a particular calculation, procedure, or discussion. Except when otherwise specified, the waveform epoch is assumed to be the span over which the waveform is measured or defined. The duration of time corresponding to a data record. For instance, for an  $M$ -sample record acquired at the uniform sampling period  $T_s$ , the epoch is  $MT_s$ .

**window:** See: **data window.**

### 3.2 Symbols and acronyms

Below are the acronyms used in this standard and the symbols that are used in more than one subclause in this standard. Other symbols are declared and defined locally as needed.

|                    |   |
|--------------------|---|
| $\varepsilon$      | general symbol for error, uncertainty, or tolerance                         |
| $\varepsilon_f$    | error in frequency  |
| $\varepsilon_{fs}$ | error in sampling rate  |
| $\varepsilon_G$    | gain error  |
| $\varepsilon[k]$   | residual error in the least squares fit method of computing gain and offset |
| $\varepsilon_m$    | upper bound on aliasing error magnitude spectrum                            |
| $\varepsilon_Q$    | quantization error  |
| $\varepsilon_{ms}$ | mean square error   |

|                      |   |
|----------------------|---|
| $\varepsilon_w$      | measured word error rate  |
| $\varepsilon_{wMax}$ | upper bound on word error rate  |
| $\eta$               | root-mean-square (rms) amplitude noise  |
| $\eta(f)$            | noise power per hertz relative to the carrier   |
| $\eta_\varphi$       | phase noise   |
| $\pi$                | constant, ratio of the circumference of a circle to the diameter  |
| $\rho$               | reflection coefficient  |
| $\sigma$             | standard deviation  |
| $\sigma^2$           | variance  |
| $\sigma_t$           | aperture uncertainty  |
| $\tau$               | time constant   |
| $\Phi[s]$            | cumulative density function for a Gaussian distribution (the fraction of the total distribution covered from negative infinity to $s$ )                 |
| $\Phi[k]$            | confidence level for $k$ standard deviations for a Gaussian distribution, expressed as a fraction   |
| $\varphi$            | phase, expressed in radians   |
| $A_{rms}$            | root-mean-square (rms) value of a fitted sine wave, rms signal  |
| ac                   | alternating current   |
| ADC                  | analog-to-digital converter   |
| BW                   | bandwidth   |
| cdf                  | cumulative distribution function  |
| CMRR                 | common-mode rejection ratio   |
| COMINT               | communications intelligence   |
| DAC                  | digital-to-analog converter   |
| dBFS                 | decibels full scale   |
| dc                   | direct current  |
| DFT                  | discrete Fourier transform  |
| DG                   | differential gain error   |
| DNL                  | differential nonlinearity (when given as one number without a code bin specification, it is the maximum differential nonlinearity of the entire range.) |
| $DNL_{rms}$          | root-mean-square (rms) value of $DNL[k]$  |
| $DNL[k]$             | differential nonlinearity of code $k$   |
| DP                   | differential phase error  |
| $E_{avm}$            | residual spectrum after the bins at dc and test frequencies have all been set to zero (deleted from the spectrum)                                       |
| ELINT                | electronic intelligence   |
| ENOB                 | effective number of bits  |
| $f$                  | frequency, expressed in hertz   |

|                  |   |
|------------------|---|
| $f_{eq}$         | equivalent sampling rate  |
| $f_h$            | subset of harmonics used in computing total harmonic energy   |
| $f_i$            | input signal reference frequency or input signal repetition rate  |
| $f_m$            | discrete Fourier transform (DFT) basis frequency  |
| $f_{ref}$        | reference frequency   |
| $f_s$            | sampling frequency  |
| $\Delta f$       | separation between two frequencies  |
| $\Delta f_{rms}$ | root-mean-square (rms) frequency deviation over one record length                                       |
| FDHM             | full duration at half of maximum  |
| FM               | frequency modulation  |
| FSR              | full-scale range (of the recorder)  |
| $G$              | gain of waveform recorder, ideally = 1  |
| $G(f)$           | dynamic gain of waveform recorder as a function of input frequency $f$                                  |
| $H(f)$           | frequency response of the waveform recorder   |
| $h(t)$           | impulse response  |
| IDFT             | inverse discrete Fourier transform  |
| IMD              | intermodulation distortion  |
| INL              | integral nonlinearity   |
| $K$              | number of data records  |
| LSB              | least significant bit   |
| LTI              | linear time invariant   |
| $M$              | number of sequential samples in a data record   |
| MSE              | maximum static error  |
| $N$              | number of bits digitized by the waveform recorder   |
| $N_{CHG}[i]$     | cumulative number of samples up to bin $i$ in sine wave histogram code transition level test            |
| $N_H$            | number of the highest order harmonic used for computing total harmonic distortion (THD)                 |
| $N_{HG}[i]$      | average number of histogram samples received in the two code bins that share the given transition level |
| $N_s$            | total number of samples processed over several records  |
| NAD              | noise and distortion  |
| NPR              | noise power ratio   |
| $NPR_{max}$      | maximum noise power ratio   |
| NNPG             | normalized noise power gain   |
| $P$              | probability   |
| pdf              | probability density function  |
| PSD              | power spectral distribution   |

|               |   |
|---------------|---|
| $Q$           | ideal code bin width, expressed in input units  |
| $Q'$          | actual average code bin width   |
| rms           | root mean square  |
| SFDR          | spurious free dynamic range   |
| SIGINT        | signal intelligence   |
| SINAD         | ratio of signal to noise and distortion   |
| SNR           | signal-to-noise ratio   |
| $T$           | time between digitized data samples or sample period  |
| $T_R$         | record length of the recorder in seconds  |
| $T_{eq}$      | interval between equivalent-time samples  |
| $t$           | time, in seconds unless otherwise specified   |
| $t_r$         | transition duration   |
| $T[k]$        | code transition level between code $k$ and code $k-1$   |
| $T[k_{in}]$   | measured level used to fine tune location of a code transition level  |
| TDR           | time domain reflectometer   |
| THD           | total harmonic distortion   |
| $u(t)$        | unit step function  |
| $u'(t)$       | non-ideal step-like function  |
| $U'(f)$       | Fourier transform of $u'(t)$  |
| $V_{in}$      | amplitude of the input signal to the waveform recorder  |
| $V_{in\ rms}$ | root-mean-square (rms) of the input signal to the waveform recorder   |
| $V_{os}$      | input offset of waveform recorder, ideally = 0  |
| $V_{out}$     | peak-to-peak amplitude of the signal in the digitized data  |
| VSWR          | voltage standing wave ratio   |
| $W[k]$        | code bin width of code bin $k$  |
| $W[n]$        | Fourier transform of the data window function $w[k]$  |
| $w[k]$        | window function [for a discrete Fourier transform (DFT)]  |
| $X[k]$        | frequency domain samples of the input sequence $x[i]$ computed via the discrete Fourier transform (DFT)   |
| $X_{avg}[m]$  | averaged spectral magnitude of the discrete Fourier transforms (DFTs) of multiple data records  |
| $X_{avnh}$    | averaged discrete Fourier transform (DFT) spectrum, $X_{avg}$ , with the components (bins) at dc, the test frequencies $f_i$ and ( $f_s - f_i$ ), and the specified harmonic frequencies $f_{h[n]}$ , all set to zero (deleted) |
| $X_{wavg}[m]$ | averaged spectral magnitude of the discrete Fourier transforms (DFTs) of multiple windowed data records   |
| $X_w[i]$      | Fourier transform of a windowed input sequence $w[i] x[i]$  |
| $X_{w,k}[i]$  | windowed Fourier transform of the $k^{\text{th}}$ record when multiple records are taken  |

|           |  |
|-----------|--|
| $x[i]$    | sequence of digitized input time domain samples          |
| $x'[i]$   | best fit points to a data record                         |
| $x(t)$    | continuous input signal as a function of time            |
| $\bar{x}$ | average value of the input signal over the record        |
| $y[i]$    | filtered input sequence of digitized time domain samples |
| $Z_0$     | transmission line impedance                              |
| $Z_i$     | waveform recorder input impedance                        |

## 4. Test parameters and methods

### 4.1 Manufacturer supplied information

#### 4.1.1 General information

Manufacturers shall supply the following general information:

- Model number
- Dimensions and weight
- Power requirements
- Environmental conditions: Safe operating, nonoperating, and specified performance temperature range; altitude limitations; humidity limits, operating and storage; vibration tolerance; and compliance with applicable electromagnetic interference specifications
- Any special or peculiar characteristics
- Compliance with military and other specifications
- Available options and accessories, including their impact on equipment performance
- Exceptions to the above parameters where applicable
- Calibration interval, if required

#### 4.1.2 Performance specification

The manufacturer shall provide the minimum specifications defined in 4.1.2.1. Additional potentially useful specifications are given in 4.1.2.2. See 3.1 for definitions.

##### 4.1.2.1 Minimum specification

The manufacturer shall provide minimum specifications for the following:

- Number of digitized bits
- Sample rates
- Memory lengths
- Input impedances
- Analog bandwidths
- Input signal ranges
- Power supply voltage ranges

- Power dissipation

#### 4.1.2.2 Additional specifications

The following additional specifications shall potentially be provided:

- Gain
- Offset
- Differential nonlinearity (DNL)
- Integral nonlinearity (INL)
- Maximum static error
- Monotonicity
- Hysteresis
- Total harmonic distortion (THD) and spurious response
- Intermodulation distortion (IMD)
- Noise power ratio (NPR)
- Ratio of signal to noise and distortion (SINAD)
- Signal-to-noise ratio (SNR)
- Effective number of bits (ENOB)
- Random noise
- Gain error versus frequency
- Frequency response
- Transition settling duration
- Transition duration of step response (rise time)
- Overshoot and precursor
- Slew limit
- Crosstalk
- Aperture uncertainty (short-term time base stability)
- Long-term time base stability
- Fixed error in sample time
- Trigger delay and jitter
- Trigger sensitivity
- Trigger hysteresis band
- Trigger minimum rate of change
- Trigger coupling to signal
- Overvoltage recovery
- Word error rate
- Cycle time

- Common-mode rejection ratio (CMRR)
- Maximum common-mode signal level
- Differential input impedance
- Maximum operating common-mode signal level

#### 4.1.3 Critical waveform recorder parameters

**Table 1** is presented as a guide for many of the most common waveform recorder applications. The wide range of waveform recorder applications makes a comprehensive listing impossible. This table is intended to be a helpful starting point for users to apply this standard to their particular applications.

**Table 1—Critical waveform recorder parameters**

| Typical applications                                | Critical waveform recorder parameters   | Performance issues   |
|---|---|--|
| Audio   | SINAD, THD, noise, frequency response   | Power consumption<br>Crosstalk and gain matching   |
| Data acquisition                                    | DNL, INL, gain, offset, noise, out-of-range recovery, settling time, full-scale step response, channel-to-channel crosstalk | Channel-to-channel interaction<br>Accuracy, traceability   |
| Digital oscilloscope/<br>waveform recorder          | SINAD, ENOB, noise, bandwidth, out-of-range recovery, word error rate   | SINAD for wide bandwidth amplitude resolution<br>Low thermal noise for repeatability<br>Bit error rate                                     |
| Geophysical   | THD, SINAD, long-term stability, noise  | Millihertz response  |
| Imaging   | DNL, INL, SINAD, ENOB, noise, out-of-range recovery, full-scale step response   | DNL for sharp-edge detection<br>High-resolution at switching rate<br>Recovery from blooming  |
| Radar and sonar                                     | SINAD, IMD, ENOB, SFDR, out-of-range recovery, noise  | SINAD and IMD for clutter cancellation and Doppler processing.   |
| Spectrum analysis                                   | SINAD, ENOB, SFDR, noise  | SINAD and SFDR for high linear dynamic range measurements.   |
| Spread spectrum communication                       | SINAD, IMD, ENOB, SFDR, NPR, noise-to-distortion ratio, noise   | IMD for quantization of small signals in a strong interference environment<br>SFDR for spatial filtering<br>NPR for interchannel crosstalk |
| Telecommunication personal communications           | SINAD, NPR, SFDR, IMD, bit error rate, word error rate, noise   | Wide input bandwidth channel bank<br>Interchannel crosstalk<br>Compression<br>Power consumption  |
| Video   | DNL, SINAD, SFDR, DG, DP, noise   | Differential gain and phase errors<br>Frequency response   |
| DVR (Digital Video Recorder)                        | Data rate, compression algorithm, power consumption, input impedance  | Video standards compliance   |
| Wideband digital receivers<br>SIGINT, ELINT, COMINT | SFDR, IMD, SINAD, noise   | Linear dynamic range for detection of low-level signals in a strong interference environment<br>Sampling frequency                         |

## 4.2 Test selection

In general, it is not worthwhile to test every parameter defined in this standard for any given waveform recorder application, nor is it possible to test parameters under the infinitely many possible test conditions. Thus, the first step in testing any waveform recorder shall be to determine the set of parameters to be measured and the conditions under which they are to be tested. No single process for making this determination will fit every need, but the general procedure outlined below is a good place to start. Users may choose to modify this outline as they gain experience in the particulars of their applications.

Test selection is typically an iterative process. At first, a core set of basic tests is run. Then, depending on the results of these tests, additional tests can be selected to more carefully measure the most significant parameters, further clarify the cause and/or extent of an error, verify an error model, etc. The core set of tests is run at several waveform recorder settings (e.g., different sample rates, input signal ranges) that form a representative sample for the intended use of the recorder, as the results of the tests can vary with the control settings. In addition, some tests (e.g., ENOB) shall be run at several different input conditions (e.g., at several input frequencies). The subclauses below define a core set of tests and input conditions, along with methods to interpret the results, and from there to select additional tests.

Several basic test methods may be used to characterize a waveform recorder. Brief description of the step response test, sine fit and harmonic distortion tests, and dc tests follow.

### 4.2.1 Step response

Start by measuring the recorder's step response using an input step from about 10% to about 90% of full scale (see 4.8). From this, calculate the recorder's analog bandwidth, frequency response, transition duration, overshoot, transition settling duration, etc. (see Clause 9 and Clause 10). Measuring the frequency response from the step response assumes the waveform recorder is a linear, time-invariant system. Note that in many recorder architectures, the step response and the parameters derived from it vary with the sample rate and/or the input signal range. Note, also, that some recorders cannot be clocked at rates that can fully record the step response, and equivalent-time sampling can be required (see 4.4).

### 4.2.2 Sine fit and harmonic distortion tests

Perform sine fit tests using a large (e.g., 90% full scale) amplitude signal at several frequencies spanning the range of major expected frequency components in the intended use of the recorder (see 4.6). The residuals of the sine fits show deviations from the linear, time-invariant model assumed in the step response testing. Calculate the ENOB of the recorder at the different frequencies (see 8.5). Also, calculate the Fourier transform of the sine wave data records, and check for harmonic distortion and other spurious components (see 7.7 and 8.7). These tests are then repeated for sample rates and input signal ranges of interest.

In the following, the sine-fit frequencies are categorized as low, medium, and high. Low frequencies are low enough to not cause significant dynamic errors in the waveform recorder. Frequencies less than a few percent of the analog bandwidth are generally safe to consider low. Medium frequencies are those high enough to cause some dynamic effects, but still well below the analog bandwidth. These will typically be in the range of 10% to 60% of the analog bandwidth. High frequencies are near enough to the analog bandwidth limit that the amplitude roll-off is a significant factor.

Also in the following, the ENOB parameter is characterized as low or falling if it is more than one-half to one bit below the number of digitized bits or below the ENOB at a lower frequency. Likewise, total harmonic distortion (THD) (expressed in decibels relative to the carrier) is considered high or rising if it is more than 3 dB to 6 dB above quantization errors or above the harmonic distortion at a lower frequency.

The ENOB will typically decrease at high frequencies. A major reason for this decrease is that aperture uncertainty effects become greater at high frequencies (see Clause 12). THD can decrease at high frequencies if the harmonics are outside the upper bandwidth limit.

If the low-frequency ENOB is low and the low-frequency THD is high, the waveform recorder can have significant static nonlinearity. Measure the code transition levels (see [4.7](#)) and calculate the integral nonlinearity (INL) and DNL (see [Clause 7](#)).

If the low-frequency ENOB is low and the low-frequency THD is low, the waveform recorder probably has fine-grained (locally varying) nonlinearity and/or additive noise. Measure the INL, DNL, and random noise (see [Clause 8](#)).

If the medium-frequency ENOB is falling and the THD is rising commensurately, the waveform recorder has dynamic nonlinearity. This dynamic nonlinearity can also cause a variation in the step response with input amplitude. Retest the step response at a low input amplitude to determine whether there is a significant difference between small-signal and large-signal frequency responses.

If the medium-frequency ENOB is falling, but the THD remains low, the waveform recorder probably has errors in sample timing. Measure the aperture uncertainty and fixed error in sample time (see [Clause 12](#)).

If the high-frequency ENOB is rising and the high-frequency THD is falling, it is likely that there is a distorting stage before the bandwidth-limiting stage and that THD is being filtered out as it exceeds the analog bandwidth. Although this reduction in THD for single-tone sine wave inputs is real, the distorting stage will likely produce distortion products at or below the input frequencies for other input signals, which would not be filtered out. Thus the reduction of THD at high frequencies does not necessarily imply an increase in accuracy in typical use. Check for other signs of high-frequency nonlinearity, such as slew limiting and intermodulation distortion (IMD).

If the Fourier transform shows spurious components at multiples of  $f_s/J$  and/or at the input frequency  $\pm$  multiples of  $f_s/J$  (where  $f_s$  is the sample rate and  $J$  is a small integer), the waveform recorder is likely implemented as  $J$  interleaved slower digitizers.

Additional information about the error sources within a waveform recorder can be gleaned from a visual inspection of plots of the residuals from the sine-fit tests. See [Annex G](#) for details on the interpretation of residual plots.

#### 4.2.3 Tests at dc

For applications where dc accuracy is of major importance, find the code transition levels, and from there calculate the gain and offset, INL and DNL, maximum static error, etc. For applications where such a detailed view of the dc transfer function is not needed, find the waveform recorder's low-frequency gain and offset using the dynamic test method shown in [6.1.2](#) instead, as this can be done using the same sine-fit data gathered above.

### 4.3 Test setup

#### 4.3.1 Setting up the recorder

The recorder shall be allowed to warm up and is then tested at specific settings of interest. These settings include some or all of the following:

- Full-scale range (FSR)
- Recorder offset adjustment
- Sample rate
- Record length
- Number of pretrigger samples

- Triggering source, level, slope, bandwidth, impedance, etc.
- Input impedance
- Bandwidth/anti-aliasing filter

Notice that testing a waveform recorder inverts the order of operations associated with normal use. For testing, first set the instrument to the desired operating settings, and then adjust the input source to provide an appropriate signal.

Note that some test methods call for relatively specific record lengths. Unnecessarily large record lengths shall be avoided because they can add additional errors due to drift or other long-term phenomena. Longer records also require more computer processing time. However, if the user is interested in the performance of the recorder over a particular record length, tests shall be performed over the length of interest. For example, the results of an ENOB test can degrade with increasing record length due to accumulated time base error.

Pre-trigger may be useful for positioning a test sample at a convenient place in the record. Having the proper input impedance selected will be very important for many tests, e.g., step pulse response, gain, over-voltage recovery.

More sophisticated recorders can have more parameters that shall be set properly. Consult the manual for the recorder for more detail. Some recorders allow the operating parameter setting either by manual or by computer control. Others can be set up only by computer control.

#### **4.3.2 Selecting signal sources**

The sources used to generate the test signals are dependent on the characteristics of the waveform recorder under test. It is important, whenever possible, that the signals, particularly the test signal, be defined at the inputs to the waveform recorder with the recorder replaced by an ideal load. Using the signal at the input points instead of at the source output eliminates the effects of cables and any signal conditioning components between the source and the recorder.

Because the properties of sine waves are easy to establish and maintain, sine waves are commonly used as sources for test signals. More complex waveforms, such as triangular, rectangular, or Gaussian, are also used, but it is more difficult to define and maintain the required frequency, amplitude, and phase relationships with high fidelity.

Combining the output of two (or more) sine wave generators can produce two-tone (or multi-tone) test signals for IMD testing. Additionally, a noise generator's output can be combined with a signal to provide low-level dither (see Gray and Stockham [B20]).

If the waveform recorder supports an external clock signal, the frequency synthesizers used to generate the test and clock signals can often be phase-locked to maintain precise phase relationships between the signal and the sampling clock. Phase-locking of synthesizers facilitates testing and simplifies subsequent digital signal processing, by preventing clock/signal walkthrough (beat patterns) that can artificially increase or reduce measured spurious output. This is the primary advantage of testing with a user-supplied clock. Both the clock and the test signals shall be suitable for the test being performed. Filters can be required in either the clock or signal paths to reduce noise or harmonic distortion. For example, sub-harmonics in the clock path can degrade waveform recorder performance; therefore, the clock signal can require filtering to smooth edges that might otherwise feed through to the signal path. Also, low-pass or band-pass filters can be required in the signal path to eliminate noise or other undesirable signals (e.g., harmonics). The relative jitter between the clock and test signals shall be low enough to prevent jitter artifacts from affecting the measured noise as described in Clause 8.

### 4.3.3 Connecting signal sources

When complex test signals are required, use of additional signal-combining circuits can be employed. These can take the form of resistive or inductive passive combiners or, in some cases, an active summing amplifier can be used. It is important to understand the effects these circuits can have on the noise, distortion, and amplitude of the newly created test signal. Impedance-matching circuits can also be inserted to accurately couple the input test signal to the waveform recorder input terminals. Back-terminating the input signal is another common method to achieve proper input connection impedance matching. It is important to carefully understand the return signal path so that a ground loop is not formed that would cause amplitude degradation and increased noise. As in all sampling systems, the appearance of sampling transients, otherwise known as “kickout” or “kickback” error signals, can be present at the waveform recorder input that shall be properly terminated to reduce their effect on the input test signal. Buffer amplifiers or attenuators with adequate bandwidth can be inserted between the signal source and the recorder to reduce these glitches.

### 4.3.4 Terminations

Several test methods call for terminating the input of the waveform recorder. This phrase means that an appropriate circuit shall be placed across the input terminals of the recorder under test. The circuit will often simply be a resistor of a specified value.

### 4.3.5 Reducing noise

Unwanted components or noise can be present on the test signal or connections to the waveform recorder input. Filters, usually low-pass, band-pass, or even high-pass, are commonly used to attenuate these undesirable frequencies and noise signals.

#### 4.3.5.1 Grounding and shielding

Proper grounding and shielding techniques are important in making accurate measurements that are not corrupted by electrical noise. The user shall minimize ground loops and provide low impedance paths to ground. The actual grounding method chosen will often be limited by features of the test equipment used and by electrical safety codes. Electronic instruments often have coaxial connectors where the cable shield is connected to the chassis, which is, in turn, connected to the ac power ground. Under those conditions, ground loops are inevitable when multiple chassis or signal cables are used. In this case, cable lengths shall be minimized and routed to minimize loop areas. Connecting electrical chassis to a high-conductivity ground plane with heavy-duty braid also helps reduce ground-loop pickup.

All connections between the test signal source(s) shall make use of shielded transmission lines such as coaxial cable to shield the test signal from radiated noise. Triaxial cable can be required in some severe noise applications. For low-frequency applications, differential data transmission techniques using twisted shielded pair cable can be used. See Morrison [B33] for more information on grounding and shielding.

“Ground” represents the reference node for all waveform recorder measurements, and it shall be as stable and quiet as possible. There are different philosophies that claim to be the best way to ground a device. Any ground system that provides an acceptably low noise floor is a good one. In connecting and grounding a waveform recorder, determining where the currents flow is essential. Most precision waveform recorders have separate digital and analog returns. Grounding problems can be minimized if proper attention is paid to where the currents flow and to where voltage drops are being generated. A block diagram of the returns in a typical modular waveform recorder application is shown in [Figure 3](#).

Seven nodes that are nominally at “ground” potential are identified in [Figure 3](#). These nodes are described as follows:

- PS1 return, labeled (1). This node is the return of one of the power supplies that are powering the analog portion of the waveform recorder.

- Analog return of the waveform recorder, labeled (2). This node is usually considered the reference node. The internal workings of the waveform recorder try to measure the specified level of the recorder input with reference to this node. The digital return and the analog return are normally connected somewhere in the system to chassis ground.
- Digital return of the waveform recorder, labeled (3). Note that the digital output currents are nominally returned through this node.
- Load return, labeled (4). The load that is applied to the digital outputs returns current to this node.
- Source LO, labeled (5). The source being applied to the recorder input has its return at this node.
- PS2 return, labeled (6). This node is a second power supply return. Current drawn by the recorder's digital section returns through this line. This power supply powers the digital portion of the waveform recorder.
- Chassis ground, labeled (7). This node is the system return that is eventually connected to the ac power line return.

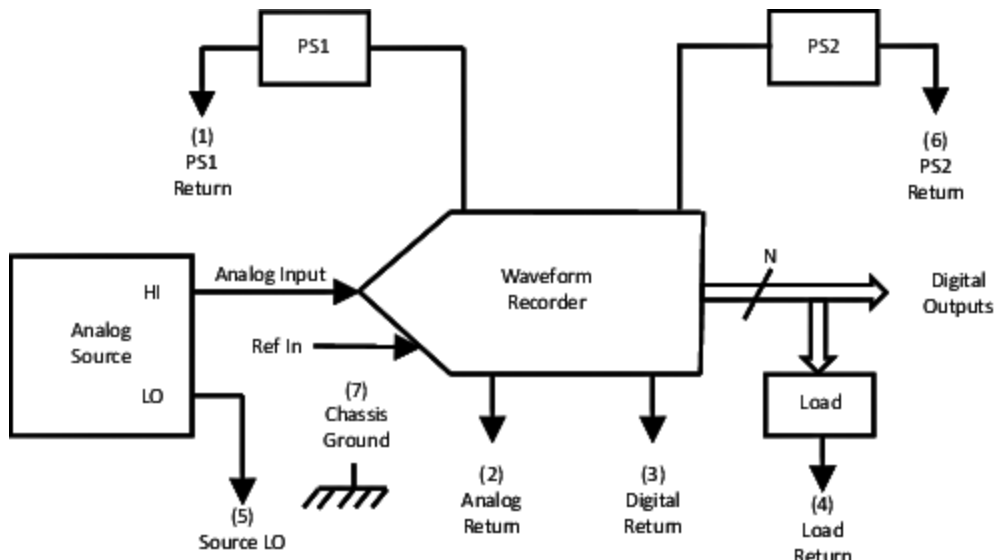


**Figure 3—Block diagram of waveform recorder “ground” nodes**

Some general rules, as follows, are vital for good measurement quality:

- Connect the source LO (5) to the analog return (2).
- Connect the chassis return (7) to the digital return (3) and to the digital power supply return (6).
- The reference input to the waveform recorder normally has its return referenced to the analog return (2).
- The analog power supply, PS1, normally has its return (6) connected through an isolated line to the analog return of the waveform recorder (2).
- The digital return (3) and the analog return (2) are normally strongly connected through a ground plane. Note that many waveform recorders have the analog and digital grounds internally connected or merged into a single pin.
- The load return (4) is normally connected with an isolated connection to the digital return (3).

Many of these rules can be judiciously violated, but the designer of the ground interconnect shall always be cognizant of the finite impedance of the ground interconnects and cognizant of the paths of the current flows—both static and dynamic.

#### **4.3.6 Taking a record of data**

A record of data is a sequential collection of samples acquired by the waveform recorder. The action of taking a record of data is defined as creating the record of data in the recorder by making a measurement and then transferring the data record to a computer for analysis.

Any test signal source(s) shall be connected to the recorder using proper cabling and auxiliary signal conditioning components. If the user has elected to use an external trigger, then the trigger signal shall also be connected, and the signal and trigger shall be synchronized. If a single-shot acquisition mode is being used, then the recorder shall be armed. After the digitizer records and possibly processes the data, the values can be read when the recorder indicates they are ready. Many recorders perform internal gain, offset, and time base corrections after the waveform is recorded.

The user can consult the recorder's manual for details in reading the data. Recorders output the data in different formats, and sometimes the user can select one of several formats. The user might need to convert the data into input units (e.g., volts) following the manufacturer's instructions.

#### **4.3.7 General test setups**

A few general test setups can be used to perform most of the waveform recorder tests presented in this standard. Test setups that use sine waves, arbitrary waveforms, and pulses are described in the following subclauses. Some tests, such as those for voltage standing wave ratio (VSWR) and out-of-range signals require setups other than those discussed in the following subclauses.

The following clauses describe general test setups for sine waves, arbitrary waveform generators, and pulses. Some waveform recorders have features such as clock and trigger outputs that facilitate these tests as shown in [Figure 4](#).

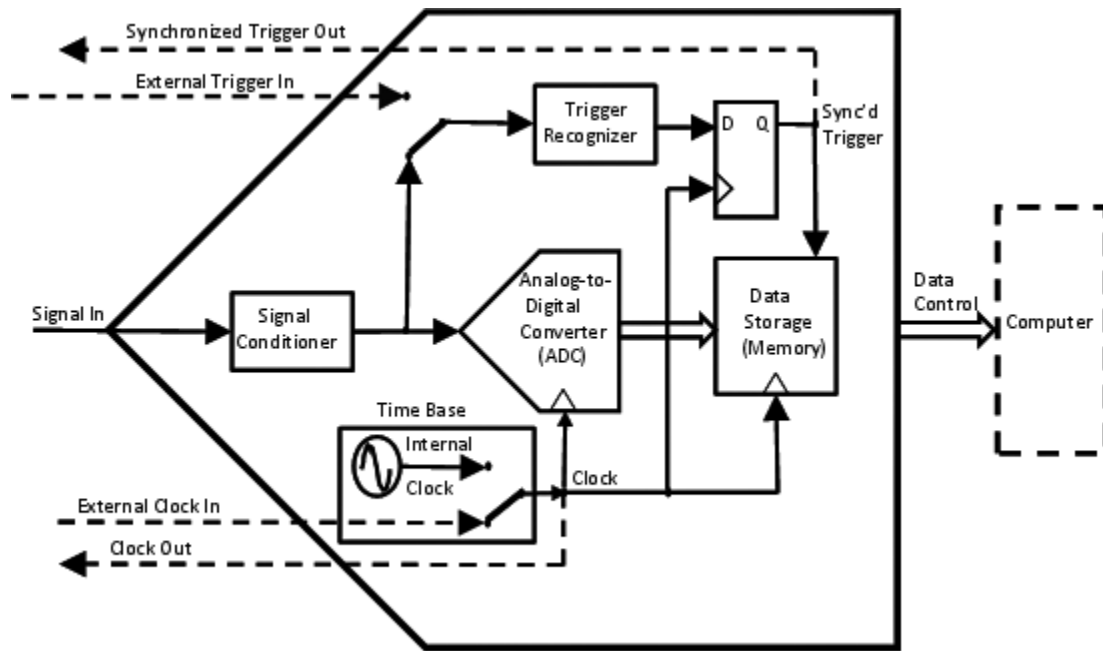


**Figure 4—Generic waveform recorder with features that facilitate testing**

It is assumed that the user/manufacturer has defined operating limits for the device under test. These limits are categorized as absolute (the limit beyond which the device will be destroyed) and operating (the limit beyond which the device will not operate properly). These limits will vary from device to device, depending on the design. It is not the intention of this document to describe the method of setting these limits, only to verify the operation within them. All test procedures described herein apply only to parameters of a device that is operated within its specified limits.

#### 4.3.7.1 General test setup for sine waves

Figure 5 shows the sine wave test setup. Sine waves are commonly used in waveform recorder testing because appropriate sine wave sources are readily available and because it is relatively easy to establish the quality of the sine wave (e.g., with a spectrum analyzer). A sine wave generator provides the test signal while a clock generator provides the clock (or conversion) signal. Also, combining the output of two (or three) sine wave generators can produce two-tone (or three-tone) test signals for intermodulation distortion testing. Additionally, a noise generator's output can be combined with a signal to provide low-level dither (Gray and Stockham [B20]).

If frequency synthesizers are used to generate the test and clock signals, the synthesizers can often be phase-locked to maintain precise phase relationships between the signal and the sampling clock. Phase-locking of synthesizers facilitates testing and simplifies subsequent digital signal processing, by preventing clock/signal walkthrough (beat patterns) that may artificially increase or reduce measured spurious output.

Both the clock and the test signals shall be suitable for the test being performed. Filters may be required in either the clock or signal paths to reduce noise or harmonic distortion. For example, sub-harmonics in the clock path will degrade waveform recorder performance, so the clock signal may require filtering to smooth edges that might otherwise feed through to the signal path. Also, low-pass or band-pass filters may be required in the signal path to eliminate noise or other undesirable signals (e.g., harmonics). The relative jitter between the clock and test signals shall be low enough to prevent jitter artifacts from affecting the measured noise floor as described in 8.5.7.

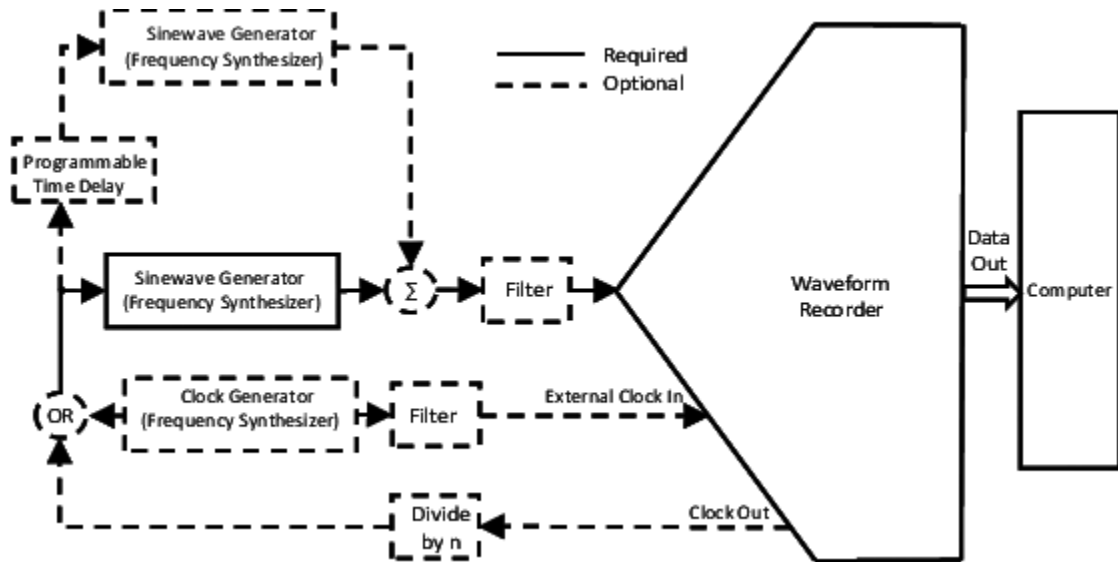


Figure 5—General sine wave test setup

#### 4.3.7.2 General test setup for arbitrary signal test

The arbitrary waveform test setup of Figure 6 can be used for arbitrary test signals, such as ramps, chirps, and steps. In this setup, the test signal is generated digitally and then converted to analog. Care shall be taken to quantify the performance of the arbitrary waveform generator and filter in order to assess (or remove) its impact on the measured performance of the waveform recorder under test. See 4.3.7.1 for comments on filters and data capture. If an arbitrary waveform generator instrument is not available, the function can be performed with local memory and a digital-to-analog converter (DAC).

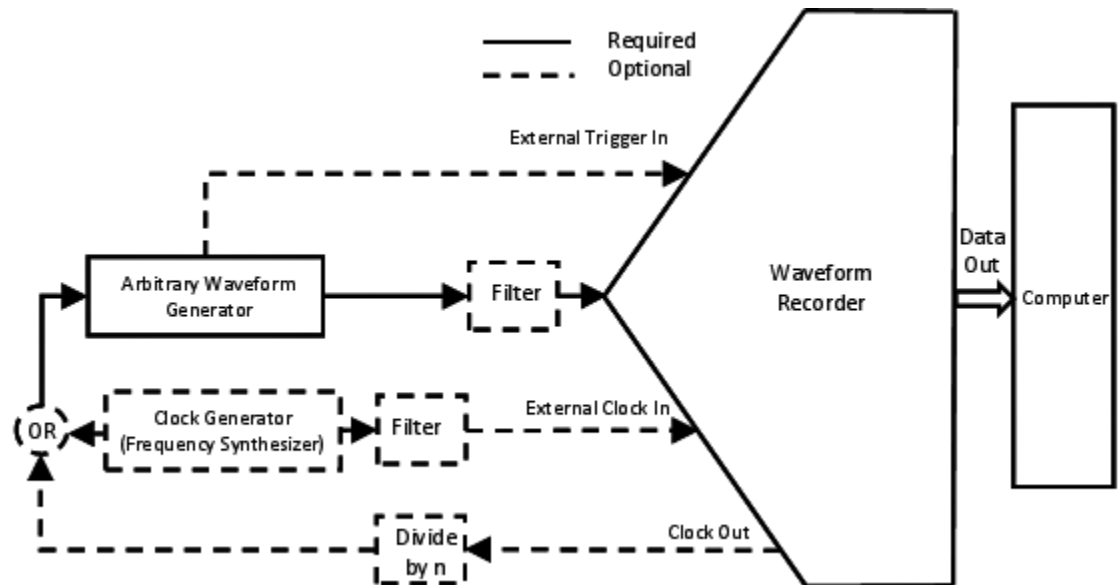


Figure 6—General setup for test using an arbitrary signal generator

#### 4.3.7.3 General test setup for pulses

Figure 7 shows a step waveform test setup to be used for testing with precision step signals that are not digitally generated. Precision pulses and step signals can be used to measure both time domain parameters (such as impulse response, transition duration, overshoot, and settling time) and frequency domain parameters (such as frequency response amplitude and phase, bandwidth, and gain flatness). Equivalent-time sampling can be employed, and certain data analysis tasks can be simplified, if the optional step repetition generator is phase locked to the sampling clock. See 4.3.7.1 for comments on data capture and on filters. Careful attention shall be paid to the phase linearity of any filters placed in the pulse/step signal path.

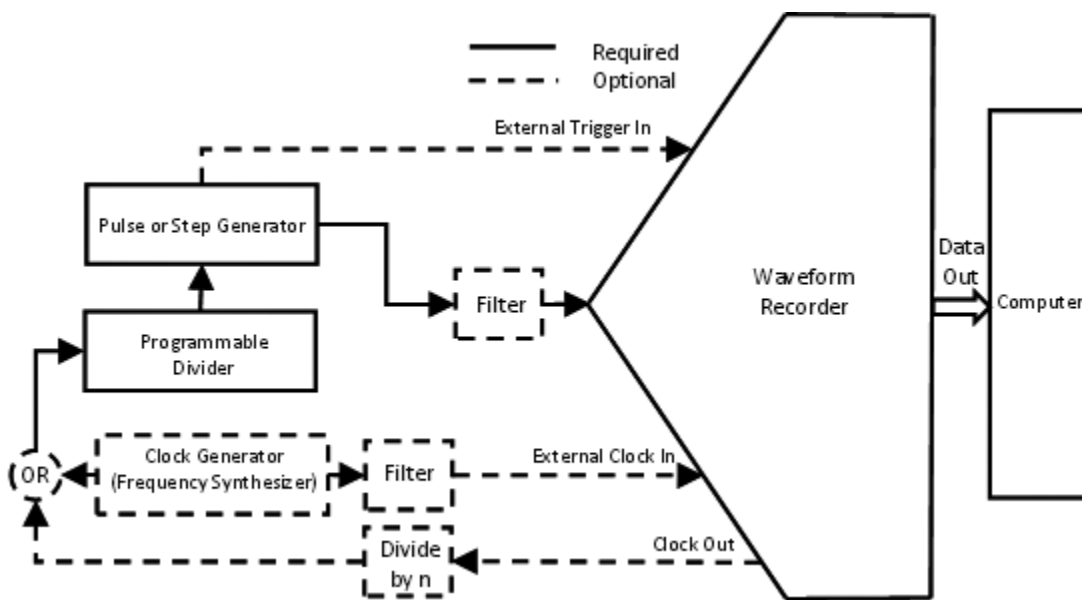


Figure 7—General setup for pulse and step signal testing

#### 4.4 Equivalent-time sampling

The sampling rate of a real-time recorder can limit the accuracy of the measurement of the recorder's bandwidth and step pulse parameters. If the sampling rate is not at least twice the frequency of the highest frequency component of the input signal, then aliasing errors can result. If the input signal is repetitive, these limitations can be reduced by equivalent-time sampling. Several methods of equivalent-time sampling exist. Two methods are described here. The first method consists of extracting equivalent-time samples from a single record using the recorder's internal time base, provided that the input signal's repetition rate is selected appropriately. The second method uses random equivalent-time sampling. These methods are needed only if the recorder does not internally support equivalent-time sampling.

##### 4.4.1 Test method for extracting data for single-record equivalent-time sampling method

If the input signal is repetitive, sampling rate limitations can be reduced by using the principle of equivalent-time sampling to effectively multiply the real-time sampling rate of the waveform recorder by an integer,  $D$ . By choosing the sampling rate of the input signal ( $f_s$ ) appropriately, at least  $D$  periods of the input waveform are recorded in a single record; then, upon rearranging the samples with a simple algorithm, a single repetition of the input signal is obtained that is effectively sampled at  $D$  times the real-time sampling rate. This is illustrated in Figure 8 for  $D = 5$ . The steps in implementing the method are given below and illustrated with an example in which the sampling frequency of the recorder is 1 MHz and the desired equivalent-time sampling rate is 5 MHz. The number of data points is kept small so the example can be easily illustrated in Figure 8.

This method is implemented via the following steps:

- Choose the integer,  $D$ , based on the requirement that  $D \geq f_{eq} / f_s$ , where  $f_s$  is the maximum sample rate of the recorder. In this example,  $D = 5$ .
- Choose  $M$ , the number of samples in the record.  $M = 20$  in this example.
- Using  $D$  and  $M$ , solve for  $L = \text{INT}(M/D)$ , the number of real-time samples taken during each repetition of the input waveform. In this example,  $L = 4$ .
- Determine the input sampling frequency using [Equation \(4\)](#).

$$f_i = f_s \frac{D}{LD-1} \quad (4)$$

In this example,  $f_i$  evaluates as 263.158 kHz. In [Figure 8](#), the horizontal axis for the upper plot can be interpreted as being in microseconds. The lower reconstructed plot can be interpreted as having units of 200 ns per sample.

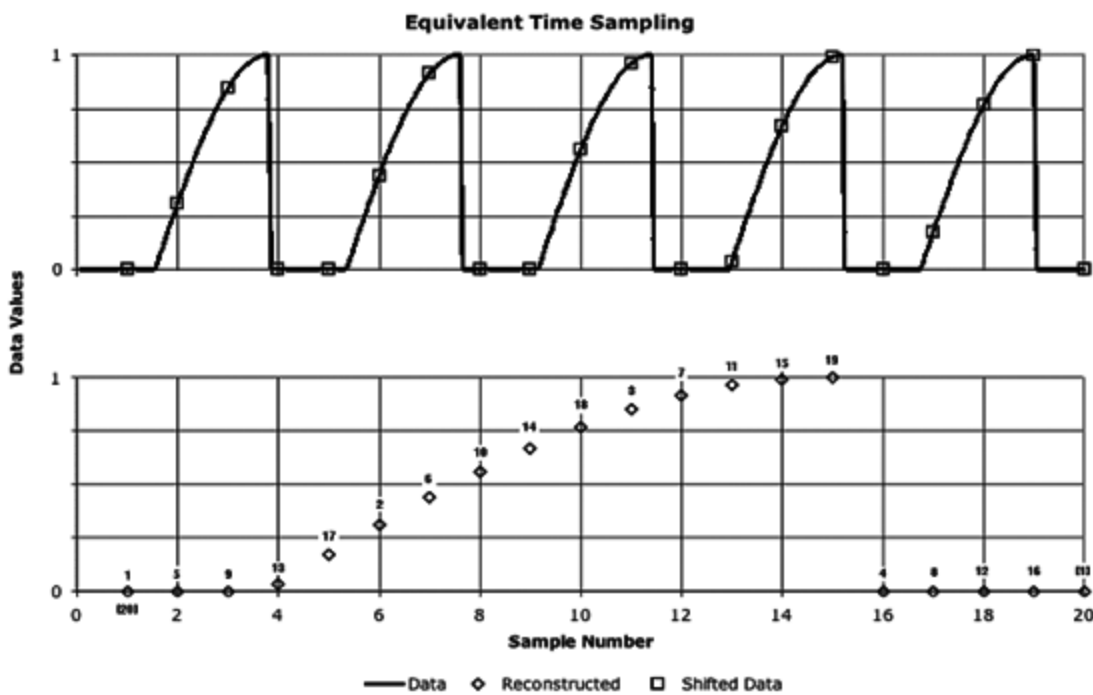


**Figure 8—Equivalent-time sampling extraction example**

The following pseudo-code program implements the algorithm to rearrange the samples in equivalent time:

```
for J = 1 to L*D
E(J) = R(1 + MOD(L*(J-1), L*(D-1)))
next J
```

where

$D$  is the sample rate multiplier (5 in the sample case)

$M$  is the record length (20 in the sample case)

|              |  |
|--------------|--|
| L            | is $\text{INT}(M/D)$ where $\text{INT}(\cdot)$ designates the integer part of $(\cdot)$ (4 in the sample case) |
| E( $\cdot$ ) | is the array containing $(L \times D)$ equivalent-time samples   |
| j            | is the equivalent-time sampling index  |
| R( $\cdot$ ) | is the array containing real-time samples  |
| MOD(A,B)     | is the remainder when A is divided by B  |

#### 4.4.2 Comments on the extraction method for single-record equivalent-time sampling

This method of achieving higher equivalent sampling rates requires that the repetition rate,  $f_i$ , of the input signal and the sample rate,  $f_s$ , be precisely controlled. While the average equivalent-time sample rate is just  $Df_s$ , independent of  $f_i$ , the relative spacing of the equivalent-time samples becomes nonuniform when  $f_i$  deviates from the value given by [Equation \(4\)](#). If  $f_i$  is too great,  $D-1$  out of  $D$  successive samples will occur too late, while one sample will be correctly placed; if  $f_i$  is too small,  $D-1$  samples will occur too soon. In either case, the maximum sampling time error,  $\varepsilon_{T_{eq}}$ , is given, to a good approximation, by [Equation \(5\)](#).

$$\varepsilon_{T_{eq}} \approx \frac{M(D-1)}{Df_s} \times \frac{\varepsilon_{tr}}{t_r} \quad (5)$$

where

|                          |   |
|--------------------------|---|
| $T_{eq}$                 | is the average equivalent-time sampling interval, i.e., $1/(Df_s)$      |
| $\varepsilon_{T_{eq}}$   | is the maximum sampling time error                                      |
| $\varepsilon_{tr} / t_r$ | is the proportional error in the repetition period (or repetition rate) |

Note, however, that the errors are not cumulative; the average equivalent-time sampling period is still given by  $1/(Df_s)$ .

The assumption is made in [Equation \(4\)](#) that  $f_s$  is exactly known. If it is not exactly known, then the additional error given by an expression similar to [Equation \(5\)](#) will occur. As an example, if  $D = 4$ ,  $M = 1024$ , and the equivalent sampling period is required to be known to 5%, then the repetition rate shall be set, and the sampling rate shall be known, each with an accuracy of  $0.05/(1024 \times 3) = 16$  ppm. To achieve such accuracy, it is usually necessary to use a frequency synthesized source. It is sometimes necessary to measure the frequency of the input signal as well as the frequency of the waveform recorder's internal clock with an accurate frequency counter to assure that they are set with sufficient accuracy. If sufficient accuracy cannot be attained for a specific record length, the accuracy can be improved by decreasing the record length. However, since the lowest frequency component that is represented in a record of length  $M$  is given by  $f_{eq}/M$ , the range of frequencies that can be represented is limited.

#### 4.4.3 Alternate extraction method for single record equivalent time sampling

Use the setup of [4.4.1](#) and the same parameters. Collect a record of length  $L^*M+1$  or larger. Use the following algorithm to extract the equivalent time samples:

```
for J = 1 to L*D
  E(J) = R(1 + (J-1)*L)
next J
```

All variables are the same as in [4.4.1](#).

#### 4.4.4 Comments on the alternate extraction method for equivalent time sampling

This extraction method requires the same precision in the setting of the ratio of  $f_i$  to  $f_s$  as the extraction method of [4.4.1](#), but the consequence of errors in this ratio is different. In the previous method an error in the frequency

ratio produced non-uniform sampling with the correct average equivalent-time sampling rate. An error in the frequency ratio in the method of 4.4.3 produces uniform equivalent time sampling that has an error in the sampling frequency given by [Equation \(6\)](#), as follows:

$$\frac{\delta f_{eq}}{f_{eq}} \cong M \frac{\delta(f_i/f_s)}{f_i/f_s} \quad (6)$$

where

|                   |                                     |
|-------------------|-------------------------------------|
| $\delta f_{eq}$   | is the error in $f_{eq}$            |
| $\delta(f_i/f_s)$ | is the error in the frequency ratio |

Also, when this extraction method is used,  $D$  is not restricted to being an integer.

#### 4.4.5 Test method for random equivalent-time sampling

The random equivalent-time sampling test method has the advantage of not requiring accurate control of the pulse repetition frequency. Instead, it requires taking many, typically 100 or more, records of data. Application of the method requires that the input signal, as recorded on the waveform recorder, have a level,  $v_0$ , with the property that the signal is increasing during a time interval  $T$  after crossing  $v_0$ , where  $T$  is the reciprocal of the sampling frequency. The method also requires that the input pulse occur at times that are random relative to the clock of the waveform recorder. With these conditions met, do the following:

- a) Collect  $K$  records of data  $x_k[i]$ , for  $k = 1\dots K$  and  $i = 1\dots M$ .
- b) Let  $i_0$  be the first index in each record for which the recorded signal value is equal to or greater than  $v_0$ . It is assumed that  $i_0$  is the same for each record. If it is not, the beginnings of some records shall be truncated to make it the same.
- c) Reorder the numbering of the records so that  $x_{k+1}[i_0] \geq x_k[i_0]$ . Because the signal is increasing in this interval, the records are now ordered in time.
- d) Construct a single record of length  $K \times M$  by taking the first point from each record (in the order of the records), followed by the second point of each record, then the third, and so on.
- e) Treat this larger record as if it had a sampling frequency of  $K \times f_s$ , where  $f_s$  is the sampling frequency of the individual records.

This approach eliminates the aliasing error and replaces it with a different error—the error due to the fact that the records are not truly uniformly distributed in time, but differ randomly from a uniform distribution. In [\[B12\]](#) Blair shows that the error in the calculated frequency response at any frequency is a random error with standard deviation,  $\sigma$ , given by [Equation \(7\)](#).

$$\sigma = \frac{1.1}{\sqrt{K}} e_{alias}(f) \quad (7)$$

where

|                |  |
|----------------|--|
| $e_{alias}(f)$ | is the aliasing error at frequency $f$ . Methods for estimating the aliasing error are given in <a href="#">10.3.2</a> |
|----------------|--|

## 4.5 Discrete Fourier transform (DFT)

The DFT is a mathematical operation that converts sampled data from the time domain to the frequency domain. (See Stearns and Hush [B41] or Oppenheim and Willsky [B35] for more information on the DFT.) In this standard, the DFT,  $X[k]$ , is defined as shown in [Equation \(8\)](#).

$$X[k] = \sum_{n=0}^{M-1} x[n] \exp(-j2\pi kn / M) \quad \text{for } 0 \leq k \leq M - 1 \quad (8)$$

where

- $x[n]$  is the samples in the data record
- $M$  is the number of samples in the data record

The inverse discrete Fourier transform (IDFT) is the mathematical operation that converts sampled data from the frequency domain to the time domain. The formula is shown in [Equation \(9\)](#).

$$x[n] = \frac{1}{M} \sum_{k=0}^{M-1} X[k] \exp(+j2\pi kn / M) \quad (9)$$

Note that in this standard, the IDFT includes the requisite  $(1/M)$  normalization. Other definitions of a DFT can use other normalization factors.

The frequency corresponding to  $X[k], f_k$ , is shown in [Equation \(10\)](#).

$$\begin{aligned} f_k &= \frac{k}{M} f_s && \text{for } 0 \leq k \leq M / 2 \\ f_k &= -\left(1 - \frac{k}{M}\right) f_s && \text{for } M / 2 + 1 \leq k \leq M - 1 \end{aligned} \quad (10)$$

where

- $f_k$  is the frequency corresponding to the  $k^{\text{th}}$  DFT component
- $f_s$  is the sampling frequency

Note that the second half of the frequency components can be interpreted as negative frequencies, and for real signals their transform values are the complex conjugates of the values for the corresponding positive frequencies. Sometimes, to simplify mathematical expressions (such as the modulo function), the upper formula will be used for all  $k$ , mapping the negative frequencies to frequencies between the Nyquist frequency and twice the Nyquist frequency. The frequencies are separated by an interval of  $\Delta f = f_s / M$ . The interval of frequencies from  $f_k - \Delta f / 2$  to  $f_k + \Delta f / 2$  is called the  $k^{\text{th}}$  frequency bin. Associated with any frequency,  $f$ , is the bin number,  $f / \Delta f$ . If  $f$  is at the center of the  $k^{\text{th}}$  frequency bin, the bin number will be the integer,  $k$ . Noninteger values of the bin number correspond to frequencies that are not at the center of a bin.

$X[f_k]$  may be written in place of  $X[k]$  to make the frequency dependence more obvious.

Example DFT plots are shown in [Figure 9](#) and [Figure 10](#). Both show the DFT of a signal sampled at 100 samples per second. The Nyquist frequency is 50 samples per second. The signal is a 21 Hz sine wave with amplitude 1, a 2nd harmonic distortion with amplitude 0.5, and a 3rd harmonic distortion with amplitude 0.25. [Figure 9](#) shows the DFT spectrum using positive and negative frequencies. All signals are symmetrical and have the same magnitude for positive and negative frequencies. The 3rd harmonic, which is at 63 Hz, is aliased down to 37 Hz. [Figure 10](#) shows the negative frequencies mapped up to the frequencies between the Nyquist frequency and twice the Nyquist frequency. They are moved to the right 100 frequency units (the sampling frequency). Note that one of the 3rd harmonic terms is at the correct frequency of 63 Hz. However, the other

frequencies that are mapped for the negative side are at locations that are not very intuitive. [Figure 9](#) gives a better visual picture, while [Figure 10](#) is often more convenient in mathematical calculations, specifically in the tracking of frequencies that are above the Nyquist frequency.

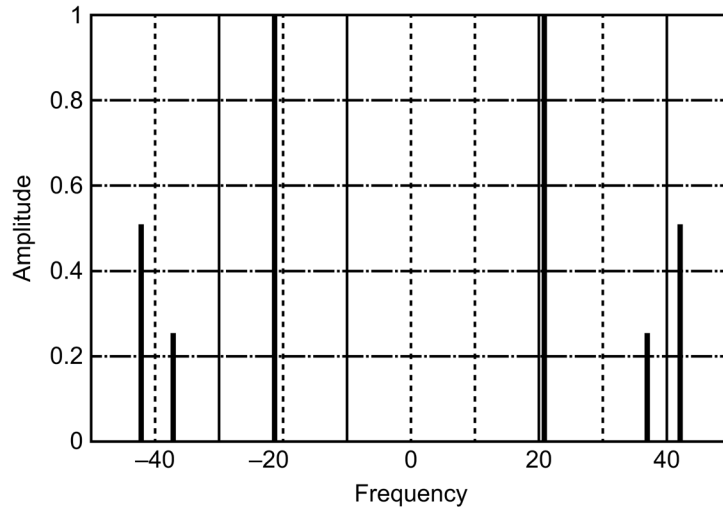


**Figure 9—Example DFT spectrum using positive and negative frequencies**

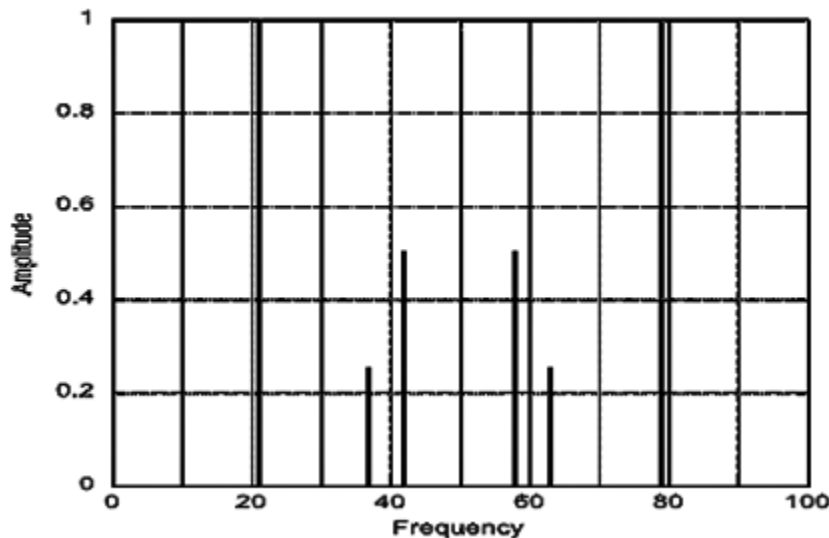


**Figure 10—Example DFT showing the negative frequencies mapped up to the frequencies between the Nyquist frequency and twice the Nyquist frequency**

The “energies” in the time and frequency representations of the data are related by the Parseval relation shown in [Equation \(11\)](#).

$$\sum_{n=0}^{M-1} |x[n]|^2 = \frac{1}{M} \sum_{k=0}^{M-1} |X[k]|^2 \quad (11)$$

#### 4.5.1 Aliasing

Aliasing is the phenomenon in sampled data systems whereby signal components at input frequencies greater than half the sampling frequency are converted to frequencies at less than half the sampling frequency in the output data record (see Stearns and Hush [B41] or Oppenheim and Willsky [B35]).

Frequency aliasing is a phenomenon that can best be understood using the plot shown in [Figure 11](#).

The horizontal axis represents the frequency being applied to the recorder. In the region of input frequencies that are less than half the sample frequency ( $f/f_s < 0.5$ ), there is an exact correspondence between the frequencies identified by the DFT and the applied frequency. When the input frequency is greater than half the sampling frequency (the Nyquist frequency), the DFT moves the frequency to a frequency that is less than the Nyquist frequency. The value of the aliased frequency can be obtained either from [Figure 11](#) or from mathematics that implement the results shown in [Figure 11](#). Note that both the positive and the negative frequencies are generated by the DFT used in this standard, but for the sake of clarity, only the positive frequencies are shown in [Figure 11](#).

The advantage of the DFT display shown in [Figure 12](#) is apparent when it is noted that the mathematics described by [Figure 11](#) become trivial when the function  $\text{mod}(f/f_s, 1)$  is used to determine the location of the DFT frequencies that are shown in [Figure 11](#).

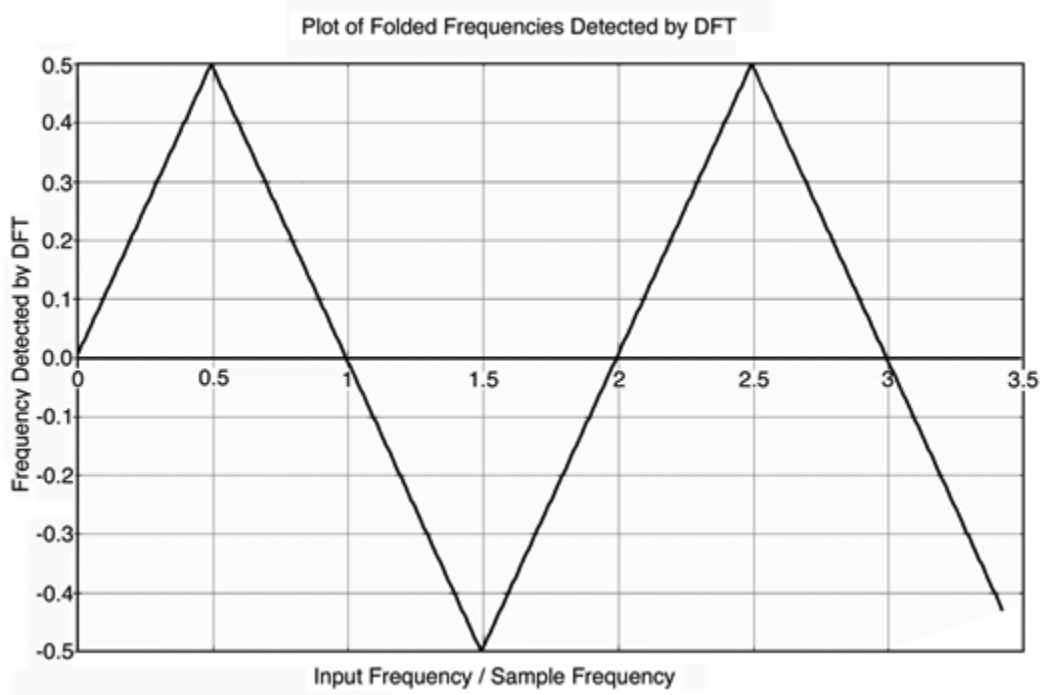


**Figure 11—Plot of DFT detected frequencies versus input frequency for a waveform recorder**

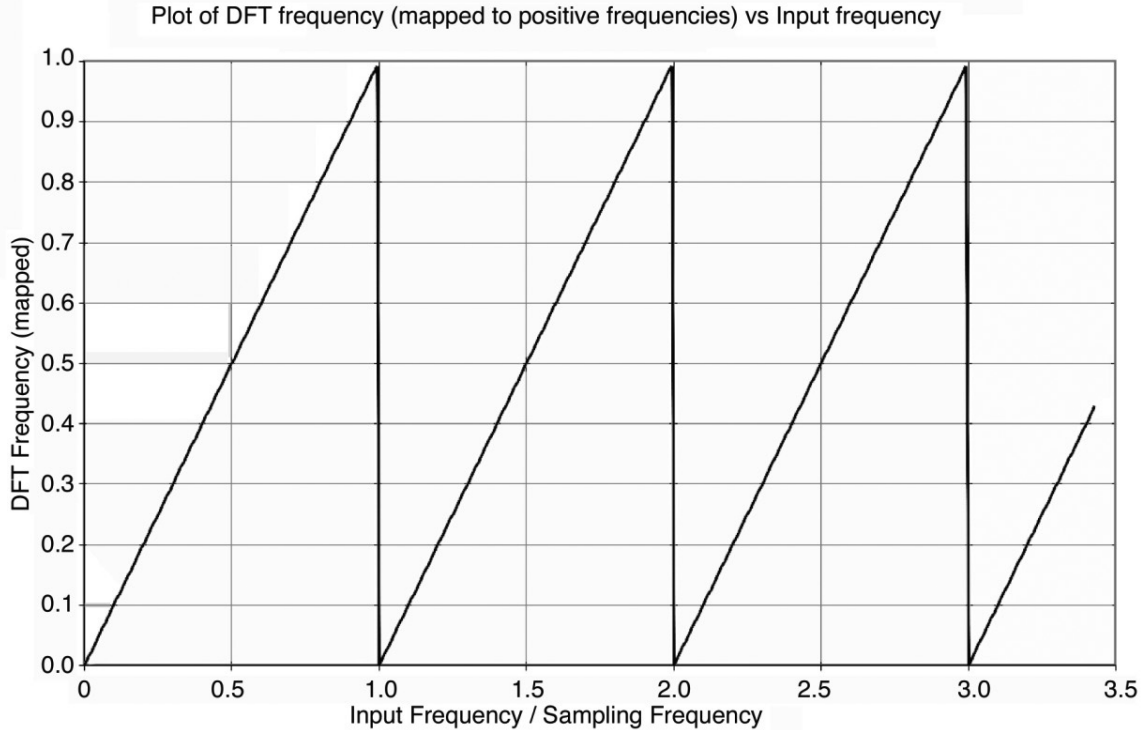


**Figure 12—Plot showing how negative DFT frequencies are mapped up to the frequencies between the Nyquist frequency and twice the Nyquist frequency**

#### 4.5.2 Windowed DFT and spectral leakage

A windowed DFT is defined in [Equation \(12\)](#). The window factors,  $w[n]$ , are near one at the center of the data interval and approach zero at the ends of the interval.

$$X_w[k] = \sum_{n=0}^{M-1} w[n]x[n]\exp(-j2\pi nk / M) \quad (12)$$

Windowing is multiplication in the time domain and corresponds to convolution in the frequency domain. Some authors refer to the function  $w[n]$  as the temporal weighting function and its Fourier transform,  $W[k]$ , as the window function; whereas some refer to  $w[n]$  as the window function. When all the window factors are one, i.e., no windowing, the window is called the rectangular window. This rectangular window is also called nonweighting. Window functions other than the rectangular are used to reduce the effects of spectral leakage, which is described in [4.5.2.1](#).

##### 4.5.2.1 Spectral leakage

The rectangular-windowed DFT of a sinusoid with a frequency at the center of a DFT bin produces a single spectral line. If the frequency of the sinusoid is not at the center of a bin, the DFT will produce lines in all frequency bins (see Stearns and Hush [\[B41\]](#) or Oppenheim and Willsky [\[B35\]](#)). The leakage is described by the continuous-time Fourier transform,  $W[f]$ , of the window function. Two examples are shown in [Figure 13](#).

The dashed line is the Hann window (defined in [4.5.2.3](#)), and the solid line is the rectangular window. The horizontal axis is the frequency converted to DFT bin number, and the vertical axis is  $W[f]$  expressed in decibels. Since  $W[-f] = W[f]$ , the data are not shown for negative values. If the signal being analyzed is a

sinusoid with amplitude  $A$  and frequency with a bin number of  $x$  (not necessarily an integer), the  $k^{\text{th}}$  spectral line will have an amplitude of  $A \times W[k-x]$ .

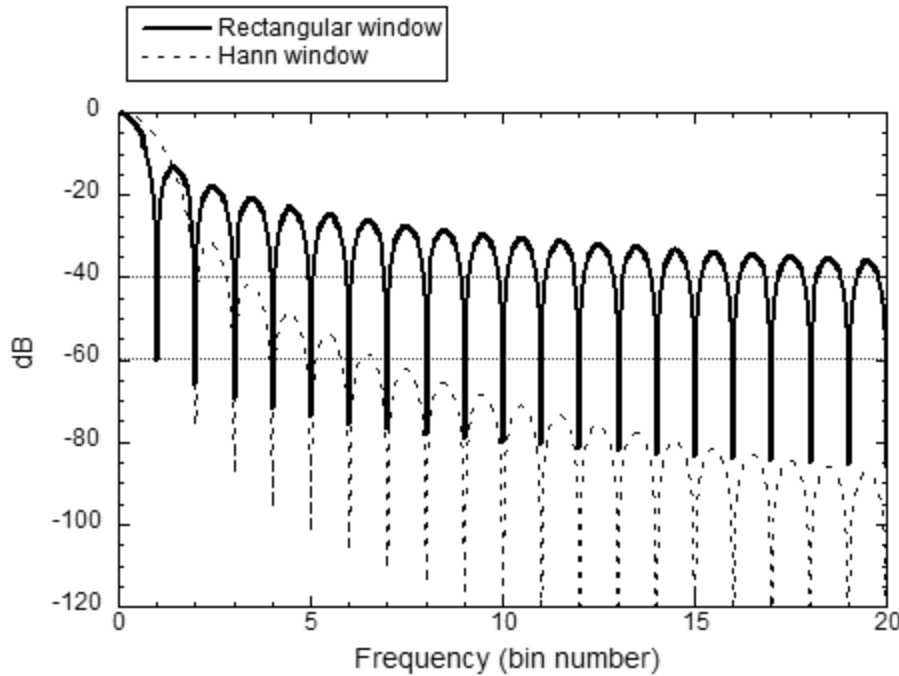


**Figure 13—Fourier transform of the Hann and the rectangular windows**

The negative spikes in the plot are where the function is zero. For the rectangular window, the function is zero at all integers except zero, while the function for the Hann window is zero at all integers except zero and  $\pm 1$ . Thus, for a coherently sampled sinusoid (one with an integer bin number), the rectangular window will produce a single line, while the Hann window will produce three lines. However, for incoherent sampling, both windows produce lines at all frequencies. The amplitudes of the lines fall off much more slowly for the rectangular window than for the Hann window.

Figure 14 shows the same information for the Hann window (dashed line) and the Blackman window (solid line; also defined in 4.5.2.3). Note that the difference is much smaller than the difference between the rectangular and Hann windows. This example illustrates that once the user chooses to use a good window other than the rectangular, it is often not critical which one is chosen.

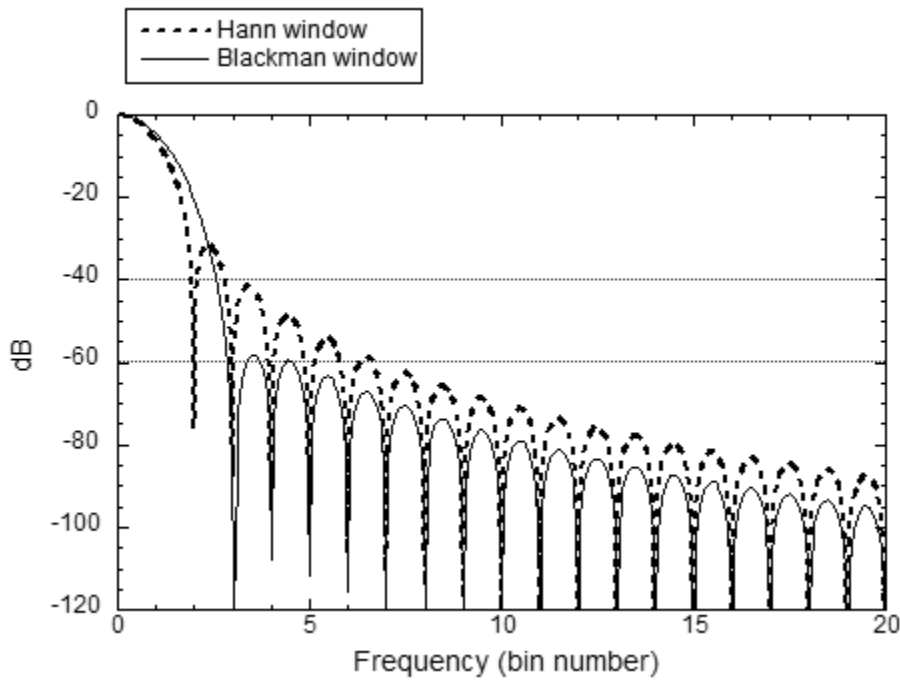


**Figure 14—Fourier transform of the Hann and the Blackman windows**

#### 4.5.2.2 Coherent-sampling and sine fitting methods of reducing spectral leakage

There are several methods of dealing with spectral leakage other than the judicious choice of windows. The basic problem is that the energy of some large sinusoidal components of the signal leaks into spectral bins that have smaller components that need to be identified. This problem is often solved simply by choosing a sufficiently long record length. As seen from [Figure 13](#) and [Figure 14](#), the simplest windows (Hann and Blackman) are both down by more than 87 dB at an offset of 20 frequency bins. As the record becomes longer, the frequency deviation corresponding to 20 frequency bins becomes smaller. For example, with a record length of 4096, 20 frequency bins is less than 1% of the Nyquist frequency.

Coherent sampling, in which the bin number of the applied signal is an exact integer, is the usually the best approach for dealing with spectral leakage. It eliminates the leakage problem completely if exact coherence is obtained. Also, the recommended frequencies given elsewhere in this standard for best achieving other ends typically result in coherent sampling. However, sometimes the accuracy and/or precision of the frequency setting of available oscillators does not allow for coherent sampling.

Sine fitting is another approach to reduce leakage problems. Use the four-parameter sine-fitting algorithm described in [4.6](#) to determine the frequency, amplitude, and phase of large incoherent sinusoidal components of the data record. Then subtract these components from the data record, and perform the DFT on the result. This approach typically reduces leakage problems by 30 dB to 50 dB. The user can also first truncate the record to a length containing approximately an integer number of periods.

#### 4.5.2.3 Useful windows and their characteristics

The only window parameter used in this standard is the normalized noise power gain (NNPG), which is given by [Equation \(13\)](#).

$$\text{NNPG} = \frac{1}{M} \sum_{n=0}^{M-1} w[n]^2 \quad (13)$$

where

- $w[n]$  is the window coefficients
- $M$  is the number of samples in the data record

The  $NNPG$  is a conversion factor that gives a Parseval-like relationship for the windowed DFT in [Equation \(14\)](#).

$$\frac{1}{M} \sum_{n=0}^{M-1} x[n]^2 = \frac{1}{M \times NNPG} \sum_{k=0}^{M-1} X_w[k]^2 \quad (14)$$

where

- $X_w[i]$  is the Fourier transform of a windowed input sequence  $w[i]x[i]$

The value of  $NNPG$  is 1 for the rectangular window and is less than 1 for all other windows.

Useful windows and their characteristics are described by Harris [\[B22\]](#) and Nuttall [\[B34\]](#). These windows are of the form shown in [Equation \(15\)](#).

$$w[n] = \sum_{l=0}^L a_l (-1)^l \cos(2\pi nl / M) \quad (15)$$

where

- $a_l$  is the  $l^{\text{th}}$  coefficient used to define the window function (the sum of the coefficients equals 1)
- $L$  is the order, or number, of coefficients in the window

These windows are commonly used and are discussed at length by Nuttall [\[B34\]](#). Any window of this form is referred to as a cosine window of order  $L$ .

For these windows, the coefficients of the DFT of the window function are proportional to the coefficients multiplying the cosine terms. There is one nonzero coefficient at zero frequency,  $L$  nonzero coefficients at positive frequencies, and  $L$  nonzero coefficients at negative frequencies. Therefore, a coherently sampled sine wave produces  $L$  lines on each side of the central bin.

From [Equation \(14\)](#), the Parseval relation, and the fact that the  $a_i$  are the Fourier coefficients of the window function, [Equation \(16\)](#) can be derived, as follows:

$$\text{NNPG} \cong a_0^2 + \frac{1}{2} \sum_{l=1}^L a_l^2 \quad (16)$$

The windows shown earlier are described in [Table 2](#).

**Table 2—Properties of various data windows**

| Name        | <i>L</i> | NNPG  | <i>a</i> <sub>0</sub> | <i>a</i> <sub>1</sub> | <i>a</i> <sub>2</sub> |
|-------------|----------|-------|-----------------------|-----------------------|-----------------------|
| Rectangular | 0        | 1     | 1                     | 0                     | 0                     |
| Hann        | 1        | 0.625 | 0.5                   | 0.5                   | 0                     |
| Blackman    | 2        | 0.305 | 0.42                  | 0.5                   | 0.08                  |

#### 4.5.2.4 Choosing a window

The spectral leakage from a large sinusoidal component can interfere with another feature a user wishes to measure. The magnitude of the problem is determined by inspection of the Fourier transform of the window sequence, as described earlier, and depends on the size of the interfering component(s) and their distance from the desired smaller components. If the chosen window causes an interference that is too large, the user shall either choose a window that is sufficiently small at the location that is important for the particular problem or use one of the other methods for ameliorating spectral leakage.

#### 4.5.3 The DFT and a spectrum analyzer display

There is a direct relationship between the DFT of a waveform and the kind of display that is generated by a spectrum analyzer. There are also confusing differences between the two. Some of the differences are described as follows:

- Some spectrum analyzers display only positive frequencies, not negative frequencies.
- The amplitudes of the spectral components displayed on a spectrum analyzer are real, not complex. The amplitudes reflect the root mean square (rms) of the signal being measured and can be displayed in decibels.
- The horizontal axis of a spectrum analyzer is frequency, not bins.
- A spectrum analyzer is not directly affected by leakage.

Consider the spectrum shown in [Figure 9](#), the spectrum of a 21 Hz sine wave sampled at 100 samples per second. A data record is collected that contains the appropriate number of points to sample an integer number of cycles. The smallest numbers of points that can be collected are 100, which generates exactly 21 cycles of the sine wave. In order to produce the results shown in [Figure 9](#), the amplitude of the fundamental 21 Hz signal is  $\sqrt{2}/50$ , or 0.02 rms. A plot of the data record is shown in [Figure 15](#). For the sake of clarity, the phases of the example are set so that the DFT results are all real.

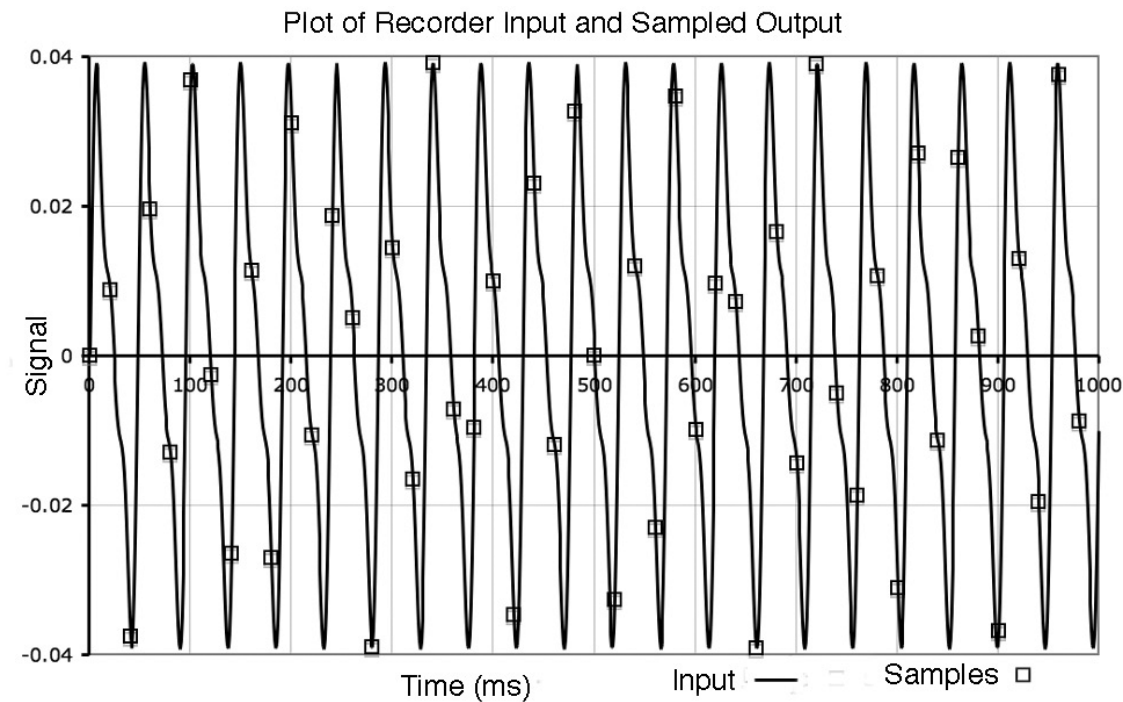


**Figure 15—Plot of signals and samples that generate the spectrum shown in Figure 9**

A spectrum analyzer that monitored the signal shown in [Figure 15](#) would produce a display similar to that shown in [Figure 16](#).

Note that the frequencies used are not compatible with most spectrum analyzers because of the large amount of time required to display low-frequency data. The results would be the same if the signal were a 21 MHz signal sampled at 100 MHz.

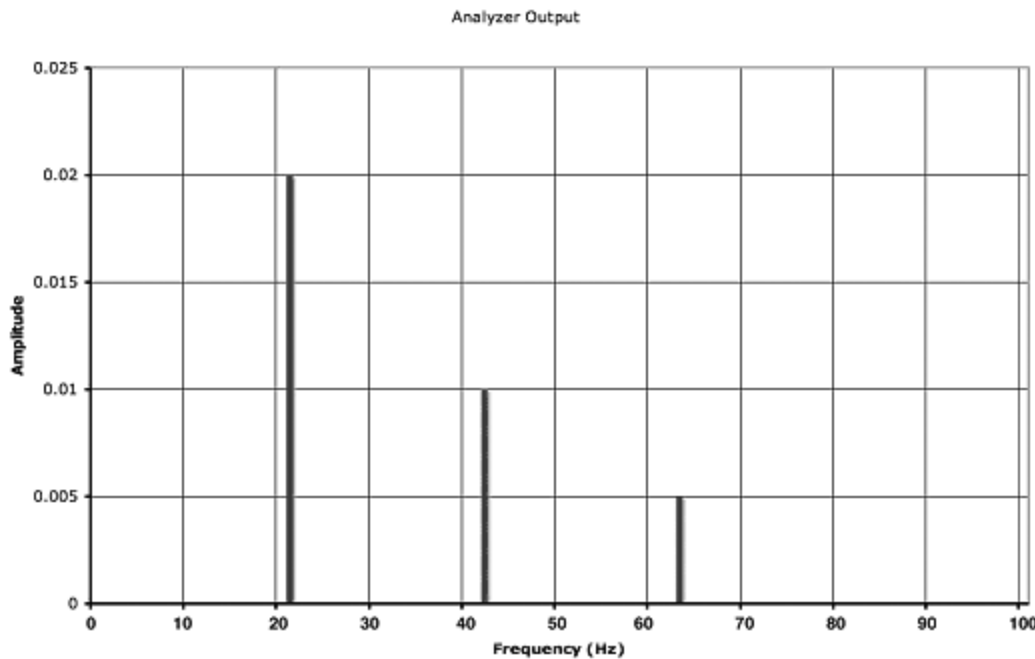


**Figure 16—Spectrum analyzer display of signal with DFT results shown in Figure 9**

Note that Parseval's relation holds. The sum of the squares of the sampled signal data as shown in Figure 15 is 0.02625. The sum of the squares of the spectral components shown in Figure 9 are  $(1 + 1 + 0.25 + 0.25 + 0.0625 + 0.0625) / 100 = 0.02625$ .

## 4.6 Sine wave testing and fitting

### 4.6.1 Sine waves as test signals

There are a number of tests that use sine waves as input signals, and there are often questions about why sine waves are used to test instruments that are often intended to record transients. The primary reason is that very accurate sine wave signals can be produced, and the accuracy of the signals can be readily tested with a spectrum analyzer. Another reason for the usefulness of sine waves as test signals is that they are eigenfunctions for linear time invariant (LTI) systems. In other words, when a pure sine wave is supplied to the input of an LTI system, the output is a pure sine wave of the same frequency but with altered amplitude and phase. Because the analysis of the test results usually assumes that both the amplitude and phase are unknown, the LTI system distortion is ignored. The test results give the nonlinear and time varying errors.

### 4.6.2 Curve fitting test method

Apply a sine wave signal with appropriate amplitude, frequency, and spectral purity to the input of the recorder. Trigger the recorder to collect a record of data. The trigger does not have to be synchronized to the signal. For the four-parameter method, calculate the values of  $A_0$ ,  $B_0$ ,  $C_0$ , and  $f_0$  that give the best fit, in the least squares sense, to the recorded signal to a function of the form as shown in Equation (17).

$$x[n] = A_0 \cos(2\pi f_0 t_n) + B_0 \sin(2\pi f_0 t_n) + C_0 \quad (17)$$

where

$t_n$  nominal time associated with the  $n^{\text{th}}$  data value

For the three-parameter fit, the known frequency is substituted for the parameter  $f_0$ . Subtract the fitted signal from the recorded signal to obtain the residuals. There are many algorithms for performing the least squares curve fits above. [Annex A](#) describes methods for both the three- and four-parameter fit.

The sine wave curve fit is used in several specific test methods described later in this standard. Analyze the residuals and fit parameters using methods described for the specific test being performed.

The amplitude and phase form of the fitted signal can be computed from [Equation \(18\)](#), as follows:

$$A_0 \cos(2\pi f_0 t_n) + B_0 \sin(2\pi f_0 t_n) = A_0 \cos(2\pi f_0 t_n + \Phi) \quad (18)$$

where

$$\begin{aligned} A &\text{ is } \sqrt{A_0^2 + B_0^2} \\ \Phi &\text{ is } -\text{ArcTan}(B_0, A_0) \end{aligned}$$

The ArcTan is the standard inverse tangent of two arguments, called ATAN2 in many programming languages, and returns a value in the range from 0 to  $2\pi$  or in the range from  $-\pi$  to  $\pi$ .

#### 4.6.3 Three-parameter versus four-parameter fit

The recommended method is the four-parameter method with a record containing at least five cycles of the signal. Even if the input frequency is accurately known a priori, the four-parameter method usually determines it to even better accuracy. The computations are more complicated with the four-parameter method. Software for carrying out these computations is available ([Annex E](#)). For records containing less than five cycles, the four-parameter method can underestimate harmonic distortion by compensating for it with a change in frequency. In this case, the three-parameter method may be more appropriate. When frequencies are chosen precisely as recommended for coherent sampling, with an exact integer number of cycles in a record, a DFT will give the same results as a three-parameter sine wave fit.

Algorithms for both the three-parameter and the four-parameter fits are given in [Annex A](#).

#### 4.6.4 Choice of frequencies and record length

Typically waveform recorders are tested at several different frequencies. There are several factors that enter into the selection of frequencies. These factors affect frequency selection on three different scales: fine, medium, and coarse. Although the frequency selection decisions are made in the order of coarse, medium, and then fine, the criteria are described here in the reverse order.

##### 4.6.4.1 Fine-scale frequency selection

On the fine scale, a user wants to select a frequency for which the sampled values will all be different. For example, if a frequency of 200 kHz was used to test a recorder with a sampling rate of 1 MHz, the same five different phases of the sine wave would be sampled many times. The recommended approach is to use a record length,  $M$ , and a frequency,  $f_i$ , so that  $M$  uniformly distributed phases will be sampled. This is easily accomplished by choosing  $f_i$  as shown in [Equation \(19\)](#).

$$f_i = \frac{J}{M} f \quad (19)$$

where

- $J$  is an integer that is relatively prime to  $M$
- $f_i$  is the sampling frequency
- $M$  is the record length

The condition of being relatively prime means that  $M$  and  $J$  have no common factors, i.e., their greatest common divisor is one. For the recommended frequency, there are exactly  $J$  cycles in a record (called *coherent sampling* in this standard). If  $M$  is a power of two, then any odd value for  $J$  meets the relatively prime condition.

If the signal frequency meets the above conditions exactly, the maximum phase difference between successive sampled phases will be  $2\pi/M$ . The accuracy required of the signal frequency depends strongly on the frequency and on whether the frequency deviation is in the positive or negative direction from the nominal value.

For any value of  $J$ , relatively prime to  $M$ , there is a unique value,  $I$ , between 0 and  $M-1$ , which satisfies  $\text{mod}(IJ, M) = 1$ . The number  $I$  is the multiplicative inverse (modulo  $M$ ) of  $J$ , and its value determines the frequency accuracy required.

For an exact input frequency, the maximum difference between successive sampled phases is  $2\pi/M$ . If the frequency does not have the exact value specified in [Equation \(19\)](#), the maximum phase difference will be larger. If the larger value is written in the form  $(1 + \rho) \times (2\pi/M)$ , the error  $\varepsilon_f$  in the frequency shall satisfy [Equation \(20\)](#).

$$\begin{aligned} \left| \frac{\varepsilon_f}{f_i} \right| &\leq \frac{\rho f_i}{IMf_i} && \text{for } \varepsilon_f > 0 \\ \left| \frac{\varepsilon_f}{f_i} \right| &\leq \frac{\rho f_i}{(M-I)IMf_i} && \text{for } \varepsilon_f < 0 \end{aligned} \quad (20)$$

where

- $\varepsilon_f$  is the error in input frequency
- $\rho$   $(1 + \rho)$  is the error limit factor between successively sampled phases as defined above
- $f_i$  is the input frequency
- $I$  is chosen so that  $\text{mod}(IJ, M) = 1$
- $M$  is the record length

For positive frequency deviations,  $I$  shall be as small as possible; for negative frequency deviations,  $I$  shall be as large as possible (the maximum value is  $M - 1$ ). In [\[B16\]](#), Blair provides tables that give values of  $J$  corresponding to small values of  $I$  and small values of  $M - I$  for all power-of-two record lengths between  $2^8$  and  $2^{20}$ . A user can choose a frequency from these tables that is close to the desired frequency and determine the accuracy requirement and required direction of deviation from information in the table. If the tables do not contain values of  $J$  with acceptable frequencies, the user can compute the value for  $I$  for an interval of acceptable values of  $J$  and select the value with the smallest values of  $I$  or  $M - I$ . The actual deviation of the frequency from the ideal value can be determined from the sine wave fitting result.

For a recorder with  $N$  bits of resolution and an ideal transfer characteristic, the minimum record size that will produce a representative sample in every code bin (in the absence of random noise) is  $2^N \times \pi$ , when the input frequency is chosen as above. The smallest power-of-two record length is  $4 \times 2^N$ . To achieve one sample in each code bin with this slightly longer record length, the user can let  $1 + \rho = 2\rho/4$ , or  $\rho = 0.57$ .

At low frequency, the accuracy requirement becomes much less stringent. However, if a four-parameter fit is being used, the frequency shall be chosen large enough so that there are at least five cycles in the record. Otherwise, errors can be underestimated.

#### **4.6.4.2 Medium-scale frequency selection**

The rules for fine-scale frequency selection give many frequencies that optimize the spacing between the samples recorded. On the medium scale, a user selects frequencies to cause errors from different sources to occur at different frequencies. For example, for a recorder with a sampling rate of 2 GSa/s, if a frequency of 400 MHz were selected, 3rd harmonic distortion would be at a frequency of 1200 MHz. Because this is above the Nyquist frequency of 1000 MHz, it would be aliased down to 800 MHz. This is the same frequency as 2nd harmonic distortion; therefore, the two would be indistinguishable. With a frequency of 420 MHz, the 2nd harmonic is at 840 MHz while the 3rd harmonic aliases down to 760 MHz, allowing the user to distinguish between the two.

If the recorder uses interleaving, i.e., multiple recorders at lower sampling rates, the user shall check and verify that interleaving errors do not occur at the same frequencies as harmonic distortion. Interleaving errors occur at frequencies that are sums and differences of the base sampling frequency and multiples of the signal frequency. For example, for a 2 GSa/s recorder that interleaves two 1 GSa/s recorders, the base sampling frequency is 1 GSa/s. An input signal of 250 MHz would induce an interleaving error at 750 MHz, the difference between the base sampling frequency and the signal frequency. This is the same frequency as the 3rd harmonic, so the two would be indistinguishable.

In the coarse-scale frequency selection, a user normally selects nice round numbers (e.g., 250 MHz, 500 MHz). These round numbers then have to be modified to separate the errors from different harmonics and from interleaving. It is important to take aliasing into account in this step. The resulting frequencies shall then be modified a second time to meet the criteria for fine-scale frequency selection.

#### **4.6.4.3 Coarse-scale frequency selection**

Select several test frequencies spanning the range of major expected frequency components in the final-use input signal. It is important that the highest frequency signal have at least as large of a maximum slew rate (derivative with respect to time) as the maximum slew rate of final-use input signal.

The test frequencies can be categorized as low, medium, and high. Low frequencies are low enough to not cause significant dynamic errors (e.g., frequency dependent distortion and time jitter) in the waveform recorder. Frequencies less than a few percent of the analog bandwidth are generally safe to consider low. Medium frequencies are those high enough to cause some dynamic effects, but still well below the analog bandwidth. These will generally be in the range of 10% to 30% of the analog bandwidth. High frequencies are near enough to the analog bandwidth that the amplitude roll-off is a significant factor. The test frequencies shall include at least one frequency in each category.

#### **4.6.4.4 Special considerations with very long record length**

It is sometimes necessary to test a recorder with a record length much longer than that for which the frequency accuracy condition in [Equation \(20\)](#) can be met. This is the case when a user wants to quantify errors that can be detected only with very long record lengths, e.g., drift and clock phase noise. In this case, the frequency selection shall be based on a shorter base record length. The long record length shall then be selected as an integer multiple of the base record length.

### **4.6.5 Selecting signal amplitudes**

One signal amplitude of between 90% of full scale and 100% of full scale shall be used for each frequency. This signal is referred to in this standard as a large amplitude signal. This amplitude is the amplitude of the signal at the input of the recorder. The frequency response of the recorder can substantially change the recorded amplitude. For example, if a 90% of full-scale signal is supplied at the -3 dB bandwidth of the recorder, the recorded signal will have an amplitude of only 63% of full scale. This result is acceptable. If the recorder has a gain of greater than 110% at a test frequency, a 90% of full-scale signal will saturate the waveform recorder.

This situation can require reducing the amplitude of the test signal. If the signal is reduced, this fact shall be reported in the test results.

It is useful to also record a lower amplitude signal at each frequency. If the lower amplitude signal is obtained by leaving the oscillator amplitude unchanged and adding an attenuator, the test results can distinguish between distortion and noise in the oscillator and distortion and noise in the recorder. Typical values for the attenuator are between 6 dB and 12 dB.

#### **4.6.6 Presenting sine wave test data**

There are three common ways of presenting the results of sine wave test data for visual analysis. Particular calculations on the test data are given at various other places in this standard. Examples of these presentations with interpretations are in [Annex G](#). The three presentations are as follows:

- Power spectrum of the residuals (see Blair [[B12](#)])
- Modulo time ( $2\pi$ ) plot of the residuals versus phase angle (see Irons and Hummel [[B25](#)])
- Plot of the residuals versus time

#### **4.6.7 Impurities of sine wave sources**

A number of tests in this standard use sine wave sources, and the analyses of the test results assume that the signal is a pure sine wave. This subclause describes how the impurities of a sine wave are quantified, how they are measured, and how users can control them.

The impurities in a sine wave are described as follows:

- Harmonic distortion
- Spurious components
- Wide-band noise
- Amplitude modulation
- Phase modulation

Harmonic distortion is the presence of sinusoidal signals at frequencies that are integer multiples of the signal frequency. If the signal is periodic at the nominal frequency but its shape is not pure sinusoidal, it will have harmonic distortion. Harmonic distortion is typically specified in decibels relative to the carrier (the signal at the desired frequency). Therefore, if the harmonic distortion is  $-30$  dBc, it is about 3% of the signal (in voltage, not power).

Spurious components are sinusoidal signals at frequencies that are not integer multiples of the signal frequency. They can result from extraneous signals coupling to the output of the signal source or from artifacts occurring in the waveform recorder. They are also specified in decibels relative to the carrier.

Wide-band noise is a random signal that is spread over a large frequency range. It is measured in decibels relative to the carrier per hertz, i.e., the power in a 1 Hz bandwidth relative to the power of the signal. This signal is often specified in units such as nanovolts per square root hertz because the noise has the property that if the measuring bandwidth is multiplied by  $H$ , the observed noise signal has an rms value that is multiplied by  $\sqrt{H}$ . Such sources of noise often have a “(1/f) corner.” Such a signal will exhibit increasing power at lower frequencies that can cause instability in measurements. Such behavior is beyond the scope of this standard.

When the signal is a pure sinusoid with an amplitude that varies with time, it is said to have amplitude modulation. Amplitude modulation is typically expressed as  $\pm x$  dB, where  $x$  specifies the fluctuations in amplitude of the signal. Amplitude modulation adds to the spectrum of the signal a spectrum that is spread over a frequency range of  $\pm BW_a$  around the signal frequency, where  $BW_a$  is the bandwidth of the fluctuations in the amplitude of the signal. Analysis of amplitude modulation usually assumes that the amplitude is changing slowly relative to the signal, in other words, that  $BW_a$  is significantly smaller than the signal frequency.

When a signal is of the form  $a(t)\sin(2\pi ft + \phi(t))$ , where  $\phi(t)$  varies with time, it is said to have phase modulation. When  $\phi(t)$  varies randomly, the phenomenon is called phase noise. Phase modulation has the same effect on the spectrum of the signal as amplitude modulation when the phase modulation is small, as it will likely be if it arises as an unwanted impurity. The added spectrum has a bandwidth equal to the bandwidth of the variations in  $\phi$ . Phase noise is usually specified in decibels relative to the carrier per hertz at specified offset frequencies from the carrier. It is difficult to relate phase noise specifications to anything of interest in waveform recorder testing.

#### **4.6.8 Estimating impurity problems from sine-fitting results**

One approach to dealing with the problem of potential sine wave impurities is to assume that they are negligible and proceed with sine-fitting tests. The results of the sine-fitting tests can then be used to determine potential problems with the signal source. This subclause gives guidance on how to accomplish this approach.

This approach requires performing the sine-fit test with two different amplitudes of the same frequency. The first is a large amplitude signal, and the second is reduced in amplitude by a factor of  $R$  from the large signal. The reduced amplitude signal shall be obtained from the large amplitude signal by applying an attenuator, rather than reducing the amplitude at the signal source. Values of  $R$  between 3 and 10 are appropriate. It is a good practice to test waveform recorders at two amplitudes in this way even if the signal source is known to be perfect.

Users shall also determine the frequency spectrum of the residuals using one of the methods given elsewhere in this standard. The accuracy with which the various distortion components can be determined improves with record length; therefore, the longest reasonable record length shall be used. Guidelines for interpreting the results for various types of impurities are as follows:

- a) *Harmonic distortion.* Observe the harmonic distortion in the residuals. If it is negligible, it is reasonable to assume that the harmonic distortion in the signal source is negligible. Usually, harmonic distortion within the waveform recorder will be a factor of  $R^{n-1}$  (for the  $n^{\text{th}}$  harmonic) or smaller relative to the signal for the low amplitude signal than for the large amplitude signal. Harmonic distortion in the signal source will remain the same relative to the signal. If the reduction factor in the harmonic distortion is less than  $R^{n-1}$ , the signal source shall be tested for harmonic distortion as discussed in [4.6.9](#).
- b) *Other spurious components.* Other spurious components are handled in much the same way as harmonic distortion. Other spurious components in the signal source will be the same, relative to the signal, for the attenuated signal. If there are significant components that remain the same relative to the signal, the signal source shall be tested. There can be components within the waveform recorder that also are proportional to the input signal. Examples of such components are difference signals between an internal clock and the input signal.
- c) Use of the frequency domain with long record lengths has the same effect as averaging. The noise (quantization included) is reduced by a factor of  $\sqrt{M}$  relative to the harmonics and spurs, where  $M$  is the record length.
- d) *Wide-band noise.* Observe the wide-band noise component of the residuals. If it is significantly smaller for the attenuated signal, the signal source shall be tested for wide-band noise.

- e) *Amplitude and phase modulation.* The spectrum of the residuals will have a peak at the signal frequency if either amplitude or phase modulation is significant. The two types of modulation can be distinguished by looking at the modulo time plot of the residuals (see Irons and Hummel [B25]). Amplitude modulation will appear as random noise multiplied by a sinusoidal envelope at the frequency of, and in phase with, the input signal. Phase modulation is the same except that the envelope is 90° out of phase with the signal. The observed phase modulation will be the difference between that of the signal and that of the clock of the waveform recorder. One way to discriminate between the two is to simultaneously test two waveform recorders that have independent clocks with the same signal. By correlating the residuals from the two waveform recorders, a user can determine how much of the phase modulation is due to the signal and how much is due to the waveform recorder clocks.

#### 4.6.9 Measuring and controlling sine wave impurities

The primary means of measuring input sine wave impurities is with a spectrum analyzer. The primary means of controlling them is with filters. Measurement and control are described as follows:

- a) *Spectrum analyzer basics.* A spectrum analyzer shows power in decibels with respect to a milliwatt on the vertical axis as a function of frequency on the horizontal axis. It is calibrated so that placing a sine wave at the input causes it to read the power of the sine wave on the vertical axis. The user sets the start and stop frequencies for the horizontal axis. There are a number of other controls. The two most important are the attenuation and the resolution bandwidth. Other controls that affect the accuracy are the vertical bandwidth and the sweep speed. The spectrum analyzer is normally put in the mode in which the vertical bandwidth and the sweep speed are automatically determined from the start and stop frequencies and the resolution bandwidth. In this discussion, it is assumed that the power shown on the vertical axis takes into account the attenuation setting. Because spectrum analyzers have a quite limited set of available attenuation values, it may be desirable to use an external attenuator. In this case, the user shall do the calculations to take the attenuator into account. When measuring noise and harmonic distortion with a spectrum analyzer, the noise and distortion (NAD) of the spectrum analyzer itself shall be considered.
- b) *Harmonic distortion.* If the signal is larger than the recommended input signal to the mixer of the spectrum analyzer, attenuate the signal with an external attenuator to get it within range. Set the start and stop frequencies to display the harmonics of interest. Reduce the resolution bandwidth until the displayed noise floor is at least 16 dB below the size of the smallest harmonic to be measured. Determine the size (in decibels with respect to a milliwatt) of the desired harmonics. Now increase the internal attenuation of the spectrum analyzer by 10 dB (usually the smallest step). If there is an accurate measurement of the signal, the size of the harmonic will stay the same, and the noise floor will rise 10 dB. In this case, the measurement is good. If the size of the harmonic changes, then the spectrum analyzer's harmonic distortion is contributing. In this case, the process of decreasing the resolution bandwidth and increasing the attenuation shall be repeated until the size of the harmonic does not change. If this state cannot be accomplished, a better spectrum analyzer is needed, with either lower resolution bandwidth or lower noise.
- c) Filtering the signal with band-pass and/or low-pass filters can reduce harmonic distortion.
- d) *Other spurious components.* The measurement here is the same as for harmonic distortion, but the spectrum analyzer is not likely to contribute. As for harmonic distortion, filtering the signal with band-pass and/or low-pass filters can reduce spurious components.
- e) *Wide-band noise.* For wide-band noise, it is best to have the signal as large as possible without damaging the spectrum analyzer. Use the minimum of attenuation and, perhaps, a low noise amplifier. The setting of the resolution bandwidth is not critical. With normal settings, the noise-floor display will look noisy. It is best to reduce this situation by averaging or by reducing the vertical bandwidth. Measure the height of the noise floor both with the signal connected and with the signal source replaced by a terminator. If these measurements are the same, then the spectrum analyzer does not

have low enough noise for this measurement. Convert each measurement from decibels with respect to a milliwatt to milliwatts. Subtract the value of the measurement without the signal from the measurement with the signal. Convert this difference back to decibels with respect to a milliwatt. Subtract 2 dB from this value to correct for the fact that the spectrum analyzer is calibrated for sine waves rather than noise. Divide the result by the resolution bandwidth to get the noise in decibels with respect to a milliwatt per hertz. The noise can be reduced with filters.

- f) The  $-2$  dB correction mentioned above is the combination of corrections for two different sources of error that occur in spectrum analyzers when measuring noise. One is a  $-2.5$  dB correction due to the fact the spectrum analyzer uses an envelope detector and a log amplifier rather than obtaining a true rms value. The other is a  $+0.5$  dB correction due to the fact that the resolution bandwidth is given as a  $-3$  dB bandwidth rather than as a noise bandwidth. This subject is discussed in detail in Application Note 1303 [B10].
- g) *Amplitude and phase modulation.* Amplitude and phase modulation cannot be measured with common spectrum analyzers. They require specialized and expensive equipment. They cannot be easily reduced. The effect of both generally decreases with record length. The best control is to use short enough record lengths that these phenomena are not significant. Their effect at a given record length can be determined using the sine-fit method of measuring them given in 4.6.8.

## 4.7 Locating code transition levels

Because a waveform recorder digitizes the signal for storage, many of the specifications describe the fidelity of the digitization process. The fidelity of digitization depends on how well the code bins into which the samples fall match the ideal. The only way of directly measuring the code bins is to identify their end points. The boundary between two adjacent code bins is the code transition level. Measurement of the code transition levels is used to determine conformance to several specifications.

The integer  $k$  is the recorder's output code, which ranges from 0 to  $2^N - 1$ , where  $N$  is the number of digitized bits (refer to Figure 2 in 3.1). The  $k^{\text{th}}$  code transition level  $T[k]$  is defined to be the input value corresponding to the transition between codes  $k-1$  and  $k$ . Therefore,  $T[k]$  is the input value for which 50% of the output codes will be less than  $k$  and 50% will be greater than or equal to  $k$ . Note that  $T[0]$  is undefined.

### 4.7.1 Static test method

For applications where dc accuracy is of major importance, find the code transition levels and, from there, calculate the gain and offset, INL and DNL, maximum static error, etc. For applications where such a detailed view of the dc transfer function is not needed, find the waveform recorder's low-frequency gain and offset using the dynamic test method as described in 6.1.2.

A programmable dc source (e.g., a DAC) is required whose range and output parameter (voltage or current) is compatible with the waveform recorder and whose resolution and accuracy are at least four times better than that required of the waveform recorder. The resolution of the source shall be less than the rms noise of the waveform recorder. The static transfer characteristic of the source shall be known. The code transition levels are then determined as in the following steps.

Connect the output of the source to the input of the waveform recorder. Perform the following steps:

- a) Begin with  $k = 1$ .
- b) Apply an input level slightly lower than the expected code transition level. For  $k = 1$ , begin with a value slightly lower than the minimum level recordable by the waveform recorder (e.g., 2% of the input range).

- c) Wait for the transition settling duration of the programmable source. Take a record of data. Evaluate the record to determine the percentage of codes in the record that are less than  $k$ . Temporarily store the percentage along with the corresponding input value.
- d) If the percentage from step c) is greater than 50%, then raise the input value by  $1/4 \times Q$  (of the waveform recorder) or less, and repeat step c), updating the stored input value and percentage.
- e) The first time the percentage drops to 50% or less, the transition has been crossed. The code transition level is computed by linear interpolation based on the recorded percentages at this level and the previous level. Record the interpolated value as the code transition level  $T[k]$ .
- f) After finding  $T[k]$ , repeat step b) to find  $T[k+1]$ . (The final level of step a) for the  $k^{\text{th}}$  code transition level will generally be a satisfactory starting point for code transition level  $k+1$ , step b).
- g) Repeat step f) until  $T[k]$  has been found for all  $k$ .

Care shall be taken to help ensure the impedance of the source and the input impedance of the recorder do not affect this measurement.

#### 4.7.2 Locating code transitions using a feedback loop

A widely used test method for determining transition levels is based on a feedback loop. In this method, an input is applied to the waveform recorder, a record of data is taken, and the record is compared to a desired value. If the waveform recorder output is below the desired value, the input is raised by a fixed amount. If the waveform recorder output is equal to or above the desired value, the input is lowered by a fixed amount. This process is allowed to run continuously until the waveform recorder input has settled to a stable average value. The algorithm was historically implemented in hardware with a hardware word comparator. With current technology, it is usually best implemented in software. The feedback loop approach can be viewed as a variation on the algorithm described in 4.7.1.

After the loop has settled, the input value can be either measured or, if the input source is well calibrated, computed from its transfer function.

A block diagram of the feedback loop used with a waveform recorder is given in Figure 17. In this diagram, a DAC generates the feedback signal. The DAC's input is decremented or incremented to produce an output change of  $\Delta V$ , after each data record of length  $M$  is collected. The increment is based on the result of the comparison between the waveform recorder's average output code,  $\text{avg}(k[1:M])$ , and a designated reference code,  $k_{in}$ . (The notation  $k[i:j]$  denotes a vector with elements from index  $i$  through index  $j$ .) Once the code transition level  $T[k_{in}]$  has been reached, the feedback loop causes the waveform recorder input signal to oscillate across this transition in steps that can be chosen to be as small as desired down to the DAC resolution. The recorder input level is calculated from the known transfer function of the DAC ( $G_{DAC}$ ,  $OFF_{DAC}$ ) or measured by an optional voltmeter. The data recorder can have one measurement per record ( $M = 1$ ), or it can make  $M$  conversions per record to reduce the effect of noise in the waveform recorder.

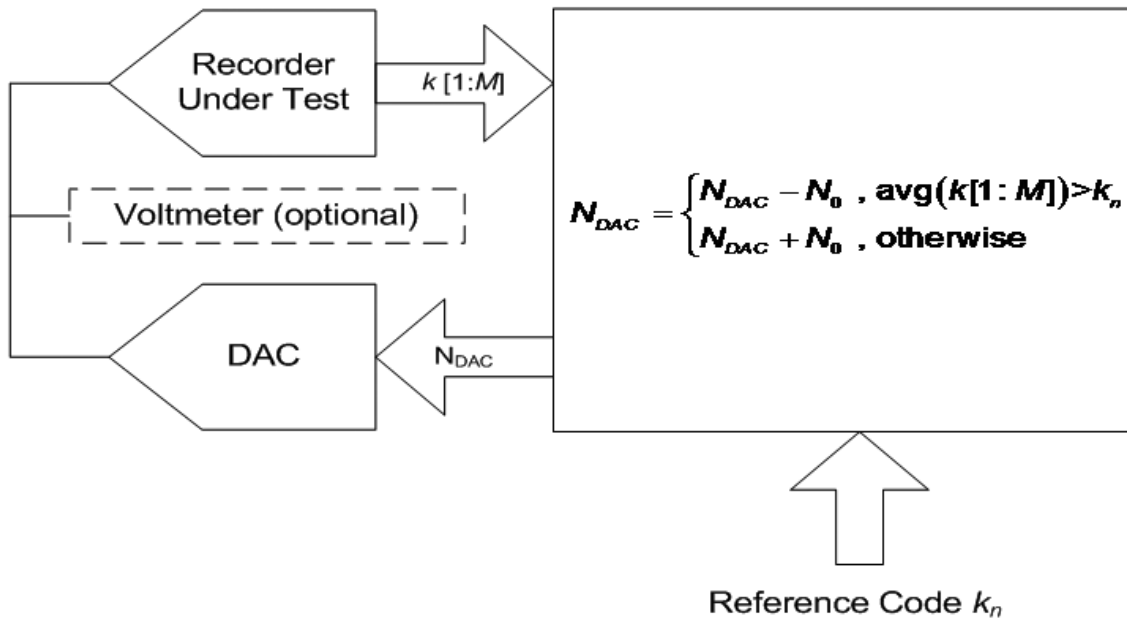


**Figure 17—Block diagram of feedback technique for determining waveform recorder code thresholds**

In an ideal noiseless data recorder, the asymptotic test result is an alternation between two DAC values, and the transition level is known only to an accuracy of  $\Delta V$ . Repeated tests with smaller values of  $\Delta V$  can determine the transition level as precisely as desired.

In a real-world waveform recorder, one with internal noise, the noise affects the properties of the asymptotic state of the test. Instead of a simple alternation about the code threshold value, there will be a random walk about the transition level. The properties of this random walk depend on the relative values of the noise, the step size,  $\Delta V$ , and the waveform recorder code bin width. Choosing the optimum step size is a tradeoff between speed of convergence and the desired accuracy. If  $\Delta V$  is well chosen, this test can be faster than either the histogram or the ramp techniques discussed in following clauses. The remainder of this discussion covers guidance in choosing the step size and the number of samples to be taken to achieve a desired accuracy. The step size,  $\Delta V$ , is typically set to the rms value of the equivalent converter noise, as given in [Equation \(21\)](#):

$$\Delta V = \eta / \sqrt{M} \quad (21)$$

where

$\eta$  is the recorder's rms noise

$M$  is the record length

The value of  $\Delta V$  is equal to  $N_0 \times G_{DAC}$

where

$G_{DAC}$  is the gain of the DAC in volts per least significant bit (LSB)

$N_0$  is the count that is used for the programmed step

Because this is a statistical process, the desired accuracy and the step size being used in the feedback loop determine the number of recorder input values that are to be averaged. In general, there will be a setup period

of  $K_1$  records, followed by an averaging period of  $K_2$  records. Optimizing the procedure requires some care in choosing  $K_1$  and  $K_2$ . Papers by Max ([B31] and [B32]) give detailed guidance for making this choice; this subclause gives rules of thumb for estimating values that work in most cases.

For the case where the step size,  $\Delta V$ , is greater than or equal to the equivalent recorder noise,  $K_1$  can be set to be 8. The initial DAC setting is assumed to differ from the true code edge by less than three times the rms value of the input noise of the recorder. This initial setting is usually evaluated by an input adjusting routine, which initially sets a large value for  $\Delta V$  and eventually reduces the size of  $\Delta V$  in binary steps to the point where the appropriate step size is reached for the final settling. If the step size is less than the noise level, the setup requires additional time. The number of setup samples is inversely proportional to the ratio of step size to noise value. For example, if the step size is one-half the noise value,  $K_1$  would be 16; for one-quarter it would be 32.

#### **4.7.3 Comment on the significance of record length and the presence of noise**

The location of code transition levels is a probabilistic process because of the inevitable presence of noise. As a consequence, the percentages estimated by the measurements of 4.7 have an associated standard deviation. Corresponding uncertainties in the estimates of the code transition levels result. The uncertainties can be reduced by choosing larger record lengths.

Assuming the noise to have zero mean and a normal distribution, the size of the record required for a given precision in the estimates of code transition levels can be computed. Table 3 gives the precision with a 99.87% (3 standard deviations,  $\sigma$ ) confidence level, expressed as a percentage of the rms noise value, computed for several record lengths.

If is necessary for the uncertainty to be known absolutely (that is, in terms of input units) rather than as a percentage of the noise, then the noise level shall be determined. Procedures are given in Clause 8 for measuring the noise level if the dominant source of noise is the waveform recorder rather than the programmable source. Alternatively, the noise can be estimated as the code transitions are located by examining the probability distribution versus input level on either side of a code transition (see Blair [B14]). Note that there is limited value in determining the code transition levels with a precision very much smaller than the noise level, unless the results of an intended application can be used in conjunction with noise-reducing signal processing.

**Table 3—Uncertainty of estimates of code transition level**

| Record length<br>(samples) | Uncertainty of estimates of code<br>transition level<br>(percentage of rms noise) |
|----------------------------|---|
| 64                         | 45%   |
| 256                        | 23%   |
| 1024                       | 12%   |
| 4096                       | 6%  |

#### **4.7.4 Test setup precautions**

The basic setup for these tests involves feeding a dc source into the waveform recorder. Usually, this dc level is generated by a precision dc source or DAC. Because the signal is dc, the waveform recorder shall be dc coupled.

The user shall be alert to the possibility of damaging levels of input signals. For example, some signal sources produce large output levels during their internal calibration procedure. If the waveform recorder is connected and is not protected, it could be damaged. It is also important to maintain a stable environment during the tests, including such factors as temperature, humidity, ac power level, and possible external noise sources.

#### **4.7.5 Test equipment performance**

As discussed above, the dc signal source, or the instrument measuring the source, shall have a precision significantly better than the precision of the waveform recorder. It is important that the high-frequency noise (noise with a frequency comparable to the clock rate of the recorder) be significantly less than the intrinsic noise of the recorder, and filtering can be used to achieve this state. Low-frequency noise (frequency components much less than the digitization frequency) can be a more difficult problem. To test whether low-frequency noise is a problem, take successive records with identical input, and look for baseline shifts or a smooth variation over the time duration of the data record. If low-frequency noise is a problem, its source shall be determined and corrected. Possible sources are ground loops, pickup from ac power sources,  $1/f$  noise in the source circuits, or poor power supply regulation.

#### **4.7.6 Noise filtering**

The accuracy of the input level, or the optional voltmeter, shall be at least four times greater than the desired accuracy of the waveform recorder. For example, to test an 8-bit recorder with an accuracy specification of  $\pm 1$  LSB, a signal source with at least 10 bits of accuracy is needed.

These tests work even when the external noise is greater than the recorder specification, but accuracy can be improved by reducing the noise of the input source to a value much less than the required measurement repeatability. A large capacitor to ground can remove high-frequency noise, but care shall be taken that it does not excessively load the source output or create an unacceptably long time constant. Low-frequency noise, such as pickup from line frequency sources, shall be controlled. In many cases, the time covered by a data record will be a small fraction of a cycle on the noise source; therefore, the noise will appear as a baseline shift between data records taken with the same input level. Often ground loops are a significant contribution to this noise, and all the standard advice for dealing with them, such as using “star” connections and grounding at only one point, applies.

#### **4.7.7 Software considerations**

When writing software to locate the transition levels, users shall not assume ideal behavior for the waveform recorder. Some of these effects have been anticipated, and care shall be taken to follow the procedures of this standard. For example, hysteresis effects are reduced by performing the scan monotonically. Also, missing codes will influence the distribution of the data in the record.

#### **4.7.8 Sine wave histogram**

The following method for locating code transitions is often easier to implement, especially if a user is interested in determining only nonlinearities. A sine wave of amplitude sufficient to slightly overdrive the recorder is recorded in a data record, and a histogram is constructed. If the input range of the recorder is not symmetrical around 0, then a dc level shall be added to the sine wave so that the peaks of the combined signal are approximately equidistant from the center of the range. The triggering of the recorder shall be asynchronous with the sine wave, and the frequency of the sine wave shall be specified. The amount of overdrive required depends on the noise level of the recorder and on the accuracy required. This subject is covered in [4.7.8.2](#). If the amplitude and offset of the sine wave are precisely known, this method gives the transition levels to the same precision. If the amplitude of the sine wave and the offset are unknown, this method gives the transition levels to within a gain and offset error, i.e., the calculated transition levels,  $T'[k]$ , will be related to the true transition levels by the relation shown in [Equation \(22\)](#).

$$T'[k] = aT[k] + b \quad (22)$$

where

$T[k]$  are the true transition levels

$a, b$  are constants

The sine wave frequency shall be chosen as described in 4.7.8.1. Take many records of data (the required amount is covered in 4.7.8.1), and keep track of the total number of samples received in each code bin. The transition levels are then given by Equation (23).

$$T[k] = C - A \cos \left[ \frac{\pi \times N_{CHG}[k-1]}{N_s} \right] \quad (23)$$

where

- $A$  is the amplitude of the sine wave
- $C$  is the offset (dc level) of the applied signal
- $N_s$  is the total number of samples
- $N_{CHG}$  is the cumulative histogram

$$N_{CHG}[j] = \sum_{k=0}^j N_{HG}[k]$$

where

- $N_{HG}[k]$  is the total number of samples received in code bin  $k$

If  $A$  and  $C$  are unknown, they can be determined from the data and an independent estimate of any two of the transition levels. Errors in the values of  $A$  and/or  $C$  do not induce any errors in the determination of DNL or INL from the calculated transition levels because they only induce gain and offset errors in the transition levels as shown in Equation (23). These results are derived by Vanden Bossche, Schoukens, and Renneboog [B44].

#### 4.7.8.1 Comment on the selection of the frequency and record length

The frequency of the sine wave and the record length of the data collected shall be carefully selected in order for the error estimates of 4.7.8.2 to apply. There shall be an exact integer number of cycles in each record, and the number of cycles in a record shall be relatively prime to the number of samples in the record. Meeting these two criteria will produce samples in each record that are uniformly distributed in phase from 0 to  $2\pi$ . If the frequency is low enough that dynamic errors do not arise, this method will give the same results as the static test method. If the frequency is chosen large enough that the dynamic errors are significant, some dynamic errors can appear in the results while others can be averaged out by the histogram calculations.

A frequency that meets the above requirements can be selected as follows: Choose the number of cycles per record,  $M_c$ , and a record length,  $M$ , so that  $M_c$  and  $M$  have no common factors. Choose the frequency by the formula shown in Equation (24).

$$f_i = \frac{M_c}{M} f_s \quad (24)$$

where

- $f_i$  is the input signal frequency
- $f_s$  is the sampling frequency
- $M_c$  is the number of cycles per record
- $M$  is the number of samples in the record

In order for [Equation \(28\)](#) in [4.7.8.2](#) to be valid, the accuracy of the signal frequency is given by [Equation \(25\)](#).

$$\frac{\epsilon_f}{f_i} \leq \frac{1}{2M \times M_c} \quad (25)$$

where

$\epsilon_f$  is the allowable error in the signal frequency

This result is derived by Carbone and Chiorboli [[B17](#)]. With larger values of  $M$ , fewer total samples (the number of records times the number of samples per record) will be required to obtain any given accuracy, but greater accuracy will be required of the signal frequency. The best approach is to use the largest value of  $M$  compatible with the frequency accuracy obtainable. The frequency accuracy specified by [Equation \(25\)](#) helps ensure that the phase separation between samples is within  $\pm 25\%$  of the ideal. This tolerance was assumed in the derivation of [Equation \(28\)](#), which defines the number of records required.

#### 4.7.8.2 Comment on the amount of overdrive and the number of records required

The minimum amount of overdrive required in the method in [4.7.8](#) depends on the combined noise level of the signal source and the waveform recorder. In the absence of noise, the overdrive need be sufficient to receive only at least one count in each of the first and last code bins. If noise is present, it will modify the probabilities of samples falling in various code bins, and the effect will be largest near the peaks where the curvature of the probability density is greatest. This effect can be made as small as desired by making the overdrive large enough. The amount of overdrive required to obtain a specified accuracy also depends on whether the specified accuracy is for the code bin widths, i.e., DNL, or for the transition levels, i.e., INL.

The overdrive required to obtain a specified tolerance in code bin widths is given by [Equation \(26\)](#).

$$V_o \geq \text{Maximum of } (3\eta) \text{ or } \left( \eta \times \sqrt{\frac{3}{2B}} \right) \quad (26)$$

where

$V_o$  is the input overdrive: the difference between the positive (negative) peaks of the sine wave and the most positive (negative) transition level of the waveform recorder  
 $\eta$  is the rms value of the random noise in input units  
 $B$  is the desired tolerance as a fraction of the code bin width

This amount of overdrive helps ensure that the error caused by the noise is  $\leq 1/3$  of the desired tolerance.

The overdrive required to obtain a specified tolerance in transition levels is given by [Equation \(27\)](#).

$$V_o \geq \text{Maximum of } (2\eta) \text{ or } \frac{\eta^2 2^N}{\text{FSR} \times B} \quad (27)$$

where

$\text{FSR}$  is the full-scale range of the instrument in input units  
 $N$  is the number of bits of the recorder

The values of  $V_o$  in [Equation \(26\)](#) and [Equation \(27\)](#) are adequate to keep the errors due to noise equal to or less than  $B/3$  code bin widths so that these errors are negligible when added to the statistical errors caused by taking a finite number of samples.

For more information about the amount of overdrive to use, see Alegria and Cruz Serra [B3] and [B5].

The number of records required depends on several factors, including the combined noise level of the recorder and the signal source, the desired test tolerance and confidence level, whether the tolerance and confidence level is for INL (transition levels) or DNL (code bin widths), and whether a user wants to obtain the desired confidence for a particular width or transition level or for the worst case for all widths or transition levels. The number of records,  $K$ , required for a given test tolerance and a given confidence in code bin widths is given by [Equation \(28\)](#).

$$K = D \left[ \frac{2^{(N-1)} K_u}{B} \right] \times \left[ \frac{c\pi}{M} \right] \times \left\{ 1.13 \left[ \frac{\eta^*}{V} + \frac{c}{2} \eta_\varphi \right] + 0.25 \left[ \frac{c\pi}{M} \right] \right\} \quad (28)$$

where

- $K$  is the minimum required number of records for obtaining the specified confidence either in an individual transition level or code bin width or in the worst-case transition level or code bin width, depending on  $K_u$
- $D$  is a scale factor ( $D = 1$  for INL, and  $D = 2$  for DNL)
- $M$  is the number of samples per record
- $c$  is  $1 + 2(V_o/\text{FSR})$

where

- $\text{FSR}$  is the full-scale range of the waveform recorder under test
- $V_o$  is the input overdrive
- $K_u$  is the value of  $Z_{u/2}$  for obtaining the specified confidence in an individual transition level or code bin width (see [Table 4](#)), or is the value of  $Z_{N,u/2}$  for obtaining the specified confidence in the worst-case transition level or code bin width (see [Table 4](#))
- $u$  is  $1 - v$ , with  $v$  the desired confidence level expressed as a fraction
- $\eta^*$  for INL, is  $\eta$ , the rms additive random noise, and for DNL, is the minimum of  $\eta$  or  $Q/2.26$
- $\eta_\varphi$  is the rms random phase difference of the sampling time relative to the input signal, in radians
- $N$  is the number of bits of the waveform recorder
- $\varepsilon_{T0}$  is the desired test tolerance as a fraction of the code bin width

The values for  $Z_{u/2}$  and  $Z_{N,u/2}$  can be obtained from [Table 4](#). For values of  $N$  between those in the table, use linear interpolation.  $Z_{u/2}$  is defined so that the probability is  $(1 - u)$  that the absolute value of a Gaussian distributed random variable, having a mean of 0 and a standard deviation of 1, is less than or equal to  $Z_{u/2}$ .  $Z_{N,u/2}$  is defined so that there is a probability of  $(1 - u)$  that the maximum of the absolute values of  $2^N$  Gaussian distributed random variables, having means of 0 and standard deviations of 1, is less than or equal to  $Z_{N,u/2}$ .

**Table 4—Values of  $Z_{u/2}$  and  $Z_{N,u/2}$**

| $u$  | $Z_{u/2}$ | $Z_{4,u/2}$ | $Z_{8,u/2}$ | $Z_{12,u/2}$ | $Z_{16,u/2}$ | $Z_{20,u/2}$ | $Z_{24,u/2}$ |
|------|-----------|-------------|-------------|--------------|--------------|--------------|--------------|
| 0.2  | 1.28      | 2.46        | 3.33        | 4.04         | 4.64         | 5.19         | 5.68         |
| 0.1  | 1.64      | 2.72        | 3.53        | 4.21         | 4.80         | 5.33         | 5.81         |
| 0.05 | 1.96      | 2.95        | 3.72        | 4.37         | 4.94         | 5.46         | 5.93         |
| 0.02 | 2.33      | 3.22        | 3.95        | 4.57         | 5.12         | 5.62         | 6.08         |
| 0.01 | 2.58      | 3.42        | 4.11        | 4.71         | 5.25         | 5.74         | 6.19         |

*Table continues*

**Table 4—Values of  $Z_{u/2}$  and  $Z_{N,u/2}$  (continued)**

| $u$   | $Z_{u/2}$ | $Z_{4,u/2}$ | $Z_{8,u/2}$ | $Z_{12,u/2}$ | $Z_{16,u/2}$ | $Z_{20,u/2}$ | $Z_{24,u/2}$ |
|-------|-----------|-------------|-------------|--------------|--------------|--------------|--------------|
| 0.005 | 2.81      | 3.60        | 4.27        | 4.85         | 5.38         | 5.85         | 6.30         |
| 0.002 | 3.09      | 3.84        | 4.47        | 5.03         | 5.54         | 6.01         | 6.44         |
| 0.001 | 3.29      | 4.00        | 4.62        | 5.16         | 5.66         | 6.12         | 6.54         |

[Equation \(26\)](#), [Equation \(27\)](#), and [Equation \(28\)](#), and the values in [Table 4](#) are derived by Blair [B14] with refinements and additions by Carbone and Chiorboli [B17] and Dallet and Machado da Silva [B19]. For further information, see Papoulis [B36], Alegria, et al. [B9], and Alegria and Cruz Serra [B7].

#### 4.7.8.3 Effect of harmonic distortion of signal source on transition levels

When the sine wave histogram is used, the harmonic distortion influences the calculated transition levels. The excitation signal with harmonic distortion is described by [Equation \(29\)](#).

$$f(t) = C + A \sin(2\pi ft) + \sum_{i=2}^N A_i \sin(i2\pi ft + \varphi_i) \quad (29)$$

where

- $C$  is the dc offset of the sine wave
- $A$  is the amplitude of the fundamental
- $A_i$  is the amplitude of the  $i^{\text{th}}$  harmonic
- $f$  is the frequency of the fundamental in hertz
- $\varphi_i$  is the phase of the  $i^{\text{th}}$  harmonic

An 8-bit waveform recorder excited with the signal described by [Equation \(29\)](#), with  $A_i = 0.0$  for all  $i$  except for one value of  $i$ , which is equal to 1 LSB, causes the deviations in the calculated transition levels shown in [Figure 18](#). The sine effects are evaluated by setting  $\varphi_i = 0.0$ . The cosine effects are identified by setting  $\varphi_i = \pi/2$ . The fundamental of the excitation signal is assumed to be a sine function with 3% overdrive. The worst-case influence on the transition levels is approximately half of the distortion component amplitude. When multiple harmonics at the worst-case phases are present, the peak errors can add up almost linearly.

The even harmonic cosine terms and the odd harmonic sine terms induce significant effects on the computed code transition levels. The even harmonic sine terms and the odd harmonic cosine terms induce much smaller effects that cluster around the 0 LSB line. An extensive analysis on the effects of harmonic distortion is given by Blair [B14]. The location of the code transition can be in error by as much as  $A_i/2$  when the phase of the distortion is unknown.

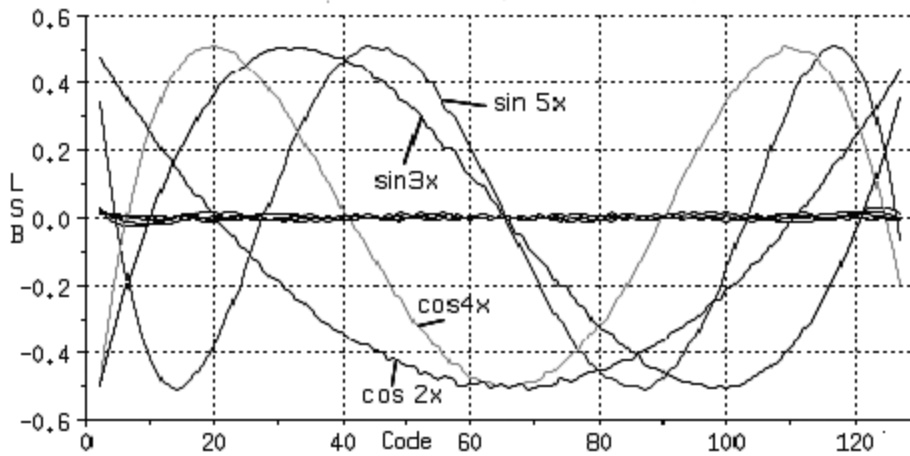


**Figure 18—Plot of perfect waveform recorder-computed transition level deviations using sine wave histogram with additive harmonic distortion (Effect of 2nd, 3rd, 4th, 5th harmonics on transition levels are shown. The harmonic amplitude is 1 LSB, sine and cosine components.)**

#### 4.7.9 Comments on histogram testing

Histogram methods can produce erroneous results if the device being tested has output codes that are swapped with other codes or exhibits other types of nonmonotonic behavior. Such waveform recorders can produce seemingly good results, yet have large errors in the actual code transitions. To avoid these issues, waveform recorders shall also be tested for signal-to-noise ratio (SNR) performance to confirm that nonmonotonic behavior is not significant (see 8.3).

#### 4.7.10 Triangle wave tests

Three methods of triangle wave testing are included in this standard.

The first test method, described in 4.7.10.1, is useful for lower resolution waveform recorders or when a highly accurate ramp signal is available.

The second test method, described in 4.7.10.2, can be used for higher resolution waveform recorders when a quasi-static, highly accurate dc source is available in combination with a lower accuracy triangle source.

The third test method, described in 4.7.10.3, can be used for high-resolution waveform recorders when a ramp generator is available whose resolution is less than the rms waveform recorder noise. It can also be used when the ramp generator can be characterized to an appropriate accuracy level.

##### 4.7.10.1 Full-scale triangle wave excitation

In the full-scale triangle wave excitation approach, a histogram of code occurrences is generated in response to an input signal level, which ramps linearly between the extremes of the full-scale range (FSR) of the waveform recorder, or equivalently, which ramps in a positive direction and a negative direction with equal slope magnitudes. After a sufficiently large number of samples, the histogram of the output provides an accurate measure of the transition levels. The DNL and INL of the waveform recorder can be extracted from the transition level data using methods described in Clause 7.

The input ramp or triangle wave can be generated either by a high-resolution DAC or by an arbitrary waveform generator (AWG) with suitable linearity. The ramp is assumed to have a positive peak level of VP and a negative peak level of VM as shown in [Figure 19](#). Best results will be achieved when the triangle wave is synchronous with the sampling clock of the waveform recorder.

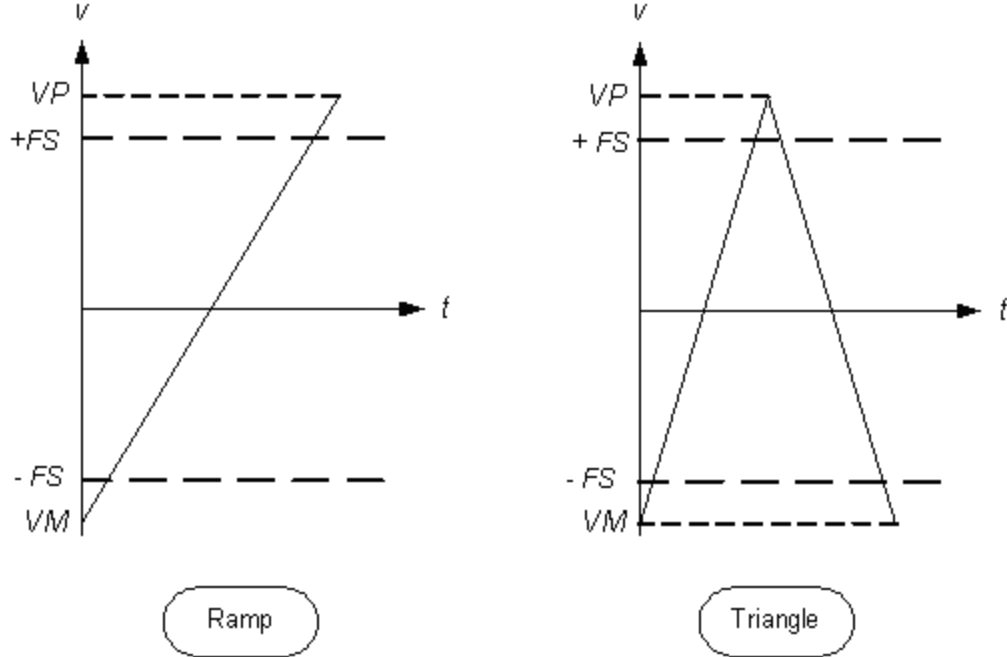


**Figure 19—Plot of acceptable ramp test input signals**

The location of the code transition levels,  $T[k]$ , can be extracted by manipulating the data that are collected in a histogram test with a ramp input. The code transition levels are given by [Equation \(30\)](#).

$$T[k] = C + A \times N_{CHG}[k-1] \quad \text{for } k = 1, 2, \dots, (2^N - 1) \quad (30)$$

where

- $A$  is a gain factor
- $C$  is an offset factor
- $N_{CHG}$  is the cumulative histogram

$$N_{CHG}[j] = \sum_{k=0}^j N_{HG}[k]$$

where

- $N_{HG}[k]$  is the total number of samples received in code bin  $k$

The values of the two end-point transitions can be computed from [Equation \(31\)](#) and [Equation \(32\)](#).

$$T[1] = VM + \frac{VP - VM}{N_s - 1} (N_{CHG}[0] - 0.5) \quad (31)$$

$$T[2^N - 1] = VM + \frac{VP - VM}{N_s - 1} (N_{CHG}[2^N - 2] - 0.5) \quad (32)$$

where

- VP      is the positive voltage peak of the ramp
- VM      is the negative voltage peak of the ramp
- $N_s$     is the total number of samples
- $S$       is  $\sum_{i=0}^{2^N-1} H[i]$  = the total number of histogram samples

The parameters  $A$  and  $C$  can then be computed from the end-point values from [Equation \(33\)](#) and [Equation \(34\)](#).

$$A = \frac{(T[2^N - 1] - T[1])}{(N_s - N_{HG}[2^N - 1] - N_{HG}[0])} \quad (33)$$

$$C = T[1] - \left( \frac{N_{HG}[0] \times (T[2^N - 1] - T[1])}{(N_s - N_{HG}[2^N - 1] - N_{HG}[0])} \right) \quad (34)$$

The gain and the offset of the waveform recorder based on the end points can be computed once the values of  $T[k]$  are known (see [Clause 6](#)).

#### 4.7.10.1.1 Comments on number of samples required per transition level for a given confidence level

The precision of the measured values of the code transition levels depends on the total number of histogram samples measured. Increasing the number of samples decreases the uncertainty. Nonlinearity of the ramp input signal will produce comparable errors in the code transition levels. Noise on the ramp signal or the waveform recorder under test will cause uncertainty in the measured code transition levels. Specifically, the uncertainty in LSBs in the estimate of a transition level,  $\varepsilon_Q$ , for large numbers of samples is approximated by [Equation \(35\)](#) (see [Max \[B31\]](#)).

$$\varepsilon_Q \approx 0.83 \sqrt{\frac{\sigma}{\bar{N}_{HG}}} \quad (35)$$

where

- $\sigma$       is the standard deviation of the converter noise, in units of ideal code bin widths (LSBs)
- $\bar{N}_{HG}$     is the average number of histogram samples received in the two code bins that share the given transition level

If the noise is low and  $\bar{N}_{HG}$  is small, the uncertainty approaches the value given by [Equation \(36\)](#).

$$\varepsilon_Q \approx \frac{1}{\bar{N}_{HG} \sqrt{12}} \quad (36)$$

The relationships described in the above equations are shown graphically in [Figure 20](#). The low-noise case is illustrated by the “mod2” graph, which identifies the region defined by [Equation \(35\)](#) for  $\bar{N}_{HG} = 2$ . The high-noise case is illustrated by the slope of 0.5, identifying the square root characteristic of [Equation \(35\)](#). The horizontal axis is the rms waveform recorder noise in units of LSBs. Each curve in the plot has a different average number of samples per LSB.

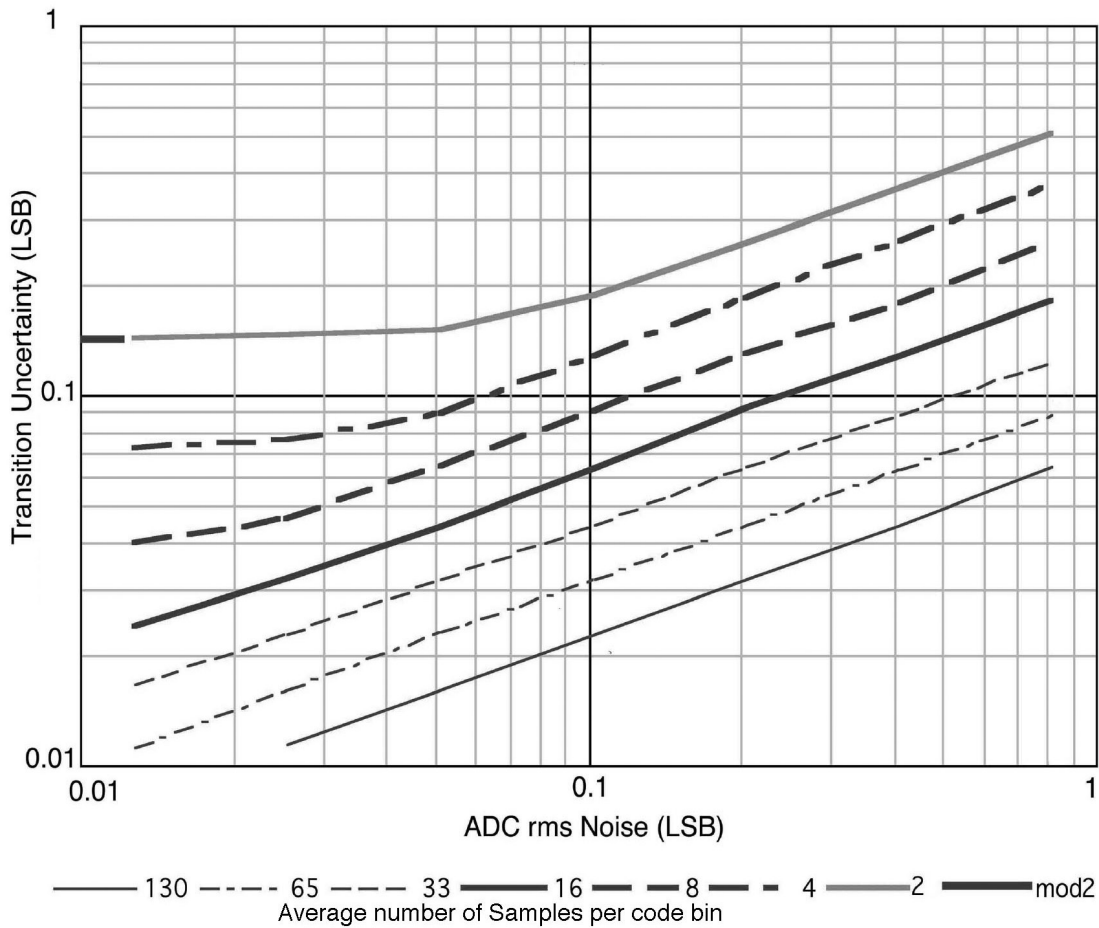


**Figure 20—Plot of transition uncertainty**

#### 4.7.10.1.2 Comments on ramp characteristics

The ramp method is generally used when static characteristics of the device under test are being measured. The sine wave histogram is generally used for dynamic testing. The ramp method is more efficient in measuring the device characteristics when a generator with the required linearity is available.

#### 4.7.10.1.3 Comments on histogram testing

See 4.7.9.

#### 4.7.10.2 Excitation using a high-precision dc source with ramp vernier

For medium- and high-resolution waveform recorders, the implementation of the test methods described earlier (in 4.7.1, 4.7.2, and 4.7.10) might not be feasible. For instance, the great number of changes in dc input level required in the static test method described in 4.7.1 can lead to excessive test time due to the dc source transition settling duration. Also the requirements on triangular wave linearity of the triangle wave excitation test described in 4.7.10 can be difficult to meet with commercially available function generators when testing waveform recorders with more than 8 bits. It might also be important to have all the output codes uniformly stimulated, and such stimulation cannot be done with the sine wave histogram described in 4.7.8 due to the shape of the test signal.

In those cases, a hybrid test can be used that combines a traditional static test philosophy of dc stimulus with a statistical approach characteristic of code density procedures (histogram) similar to those described in IEEE Std 181-2011. Instead of determining each individual code transition voltage as in the static test method described in 4.7.1 or determining all the transition voltages at the same time as in the triangle wave method described in 4.7.10.1, this test procedure determines a fraction of the code transition voltages at a time. It uses a precision dc source to produce a dc voltage, which is added to a small-amplitude triangular wave.

This procedure drastically decreases the number of dc source output changes by determining several code transitions with the same dc voltage and leads to a substantial decrease in test duration. The linearity requirements of the triangular wave are reduced due to the small amplitude required from the ramp generator. This small amplitude together with a low frequency used lead to a small input stimulus slope and consequently to quasi-static conditions.

**Figure 21** shows the several test signals,  $N_s$ , used to cover all of the waveform recorder input range ( $v$ ). The different values of dc voltage are represented by  $V_j$ , with  $j = 0, 1, \dots, N_s - 1$  and the triangular wave amplitude by  $A$ .

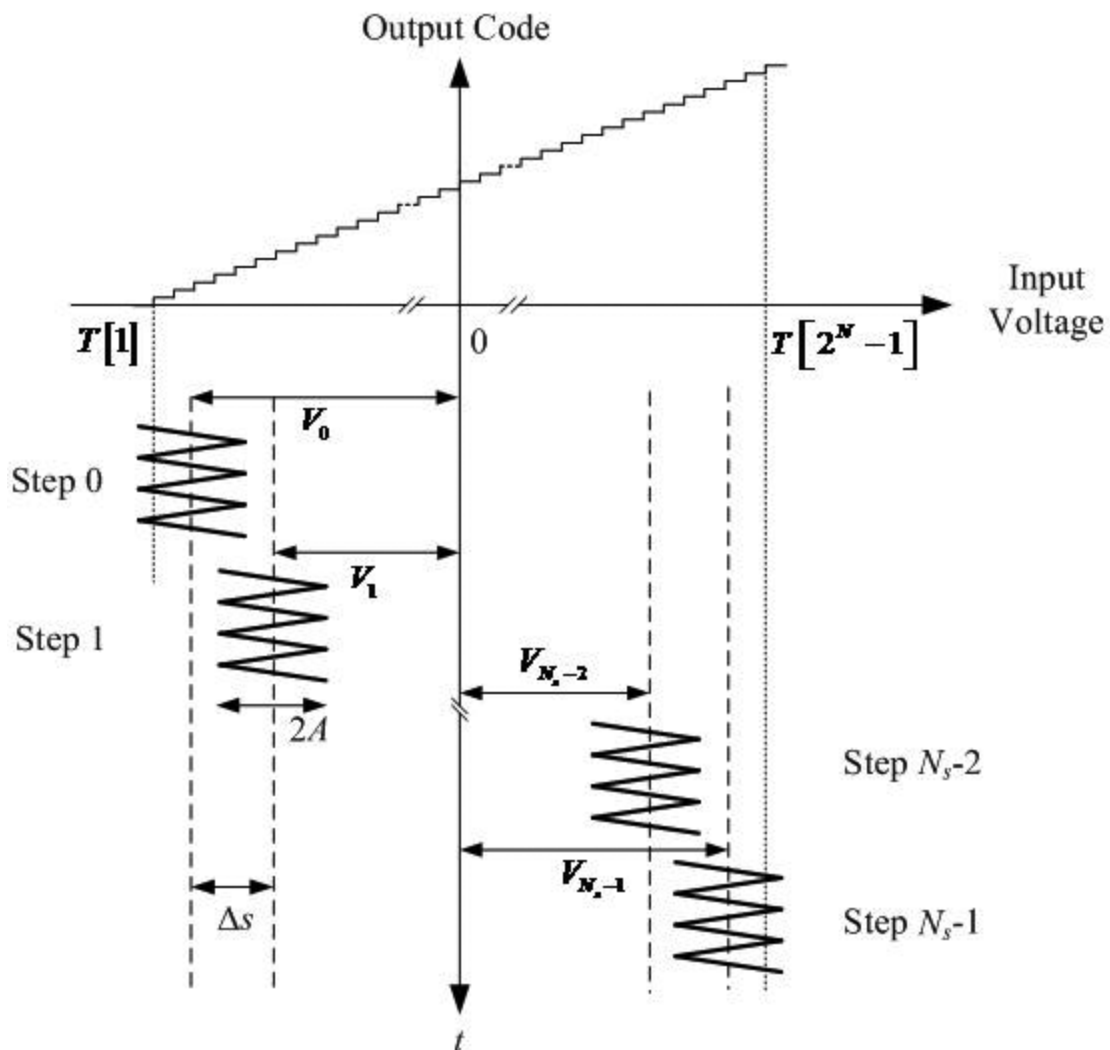


**Figure 21—Ramp vernier test signals applied to waveform recorder**

The procedure for making the measurement is given in the following steps. (See [Annex F](#) for a discussion on setting various test parameters.)

- a) Program the triangular wave generator with the amplitude  $A$  and frequency  $f$ .
- b) Set the dc source voltage to the offset of the triangular wave to use in the first step ( $j = 0$ ), namely  $V_0$ .
- c) Acquire  $K$  records of  $M$  samples each.
- d) Compute the cumulative histogram for the current step ( $N_{CHG}[k]$ ) by counting the number of samples equal to or lower than each output code  $k$ , with  $k = 0$  to  $2^N - 1$ . From the cumulative histogram, compute the transition voltages for the current step ( $T_j[k]$ ) using [Equation \(37\)](#).

$$T_j[k] = V_j + A \times \left( 2 \frac{N_{CHG}[k]}{K \times M} \right) \quad \text{for } k = 1, 2, \dots, (2^N - 1) \quad (37)$$

- e) If there are more steps ( $j < N_s$ ), then increase the dc source voltage by  $\Delta V$  to  $V_j$  and go to step d).
- f) Combine the  $N_s$  arrays of transition voltages  $T_j[k]$  obtained in each step into a single array  $T[k]$ . Because of the use of overdrive, the arrays obtained in each step overlap. To combine them, the transitions at the beginning and at the end of each array shall be discarded one at a time until no overlap occurs anymore, and the resulting array is concatenated. It is important that the values of transition voltages at the edges of the arrays be discarded because they are obtained at an extreme of the triangular wave, which is more distorted than the middle of the wave due to the discontinuity of the derivative, and also is more affected by additive random noise.

[Figure 22](#) shows a flowchart for this procedure.

An example of successive cumulative histograms is presented in [Figure 23](#) for a 5-bit waveform recorder and a test with four steps.

This test can also be used when testing very high resolution waveform recorders (24 or more bits) for which all the other tests presented here become unfeasible due to the excessive time required to complete the test. This time can reach months for a single waveform recorder if an exhaustive test were to be carried out. The only solution envisioned at present would be to just determine some of the transition voltages in the regions where problems are known to happen, e.g., in the most significant bits transitions. This test could then be partially executed by skipping some of the steps.

This test shall be used only when it is possible to add the signal from the dc source with the signal from the triangular wave generator. This step can be done by means of a precision adder, by using the waveform recorder inputs in differential mode if available or by connecting the dc source and the function generator in series. In the latter case, special care shall be taken with the impedances and the floating inputs. In general, it is not possible to use only a function generator because the controllable offset does not have the precision required and some units cannot generate a wave with an offset much higher than the amplitude.

In the test design, the following values of its main parameters have to be defined:

- The amplitude  $A$  of the small wave
- The offset  $V_j$  in the  $j^{\text{th}}$  step
- The number of samples  $M$  in each record
- The frequency  $f$  of the small wave

Analytical relations for selecting these parameters are provided in [Annex F](#).

For more information on this test method, see Alegria, et al. [[B1](#)] and [[B2](#)].

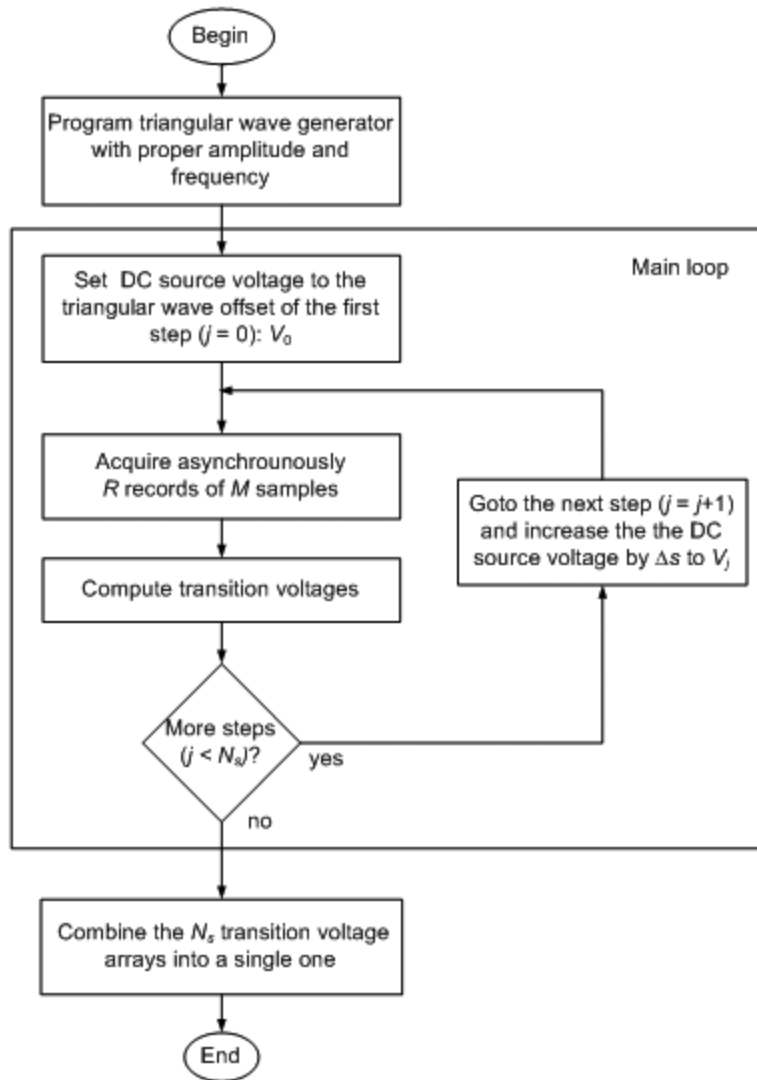
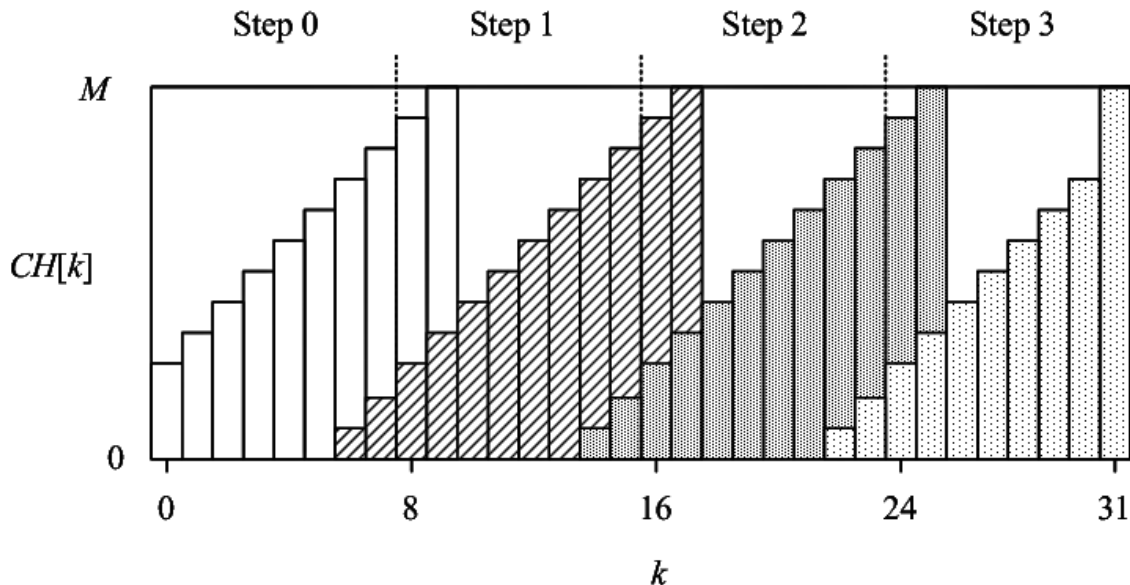


Figure 22—Test procedure for excitation using a high-precision dc source with ramp vernier



**Figure 23—Representation of the cumulative histograms computed in each step in the case of a 5-bit converter and a test with four steps**

#### 4.7.10.3 Excitation with limited accuracy ramp sources

In the excitation approach with limited accuracy ramp source, histograms of code occurrences are generated in response to an input signal level, which ramps at discrete levels between the extremes of the FSR of the waveform recorder. After a sufficiently large number of samples, the histograms of the output provide an accurate measure of the transition levels.

The input ramp shall be generated synchronously with the sampling clock, by a DAC or AWG with appropriate resolution whose values can be identified to an appropriate accuracy level. The ramp is assumed to have a positive peak level of VP and a negative peak level of VM as shown in [Figure 19](#). It is important that the resolution of the input ramp be less than the rms noise of the waveform recorder system. The values of each input level are stored in the array  $V[1:J]$ , where  $V[1] = VM$  and  $V[J] = VP$ . (The notation  $V[i:j]$  denotes a vector with elements from index  $i$  through index  $j$ .) The waveform recorder is assumed to have  $2^N - 1$  output codes where  $N$  is the number of bits. At each input level, the waveform recorder is triggered  $K$  times. The values generated by the voltage input  $V[j]$  are counted in the array  $d[j, 1:2^N - 1]$ . For example, if  $K = 100$  and  $v[j] = 5.2$  V, the values present in  $d[j, 0:8]$  are shown in [Figure 24](#).

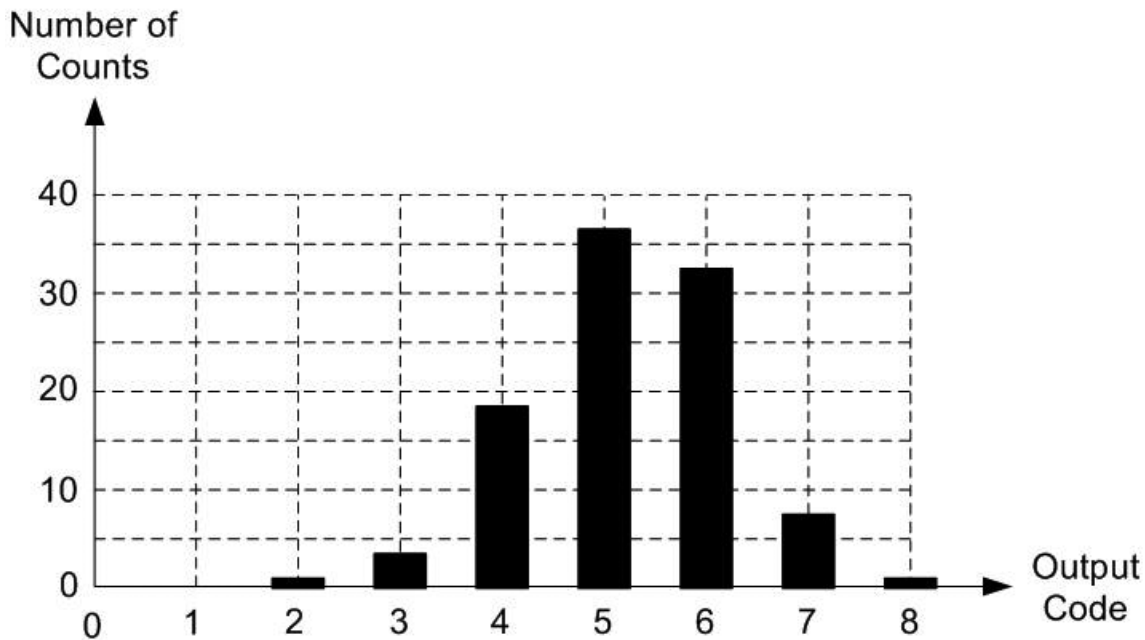


**Figure 24—Example data for limited accuracy triangle wave measurement of code transition levels (Data are for an input voltage of 5.2 V,  $Q = 1 \text{ V/count}$ , and a noise level of  $1 \text{ V}_{\text{rms}}$ )**

Once all the arrays are collected, the mathematical algorithm described by the pseudo-code shown below is run.

```

for j = 1 to J do      - J is number of waveform recorder
levels in the input ramp
for i = 1 to N do      - N is number of codes
Hc[i, j] = sum(d[j, 1:i])
endfor
endfor
for i = 1 to N do
Hc[i] = Hc[i] / Hc[i, 1]
endfor

```

The transition voltage,  $T[i]$ , is then evaluated from the mathematical algorithm generated by the pseudo-code shown below.

```

pd[i, 1:J-1] = Hc[i, 2:J] - Hc[i, 1:J-1]
v_avg[1:J-1] = (v[1:J-1] + v[2:J]) / 2.0
T[i] = sum(pd[i, 1:J-1] * v_avg[1:J-1])

```

#### 4.7.10.4 Comments on number of samples to be averaged per transition level for a given confidence level

The uncertainty of the measured values of the code transition levels is identical to the values shown in Figure 20. The algorithm is robust if the resolution of the source is less than twice the rms system noise. If the resolution of the source is larger, the calculated threshold values can be in error by as much as half of the source resolution.

#### 4.7.11 Determining the static transfer curve

The transfer curve of a waveform recorder is the average output code,  $\bar{y}$ , as a function of a particular input signal level,  $x$ . The transfer curve,  $\bar{y}(x)$ , is used as a basis for alternate definitions of many of the static parameters of a waveform recorder, e.g., gain and offset, *INL*, and monotonicity. The transfer curve (and the parameter definitions based on it) is especially useful in specifying waveform recorders where it may be impractical or impossible to measure the code transition levels. Examples of such waveform recorders are those with a high number of digitized bits (it may be impractical to search for all  $2^{20}$  code transition levels for a 20-bit waveform recorder), those with non-monotonic behavior and/or output-to-input crosstalk (which can result in either undefined or multiply-defined code transition levels), and those waveform recorders that are actually composed of multiple time-interleaved sample-holds and/or ADCs.

Another useful measurement that can be made at the same time as the transfer curve is the deviation of the output codes about the average, again as a function of the input signal value,  $x$ .

To estimate the transfer curve,  $\bar{y}(x)$ , and the standard deviation of the output as a function of the input,  $\sigma_y(x)$ , a dc input source is required whose output signal range spans slightly more than the full-scale range of the waveform recorders, and that has an accuracy, resolution, and noise better than the desired accuracy of the measurement. To make the estimate, perform the following steps:

- a) Set the level of the input signal,  $x$ , slightly below the bottom of the waveform recorder input range (such that further lowering of the input level would not change the waveform recorder output).
- b) Acquire a record of  $M$  samples from the waveform recorder:  $y_0, y_1, y_2, \dots, y_{M-1}$ .  $M$  shall be chosen large enough that the standard deviation of the sample mean (the standard deviation of the samples divided by the square root of  $M$ ) is small compared to the desired accuracy of the measurement.
- c) Record the sample mean (estimated average),  $\bar{y}(x)$ , and standard deviation,  $\sigma_y(x)$ , of these  $M$  samples in arrays indexed by the current input level  $x$ .
- d) Increment the input level  $x$  by a specified amount. Preferably, the increment is roughly equal to the deviation of the additive random noise present within the waveform recorder at the analog input, or  $Q/8$ , whichever is larger.
- e) Repeat steps b), c), and d) until the input level  $x$  is set slightly above the top of the waveform recorder input range (such that increasing the input level further would not change the waveform recorder output).

### 4.8 Step function response measurements

This subclause covers topics related to using step functions to evaluate the performance of a waveform recorder. The step response is the recorded output response for an ideal input step with designated low state and high state (see IEEE Std 181-2011 for more information on low and high states). If unspecified, the low state of the input step is 10% and the high state is 90% of full scale. The parameters derived from the step response waveforms are described in detail in [Clause 9](#) and [Clause 10](#).

#### 4.8.1 Purposes and limitations of step response measurements

##### 4.8.1.1 Predict output from input

A well-designed waveform recorder has a behavior very much like an LTI system. In other words, the output resulting from the sum of any two input signals is the sum of the outputs from the individual signals (so long as both inputs and their sum are within the range of the recorder) and that time-shifting an input by any amount results in the output being time-shifted by the same amount.

To the extent that a waveform recorder behaves as an LTI system, knowledge of the step response allows a user to calculate the output signal for any given input signal. The output signal is the convolution of the input signal with the derivative of the step response, the latter being the impulse response of the recorder. The deviation between the input signal and its convolution with the impulse response is called the LTI error.

#### **4.8.1.2 Determine pulse parameters**

There are several parameters of the step response that are considered important in themselves and are commonly specified for waveform recorders. These parameters include the transition duration, slew limit, overshoot, precursor, and transition settling duration. [Table 5](#) shows the subclauses that cover these parameters.

**Table 5—Step response parameters**

| Parameter                     | Subclause |
|-------------------------------|-----------|
| Transition settling durations | 9.1       |
| Transition duration           | 9.2       |
| Slew limit                    | 9.3       |
| Overshoot                     | 9.4       |
| Precursors                    | 9.4       |
| Aperture duration             | 9.5       |

#### **4.8.1.3 Determine frequency response**

One of the most important applications of step response measurements is to obtain the frequency response of the recorder. The frequency response of a system is the Fourier transform of the system's impulse response. Because the impulse response is the derivative of the step response, a user calculates the frequency response by numerically differentiating the step response and numerically calculating the Fourier transform of the result. See [Clause 10](#) for details of computing frequency response from step response.

#### **4.8.2 Test method for measuring step response**

The method given in this subclause applies to the situation in which external equivalent-time sampling is not used. This situation applies when the sampling rates supported by the waveform recorder, perhaps using internal equivalent-time sampling, are adequate to measure a step response. Adequacy of the sampling rate is determined by the magnitude of the aliasing error. If the waveform recorder does not have a sampling rate large enough to make a step response measurement with sufficiently low aliasing error, then external equivalent-time sampling shall be used to increase the effective sampling rate (see [4.4](#)).

[Figure 25](#) shows the setup for a simple step response measurement. The cable from the signal output of the pulse generator to the input of the waveform recorder shall be as short as possible.

If the waveform recorder has internal triggering capabilities and has the capability of recording a signal prior to the trigger, the cable connecting the trigger output of the step generator to the trigger input of the waveform recorder is not needed.

The step response measurement can be either a single-shot measurement or an average measurement. Generally, sophisticated techniques are required to correctly utilize signal averaging on waveform recorders. It is assumed here either that the operator is using single-shot measurements or that techniques necessary for averaging are built into the waveform recorder.

In either case (single-shot or average), what is required is to obtain a measurement of the signal from the step generator that begins early enough to record any precursors of the step response and continues until the step response has reached a constant value.

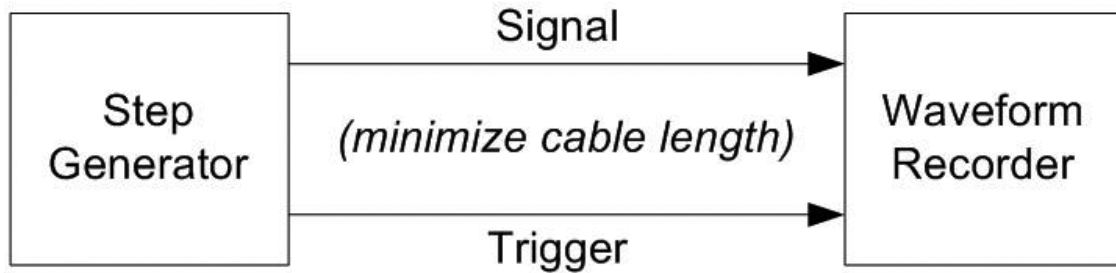


**Figure 25—Setup for a simple step response measurement**

To start the recording early enough, the trigger signal shall occur prior to the step transition, or the waveform recorder shall be set to record prior to the trigger signal. The record length shall be set long enough to record the signal until the step response becomes constant.

If waveform averaging or internal equivalent-time sampling is being used, the data are to be collected following the manufacturer's instructions. For single-shot measurements, the user merely triggers the step generator once and collects a waveform.

#### 4.8.3 Sources of error

There are a number of sources of error associated with real step pulses. These errors can adversely affect the measurements of parameters associated with the waveform recorder's step response. The effects of specific error sources on specific step pulse response parameters are described in [Clause 9](#) and [Clause 10](#), along with some suggestions on how to mitigate the effects.

##### 4.8.3.1 Cable losses and reflections

Electrical cables attenuate the high-frequency components of the signals they transmit. The amount of attenuation in decibels at a given frequency is proportional to the cable length. Different types of cables have different attenuation characteristics. In general, smaller diameter cables have greater losses than larger diameter ones. Cables with high-density polyethylene dielectric insulation have higher losses than cables with foam polyethylene dielectric. This low-pass filtering effect will increase the transition duration of the test step pulse at the input to the waveform recorder. Cables also exhibit an effect called dribble-up where the time it takes the step to go from, for example, 90% to 99% of the final value is much longer than it takes for a one-pole or a two-pole lumped circuit. Cables also exhibit dispersion whereby different frequencies propagate down the cable at slightly different velocities.

It is usually practical to use short (~2 m) cables in testing waveform recorders. The increase in transition duration time is less than 100 ps for this length of common coaxial cable types, e.g., RG-58 and RG-214. A 1.8 m length of RG-58 cable has a 90%–99% time duration of about 12 ns; and the duration for RG-214 is 2.6 ns when the input is a 1 ns transition duration “step” pulse (see Harper [\[B21\]](#)). The cable output to a unit step is given quantitatively by  $1 - e(t)$ , with  $e(t)$  given by [Equation \(38\)](#).

$$e(t) = Clt^{-1/2} \quad (38)$$

where

- $\ell$  is the length of the cable in meters
- $t$  is the time in nanoseconds from the step transition
- $C$  is a constant dependent on the cable type (The value of  $C$  is 0.019 for RG-58 and 0.0089 for RG-214.)

From [Equation \(38\)](#), it can be seen that the time for the error to be reduced to any particular value is proportional to the square of the cable length. Thus, increasing the cable length by a factor of two will increase the transition settling duration by a factor of four. The value of  $C$  can be calculated for any other cable from one attenuation measurement. It is given by [Equation \(39\)](#).

$$C = \frac{0.120 A_{dB}}{\ell \sqrt{f}} \quad (39)$$

where

- $A_{dB}$  is the attenuation in decibels
- $f$  is the frequency in gigahertz at which the attenuation is known
- $\ell$  is the length of the cable in meters

The above relations were derived using the results by Wiggington and Nahman [\[B45\]](#). The frequency,  $f$ , shall be small enough that dielectric losses are negligible. If not, the calculated  $C$  will be larger than the true value, and the error will be overestimated.

In summary, the cable length between the step pulse generator and the waveform recorder shall be kept as short as possible. The type of cable selected shall be consistent with the desired transition duration.

If there are aberrations in the step response delayed from the major part of the transition by an amount equal to the round-trip delay of the cabling from the step generator to the recorder under test, redo the test with a cable of different length. If the aberrations shift in time accordingly, they are due to reflections in the cabling between the generator and recorder. In this case, check the input impedance of the waveform recorder and output impedance of the step generator.

#### 4.8.3.2 Aliasing effects on step response measurements

Aliasing error is the error due to insufficient sampling rate. In calculations of the frequency response, the value of the response at frequencies higher than  $f_s/2$  (where  $f_s$  is the sampling frequency) appear “aliased” at frequencies lower than  $f_s/2$ , hence the name. Aliasing also affects the determination of parameters other than the frequency response. It causes an underestimate of the amount of overshoot because the peak overshoot is likely to occur between samples. Aliasing can cause the measured transition time to be either lower or higher than the true value. The error in transition duration is due to the error in the interpolation used to find the 10% and 90% times.

The magnitude of the aliasing error depends on the ratio of the sampling frequency  $f_s$  to the 3 dB bandwidth, BW, of the recorder. The exact functional form depends on the waveform recorder’s particular frequency response. In [9.6.5](#), a method is presented for transition duration measurement error estimates for single-pole and two-pole frequency response models. In [10.3.2](#), a method is presented for frequency response magnitude and phase error estimates for the two models.

#### 4.9 Tests using a dc input

Tests with dc input signal levels are used both for a quick survey of a waveform recorder at the start of testing and for locating code transitions. From the code transitions, users can calculate code bin widths from which they can derive other quantities, such as the differential and integral nonlinearities. Because they use dc levels as inputs, these tests establish baseline performance that can be compared with dynamic tests at higher slew rates. The major drawbacks of these tests are the time they take, particularly for high resolution devices, and the fact that they are static tests. Locating code transitions using a dc signal source is described in [4.7.1](#).

One use for dc tests is to perform an initial survey before proceeding with more comprehensive tests. This survey can quickly establish the upper and lower operating limits, find gross problems such as missing or stuck high order bits, and determine that the recorder is operating at least at a basic level over its entire range.

## 5. Input impedance

The input impedance is the impedance between the signal input terminal and a specified reference terminal and can be specified at various frequencies. When the frequency is not specified, the input impedance given is the low-frequency impedance. Alternatively, the input impedance can be represented as the parallel combination of a resistance and a capacitance.

### 5.1 Test method

Connect a vector impedance meter of desired accuracy and appropriate output level that matches the desired input signal range of the waveform recorder, and take readings with the input range of the recorder set to values of interest. Sweep the vector impedance meter over the frequency range of interest.

### 5.2 Alternate test method using a time domain reflectometer (TDR)

Use of a TDR may be more appropriate when the reason for measuring the input impedance is to determine how well the waveform recorder is impedance-matched to the rest of the system. A TDR gives direct dynamic measurement of a cable system or instrument reflection coefficient,  $\rho$ . The reflection coefficient can easily be converted to impedance, VSWR, and power loss factors using simple equations or nomographs. A TDR can be used to measure dc resistance, series inductance, and parallel capacitance. The TDR method is used primarily for  $50\ \Omega$  systems, but can also be used for other low-impedance systems.

Connect a TDR of appropriate output level to the input of the waveform recorder. It is desirable to use a high-quality cable whose impedance is well-defined. Unless otherwise specified, use a  $50\ \Omega$  cable. The first step is to measure the dc resistance. Adjust the horizontal display sweep rate of the TDR to a window long enough to show where the terminating reflection has settled to its final value. Set the vertical sensitivity high enough to measure any difference in step heights between the test cable and the recorder. Note the position on the screen of the settled reflection. Now repeat the measurement using a high-accuracy terminating impedance in place of the recorder. The waveform recorder input impedance can be computed from the difference in settled reflection coefficients  $\rho$  from [Equation \(40\)](#).

$$Z_i = Z_0 \frac{1+\rho}{1-\rho} \quad (40)$$

where

- $Z_i$  is the recorder impedance
- $Z_0$  is the input transmission line impedance
- $\rho$  is the reflection coefficient

If the user is interested in small reactive components of the input impedance, a positive reflection pulse corresponds to series inductance, and a negative pulse corresponds to parallel capacitance. For details, see Strickland [\[B43\]](#).

### 5.3 Input impedance for out-of-range signals

Sometimes waveform recorders are used in applications where the input signal can be greater than the FSR of the recorder but within the maximum safe operating level. The input impedance for signal levels greater than the FSR can be different from the input impedance for signals within the FSR. There can be a problem with

reflected signals when the impedance for out-of-range signals no longer matches the input transmission line impedance.

### 5.3.1 Test method

Determine the maximum signal level to be used. The level shall be less than the maximum safe operating level of the recorder. If a vector impedance meter is available with sufficient output level, use the method described in 5.1. Otherwise, connect a signal source capable of the required output level to the input of the recorder. Adjust the output signal level to the desired value. Measure the voltage and current at the input to the recorder. For dc measurements, simply divide the voltage by the current to get the impedance. For ac measurements, use a sine wave source and divide the peak-to-peak voltage by the peak-to-peak current to get the magnitude of the impedance. Measure the phase shift between the voltage and the current to get the resistive and reactive components of the impedance. Perform these measurements at frequencies of interest.

A dual-channel waveform recorder can be used to make the phase-sensitive voltage and current measurements. A calibrated attenuator can be required to measure the voltage because the level will be somewhat large due to the nature of this test. An amplifier can be required to measure the current if the recorder under test has a high input impedance. The network for measuring voltage and current will perturb the amplitude of the signal into the recorder under test. These perturbations shall be taken into account when computing the input impedance. The waveform recorder used to measure voltage and current shall have a high input impedance. If current is measured using a series resistor, the series resistor shall be small, and the measuring waveform recorder shall be capable of making a floating measurement. A pickup coil can also be used to measure ac currents.

### 5.3.2 Alternate method using time domain reflectometry

If a TDR is available with sufficient output level, use the method described in 5.2. Otherwise, the user will have to arrange a network similar to that shown in Figure 26. The key components are a pulse generator, an isolating coupler, well-characterized transmission lines, and a second waveform recorder. The pulse source shall have a fast leading transition duration and a flat top. The duration of the pulse shall be less than the two-way transit time between the recorder under test and the recorder being used to make the measurement. A competing requirement is that all cable lengths shall be relatively short to not attenuate the high-frequency components of the test pulse so much that the various measured pulses do not reach a stable final level.

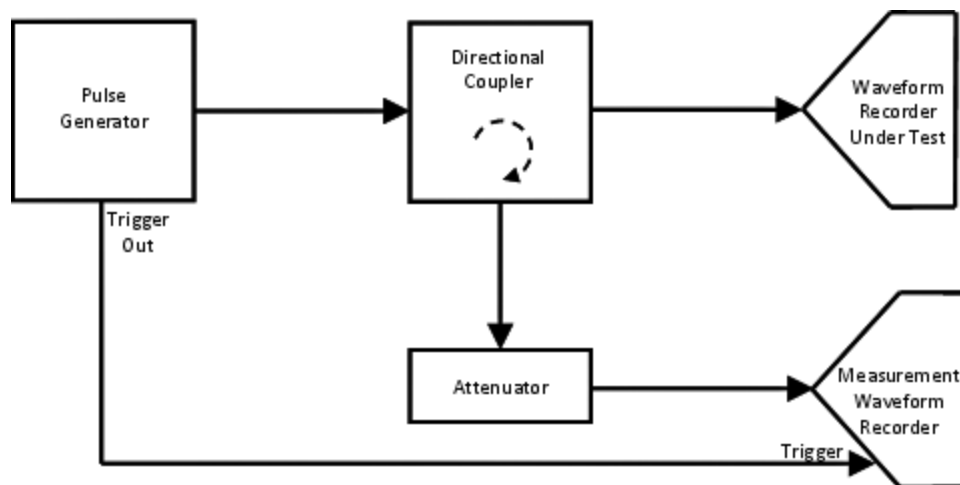


**Figure 26—Test setup for measuring input impedance for out-of-range signals by time domain reflectometry**

Adjust the output level of the pulse generator to the desired level. Again, the level shall be less than the maximum safe operating level of the recorder under test. Measure the test pulse level at the recorder input using a calibrated attenuator. Then record the pulse reflected from the input of the recorder under test. Compute the reflection coefficient,  $\rho$ , from the [Equation \(41\)](#).

$$\rho = \frac{V_{ref}}{V_{in}} \quad (41)$$

where

$V_{in}$  is the amplitude of the incident pulse at the recorder under test

$V_{ref}$  is the amplitude of the reflected pulse corrected for losses in the coupler and attenuation

Use [Equation \(40\)](#) to compute the desired input impedance. Again, reactive components can be estimated as described in [5.2](#).

## 6. Static gain and offset

Independently based gain and offset are the values by which the transition levels are multiplied and, then, to which the transition levels are added, respectively, to minimize the mean squared deviation from the ideal transition levels. Terminal-based gain and offset are the values by which the transition levels are multiplied and, then, to which the transition levels are added, respectively, to cause the deviations from the ideal transition levels to be zero at the terminal points, that is, at the first and last code transitions.

Gain and offset are nominally 1.0 and 0.0, respectively. Departures from these values represent the degree to which the device deviates from nominal performance. A gain greater than 1.0 implies that a voltage smaller than the nominal full-scale voltage can generate the full-scale output transition (exclusive of the offset).

Unless otherwise specified in this standard, gain and offset will be taken to mean independently based gain and offset.

Gain and offset values are computed from the array of measured code transition levels described in [4.7](#). The ideal code transition levels can be calculated from the slope and displacement of a linear fit to the actual transition levels. If the slope and displacement are determined by a linear least squares fit to the array of transition levels for all codes, the gain and offset are independently based. If the slope and displacement are determined by the fit that connects the first and last transition points with a straight line, the gain and offset are terminal based. The independently based method gives lower errors, while the terminal-based method is appropriate for quick adjustment of the gain and offset of the recorder. Manufacturers may specify either.

Once the array of transition levels is measured, the calculations of gain and offset are straightforward using [Equation \(43\)](#) and [Equation \(44\)](#).

### 6.1 Independently based gain and offset

#### 6.1.1 Static test method

Locate the code transition levels per [4.7](#). The transfer characteristic can then be represented by [Equation \(42\)](#).

$$G \times T[k] + V_{os} + \varepsilon[k] = Q \times (k - 1) + T_1 \quad (42)$$

where

|                  |  |
|------------------|--|
| $T[k]$           | is the input quantity corresponding to the code transition level between codes $k-1$ and $k$<br>( $T[k]$ is undefined for $k = 0$ .) |
| $k$              | is the waveform recorder output code ( $0 < k \leq 2^N - 1$ , where $N$ is the number of digitized bits.)                            |
| $T_1$            | is the first ideal transition voltage corresponding to $T[1]$  |
| $V_{os}$         | is the output offset in units of the input quantity, nominally = 0   |
| $G$              | is the gain, nominally = 1 ( $G$ is greater than 1 if a given input voltage generates a larger than nominal output code.)            |
| $Q$              | is the ideal width of a code bin, that is, the full-scale input range divided by the total number of code states                     |
| $\varepsilon[k]$ | is the residual error in the least squares fit method of computing $G$ and $V_{os}$ as described in Equation (43)                    |

(The expression on the right-hand side gives the ideal code transition levels, in input units, as a function of  $k$ , assumed to be the value of the binary coded output. For waveform recorders that can output the data already formatted in input units, the data shall be read out in or converted to a binary form before using the equation.)

Using conventional linear least squares estimation techniques, independently based offset and gain are the values of  $V_{os}$  and  $G$  that minimize  $\varepsilon$ , the mean squared value of  $\varepsilon[k]$ , over all  $k$ . The value of  $G$  that minimizes  $\varepsilon$  is given by [Equation \(43\)](#).

$$G = \frac{Q(2^N - 1) \left( \sum_{k=1}^{2^N-1} kT[k] - 2^{(N-1)} \sum_{k=1}^{2^N-1} T[k] \right)}{(2^N - 1) \sum_{k=1}^{2^N-1} T^2[k] - \left( \sum_{k=1}^{2^N-1} T[k] \right)^2} \quad (43)$$

The value of  $V_{os}$  that minimizes  $\varepsilon$  is given in [Equation \(44\)](#).

$$V_{os} = T[1] + Q(2^{N-1} - 1) - \frac{G}{2^{N-1} - 1} \sum_{k=1}^{2^N-1} T[k] \quad (44)$$

Given these values for  $G$  and  $V_{os}$ ,  $\varepsilon[k]$  is the independently based INL (see [7.1](#)).

### 6.1.2 Alternate method for determining gain and offset

The independently based static gain and offset may alternatively be found by using a least-squares fit of a straight line to the transfer curve. In order to avoid having the ends of the transfer curve, where the waveform recorder is overdriven, affect the fit, the straight line is fitted just to that portion of the transfer curve where the average output code is between its minimum value plus twice its deviation and its maximum value minus twice its deviation. This method may give slightly different results to those of the fit of straight line to the code transition levels, but the differences are insignificant in practical cases.

### 6.1.3 Comment on number of samples required

The record shall be long enough to allow the fitting algorithm to find a solution. In particular, records that are significantly shorter than the inverse of the input frequency can fail to converge on a solution.

## 6.2 Terminal-based gain and offset

### 6.2.1 General information

Terminal-based gain and offset are the values by which the transition levels are multiplied and then to which the transition levels are added, respectively, to cause the deviations from the ideal transition levels to be zero at the terminal points, that is, at the first and last code transitions. The equations for the terminal-based gain and offset are shown as [Equation \(45\)](#) and [Equation \(46\)](#).

$$G = \frac{Q(2^N - 2)}{T[2^N - 1] - T[1]} \quad (45)$$

$$V_{os} = T_1 - GT[1] \quad (46)$$

### 6.2.2 Test method

Locate the code transition levels per [4.7](#). The transfer characteristic can be represented by [Equation \(42\)](#). Terminal-based gain and offset are the values of  $G$  and  $V_{os}$  that cause  $\varepsilon[1] = 0$  and  $\varepsilon[2^N - 1] = 0$ , where  $N$  is the number of digitized bits and  $2^N - 1$  is the highest code transition defined.

For more information about the accuracy of the estimates of terminal-based gain and offset error, see Alegria and Cruz Serra [[B3](#)].

## 7. Linearity

For a perfectly linear waveform recorder, all of the code bin widths measured in [4.7](#) would be exactly equal. This clause describes a number of common measurements of nonlinearities and related effects in both the time and frequency domains.

### 7.1 Integral nonlinearity (INL)

#### 7.1.1 General information

INL is the differences between the ideal and actual code transition levels after correcting for gain and offset. INL is usually expressed as a percentage of full scale or in units of LSBs. It will be independently based or terminal based depending on how gain and offset are defined. INL is defined here to be a static parameter. For dynamic effects, see [7.7](#).

When INL is given as a single number, it is the maximum absolute value over all code bins.

#### 7.1.2 Test method

Locate the code transition levels by any of the methods in [4.7](#); then determine gain and offset per [6.1.1](#) or [6.2.2](#), as appropriate. The INL is given in percent by [Equation \(47\)](#).

$$\text{INL}[k] = 100 \frac{\varepsilon[k]}{Q \times 2^N} \quad (47)$$

where

$\varepsilon[k]$  is the residual error for code bin  $k$

$Q$  is the ideal width of a code bin, that is, the full-scale input range divided by the total number of code states

$N$  is the number of digitized bits per sample for the waveform recorder

Note that if code transitions are determined by a histogram method and the test signal parameters are inaccurately known, then the gain and offset determined here can be in error. However, the error in gain and offset will not materially affect the calculated INL.

Note that code transition levels are undefined at any codes where the recorder is not monotonic or where the codes are missing.

## 7.2 Maximum static error (MSE)

### 7.2.1 General information

MSE is the maximum difference between any code transition level and its ideal value. It is often expressed as a percentage of full scale or in LSBs.

### 7.2.2 Test method

Locate the code transition levels per 4.7. The MSE is given in percent by Equation (48) and in LSBs by Equation (49).

$$\text{MSE} = 100 \times \frac{\max\{T[k] - Q \times (k-1) - T[1]\}}{Q \times 2^N} \quad (48)$$

$$\text{MSE} = \frac{\max\{T[k] - Q \times (k-1) - T[1]\}}{Q} \quad (49)$$

where

- $T[k]$  is the code transition level for the  $k^{\text{th}}$  transition (between codes  $k-1$  and  $k$ )
- $Q$  is the ideal width of a code bin

## 7.3 Differential nonlinearity (DNL) and missing codes

### 7.3.1 General information

DNL is the difference between a specified code bin width and the average code bin width, divided by the average code bin width. When given as one number without a code bin specification, it is the maximum DNL of the entire range. A code is generally defined to be a missing code if the DNL for the code is less than  $-0.9$ .

### 7.3.2 Test method

Locate the code transition levels by any of the methods of 4.7. A set of code bin widths can then be calculated from Equation (50).

$$W[k] = T[k+1] - T[k] \quad \text{for } 1 \leq k \leq 2^N - 2 \quad (50)$$

DNL can then be calculated by Equation (51).

$$\text{DNL}[k] = (W[k] - Q')/Q' \quad (51)$$

where

- $W[k]$  is the width of code bin  $k$ ,  $T[k+1] - T[k]$
- $Q'$  is the actual average code bin width and =  $Q/G$

where

- $Q$  is the ideal code bin width
- $G$  is the static gain

Neither the width of the top bin  $W[2^N-1]$  nor that of the bottom bin  $W[0]$  is defined. Unless otherwise specified, a code  $k$  is defined to be a missing code if [Equation \(52\)](#) is true.

$$\text{DNL}[k] \leq -0.9 \quad (52)$$

Perfect DNL is defined as  $\text{DNL} = 0$ . The maximum DNL is the maximum value of  $|\text{DNL}/k|$  for all  $k$ . In addition, the rms value of the DNL can be given by [Equation \(53\)](#).

$$\text{DNL}_{\text{RMS}} = \left( \frac{1}{2^N - 2} \sum_{k=1}^{2^N-2} \{\text{DNL}[k]\} \right)^{\frac{1}{2}} \quad (53)$$

#### 7.4 Example INL and DNL data

[Figure 27](#) and [Figure 28](#) show sample plots based on the measurement of transition levels per [4.7](#) for a 12-bit recorder from an end-point calibration. [Figure 27](#) shows the INL error, and [Figure 28](#) shows DNL error.

Note that a DNL of 0 for a particular code means that code width was equal to the average width. A DNL of  $-1$  means the code was missing. A DNL of  $+1$  means the code width was twice as wide as the average.

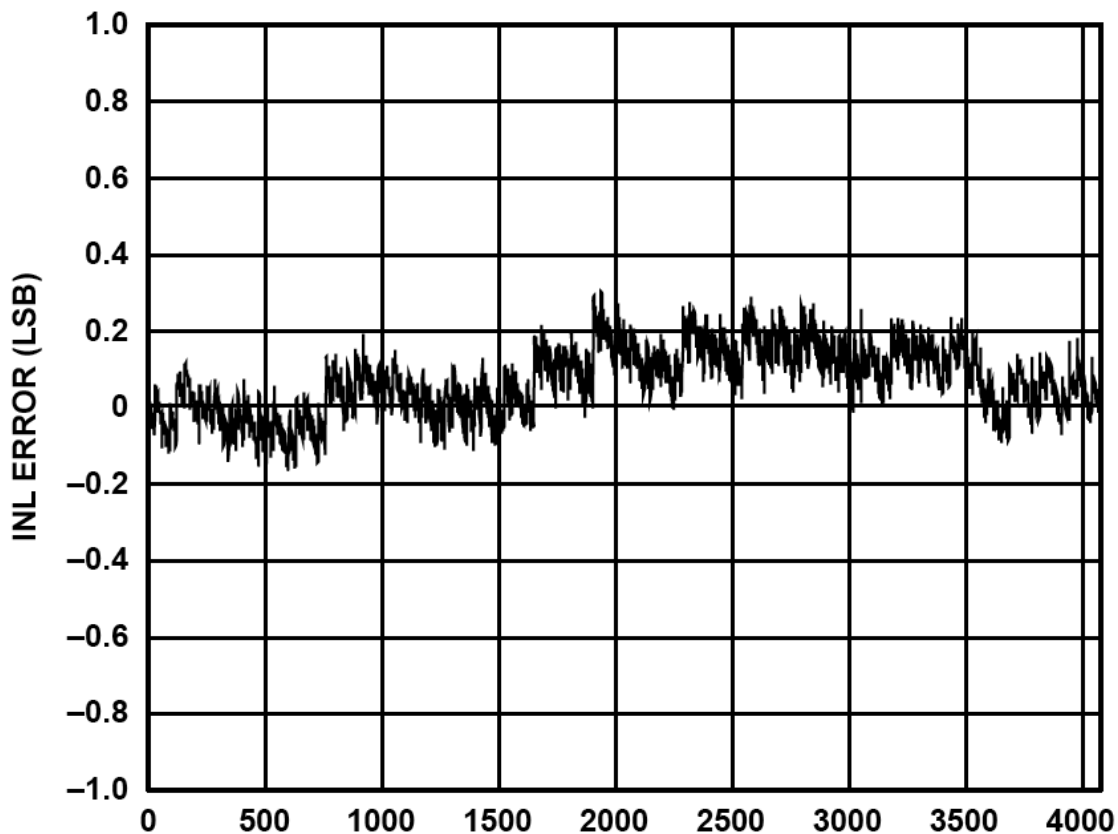
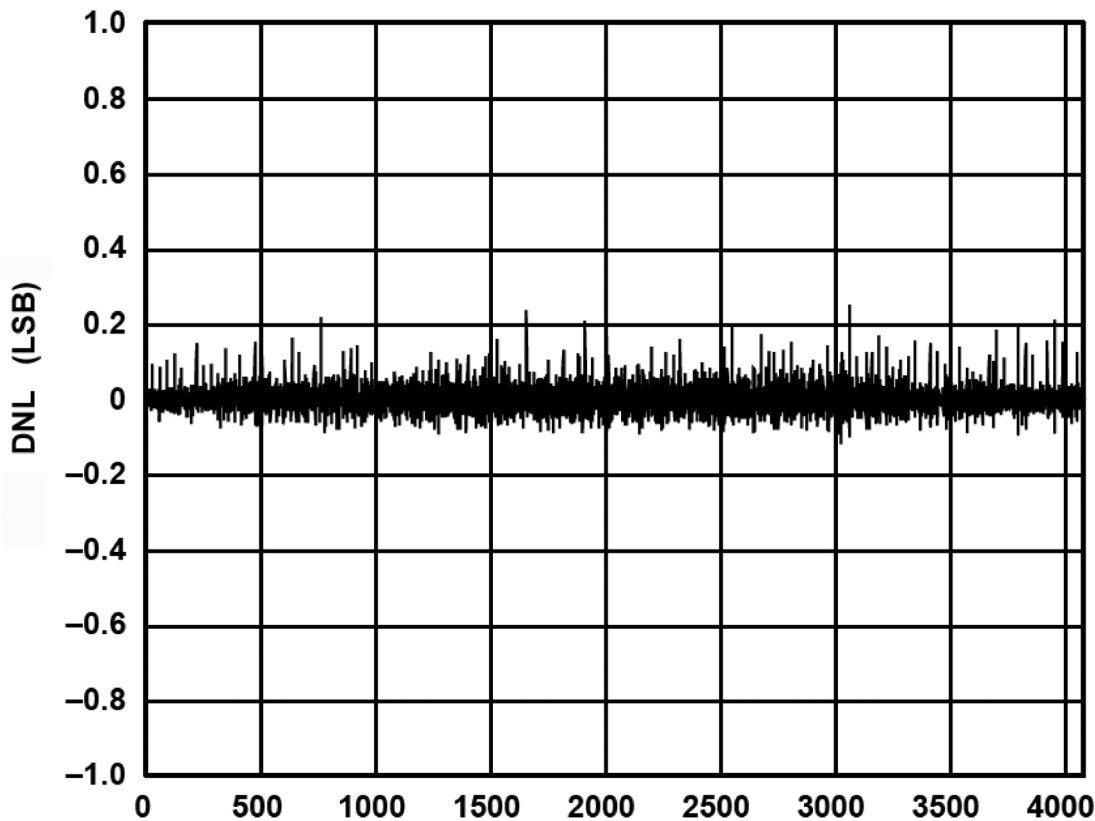


Figure 27—Example of calculated INL from a terminal-based calibrated 12-bit device



**Figure 28—DNL from a terminal-based calibrated 12-bit device**

## 7.5 Monotonicity

### 7.5.1 General information

A monotonic non-inverting waveform recorder produces output codes that are consistently increasing with increasing input stimulus and consistently decreasing with decreasing input stimulus, changing in the same direction relative to the change in input stimulus. If the input stimulus and output codes change consistently in opposite directions, e.g., a higher input produces a lower output code; the waveform recorder is monotonic and inverting.

### 7.5.2 Test method

Determine the transfer curve of the waveform recorder using both increasing and decreasing input levels, according to 4.7.11. Then the waveform recorder is considered non-monotonic if, for any pair of input levels  $x_1$  and  $x_2$ , with  $x_1 < x_2$  as shown in Equation (54) and Equation (55):

$$\bar{y}(x_1) - \frac{3 \times \sigma_y(x_1)}{\sqrt{M}} > \bar{y}(x_2) + \frac{3 \times \sigma_y(x_2)}{\sqrt{M}}, \text{ (non-inverting)} \quad (54)$$

$$\bar{y}(x_2) - \frac{3 \times \sigma_y(x_2)}{\sqrt{M}} > \bar{y}(x_1) + \frac{3 \times \sigma_y(x_1)}{\sqrt{M}}, \text{ (inverting)} \quad (55)$$

using the notation of 4.7, where  $\bar{y}(x)$  is the mean output code value and  $\sigma_y(x)$  is the standard deviation of the output code value, for a given static input signal level  $x$ , and  $M$  is the number of samples taken at each  $x$  value. Note that it is best to keep  $M > 20$  so that the standard deviation estimates  $\sigma_y(x_1)$  and  $\sigma_y(x_2)$  are statistically valid.

## 7.6 Hysteresis

The measured value of the waveform recorder transfer curve may depend on the direction by which the transfer curve is traversed (i.e., increasing or decreasing signal). The reported hysteresis of the waveform recorder, if any, is the maximum of such differences.

### 7.6.1 Test method

Determine the transfer curve of the waveform recorder using both increasing and decreasing input levels (see 4.7.11). Let  $(x)$  and  $(x)$  denote the mean output values measured at input level  $x$  for increasing and decreasing input levels, respectively, and let  $\sigma_{y+}(x)$  and  $\sigma_{y-}(x)$  be the calculated standard deviation of those measured values, for increasing and decreasing input levels, respectively. Let  $M_+(x)$  and  $M_-(x)$  be the number of measurements of the output value at input value  $x$ , for increasing and decreasing input values, respectively.

If, for all levels  $x$ , the difference between the measured mean ADC output values for increasing and decreasing input levels is within the random measurement uncertainty, i.e., if Equation (56) is true, then the waveform recorder is said to have no hysteresis.

$$|\bar{y}_+(x) - \bar{y}_-(x)| \leq \left| \frac{3 \times \sigma_{y+}(x)}{\sqrt{M_+(x)}} - \frac{3 \times \sigma_{y-}(x)}{\sqrt{M_-(x)}} \right| \quad (56)$$

Note that it is best to keep  $M_+$  and  $M_-$  greater than about 20, so that the standard deviation estimates are statistically valid. If the waveform recorder does have hysteresis, the amount is given by the magnitude of the largest observed difference, converted to the units of the input signals. Thus, in Equation (57):

$$\text{hysteresis} = \frac{|\bar{y}_+(x) - \bar{y}_-(x)|_{\max}}{G} \quad (57)$$

### 7.6.2 Comment on hysteresis and alternation

It is important to distinguish between real hysteresis and the effect of transition noise. Hysteresis is present only when the rising and falling transitions differ significantly from the transition noise.

Hysteresis can be present only when there is a significant rate of change of the input. If the effect of the slope of the input is a significant parameter, then the specification shall specify the rate of change of the input that resulted in the measured hysteresis.

A phenomenon called alternation can also be observed. It occurs when a significant range of input voltages results in adjacent recorder output codes being alternately expressed. Alternation is a complementary function to hysteresis because both hysteresis and alternation are unwanted feedbacks to the input from previous output codes. If the feedback is positive, then hysteresis is observed. If the feedback is negative, then alternation is observed.

To illustrate the phenomenon of hysteresis and alternation, consider the 1-bit ADC shown in Figure 29.

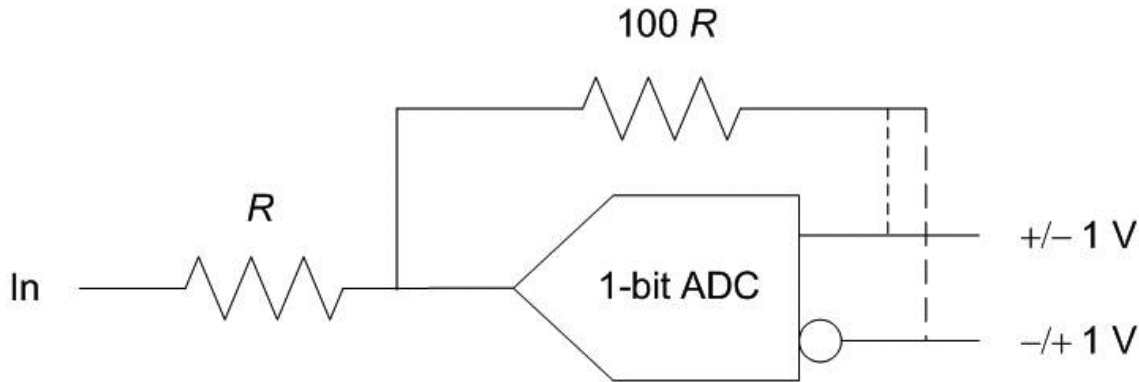


**Figure 29—Block diagram of hysteresis and alternation**

Consider the case when the “True” output is connected to the divider. The input is gradually changed from a negative voltage, which has caused the “True” output to be at the  $-1\text{ V}$  level. The output of the ADC will go to its high state only after the input voltage has exceeded  $10\text{ mV}$ . If the initial voltage had started from a positive value and then decreased, it would have to go lower than  $-10\text{ mV}$  to force the output to the low level. This phenomenon is hysteresis.

Consider the case when the “False” output is connected to the divider. The input is gradually changed from a negative voltage that has caused the “False” output to be at the  $+1\text{ V}$  level. The “True” output of the ADC will go to its high state after the input voltage has exceeded  $-10\text{ mV}$ . From that point onward, the output will alternate between the high and low states until the input voltage exceeds  $+10\text{ mV}$ . If the initial voltage had started from a positive value and then decreased, the alternation would resume when the input dropped below  $+10\text{ mV}$ . This phenomenon is alternation.

## 7.7 Total harmonic distortion (THD)

THD is the scaled square root of the sum of squares of a specified set of harmonic distortion components including their aliases for an input of a pure sine wave of specified frequency and amplitude. THD amplitude is always expressed relative to the amplitude of the applied signal, either as a percent or in decibels.

The THD is given by the ratio shown in [Equation \(58\)](#).

$$\text{THD} = \frac{\sqrt{\frac{1}{M^2} \sum_h |X[f_h]|^2}}{A_{rms}} \quad (58)$$

where

$A_{rms}$  is the rms value of the input sine wave as shown in [Equation \(59\)](#)

$$A_{rms} = \frac{1}{M} \sqrt{|X[f_i]|^2 + |X[f_s - f_i]|^2} \quad (59)$$

where

$f_i$  is the frequency of the input signal

$f_s$  is the sampling frequency (Note the use of the DFT frequency range of 0 to  $f_s$  rather than  $-f_s/2$  to  $+f_s/2$ .)

|          |   |
|----------|---|
| $X[f_h]$ | is the complex value of the spectral component at frequency $f_h$ , where $f_h$ is the $h^{\text{th}}$ harmonic frequency of the DFT of the waveform recorder output data record computed using Equation (8) in 4.5 |
| $M$      | is the number of samples in the data record   |
| $h$      | is the set of harmonics over which the sum is taken   |

The summation is taken over all of the  $h$  harmonics used that are described in the various test methods given below. The members of the set of harmonics,  $f_h$ , used in [Equation \(58\)](#) shall be specified. The choice of harmonic components included in the set is a tradeoff between the desire to include all harmonics with a significant portion of the harmonic distortion energy, but to exclude DFT bins whose energy content is dominated by random noise.

Unless otherwise specified, to estimate THD, the set normally comprises the lowest nine harmonics, i.e., 2nd through 10th inclusive, of the input sine wave.

The THD is also often expressed as a decibel ratio with respect to rms amplitude of the fundamental component of the output or as a percent.

The THD depends on both the amplitude and frequency of the applied signal. Thus, the amplitude and frequency of the input for which THD measurement(s) are made shall be specified. There are three test methods for THD based on three different methods for reducing the effects of spectral leakage.

The summation is taken over all of the  $h$  harmonics used that are described in the various test methods given below. The members of the set of harmonics,  $f_h$ , used in [Equation \(58\)](#) shall be specified. The choice of harmonic components included in the set is a tradeoff between the desire to include all harmonics with a significant portion of the harmonic distortion energy, but to exclude DFT bins whose energy content is dominated by random noise.

Unless otherwise specified, to estimate THD, the set normally comprises the lowest nine harmonics, i.e., 2nd through 10th inclusive, of the input sine wave.

The THD is also often expressed as a decibel ratio with respect to rms amplitude of the fundamental component of the output or as a percent.

The THD depends on both the amplitude and frequency of the applied signal. Thus, the amplitude and frequency of the input for which THD measurement(s) are made shall be specified. There are three test methods for THD based on three different methods for reducing the effects of spectral leakage.

### 7.7.1 Coherent sampling test method

To estimate THD, apply a test signal consisting of a pure, large amplitude sine wave at frequency  $f_i$  chosen to meet the criteria for coherent sampling. See [4.3.7.1](#) for the general sine wave test setup. See [4.5.2.2](#) for a discussion of coherent sampling and the DFT. The sine wave frequency shall not be Nyquist or any multiples thereof.

Acquire  $K$  data records of  $M$  points each from the recorder under test at sample frequency,  $f_s$ . Let  $x_k[n]$  represent the  $k^{\text{th}}$  record of sine wave data for  $k = 1, 2, \dots, K$ . For each  $x_k[n]$  record, compute the DFT,  $X_k[m]$ , where  $m$  is an integer between 0 and  $M-1$ . The  $K$  sets of data are used to compute an averaged magnitude spectrum of the DFT at each basis frequency  $f_m$  as shown in [Equation \(60\)](#).

$$X_{\text{avg}}[m] = \frac{1}{K} \sum_{k=1}^K |X_k[m]|, \quad m = 0, 1, 2, \dots, M-1 \quad (60)$$

The averaged spectral magnitude,  $X_{avg}$ , is used because it has a smaller variance than the nonaveraged spectral magnitude,  $X$ . The standard deviation of the random errors in  $X_{avg}$  is less than  $|X|$  by a factor approximately equal to the square root of  $K$  (see Jenkins and Watts [B27]).

Identify the set of bin numbers,  $n_h$ , which corresponds to the chosen set of harmonics of the input test frequency. For a test tone at frequency  $f_i$ , the harmonics are aliased so that  $f_h$  lies between zero and the sampling frequency  $f_s$ . Aliasing is accounted for by means of [Equation \(61\)](#). The default value for  $N_H$  is 10.

$$n_h = \text{mod}(hn_i, M) \quad h = \pm[2, 3, \dots, N_H] \quad (61)$$

where

- $n_i$  is the bin number of the input frequency,  $n_i = Mf_i/f_s$
- $N_H$  is the number of the highest order harmonic used

This procedure locates both Euler components of the aliased harmonics. It is important that  $n_i$  be chosen so that all of the  $n_h$  are different and that none of them is equal to either  $n_i$  or 0. THD is then given by [Equation \(62\)](#).

$$\begin{aligned} \text{THD} &= \frac{1}{M} \left( \sum_{h=2}^{N_H} X_{avg}[n_h]^2 + \sum_{h=-N_H}^{-2} X_{avg}[n_h]^2 \right) \\ A_{rms} &= \frac{1}{M} \sqrt{X_{avg}[n_i]^2 + X_{avg}[M-n_i]^2} \end{aligned} \quad (62)$$

### 7.7.2 Noncoherent sampling test method 1 (windowed DFT)

This method uses the windowed DFT to reduce the problems caused by spectral leakage. It is of value when the input frequency does not satisfy the condition for coherent sampling with sufficient accuracy. Because the windowed DFT is used, each spectral line splits into several lines, the number depending on the window. Therefore, it is necessary to use the values from several DFT bins to calculate the rms value of the input signal and each harmonic. Choose an  $L^{\text{th}}$  order cosine window, for some small integer  $L$ , following the guidance in [4.5](#).

To estimate THD, apply a test signal consisting of a pure, large amplitude sine wave. See [4.3.7.1](#) for the general sine wave test setup. Acquire  $K$  data records of  $M$  points each from the recorder under test at sample frequency  $f_s$ . Let  $x_k[n]$  represent the  $k^{\text{th}}$  record of sine wave data for  $k = 1, 2, \dots, K$ . For each  $x_k[n]$  record, compute the windowed DFT,  $X_{w,k}[m]$ , where  $m$  is an integer between 0 and  $M-1$ . The  $K$  sets of data are used to compute an averaged magnitude spectrum of the windowed DFT at each basis frequency  $f_m$  as shown in [Equation \(63\)](#).

$$X_{wavg}[m] = \frac{1}{K} \sum_{k=1}^K |X_{w,k}[m]| \quad m = 0, 1, 2, \dots, M-1 \quad (63)$$

where

- $X_{wavg}[m]$  is the spectrum averaged over  $K$  records of the DFTs of the windowed data records
- $|X_{w,k}[m]|$  is the magnitude of the DFT of each windowed record computed using [Equation \(8\)](#)

Identify the set of bin numbers,  $n_h$ , that corresponds to the chosen set of harmonics of the input test frequency. For a test tone at frequency  $f_i$ , the harmonics are aliased so that  $f_h$  lies between zero and the sampling frequency  $f_s$ . Aliasing is accounted for by means of [Equation \(64\)](#). The default value for  $N_H$  is 10.

$$n_h = \text{mod}(hn_i, M) \quad h = \pm[2, 3, \dots, N_H] \quad (64)$$

The resulting values will not be integers if the input frequency does not exactly fulfill the requirement for coherent sampling. This procedure locates both Euler components of the aliased harmonics. It is important that  $n_i$  be chosen so that all of the  $n_h$  are sufficiently different that the range of bin numbers used in their calculations (given below) do not overlap and that none of them contains either 0 or the range of bin numbers used for calculating  $X_{avg}[n_i]$ . Let  $X_{avg}[n]$  be as shown in [Equation \(65\)](#).

$$X_{avg}[n]^2 = \frac{1}{NNPG} \sum_{k=-(L+1)}^{L+1} X_{wavg}[n+k]^2 \quad \text{for } n=n_i, \text{ and } n=n_h \text{ for } h=\pm[2, 3, \dots, N_H] \quad (65)$$

where

- NNPG is the normalized noise power gain of the window, which is defined in [4.5.2.3](#)
- $n$  is the values for  $n_i$  and  $n_h$  rounded to the nearest integer
- $X_{wavg}$  is given by [Equation \(63\)](#)
- $L$  is the order of the cosine window function used

THD can then be estimated by [Equation \(66\)](#).

$$\begin{aligned} \text{THD} &= \frac{\frac{1}{M} \left( \sum_{h=2}^{N_H} X_{avg}[n_h]^2 + \sum_{h=-N_H}^{-2} X_{avg}[n_h]^2 \right)}{A_{rms}} \\ A_{rms} &= \frac{1}{M} \sqrt{X_{avg}[n_i]^2 + X_{avg}[M-n_i]^2} \end{aligned} \quad (66)$$

### 7.7.3 Noncoherent sampling test method 2 (sine fitting)

This method uses sine fitting to determine the input signal and harmonic amplitudes rather than the DFT. It is somewhat more computationally intensive than using fast algorithms for the DFT, but that is usually not a problem with today's computers. Its advantage over the method in the previous subclause is that it is less sensitive to noise and more thoroughly eliminates spectral leakage.

The data used are the same as for the other methods. To maximize accuracy, each data record shall be truncated so that it has approximately an integer number of cycles of the input signal. It is assumed that this truncated record is being used throughout this subclause. The sine fits are performed as described in [4.6](#).

Perform either a three-parameter or four-parameter sine fit to the data to determine the input amplitude  $A_1$  and, if using a four-parameter fit, the input frequency  $f_i$ . Calculate the residuals as described in [4.6.2](#).

For each harmonic number,  $h$ , between 2 and  $N_H$ , perform a three-parameter sine fit to the residuals with a frequency of  $hf_i$  to determine the harmonic amplitude  $A_h$ .

Use [Equation \(67\)](#) to calculate THD.

$$\text{THD} = \frac{\sqrt{\sum_{h=2}^{N_H} A_h^2}}{A_1} \quad (67)$$

where

- $A_h$  is the amplitude of the  $h^{\text{th}}$  harmonic

The reason for truncating the records to an approximate integer number of cycles is to allow each harmonic amplitude to be accurately determined separately.

If multiple records are used, the value for the  $A_h$  used in [Equation \(67\)](#) shall be the average of the values from the individual records.

#### 7.7.4 Comments record lengths, sample rate, and input frequency for noncoherent sampling using curve fitting

The uncertainty in the calculated harmonic distortion due to noise is proportional to the square root of the reciprocal of the record length. Thus, longer record lengths reduce the effects of noise. However, longer record lengths are more susceptible to errors due to frequency instability, which could cause the frequency to be not constant throughout the record. The record length can be truncated to minimize leakage between components by including in the record only the number of points that are close to an integer number of cycles of the fundamental. If the record length is not truncated to approximate an integer number of cycles, there will be some “leakage” between the calculated harmonic values. If the harmonics are at random phases with respect to the fundamental and the harmonics are all 1% of the fundamental, then [Figure 30](#) shows distribution of deviation from the nominal of the THD and the fundamental when 6.5 cycles of the signal are present in the record. The observed leakage can theoretically be reduced by solving many simultaneous equations, but the simplified algorithm has well-bounded errors as shown in the plot in [Figure 30](#). The errors introduced by noncoherent sampling can be reduced by taking multiple records and averaging the results.

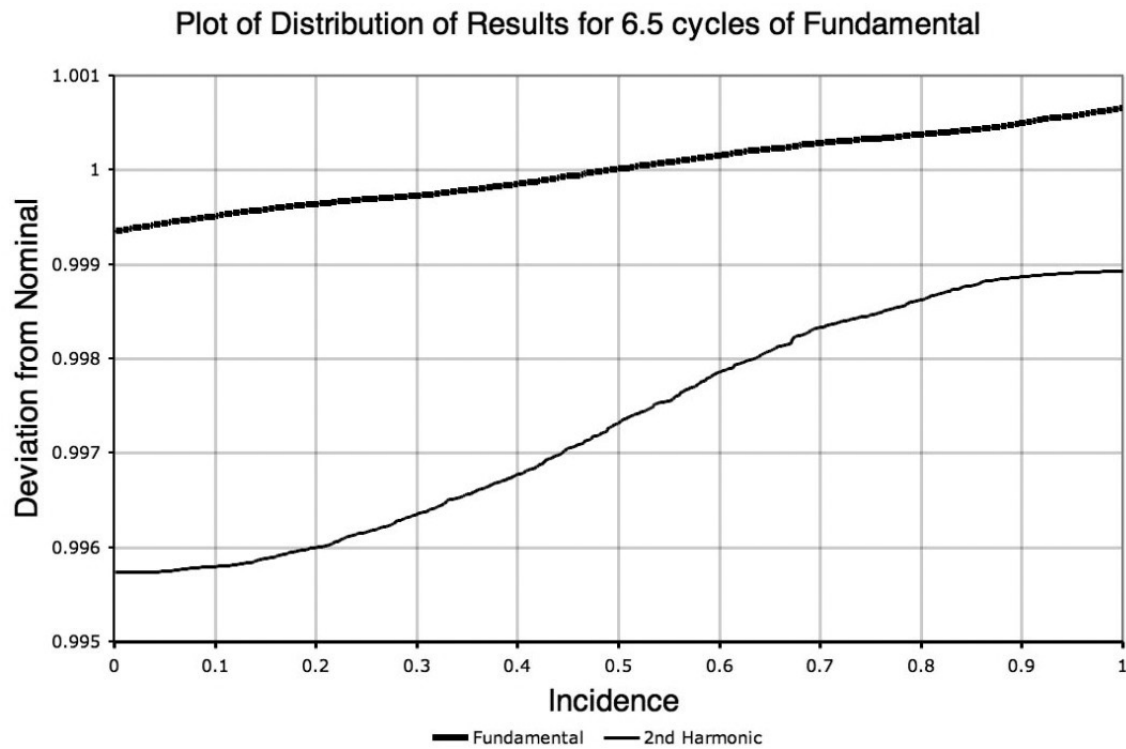


**Figure 30—Plot of distribution of calculated values of fundamental and harmonic amplitudes for noncoherent sampling with random phase between the 2nd harmonic and the fundamental**

The error in the calculation of THD is a strong function of the number of cycles of the waveform that are included in the record. The worst deviations occur when  $M+0.5$  cycles of the fundamental are included in the record. The plot in [Figure 31](#) illustrates the variation in the THD as  $M$  is increased (the phases of the harmonics are fixed in this plot at  $\pi/4$ , and the record length is fixed at 16 384 samples). The error in the THD is interpreted

as a fraction of the measured THD. From the graph, a user can observe that with a 10-cycle record, a measured THD of 1% could actually be between 1.014% and 0.986%.

It can be observed that the THD deviation varies inversely with the number of cycles over a wide range. The largest deviations are concurrent with a smaller number of cycles. When a small number of cycles are present in the record, it is fairly easy to correct the THD deviations by truncating the record length.

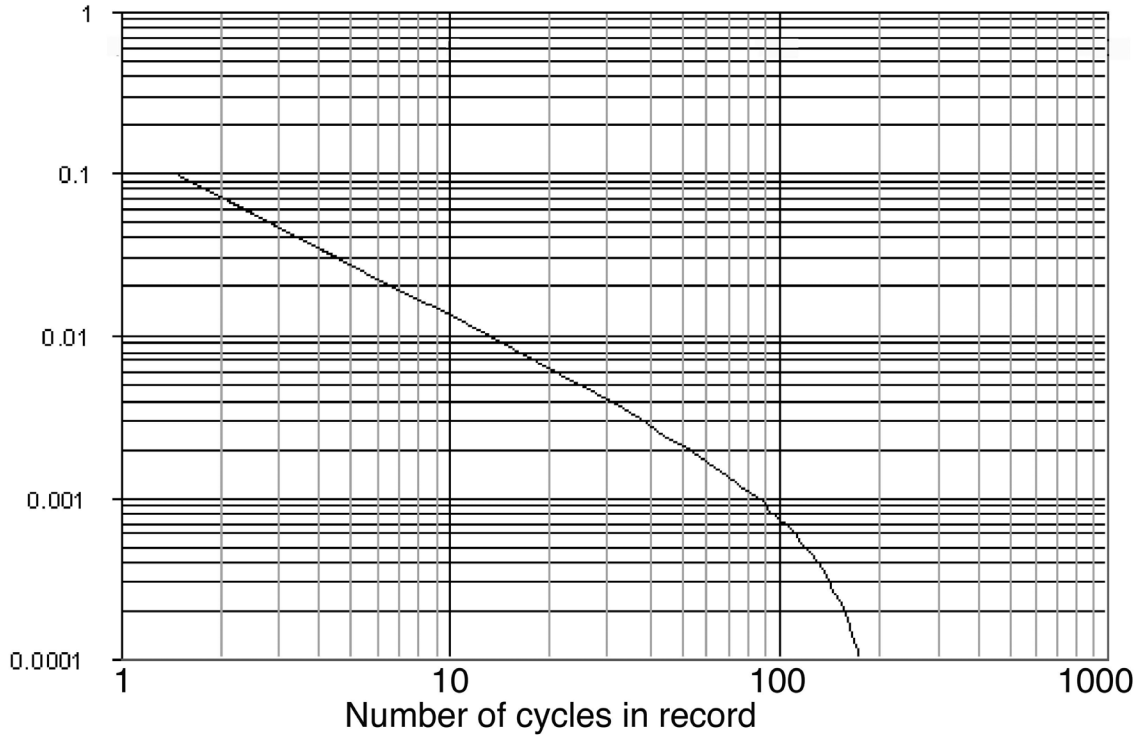


**Figure 31—THD deviation from true value as a function of number of cycles in the record**

## 7.8 Intermodulation distortion (IMD)

IMD is the generation of distortion signals at the sum and difference frequencies of the inputs due to nonlinearities in the waveform recorder frequency response when there is an input signal with multiple frequencies at the input to the recorder. IMD can occur whenever a waveform recorder is sampling a signal composed of two or more sine waves or narrow-band signal groups. This subclause describes different measures that are used to quantify such behavior. IMD spectral components can occur at sum and difference frequencies for all possible integer multiples of the input frequency tones or signal group frequencies. It is a phenomenon due to modulation and can be explained through the use of power series to model the nonlinear transfer function, or integral characteristic, of the device under test.

The measure described in 7.8.1 is based upon the use of an input composed of two independent pure sine waves. The cautionary comments given in 7.7.4 also apply to this test.

### 7.8.1 Two-tone intermodulation test method

Apply a test signal consisting of two independent pure sine waves with test frequencies  $f_{r1}$  and  $f_{r2}$  at values that are an odd number of DFT bins away from  $f_s/2$  with  $f_{r2} > f_{r1}$ . The difference,  $\Delta f$ , between  $f_{r2}$  and  $f_{r1}$  is then always an even number of DFT bins. See 4.3.7.1 for the general sine wave test setup.

Take  $K$  records of data. Compute the averaged magnitude spectrum  $X_{avg}[m]$  using Equation (60) in 7.7.1 as described for the THD test.

IMD magnitudes for a two-tone input signal are found at specified sum and difference frequencies,  $f_{imf}$ .

The difference frequencies are noted in Equation (68).

$$f_{imf} = |(i)f_{r2} - (j)f_{r1}| \quad (68)$$

And the sum frequencies are noted in Equation (69).

$$f_{imf} = (i)f_{r2} + (j)f_{r1} \quad (69)$$

where

$i, j$       is integers so that  $|i| + |j| > 1$

#### 7.8.1.1 Comments on test procedure

There are no specific guidelines to specify what frequencies and signals are to be used to perform intermodulation tests because the test parameters are influenced by each individual application. The size of  $\Delta f$  depends upon the application and the information desired.

The range for the integers  $i$  and  $j$  only needs to span nonnegative values; however, conjugate Euler frequencies can be determined using negative integers if desired. Range limits of three or four are appropriate for a waveform recorder whose harmonic distortion test (see 7.7) shows that 2nd and 3rd harmonic distortion are dominant. Note that for small  $\Delta f$ , the intermodulation frequencies are clustered around harmonics of  $f_{r1}$  and  $f_{r2}$ . The location of the aliased intermodulation frequencies, within the sampling band, follows the modulo  $f_s$  procedure specified in Equation (61) in 7.7.1.

Two-tone IMD is generally a function of the amplitudes  $X_{avg}[f_{r1}]$  and  $X_{avg}[f_{r2}]$  and the frequencies  $f_{r1}$  and  $f_{r2}$  of the input components. Thus, the amplitudes and frequencies of the input components for which IMD measurement(s) are made shall be specified.

#### 7.8.1.2 Additional comments

Note that the term “ $m^{\text{th}}$ -order” is commonly used to describe specific nonlinear system behavior such as “third-order” intercept points, etc. The “ $m^{\text{th}}$ -order intermodulation products” are found for the values of  $i$  and  $j$  that satisfy  $m = |i| + |j|$  for the sum and difference frequencies defined by Equation (68) and Equation (69). For example, for  $m = 3$ ,  $(i, j) = (3, 0), (2, 1), (1, 2)$ , and  $(0, 3)$ . The frequencies found for  $i = 0$  or  $j = 0$  correspond to harmonic distortion. However, the measured distortion can be different from that measured for single sine wave input due to the presence of the other input sine wave.

A typical set of IMD tests might involve three pairs of frequencies  $f_{r1}$  and  $f_{r2}$ , e.g., pairs of frequencies close to 0,  $f_s/4$ , and  $f_s/2$  for a conventional Nyquist-band-limited waveform recorder application. The three pairs of frequencies would also be exercised at different input amplitude combinations, e.g., each at  $-7$  dB,  $-20$  dB, and  $-40$  dB full scale (dBFS); or one tone could be held at  $-7$  dBFS while the other is incremented in equal

steps from the noise floor to  $-7$  dBFS. Other waveform recorder applications, such as intermediate-frequency sampling, can require IMD tests with input frequencies spanning from  $f_s/2$  to  $f_s$ , etc.

One caution about this test is that it is important that the test-input signal be free of any significant amount of IMD. This is not easy when a high-resolution waveform recorder (12 bits or greater) and wide bandwidths are involved. IMD can easily occur between two signal generators that have output-leveling circuitry and are coupled to one another through balanced, or so-called isolated, ports of a hybrid and other coupling circuits. In addition, the hybrids, or passive filters, used to combine two tones shall be operated well within their linear range limits in order to avoid the generation of IMD in the resulting test signal input to the waveform recorder.

### **7.8.2 Multi-tone IMD**

Multi-tone IMD tests are often used to assist in the system design process to determine limits for signal dynamic range, useful frequency bands for different signal groups, and the location of the input signal noise floor to mask small intermodulation components for a given waveform recorder. Single-tone harmonic distortion measures are useful to obtain general ideas about the linearity of a given waveform recorder, but such data do not lead directly to models that predict useful intermodulation performance measures for independent input signal groups.

A typical test procedure uses a computer-controlled DAC to generate a signal composed of a set of sine waves having frequencies that are set at DFT bin center frequencies. Gaps between the tones are used as observation points to measure IMD in the spectrum of  $X_{avg}$  as the amplitudes of the tones are uniformly increased from the noise floor to a level where the signal starts to be clipped as it exceeds the waveform recorder FSR. Such a test provides results similar to the NPR test, but allows for better simulation of expected signal group waveforms. Because such tests are application-specific, there are no useful equations provided here to describe this procedure or the quantification of its results.

## **7.9 Noise power ratio (NPR)**

### **7.9.1 General information**

NPR is the ratio of the average out-of-notch to the average in-notch power spectral density magnitudes for the DFT spectrum of the waveform recorder output sample set computed by using a notch-filtered broadband white-noise generator as the input.

The dynamic performance of a waveform recorder with broad bandwidth input is sometimes characterized by measuring NPR. In waveform recorder applications where the input signal contains a large number of incoherent tones or narrow bandwidth signals, it is generally desired that distortion, due to combinations of strong signal components, not interfere with detection of weaker signal components. An example of such an input signal is one that contains a large number of frequency-division multiplexed voice channels. Because it is impossible to design a test that embodies the specific features of all possible applications, NPR has been adopted as a figure of merit for characterizing waveform recorder performance in response to broad bandwidth signals. As explained below, the test leads to a number, the maximum NPR, by comparison of measured data to an ideal curve.

Waveform recorders possessing measured NPRs that closely match theoretical NPR, for an ideal  $N$ -bit device, are desirable candidates for broadband signal applications, e.g., a signal containing many frequency-division multiplexed channels.

### **7.9.2 Test method for NPR**

Use an arbitrary waveform generator (AWG) or a noise generator as the input test signal. Use the test setup shown in [Figure 32](#). The normal procedure is to create a curve in a series of steps that proceeds as follows. A random noise process is generated so that it possesses an approximately uniform spectrum up to a chosen

cutoff frequency,  $f_{co}$ , which is less than half the sampling frequency. A narrow band of frequencies is then removed from the noise using a notch filter, or preferably, the AWG pattern is tailored to remove the signals in the notch. To obtain a meaningful measurement, the depth of the notch shall be at least 10 dB greater than the NPR value being measured. In addition, the width of the notch shall be narrow compared to the overall noise bandwidth. With the notched noise applied to the waveform recorder input, the frequency spectrum of a captured code sequence is computed. See [Figure 33](#) for an example spectrum and [Figure 34](#) for the time domain equivalent signal. The *NPR* is then calculated in decibels from [Equation \(70\)](#) as follows:

$$\text{NPR} = 10 \log_{10} \left( \frac{P_{No}}{P_{Ni}} \right) \quad \text{dB} \quad (70)$$

where

$P_{No}$  is average power spectral density outside the notched frequency band

$P_{Ni}$  is the average power spectral density inside the notched band

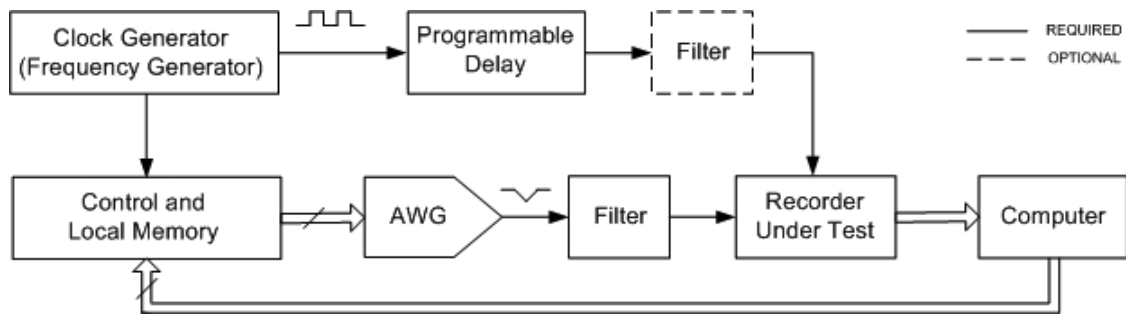


**Figure 32—Test setup for measuring NPR**

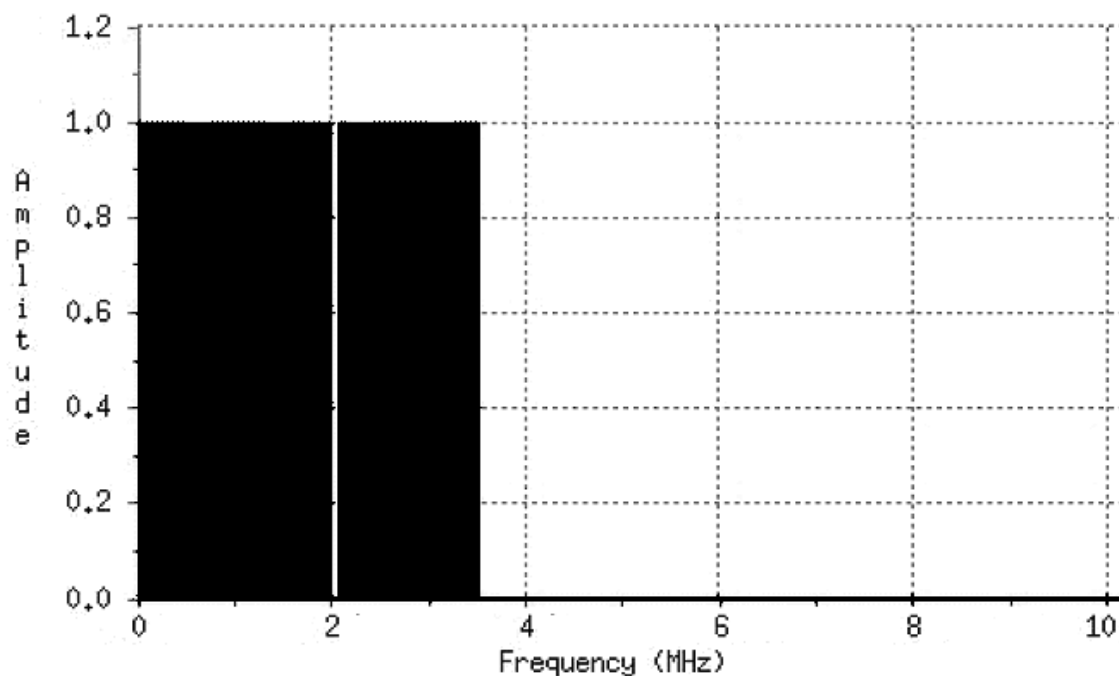


**Figure 33—Spectrum of NPR test signal**

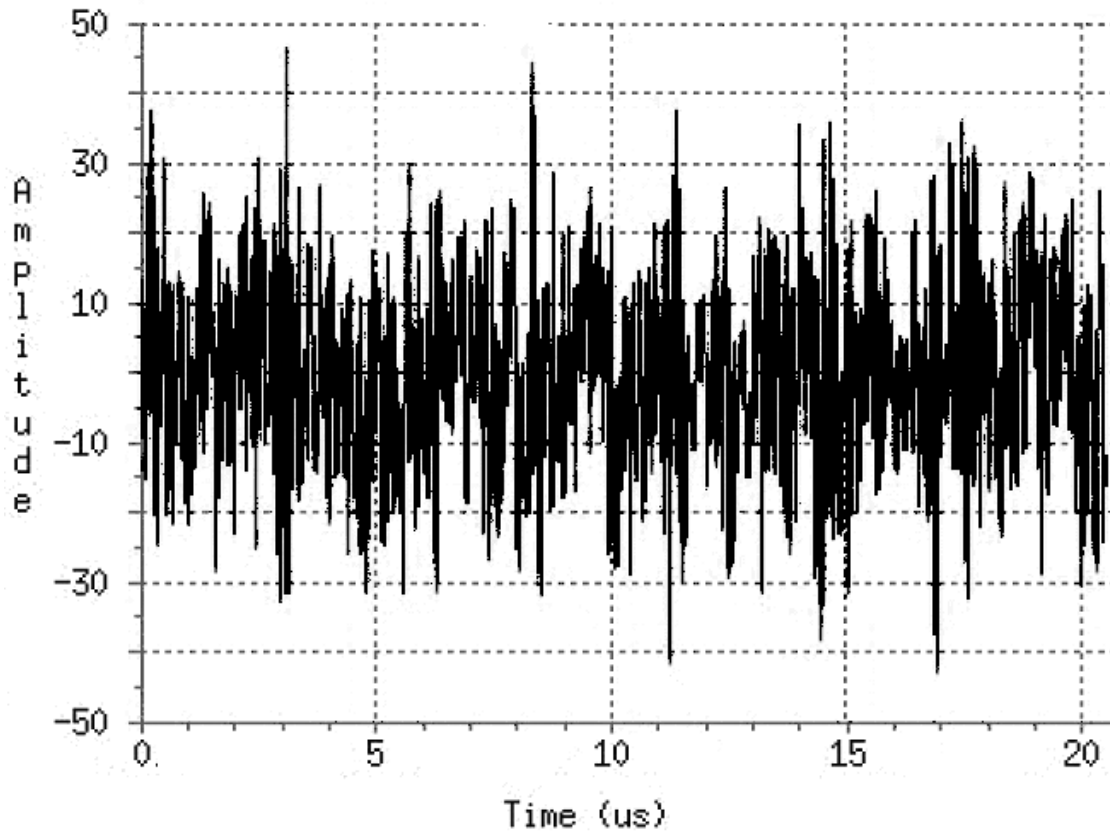


**Figure 34—Time domain representation of NPR test signal**

**Table 6** lists theoretical maximum NPR,  $NPR_{max}$ , values for ideal  $N$ -bit quantizers for both Gaussian and uniform random noise sources. These values were obtained from [Equation \(71\)](#) and [Equation \(72\)](#) given in [7.9.2.3](#). The parameter  $\alpha$  is the signal input level relative to the FSR in decibels.

**Table 6—Maximum NPR for Gaussian and uniform noise sources**

| Source no.<br>of bits | Uniform<br>$\alpha$ (dB) | $NPR_{max}$ (dB) | Gaussian<br>$\alpha$ (dB) | $NPR_{max}$ (dB) |
|-----------------------|--------------------------|------------------|---------------------------|------------------|
| 6                     | -4.65                    | 36.20            | -10.31                    | 29.94            |
| 8                     | -4.77                    | 48.16            | -11.87                    | 40.60            |
| 10                    | -4.77                    | 60.21            | -13.04                    | 51.56            |
| 12                    | -4.77                    | 72.25            | -14.02                    | 62.71            |
| 14                    | -4.77                    | 84.29            | -14.80                    | 74.01            |
| 16                    | -4.77                    | 96.33            | -15.45                    | 85.40            |
| 18                    | -4.77                    | 108.37           | -16.04                    | 96.88            |
| 20                    | -4.77                    | 120.41           | -16.62                    | 108.41           |

#### 7.9.2.1 NPR testing issues

Some experimentation with the test procedures in [7.9.2](#) may be necessary to obtain reliable measures of the NPR.

### 7.9.2.2 Input signal filtering

In practice, it is usually necessary to low-pass-filter the input noise signal to prevent aliasing and to obtain a uniform noise power across the input signal spectrum. When the noise bandwidth is low-pass-filtered to obtain a bandwidth less than the Nyquist frequency, the peak data listed in [Table 6](#) are valid for the Gaussian input signal because they are dependent upon the average input power. However, for the uniformly distributed input, the data deteriorate toward the Gaussian values because, as the signal is low-pass-filtered, the convolution of signal with filter response converges toward a Gaussian process as the bandwidth is lowered from the full Nyquist band. If a user plots NPR measurements based upon the input prior to low-pass filtering, then the input at maximum NPR will shift according to the bandwidth ratio, in decibels, of the filter cutoff frequency  $f_{co}$  to the Nyquist frequency  $f/2$ .

#### 7.9.2.2.1 Notch filter width

Another factor that affects measured NPR is the width of the notch filter. Assuming that the measured NPR is obtained from DFT spectral estimates, widening of the notch filter and averaging the noise power contained in the DFT bins inside the notch improves the estimated NPR when compared to using a single bin for the estimate of average noise power in the notch. Making the notch too wide, however, degrades the estimated NPR because the assumption for a uniform noise spectrum could be jeopardized.

#### 7.9.2.2.2 Windowing

For some cases, the depth of the filtered notch can be degraded due to spectral leakage. The use of windowing eliminates this effect at the expense of a small change in the noise floor. See [4.5.2](#) for additional details on the effects of windowing.

#### 7.9.2.3 Measured and theoretical NPR

It is customary to plot measured and theoretical NPR versus the mean noise power of the input noise process as described by Daboczi [[B18](#)] and Irons, Riley, and Hummel [[B26](#)]. For a non-ideal  $N$ -bit waveform recorder, measured NPR curves follow theoretical response at small input power levels given that the waveform recorder does not have excess internal noise. Measured NPR curves normally depart from theory prior to reaching theoretical maximum NPR due to waveform-recorder-generated harmonic distortion and IMD. It is also true that the measured curve will depart from theory for very small power levels where peak-to-peak signals are less than 1 LSB of the recorder.

The maximum measured NPR value is used to specify waveform recorder response to broadband signals with a single number, but it is also necessary to specify the type of noise source used for the test. The theoretical NPR equations for Gaussian and uniform distribution signals are given in [Equation \(71\)](#) and [Equation \(72\)](#), respectively. See Irons, Riley, and Hummel [[B26](#)] for more information.

$$\text{NPR}_G = \frac{\alpha^2}{\left[ \frac{2^{-2N}}{3} - \frac{2\alpha}{\sqrt{2\pi}} e^{-\frac{1}{2\alpha^2}} + (1+\alpha^2) \frac{2}{\sqrt{\pi}} \int_{\frac{1}{\sqrt{2\alpha}}}^{\infty} e^{-v^2} dv \right]} \quad (71)$$

$$\text{NPR}_U = \frac{(\sqrt{3}\alpha)^3}{(\sqrt{3}\alpha)2^{-2N} + (\sqrt{3}\alpha - 1)^3 u(\sqrt{3}\alpha - 1)} \quad (72)$$

where

$$\alpha \text{ is } 2 V_{in rms} / \text{FSR}$$

where

- $V_{in\ rms}$  is the rms of the actual input to the waveform recorder
- $N$  is the number of waveform recorder bits
- $u$  is the unit step function
- $v$  is a dummy integration variable

Example plots of [Equation \(71\)](#) and [Equation \(72\)](#) compared with simulated measured data are shown in [Figure 35](#) and [Figure 37](#), respectively, for an 8-bit quantizer. An example simulated broadband signal for a 12-bit AWG-generated notch-filtered uniform distribution spectrum is shown in [Figure 37](#). The plot has several notable features. It is symmetric about its center,  $f_s/2$ ; the middle notch is an anti-aliasing filter with cutoff  $f_{co}$ ; and the left notch is the NPR measuring filter. The corresponding histogram for a 16 K-sample set is shown in [Figure 38](#). Note that this histogram looks nearly uniform, but the rounding is due to spectral convolution with the anti-aliasing and notch filters.

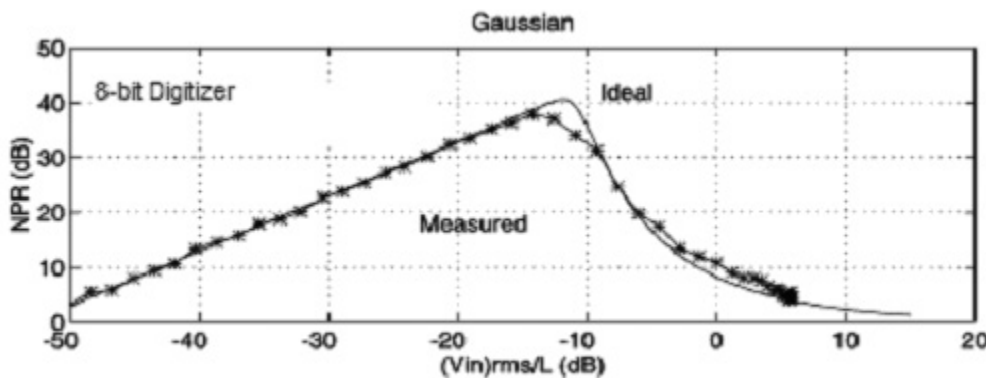


**Figure 35—Plot of ideal and measured NPR for a Gaussian noise input from [Equation \(71\)](#)**

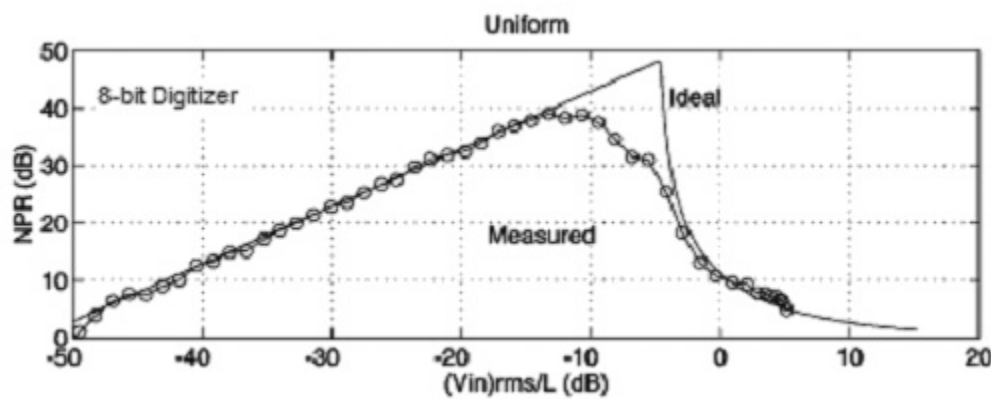


**Figure 36—Plot of ideal and measured NPR for a uniform noise input from [Equation \(72\)](#)**

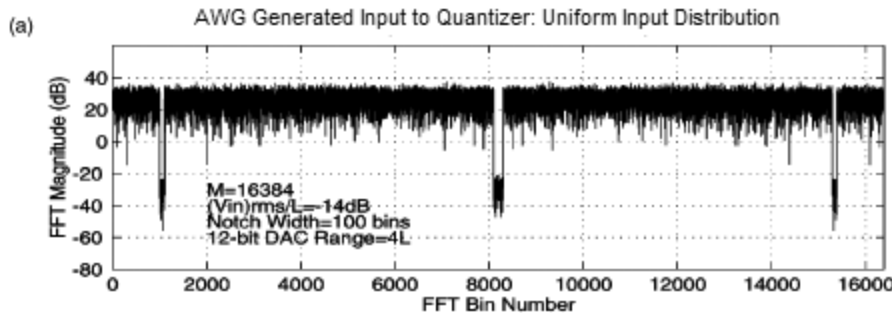


**Figure 37—Frequency domain AWG generated NPR test input to the waveform recorder**

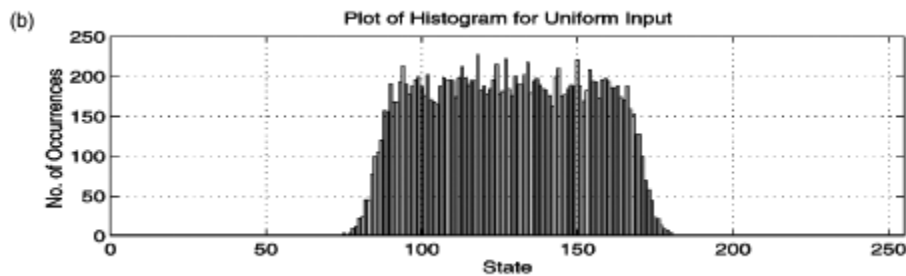


**Figure 38—Histogram from 16 K sample set**

#### 7.9.2.4 Comments on NPR

Insight into the NPR response can be obtained by considering an ideal  $N$ -bit waveform recorder. The mean-squared quantization error for such a device is  $Q^2/12$ . Assuming that the input signal does not saturate the waveform recorder, the quantization error is independent of the input power level. This ideal quantization noise exhibits a uniform spectrum with the noise power evenly distributed over the full Nyquist band. When the input noise power is greater than the quantization power, an increase of 1 dB in input power yields a 1 dB increase in NPR because the quantization power spectral density in the notch remains constant. The linear slope of the NPR curve is thus maintained as long as the waveform recorder operates within its unsaturated signal range and other nonlinearities are not present in the waveform recorder's response to the broadband test signal.

## 8. Noise<sup>7</sup>

Noise is any deviation between the output signal (converted to input units) and the input signal. Noise does not include deviations caused by linear time invariant system response (gain and phase shift), a dc level shift, THD, or an error in the sample rate.

<sup>7</sup>This definition of noise differs from the definition in a previous version of this standard (IEEE Std 1057-1994). It also differs from the definition in IEEE Std 1241-2000. It agrees with the definition of noise in IEEE Std 1241-2010 [B24]. The difference is that the older definitions included THD, while the new ones do not.

## 8.1 Comments on noise

Noise has historically been an ambiguous term. In this standard, noise is defined as indicated in this clause. Noise includes the effects of random errors, nonlinearities producing harmonics at frequencies greater than those used in measuring THD, quantization errors, spurious signals, and time base errors (fixed error in sample time and aperture uncertainty).

## 8.2 Ratio of signal to noise and distortion (SINAD)

SINAD is the ratio of rms signal to rms NAD. Unless otherwise specified, SINAD is measured using sine wave input signals. SINAD depends on the amplitude and frequency of the applied sine wave. The amplitude and frequency at which the measurement is made shall be specified.

### 8.2.1 Test method for SINAD

Apply a sine wave of specified frequency and amplitude to the waveform recorder input. See [4.3.7.1](#) for the general sine wave test setup. A large signal is preferred. The frequency of the input sine wave is called the fundamental frequency. Almost any error source in the sine wave other than frequency accuracy, gain accuracy, and dc offset can affect the test result; therefore, it is recommended that a sine wave source of good short-term stability be used and that it be highly filtered to remove distortion and noise.

Take a record of data. To find NAD, fit a sine wave to the record at the fundamental frequency per [4.6](#) and use [Equation \(73\)](#).

$$\text{NAD} = \left[ \frac{1}{M} \sum_{n=1}^M (x[n] - x'[n])^2 \right]^{1/2} \quad (73)$$

where

- $x[n]$  is the sample data set
- $x'[n]$  is the data set of the best-fit sine wave
- $M$  is the number of samples in the record

The SINAD is given by [Equation \(74\)](#).

$$\text{SINAD} = A_{\text{rms}} / \text{NAD} \quad (74)$$

where

- $A_{\text{rms}}$  is the rms signal and is equal to the peak amplitude of the fitted sine wave divided by  $\sqrt{2}$
- NAD is given by [Equation \(73\)](#)

### 8.2.2 Coherent sampling test method for SINAD in the frequency domain

SINAD can be determined equivalently from the frequency domain as a consequence of Parseval's Theorem. Apply an appropriate sine wave as described in the test procedures in [8.2.1](#). Compute the DFT of the measured waveform. Both quantities required to compute SINAD, the rms input signal and the rms NAD, can be determined from the DFT of data records as was done for THD in [7.7.1](#). The rms signal,  $A_{\text{rms}}$ , is obtained from [Equation \(62\)](#) in [7.7.1](#). NAD is found from the sum of all the remaining Fourier components after the bins at dc and at the test frequencies have been deleted from the spectrum as shown in [Equation \(75\)](#).

$$\text{NAD} = \frac{1}{\sqrt{M(M-3)}} \left[ \sum_{m \in S_0} X_{\text{avg}}[m]^2 \right]^{1/2} \quad (75)$$

where

- $S_0$  is the set of all integers between 1 and  $M-1$ , excluding the two values that correspond to the fundamental frequency and the zero-frequency term
- $X_{\text{avg}}$  is the averaged spectral magnitude, as defined in [Equation \(60\)](#) in [7.7.1](#)

SINAD is then given by substitution of NAD and  $A_{\text{rms}}$  into [Equation \(74\)](#).

### 8.3 Signal to noise ratio (SNR)

The SNR is the ratio of the rms signal to the rms noise for a sine wave input signal of a specified frequency and amplitude. The rms noise is determined by determining the rms noise and distortion as described in [8.2.1](#) or [8.2.2](#) and then determining the distortion as described in [7.7.1](#), [7.7.2](#), or [7.7.3](#). The SNR is given by [Equation \(76\)](#).

$$\text{SNR} = \frac{A_{\text{rms}}}{\eta} \quad (76)$$

where

- $A_{\text{rms}}$  is the rms signal as determined in [8.3.1](#), [8.3.2](#) or [8.3.3](#)
- $\eta$  is the rms noise as determined in [8.3.1](#), [8.3.2](#) or [8.3.3](#)

#### 8.3.1 Coherent sampling test method for SNR

Determine the NAD as described in [8.2.2](#). Determine  $A_{\text{rms}}$  and THD as described in [7.7.1](#). Let

$$\eta = \sqrt{\text{NAD}^2 - A_{\text{rms}}^2 \text{THD}^2} \quad (77)$$

SNR is defined by [Equation \(76\)](#).

#### 8.3.2 Noncoherent sampling test method 1 for SNR (windowed DFT)

Determine the NAD as described in [8.2.1](#). Determine  $A_{\text{rms}}$  and THD as described in [7.7.3](#). Use [Equation \(77\)](#) and [Equation \(76\)](#) to determine SNR.

#### 8.3.3 Noncoherent sampling test method 2 for SNR (sine fitting)

Determine the NAD as described in [8.2.1](#). Determine  $A_{\text{rms}}$  and THD as described in [7.7.3](#). Use [Equation \(77\)](#) and [Equation \(76\)](#) to determine SNR.

### 8.4 Comments on SINAD and SNR

These ratios are both dependent on the amplitude of the test signal  $A_{\text{rms}}$ . It is customary to use a near full-scale signal for these measures. However, if clipping does occur, the measures will be severely degraded. In addition, these measures are generally a function of the frequency  $f_i$  of the input sine wave. Thus, the amplitude and frequency of the input for which the SINAD and/or SNR measurements are made shall be specified.

## 8.5 Effective number of bits (ENOB)

### 8.5.1 Calculating ENOB

For an input sine wave of specified frequency and amplitude, ENOB is the number of bits of an ideal waveform recorder for which the rms quantization error is equal to the rms NAD of the waveform recorder under test. ENOB is given by [Equation \(78\)](#).

$$\text{ENOB} = \log_2 \left( \frac{\text{FSR}}{\text{NAD}\sqrt{12}} \right) \approx N - \log_2 \left( \frac{\text{NAD}}{\epsilon_Q} \right) \quad (78)$$

where

- $N$  is the number of bits digitized
- FSR is the full-scale range of the recorder
- NAD is rms noise and distortion and is defined in [Equation \(73\)](#)
- $\epsilon_Q$  is the rms ideal quantization error

The second equality in [Equation \(78\)](#) comes from [Equation \(79\)](#).

$$\epsilon_Q = \frac{Q}{\sqrt{12}} \quad (79)$$

The quantity ENOB depends on the amplitude and frequency of the applied sine wave. The amplitude and frequency at which the measurement was made shall be specified.

### 8.5.2 Test method for ENOB

Because ENOB is completely determined by the NAD, the test method is identical to that for NAD. Find the actual NAD described in [8.2.1](#) and apply [Equation \(78\)](#).

### 8.5.3 Low noise test method for ENOB

When the noise level of the waveform recorder is low enough so that the quantization error is significant compared to the random noise, the ENOB calculation can be affected by the amplitude and offset of the applied signal in an undesirable way. This effect can be greatly reduced by changing the calculation as follows:

- a) Collect a record of data as described in [8.2.1](#).
- b) Let  $x_0$  be the average of the maximum and minimum data values collected.
- c) Form a histogram of the values of the data samples collected.
- d) Let  $x_{\max}$  be the data value greater than  $x_0$  with the highest histogram count.
- e) Let  $x_{\min}$  be the data value less than  $x_0$  with the highest histogram count.
- f) Remove from the data record any values with  $x \geq x_{\max}$  or with  $x \leq x_{\min}$ .
- g) Fit a sine wave to the reduced data set (which will not have uniform time spacing).
- h) Calculate NAD using [Equation \(73\)](#) with the reduced data set.
- i) Calculate ENOB using [Equation \(78\)](#).

This procedure eliminates the data near the peaks of the sine wave and is illustrated in [Figure 39](#), where the omitted code bins are cross-hatched. See Blair [B14] for a thorough discussion of the advantages of this approach.

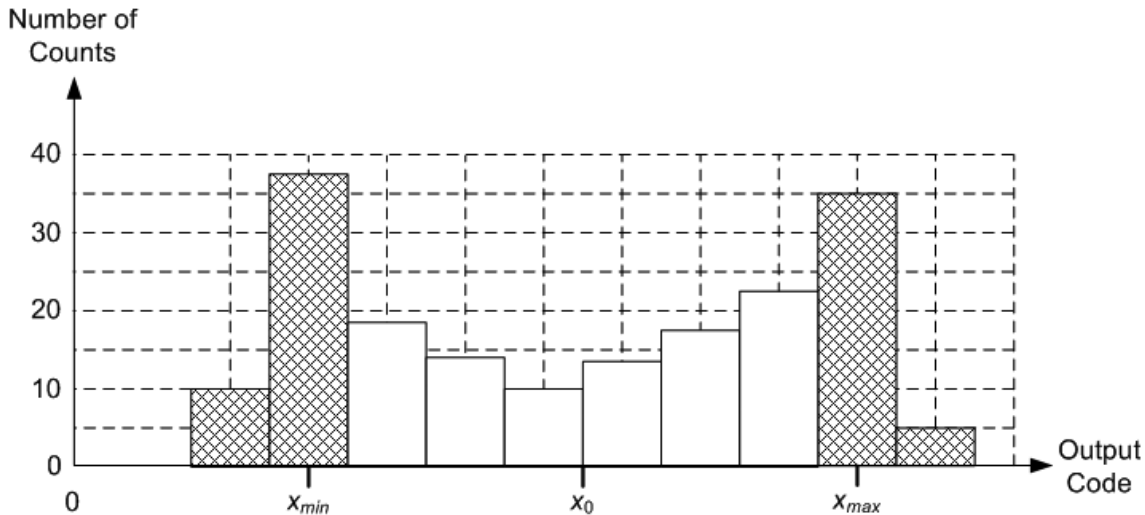


**Figure 39—Illustration of the use of the histogram to remove the sine wave peaks**

#### 8.5.4 Comment on ideal quantization error

When using quantized data, the input value corresponding to a code bin is assumed to be the center of the bin. A signal falling into a code bin not at the center generates quantization error amounting to the distance of the signal from the center of the bin. To evaluate the size of this error over many samples, the probability distribution of the signal over a code bin shall be known.

Approximating the ideal rms quantization error  $\varepsilon_Q$  by  $Q / \sqrt{12}$ , as used in [Equation \(79\)](#), arises in the following way. For large sine waves, quantization error is uniformly distributed over a code bin. The standard deviation of a uniform distribution of width  $Q$  is  $Q / \sqrt{12}$ .

#### 8.5.5 Comment on the relationship of SINAD and ENOB

SINAD and ENOB are related as shown in [Equation \(80\)](#) and [Equation \(81\)](#).

$$\begin{aligned} \text{ENOB} &= \log_2(\text{SINAD}) - \frac{1}{2} \log_2(1.5) - \log_2\left(\frac{A}{(\text{FSR}/2)}\right) \\ &= \log_2(\text{SINAD}) - \log_2\left(\frac{A}{(\text{FSR}/2)}\right) - 0.292 \end{aligned} \quad (80)$$

$$\text{SINAD} = \sqrt{1.5} \left( \frac{A}{(\text{FSR}/2)} \right) \times 2^{\text{ENOB}} \quad (81)$$

where

$A$  is the amplitude of the fitted sine wave during the test  
 $\text{FSR}$  is the full-scale range of the waveform recorder input

#### 8.5.6 Comment on significance of record size

See [4.6.4](#), [8.5.7](#), and [8.5.8](#) for a complete discussion of the significance of the record size.

### 8.5.7 Comment on effects of jitter or phase noise on sine wave tests

Time jitter (also called phase noise in the frequency domain) in the sine wave signal source produces both random and systematic errors for sine wave tests. A consequence of jitter (see Souders et al. [B40]) is that it spreads the energy of the original sine wave over a broad spectrum of frequencies, reducing the amplitude of the fundamental component (for  $\sigma_t \ll 1/f$ ) approximately by the factor shown in [Equation \(82\)](#).

$$\text{Amplitude multiplicative factor} = 1 - \frac{(2\pi f \sigma_t)^2}{2} \quad (82)$$

where

$f$  is the signal frequency fundamental component, in hertz

$\sigma_t$  is the standard deviation of the jitter, in seconds

The energy lost in the fundamental component shows up as broadband noise that has an rms value (computed over a complete period of the input sine wave) given by [Equation \(83\)](#)

$$V_{\text{noise}} \approx V_p \frac{2\pi f \sigma_t}{\sqrt{2}} \quad (83)$$

where

$V_p$  is the sine wave peak amplitude

The jitter-induced noise is distributed according to the time-derivative of the signal, approaching zero at the sine wave peaks, and reaching a maximum at the zero crossings given approximately by [Equation \(84\)](#)

$$\sigma_{\text{max}} = 2\pi f V_p \sigma_t \quad (84)$$

If a sine fit is performed on the sampled sine wave with jitter, the amplitude of the estimated sine wave will be reduced by the factor given in [Equation \(82\)](#). Furthermore, if repeated acquisitions of the waveform are averaged, the result will be a sine wave with amplitude reduced by the same factor. Note that if the original sine wave were measured using a “true rms” responding instrument, e.g., an instrument that uses thermal transfer techniques, the measured value will not be reduced by this factor; this is because the total energy is not changed by jitter, it is only redistributed.

Jitter in the sine wave source limits the signal-to-noise ratio and the number of effective bits that can be measured. Substituting [Equation \(83\)](#) for rms noise in the effective bits formula [Equation \(78\)](#) gives:

$$\text{ENOB}_{MAX} = \log_2 \left[ \frac{\text{FSR}}{V_{\text{noise}} \times \sqrt{12}} \right] \quad (85)$$

and, for a large signal sine wave (where  $V_p$  approximately equals FSR/2), this gives [Equation \(86\)](#).

$$\text{ENOB}_{MAX} = -0.7925 - \log_2 \left[ \frac{2\pi f \sigma_t}{\sqrt{2}} \right] = -0.2925 - \log_2 [2\pi f \sigma_t] \quad (86)$$

[Table 7](#) gives the maximum effective bits that can be measured as a function of the jitter standard deviation, expressed as a fraction of the sine wave period.

**Table 7—Maximum effective bits versus normalized jitter (fraction of sine wave period)**

| $\sigma_t f$ | $10^{-1}$ | $10^{-2}$ | $10^{-3}$ | $10^{-4}$ | $10^{-5}$ | $10^{-6}$ |
|--------------|-----------|-----------|-----------|-----------|-----------|-----------|
| $ENOB_{max}$ | 0.4       | 3.7       | 7.0       | 10.3      | 13.7      | 17.0      |

It is unusual to find jitter specified for sine wave sources; instead, phase noise is more commonly specified. Unfortunately, it is not a simple task to compute jitter from typical phase noise specifications. An alternative approach is to measure the jitter directly. Wideband sampling oscilloscopes, e.g., often provide simple procedures for measuring signal jitter, with resolution that is usually adequate for most waveform recorder applications.

### 8.5.8 Comment on errors included in and omitted from SINAD and ENOB

Both SINAD and ENOB are based on total rms error with respect to a best-fit sine wave. Both include quantization error, DNL, harmonic distortion, aperture uncertainty, spurious response, and random noise. Because the sine wave fitting procedure permits frequency, amplitude, phase, and offset to vary to obtain the best fit, errors in these parameters are excluded from the rms error derived and, hence, from SNR or ENOB. For example, neither SNR nor ENOB is a measure of amplitude flatness, phase linearity versus frequency, or long-term variations. For further information, see Linnenbrink [B29].

## 8.6 Random noise

Random noise is a nondeterministic fluctuation in the output of a waveform recorder, typically described by its frequency spectrum and its amplitude statistical properties. For the measurements in this subclause, the following noise characteristics are assumed:

- The amplitude probability density function (pdf) is stationary and has zero mean. (A nonzero mean is the same as offset error.)
- The noise is assumed to be additive and signal independent

Random noise test results shall include a description of the termination used at the input to the recorder.

### 8.6.1 Test method for random noise

A noise record can be obtained by digitizing two records at a specified input range with no input signal and subtracting them. The input of the waveform recorder shall be terminated as specified (see 4.3.4). The subtraction eliminates fixed-pattern errors that occur in the same location in successive records. The mean squared noise can be estimated from Equation (87).

$$\eta^2 = \delta = \frac{1}{2M} \sum_{n=1}^M (x_a[n] - x_b[n])^2 \quad (87)$$

where

- |                  |   |
|------------------|---|
| $\delta$         | is the mean squared difference between the two test records |
| $\eta^2$         | is the mean squared noise                                   |
| $x_a[n], x_b[n]$ | are the samples from the two noise records                  |
| $M$              | is the number of samples in each record                     |

When the noise is  $Q/2$  or less, the method above can produce either an underestimate or an overestimate of the noise. If the signal is near the center of a code bin, the noise will not affect the result, and an underestimate will be obtained. If the signal is near the boundary of two code bins, the recorded value will randomly toggle between two adjacent values and give an overestimate. To overcome these difficulties, use the method in 8.6.2.

Also if the input dc level is equal to a code transition level, then the recorder would appear to have an rms noise level of  $Q/2$ . If the dc level is in the center of a code bin, then the measured noise would be zero. Because neither of these situations is correct, the alternate method in 8.6.2 shall be used. The alternate method can also be appropriate for recorders with random noise that varies with input level (e.g., due to feedback from digital outputs to inputs).

### 8.6.2 Alternate test method for low-noise recorders

Connect the output of a triangle wave generator to the signal input of the digitizer. See 4.3.7.2 for the general arbitrary waveform test setup. Adjust the output amplitude to approximately  $10Q$  peak-to-peak. Trigger the digitizer to collect a record that starts at the beginning of the positive-going portion of the triangle. Adjust the frequency of the triangle wave generator so that the record contains an integer number of periods of the triangle waveform. Capture two records, and use Equation (87) and Equation (88).

$$\eta^2 = \frac{1}{\sqrt{\left(\frac{2}{\delta}\right)^2 + \left(\frac{Q}{0.866\delta}\right)^4}} \quad (88)$$

where

- $\delta$  is the mean square difference between the samples in the two test data records and is given by Equation (87)
- $\eta^2$  is the mean squared noise

As random noise increases, this equation converges to that used in 8.6.1. For a derivation of Equation (88), see Annex D.

For information about the precision of the estimates of random noise see Alegria and Cruz Serra [B8].

The analysis above is for noise whose amplitude can be described by a Gaussian pdf. Equation (88) can be modified for other pdfs. For example, for a uniform pdf, the factor 0.886 changes to 0.866; and for a bimodal pdf, the factor is 1.000.

#### 8.6.2.1 Comment on amplitude of triangle wave used for random noise test

The triangle wave provides a means of slowly slewing the digitizer over a plurality of code bin thresholds at a relatively constant rate. The subtraction process removes the contribution of the triangle wave to the result to the extent that the two repetitions are identical. Any differences due to noise, jitter, etc., will contribute to the apparent result. Consequently, unless the output of the generator can be independently judged to have a sufficiently low noise level, it is best to keep the amplitude low. In other words, only a part of the FSR of the digitizer can be explored with each measurement.

#### 8.6.2.2 Test equipment performance

A low-noise generator (both white noise and  $1/f$  noise) is required for these tests. A high-amplitude generator and attenuator are recommended. The triangle generator shall be able to trigger the waveform recorder in a stable fashion with low jitter. The additional noise generated will be approximately equal to the trigger jitter times the slew rate. The user can check this state by increasing the signal amplitude level to the input of the waveform recorder. If the measured random noise gets significantly worse, there might be a test equipment problem.

## 8.7 Spurious components

Spurious components are persistent sine waves at frequencies other than any input or harmonic frequencies.

### 8.7.1 Test method 1, with no applied signal

A waveform recorder can generate spurious components without an applied signal. For example, spurious components can be due to internal clock coupling or interleaving. These can be observed without applying any test signal.

The test procedure is given as follows:

- a) Terminate the input of the recorder as specified.
- b) Collect  $K$  records of data,  $x_k[m]$ , each containing  $M$  samples.
- c) Apply an appropriate window function to each record per [4.5.2.4](#).
- d) Compute the magnitude of the DFT of each windowed record,  $|X_{w,k}[m]|$ , using [Equation \(8\)](#) in [4.5](#).
- e) Compute the average over all of the DFT records,  $X_{avg}[m]$ , at each spectral component as shown in [Equation \(89\)](#).

$$X_{avg}[m] = \frac{1}{K} \sum_{k=1}^K |X_{w,k}[m]| \quad m = 0, 1, 2, \dots, M-1 \quad (89)$$

Spurious components are any resulting spectral lines above the noise floor.

Averaging the results over  $K$  records will reduce the standard deviation of any spectral line measurements by the square root of  $K$  (see Jenkins and Watts [\[B27\]](#)).

### 8.7.2 Test method 2, with applied signal

It is possible that an applied signal could cause spurious spectral lines that will not be measured by the method described in [8.7.1](#). Two test methods are described in [8.7.2.1](#) and [8.7.2.2](#): one for coherent sampling and one for noncoherent sampling.

#### 8.7.2.1 Coherent sampling test method

Perform the coherent sampling THD test described in [7.7.1](#). Remove the fundamental and harmonic components identified in [Equation \(60\)](#). Any remaining spectral lines are spurious components.

#### 8.7.2.2 Noncoherent sampling test method

Perform a noncoherent sampling THD test described in either [7.7.2](#) or [7.7.3](#). Remove the fundamental and harmonic components. Any remaining spectral lines are spurious components.

## 8.8 Spurious-free dynamic range (SFDR)

The frequency domain difference in decibels between the input signal level and the level of the largest spurious or harmonic component for a large, pure sine wave signal input. (Note that including harmonics in the frequencies in the definition of SFDR is not consistent with the description of “spurious components” given in [8.7](#). Including harmonics was done to reflect common usage of the term SFDR.)

### 8.8.1 Coherent sampling test method

The test procedure for estimating SFDR using coherent sampling is given below:

- a) Apply a test signal consisting of a pure, large amplitude sine wave at frequency  $f_i$  chosen to meet the criteria for coherent sampling. See [4.3.7.1](#) for the general sine wave test setup. See [4.5.2.2](#) for a discussion of coherent sampling and the DFT.

- b) Collect  $K$  records of data,  $x_k[n]$ , each containing  $M$  samples.
- c) Compute the magnitude of the DFT of each record,  $|X_k[n]|$ , using [Equation \(8\)](#) in [4.5](#).
- d) Compute the average over all of the  $K$  DFT records,  $X_{avg}[n]$ , at each spectral component using [Equation \(60\)](#) in [7.7.1](#).
- e) Compute SFDR using [Equation \(90\)](#).

$$SFDR = 20 \log_{10}(A_{rms}) - 20 \log_{10} \{ \max(X_{avg}[n_{nf}] \} \quad (90)$$

where

- $A_{rms}$  is the rms level of the input signal given by [Equation \(60\)](#) in [7.7.1](#)
- $X_{avg}[n]$  is the averaged magnitude of the spectral component at frequency index  $n$
- $n_{nf}$  is the set of frequency indices that are not the fundamental or dc

### 8.8.2 Noncoherent sampling test method

The test procedure for estimating SFDR using noncoherent sampling is given as follows:

- a) Apply a test signal consisting of a pure, large amplitude sine wave at frequency  $f_i$ . See [4.3.7.1](#) for the general sine wave test setup.
- b) Collect  $K$  records of data,  $x_k[n]$ , each containing  $M$  samples.
- c) Apply an appropriate window function to each record per [4.5.2.4](#).
- d) Compute the magnitude of the DFT of each windowed record,  $|X_{w,k}[n]|$ , using [Equation \(8\)](#) in [4.5](#).
- e) Compute the average over all of the  $K$  DFT records,  $X_{avg}[n]$ , at each spectral component using [Equation \(89\)](#) in [8.7.1](#).
- f) Compute SFDR using [Equation \(90\)](#) in [8.8.1](#).

## 9. Step response parameters

Step response parameters are the recorded output response for an ideal input step with designated low state and high state (see IEEE Std 181-2011 for more information on low and high states). If unspecified, the low state of the input step is 10%, and the high state is 90% of full scale. Several parameters of the step response are considered important in themselves and are commonly specified for waveform recorders. These parameters include the transition settling duration, transition duration, slew limit, overshoot, and precursor parameters and are covered in [9.1](#) through [9.5](#). All of the test methods described below require measuring the step response of the waveform recorder (see [4.8](#)). See IEEE Std 181-2011 for more information on computing step pulse response parameters, especially the use of histogram techniques.

### 9.1 Settling parameters

Settling parameter measurements consist of ordered pairs of settling error and time, either of which can serve as the independent variable. When measuring transition settling duration, the settling error is specified. When measuring settling error, the corresponding time is specified.

#### 9.1.1 Transition settling duration

Measured from the 50% reference level instant of the waveform, the transition settling duration is the time at which the step response enters and subsequently remains within a specified error band around the final value

for the duration of the data record. Unless otherwise specified, the final value is defined to occur 1 s after the beginning of the step.

### 9.1.2 Settling error

Settling error is the maximum absolute difference between the waveform and the final value at all times between a specified time measured from the 50% reference level instant of the waveform and the end of the data record expressed as a percentage of step amplitude. The final value is defined to occur 1 s after the beginning of the step unless otherwise specified.

### 9.1.3 Short-term transition settling duration

Measured from the 50% reference level instant of the waveform, the short-term transition settling duration is the time at which the step response enters and subsequently remains within a specified error band around the final value. The final value is defined to occur at a specified instant *less than* 1 s after the beginning of the step.

### 9.1.4 Short-term settling error

Short-term settling error is the maximum absolute difference between the waveform and the final value at all times between a specified time measured from the 50% reference level instant of the waveform and the end of the data record expressed as a percentage of step amplitude. The final value is defined to occur at a specified instant less than 1 s after the beginning of the step.

### 9.1.5 Comments on the choice of settling parameter

In the absence of any noise, transition settling duration and settling error measurements produce identical ordered pairs of error and time under identical test conditions. However, in the presence of noise, this situation is generally not the case. Therefore, when choosing between a transition settling duration and a settling error measurement, the following shall be considered:

The time at which the step response enters and subsequently remains within a specified error band around the final value can vary considerably in the presence of noise. For this reason, the sensitivity of a transition settling duration measurement to noise is highest where the waveform rate of change is small and noise is the dominant source of variance among samples within the specified error band. On the other hand, a settling error measurement is generally less sensitive to noise because, for a specified time, the settling error depends only on the maximum absolute error between the waveform and the final value regardless of where the error occurs after the specified time. For a transition settling duration measurement, it is, therefore, advisable to verify that the noise level is small compared to the specified settling error either by specifying an appropriately large settling error or by filtering the waveform data to reduce the noise.

### 9.1.6 Comment on the choice of final value

By specifying a final value at 1 s, the measured settling response can be tied to static scale-factor calibrations of the recorder, which typically involve measurement times on the order of 1 s. However, if the final value is specified at a time much shorter than 1 s, then the settling response is no longer known in terms of the static calibration. It is then possible, for example, for a waveform recorder having a short-term settling error of 0.1% at 10 ns with respect to a final value specified at 50 ns to be in error by 1% at 10 ns with respect to the static final level at 1 s. This situation is illustrated in [Figure 40](#).

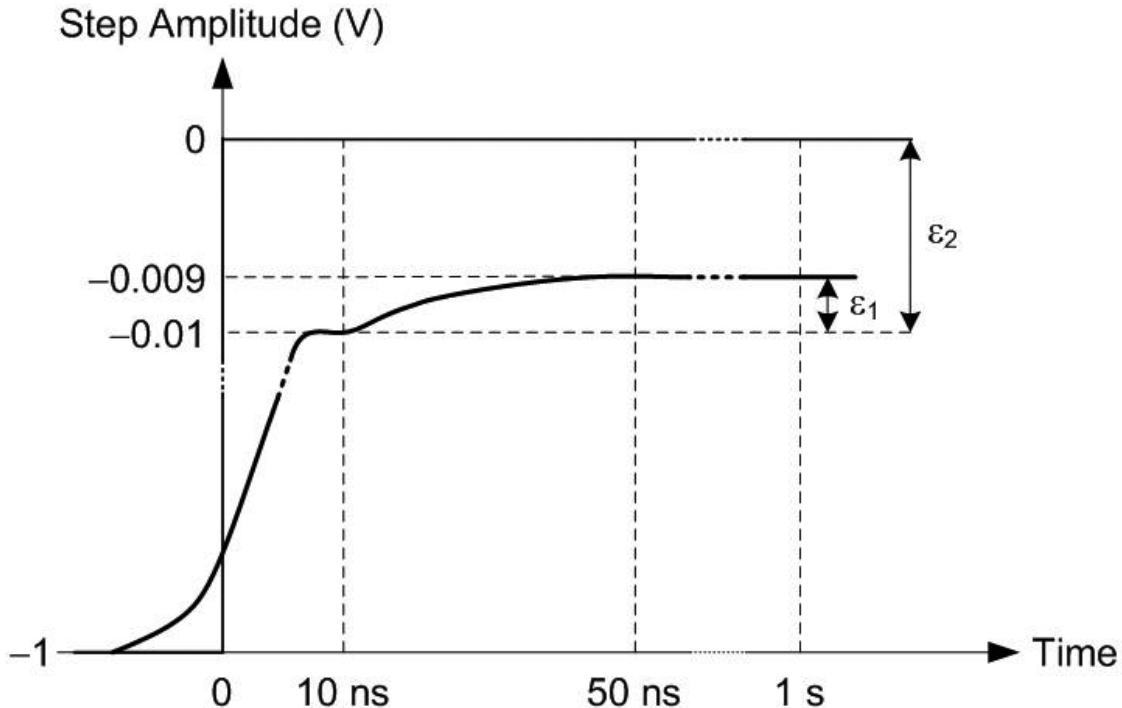


**Figure 40—Example of potential errors in measuring the final value of a step pulse response waveform when a final time shorter than 1 s is used (In the plot,  $\varepsilon_1$  is the short-term settling error, and  $\varepsilon_2$  is settling error. In this case, the final value at 1 s is 0.0 V.)**

#### 9.1.7 Comment on the use of filtering to improve transition settling duration measurement

Some caution in applying filters to improve a transition settling duration measurement time is prudent. The filter shall balance the need to reduce noise with the requirement that useful spectral information not be lost, thereby adversely affecting the measured settling response. This balance can be difficult to achieve. For determining step settling parameters, the best approach may be to rely upon averaging alone to reduce the noise to an acceptable level. For a step response settling measurement, the goal of averaging is to reduce the noise so that to a specified confidence level, the maximum value of the noise over all samples between the specified time and the end of the record is less than the uncertainty in the estimate of settling error that is acceptable.

A guideline for the number of averages  $n$  required for a given error bias is shown in [Equation \(91\)](#).

$$n \cong 2(\eta / \Delta\varepsilon)^2 [\ln(M) - \ln(u)] \quad (91)$$

where

$\eta$  is the rms value of the noise

$\Delta\varepsilon$  is the amount of acceptable bias in the settling error measurement

$M$  is the number of samples between the specified time and the end of the record

$u$  equals  $1-v$ , with  $v$  being the desired confidence level expressed as a fraction between 0 and 1

As an example, suppose the data record length is 1000 samples, and the rms of the noise equals 400  $\mu$ V. To measure the settling error of a step whose amplitude is 0.5 V with 95% confidence that the measurement bias

due to noise will be less than 200  $\mu\text{V}/\text{V}$  of the step amplitude, the number of waveform data records to be averaged is  $n = 2[(400 \times 10^{-6} \text{ V})/(200 \times 10^{-6} \text{ V}/\text{V} \times 0.5 \text{ V})]^2[(\ln(1000) - \ln(0.05))] \approx 317$ .

### **9.1.8 Test method for transition settling duration and short-term transition settling duration**

Record the response to an input step using a record length sufficient to represent the step over the duration specified or for at least 1 s when the duration is not specified. See 4.3.7.3 for the general pulse waveform test setup. Two or more overlapping records with different sample rates may be required to achieve the necessary time resolution and the required duration. To reduce noise or quantization errors, it may be desirable to digitally filter the step response data before computing transition settling duration parameters. A suitable filter is defined in Equation (92).

$$y[n] = \frac{1}{2R+1} \sum_{j=-R}^R x[n-j] \quad (92)$$

where

$x[n-j]$  is the value of the  $(n-j)$  data point of the unfiltered step response

$y[n]$  is the value of the  $n^{\text{th}}$  data point of the filtered step response

$R$  is an integer defining the duration of the moving average window

If a filter is used, the duration of the window ( $2R + 1$ ) shall be specified.

Determine the time of occurrence of the 50% reference level of the recorded waveform. Counting from that time, the transition settling duration (or the short-term transition settling duration) is the time at which the output waveform last enters the bound given by  $V(t) \pm \varepsilon$ , where  $V(t)$  is the value at the end of the specified duration and  $\varepsilon$  is the specified error. (If the specified duration is less than 1 s, then the time thus determined is the short-term transition settling duration.) When the duration is not specified,  $V(t)$  is the value 1 s after the beginning of the step.

To measure the long-term settling error, record the same step used to determine the short-term transition settling duration with a record that spans at least a 1 s interval from the beginning of the step. The long-term settling error is the absolute difference between the value 1 s after the beginning of the step and the value at the end of the specified duration following the step, expressed as a percentage of the step amplitude.

### **9.1.9 Alternate test method for recorders not allowing records of 1 s or more**

For recorders that do not allow records of 1 s or more to be taken, suitably delay the trigger so that the record includes the time 1 s after the step, and take another record. The long-term settling error is the absolute difference between the value of this record 1 s after the step and the value at the end of the specified duration when the step was applied, expressed as a percentage of the step amplitude.

### **9.1.10 Comment on transition settling duration**

The term transition settling duration refers to the time required to settle to the steady state, dc value, to within the given tolerance. The dc value is assumed to be the value after a constant input has been applied for at least 1 s. Changes that occur after 1 s are considered drift and can be due to room temperature fluctuations, component aging, and similar effects.

The term short-term transition settling duration refers to the time required to settle to a relative value (perhaps different from the steady-state value), defined as the value at the end of a specified duration, for record lengths less than 1 s. If static offset, gain, and linearity corrections are used to assign true values to short-term settling data, the results will have an uncertainty given by the long-term settling error. The uncertainty results because

of longer term settling phenomena, such as thermal imbalances that can occur after the short-term duration is complete, but that affect a steady-state measurement.

Note that only short-term transition settling duration can be specified for ac coupled recorders.

#### **9.1.10.1 Inadequate length of input step**

It is important that the duration of the input signal be long enough for the step response to reach a constant value by the end of the pulse. If this condition is not met, measurement of transition settling duration is virtually impossible. If, by the end of the input pulse, the step response still deviates by  $p\%$  from its final value, parameters such as transition duration, overshoot, precursors and the values of the frequency response can be in error by (on the order of)  $p\%$ .

#### **9.1.10.2 Effects of non-ideal step on transition settling duration**

The transition settling duration definition uses two parameters, an error band  $\varepsilon$  and a transition settling duration  $t$ . By that definition, a waveform recorder satisfies the transition settling duration condition  $[\varepsilon, t]$  if the step response remains within  $\pm \varepsilon$  of its final value for all time later than  $t$ . The settling performance of the input step affects the measured transition settling duration of the waveform recorder. As a rule of thumb, if  $[\varepsilon, t]$  is the transition settling duration requirement to be demonstrated for the waveform recorder, then the input step used for testing shall simultaneously satisfy the transition settling duration requirements,  $[\varepsilon, t/n]$  and  $[\varepsilon/n, t]$ , to achieve an accuracy of  $1/n$  in the determination of  $t$ . It is recommended that  $n$  be four or greater. This rule is demonstrably sufficient for one- and two-pole systems; it also provides a reasonable bound for other, more complex, responses.

### **9.2 Transition duration of the step response**

The transition duration of the step response is the duration between the first 10% reference level instant and the last 90% reference level instant on the recorded output response transition for an ideal input step with specified low state and high state.

#### **9.2.1 Test method**

Record the step response, and determine the 10% reference level and the 90% reference level of the output transition. Linear interpolation shall be used to determine the two reference levels when insufficient data points are available on the transition. The transition duration of the step response is the difference between the first 10% reference level instant and the last 90% reference level instant on the transition.

#### **9.2.2 Comment on pathological test results**

On some recorders, typically those that do not employ sharp cutoff anti-aliasing filters, the step response can be a nonlinear function of the input signal. The degree of nonlinearity increases with the steepness of the applied step. Because of these nonlinear effects, the step response of such a recorder can be misleading. To eliminate the gross nonlinearities, the transition duration of the applied step shall be limited to above a minimum value. The value of this limiting transition duration is dependent upon the recorder under test. The statement of results shall include the transition duration of the applied pulse. Also see 9.3 for a discussion of slew rate effects.

##### **9.2.2.1 Effects of a non-ideal step on transition duration and overshoot**

It is important that the transition duration of the input test pulse be equal to or less than one-fourth of the transition duration of the waveform recorder. If not, the observed transition duration of the waveform recorder will appear longer than the actual duration, and the calculated frequency response will roll off faster than the actual response. Use of the one-fourth rule will keep errors in transition duration and frequency response (out to the 3 dB frequency) to less than 3%.

A correction procedure for a non-ideal step is given in 9.6.1. Even if this correction procedure is used, it is important that the transition duration of the input step be smaller than that of the waveform recorder's step response. If not, the correction procedure can introduce excessive high-frequency noise. An overshoot in the input step will cause an underestimate of the transition duration of the waveform recorder and cause the calculated frequency response to roll off slower than the actual frequency response.

An overshoot of  $p\%$  can cause an underestimate by about  $p\%$  of the transition duration and an increase in the magnitude of the frequency response of about  $p\%$  at high frequency.

### 9.2.2.2 Effect of time jitter on transition duration

Time jitter contributes both a systematic and a random component of error to a transition duration measurement. The random component can be reduced with averaging, but a bias will remain.

In the frequency domain, the bias can be represented by a low-pass filter as described in 10.3.4. In the time domain, averaging a signal  $x(t)$  in the presence of jitter results in the signal  $x_j(t)$ , which can be approximated by Equation (93).

$$x_j(t) = x(t) + \frac{\sigma_t^2}{2} \frac{d^2 x(t)}{dt^2} \quad (93)$$

where

$\sigma_t$  is the standard deviation of the time jitter

For a transition duration measurement, this relation provides a good approximation to the bias in the time domain when the jitter distribution spans a time window that is small compared to the true transition duration of the signal.

The transition duration of a signal averaged in the presence of jitter is increased according to the relation shown in Equation (94).

$$t_{r,jitter} \approx \sqrt{t_r^2 + (2.5\sigma_t)^2} \quad (94)$$

where

- $t_{r,jitter}$  is the approximate transition duration increased due to jitter
- $t_r$  is the transition duration without jitter
- $\sigma_t$  is the standard deviation of the time jitter

This relation assumes that both the jitter distribution and the applied step signal are Gaussian or nearly so. The factor of  $2.5\sigma_t$  is the 10% to 90% transition duration of the integral of the Gaussian jitter distribution.

Conversely, the true transition duration of a signal can be approximated from a jittered measurement,  $t_{r,jitter}$ , using the relation shown in Equation (95).

$$t_r \approx \sqrt{t_{r,jitter}^2 - (2.5\sigma_t)^2} \quad (95)$$

This expression shall be applied with some caution. The closer  $\sigma_t$  is to  $t_{r,jitter}$ , the more sensitive this expression becomes to a user's knowledge of  $\sigma_t$  and to variance in the estimate of  $t_{r,jitter}$ . As a general rule, the expression is most useful for cases when  $\sigma_t$  is less than one-fourth of  $t_{r,jitter}$ .

These relations assume that both the jitter distribution and the applied step signal are Gaussian or nearly so.

### 9.3 Slew rate limit

#### 9.3.1 General information

Slew rate limit is the value of output transition rate of change for which an increased amplitude input step does not cause a proportional change.

#### 9.3.2 Test method

Record the step response for an input step having an amplitude 10% of full scale. Determine and store the maximum rate of change of the output transition. Repeat the process of increasing the amplitude of the input step and noting the maximum rate of change of the output transition. When the maximum rate of change ceases to increase proportionally with increasing step amplitude, slew rate limiting is taking place, and the slew rate limit is the largest recorded value for the maximum rate of change.

### 9.4 Overshoot and precursors

#### 9.4.1 General information

Overshoot is the maximum amount by which the step response exceeds the high state for a positive-going transition or is below the low state for a negative-going transition, specified as a percentage of (recorded) pulse amplitude (see IEEE Std 181-2011 for more information on low and high states). Precursors are any deviations from the low state for a positive-going transition or from the high state for a negative-going transition prior to the step transition. They are specified in terms of their maximum amplitude as a percent of the step amplitude.

#### 9.4.2 Test method for overshoot and precursors

Record the step response. Determine the maximum overshoot and precursors by following the method in Algorithm 5.3.5 in IEEE Std 181-2011.

### 9.5 Aperture duration

#### 9.5.1 General information

Aperture duration may be closely related to the transition duration of the step response. Unless otherwise indicated, aperture duration is the full width at half maximum (FWHM) of the aperture weighting function. For a Gaussian aperture, this is roughly 0.92 times the 10% to 90% transition duration of the step response. Aperture duration can also be described as the length of time necessary to encompass a specified percentage of the area under the aperture weighting function. See 3.1 for the complete definition. The length of time necessary to encompass the center 80% of the area under the aperture is identically the 10% to 90% transition duration of the step response. Some waveform recorders, such as those using successive approximation converters without sample-and-holds or track-and-holds, will have aperture duration equal to the total conversion time, and the output will represent some value that has occurred during the conversion time. In this case, the waveform recorder's ADC output value is a highly non-linear function of the input signal. Because the concept of an aperture weighting function is based on a linear model for the waveform recorder's ADC, the term aperture weighting function is not meaningful in this and similar situations. Other converter architectures will have other aperture effects.

The assignment of a definite aperture weighting function to an ADC is only valid if the sampling process is linear. In some cases this is a good approximation, while in other cases it is not. Considering the linear case, the output of a sample at sampling time,  $t_0$ , has the form:

$$v = \int_{-\infty}^0 w(t)v_{in}(t+t_0)dt \quad (96)$$

where

- $w(t)$  is the aperture weighting function, satisfying  $w(t) = 0$  for  $t > 0$
- $v_{in}(t)$  is the input signal

This expression is valid, because it is the most general expression for a value that depends linearly on  $v_{in}(t)$ , and that is causal (i.e., depends only on the past of  $v_{in}(t)$ ). It is assumed that the units are adjusted so that the integral of  $w$  is one, i.e., so that the output equals the input if the input is constant. Let  $g(t) = w(-t)$ , then:

$$v = \int_{-\infty}^0 g(-t)v_{in}(t+t_0)dt = \int_{-\infty}^{t_0} g(t_0 - t')v_{in}(t')dt' = \int_{-\infty}^{\infty} g(t_0 - t')v_{in}(t')dt' \quad (97)$$

The substitution  $t' = t + t_0$  was made. The change in the upper limit of integration in the last step is valid, because  $g(t_0 - t') = 0$  for  $t' > t_0$ .

The last expression shows that the output is equal to the result of passing the input signal through a filter whose impulse response is the time reversal of the aperture weighting function. This has significant implications for the testing and analysis of waveform recorders. It means that any method for measuring the impulse response or the step response yields a method for measuring the aperture weighting function. It also means that the combined effect of two or more components, such as an input buffer amplifier and a sample-and-hold circuit, can be obtained by convolving their individual impulse responses.

The following figures illustrate the meaning of the  $p\%$  aperture duration defined in 3.1. Figure 41 shows the impulse response of a sample-and-hold circuit while it is in the sample mode.

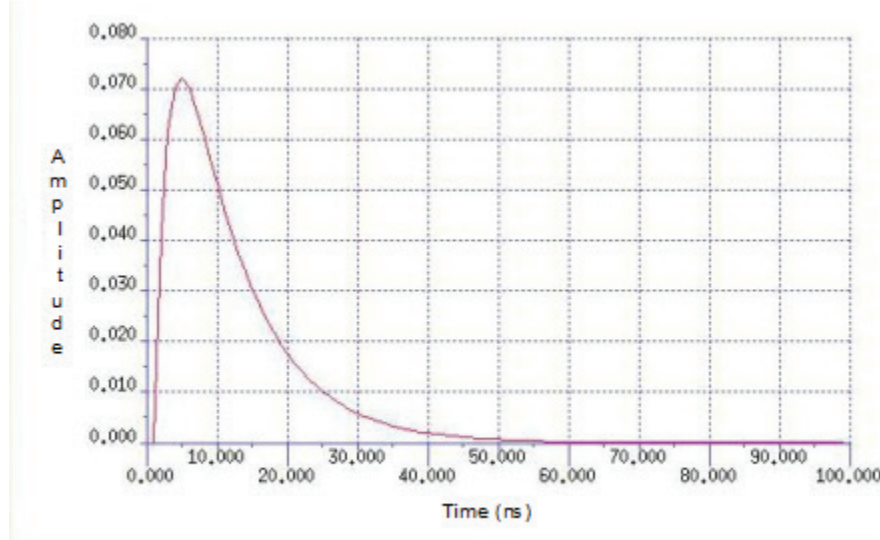


**Figure 41—Impulse response of a sample-and-hold amplifier while in the sample mode**

The step response of the sample and hold amplifier whose impulse response is shown in [Figure 41](#) is shown in [Figure 42](#).

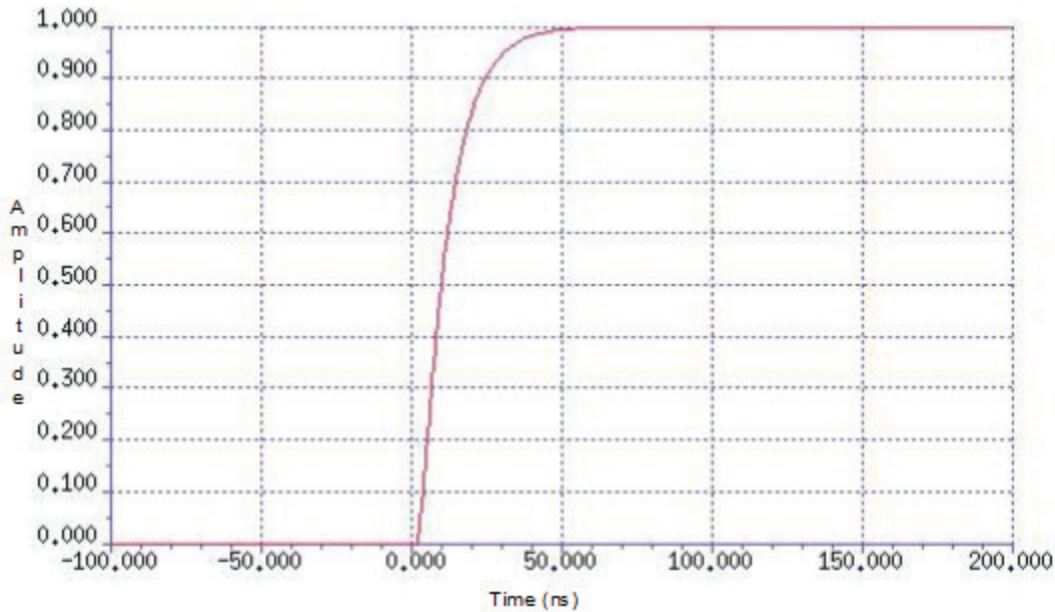


**Figure 42—The step response corresponding to the impulse response of [Figure 41](#)**

The aperture-duration is illustrated for the cases of  $p = 50$ ,  $80$ , and  $99.9$  in [Figure 42](#) through [Figure 47](#).

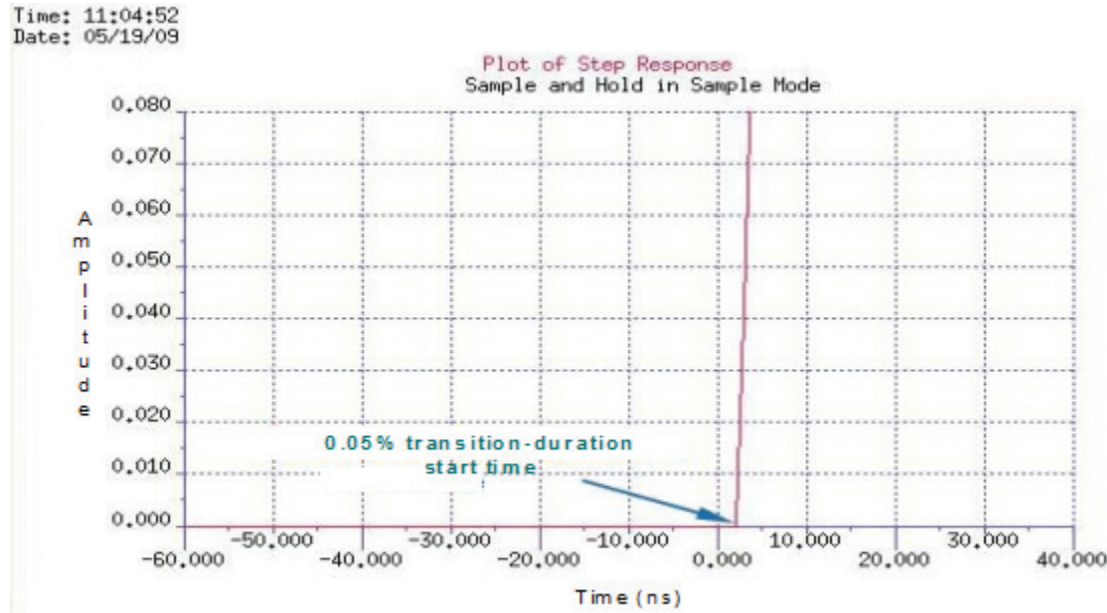


**Figure 43—View of start of transition duration for  $p = 99.9\%$**

The transition duration start time is at  $t = 2$  ns for the step response shown in Figure 42.

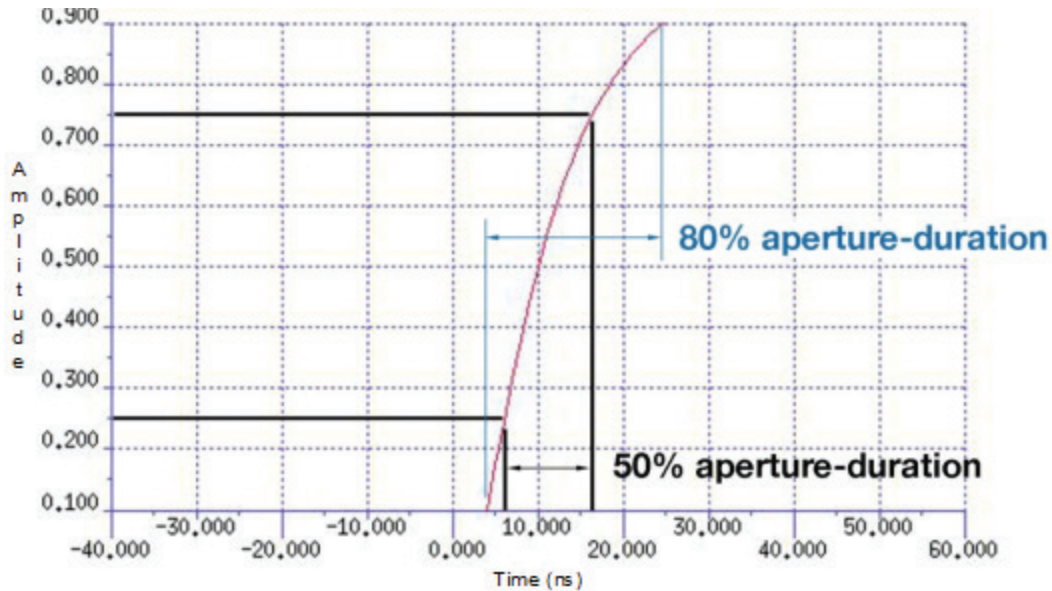


**Figure 44—Aperture duration for  $p = 50\%$  and  $p = 80\%$**

The aperture-duration shown in Figure 44 for  $p = 50\%$  and  $p = 80\%$  are 12 ns and 20 ns, respectively. The 99.9% aperture-duration is computed from Figure 45 and Figure 43.

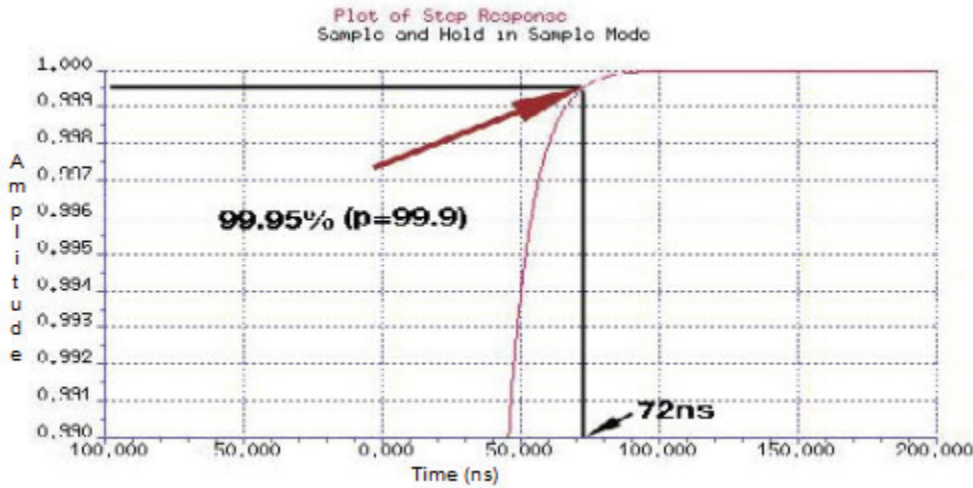


**Figure 45—Evaluation of aperture-duration stop time for  $p = 99.9\%$**

The impulse response is frequently a ringing response as is shown in Figure 46.

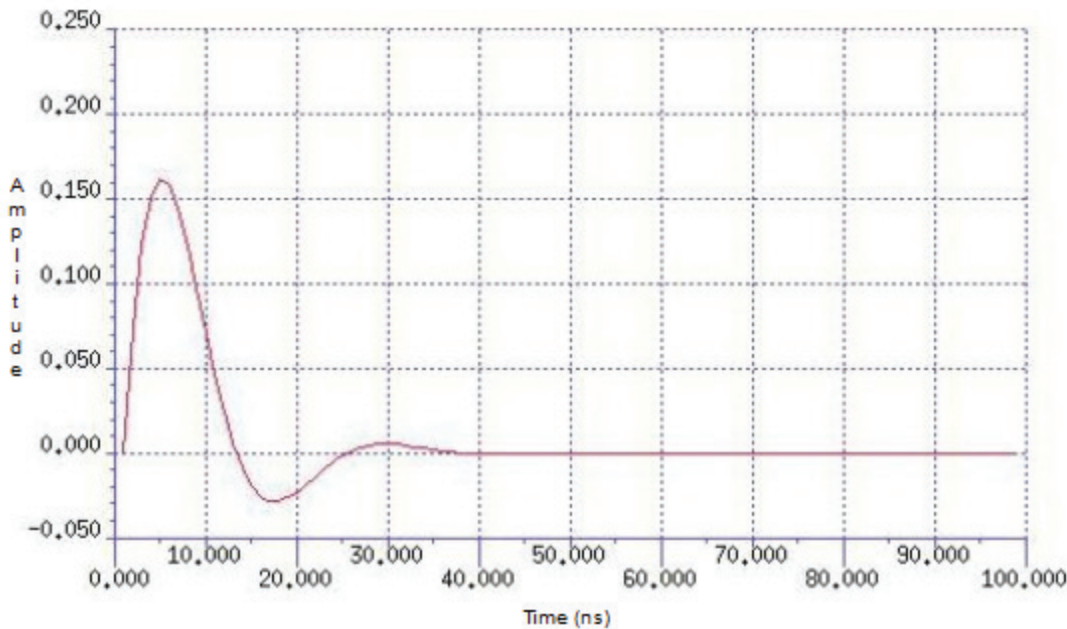


Figure 46—Ringing impulse response

This results in a ringing step response as shown in Figure 47.

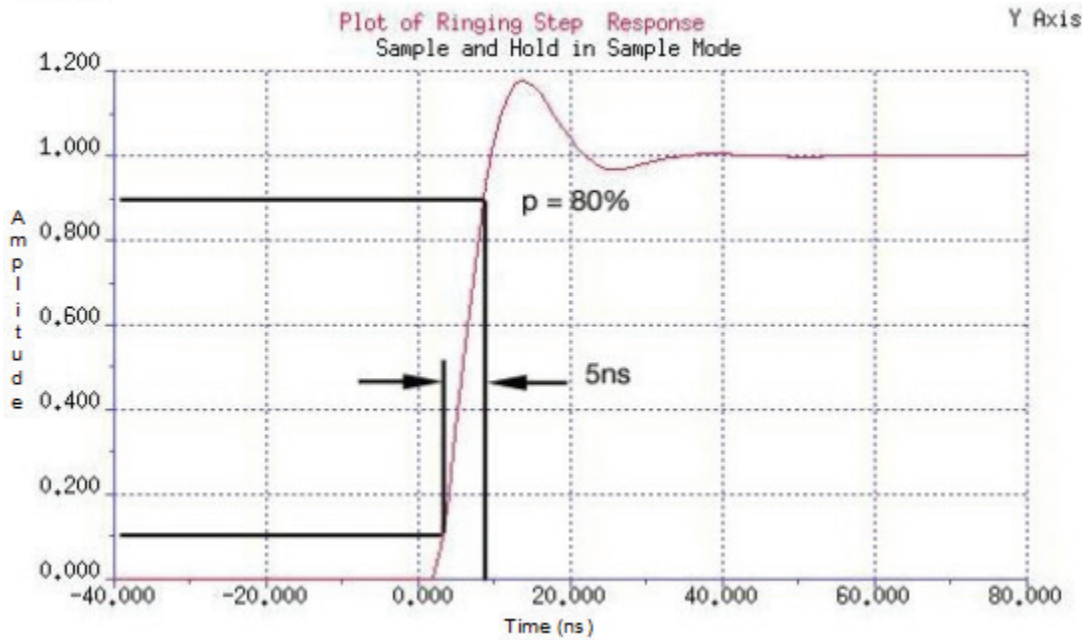
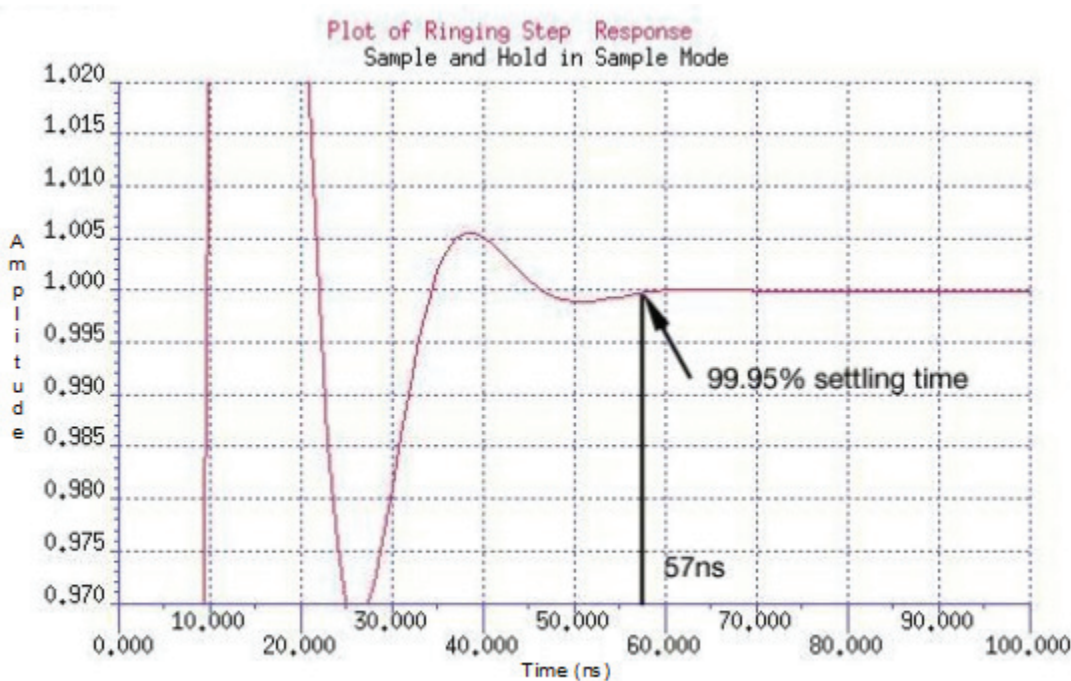


Figure 47—Ringing step response

The transition-duration ends at the last crossing of the reference level as illustrated by Figure 48.



**Figure 48—Zoomed ringing transition**

The mathematical description is valid for a linear system, which is often a good approximation. However, it is seldom exact. For example, a sample-and-hold circuit usually charges a capacitor through a forward-biased diode or transistor junction, which is not linear. A more extreme case is a successive approximation ADC without a sample-and-hold. The output value depends in a very nonlinear (but calculable) manner on the input signal during the entire conversion time. For a nonlinear system, the step response, and its  $p\%$  duration, will depend on the initial and final values of the step used for its measurement, which shall be specified along with any specification of the aperture duration.

### 9.5.2 Test method for aperture duration

Record the step response of the waveform recorder under test. Take the discrete derivative of this record to find the impulse response as described in 10.3.1. Reverse the impulse response in time to find the aperture. The full duration at half of maximum (FDHM) aperture duration can then be determined by measuring the time from when the aperture first crosses above half of its maximum value until it last crosses below half its maximum value.

## 9.6 Limitations on the use of step responses

The algorithms for analyzing step response data assume that the applied signal is an ideal step. Any deviation from this idealness will cause an error in any calculated results. The effects of various deviations from idealness of the applied step signal are discussed in 9.6.1 through 9.6.5.

### **9.6.1 Non-ideal step signal**

If the input signal is not ideal but is accurately known, the errors due to non-idealness can be corrected by using [Equation \(98\)](#).

$$H'(f) = \frac{H(f)}{U'(f)} \quad (98)$$

where

- $H'(f)$  is the frequency response corrected for a non-ideal step input
- $H(f)$  is the measured frequency response for a non-ideal step input
- $U'(f)$  is the Fourier transform of the derivative of the actual step signal  $u'(t)$

The corrected step response is obtained by integrating the inverse Fourier transform of  $H'(f)$ . All parameters of interest shall then be calculated from the corrected step response.

### **9.6.2 Recorder nonlinearities**

Most of the usefulness of the step response measurement is predicated on the fact that the recorder is a linear time invariant system. To the extent that it is not, the results of step response measurements will lose their meaningfulness. A recorder can show no nonlinearities at all for dc or slowly varying signals but still have the meaningfulness of step response measurements compromised by nonlinearities.

The magnitude of the problem can be estimated by recording the response to both a large amplitude and a small amplitude step. The user then calculates the frequency response using both step response measurements and compares the results as a function of frequency. Differences will usually increase with increasing frequency.

The magnitude of nonlinearities and their effect on step response measurements can also be estimated through the use of sine wave measurements.

### **9.6.3 Lack of time invariance**

Because the use of the step response is predicated on the recorder being both linear and time invariant, any deviation from time invariance also decreases the meaningfulness of step response measurements. If the recorder is not time invariant, the step response can change depending on the time location of the measurement.

There is a common source for lack of time invariance in high-speed waveform recorders. Many such recorders obtain their high sampling rates by interleaving the data recorded on several channels that each records at a lower sampling rate. If the several channels have slightly different roll-offs of their frequency responses (either amplitude or phase) at high frequencies, the result will be a lack of time invariance of the recorder. The magnitude of this problem can be determined through sine wave testing and looking for spurious components at frequencies separated from the applied frequency by plus or minus the interleaving frequency.

### **9.6.4 Noise**

For most waveform recorders, the inherent noise in the recorder provides a major limitation on the accuracy of quantities calculated from step response measurements.

### **9.6.5 Aliasing**

Aliasing error is the error due to insufficient sampling rate. The value of the response at frequencies higher than  $f_s/2$  (where  $f_s$  is the sampling frequency) appear “aliased” at frequencies lower than  $f_s/2$ , hence the name. Aliasing can cause an underestimate of the amount of overshoot because the peak overshoot is likely to occur between samples. Aliasing can also cause the measured transition duration time to be either lower or higher

than the true value. The error in transition duration is due to the error in interpolation to find the 10% and 90% reference level instants.

For a waveform recorder with a particular shape of its frequency response function, the magnitude of the aliasing error depends on the ratio of the sampling frequency  $f_s$  to the 3 dB bandwidth, BW, of the recorder. The exact functional form depends on the particular frequency response. Estimates are given [Table 8](#) for two different frequency response models.

Each error estimate is given as a function of frequency  $f$ , sampling frequency  $f_s$ , and bandwidth BW. For each estimate, the value of the ratio  $f_s/\text{BW}$  is given, which helps ensure an error of less than 3% for all frequencies less than BW. In all cases, this ratio is between 8.5 and 11.5.

Aliasing errors are determined for two models for the recorder's frequency response: the single-pole model and the two-pole model. The single-pole model assumes a frequency response of the form shown in [Equation \(99\)](#).

$$H(f) = \frac{1}{1 + j2\pi f\tau} \quad (99)$$

where

$\tau$  is the single pole time constant

The step response is of the form shown in [Equation \(100\)](#).

$$h(t) = 1 - \exp(-t/\tau) \quad (100)$$

The time constant  $\tau$  is related to the 3 dB bandwidth BW by the relation shown in [Equation \(101\)](#):

$$\tau = \frac{1}{2\pi \text{BW}} \quad (101)$$

The two-pole model has a frequency response of the form shown in [Equation \(102\)](#):

$$H(f) = \frac{1}{(1 + j2\pi f\tau)^2} \quad (102)$$

and a step response of the form shown in [Equation \(103\)](#).

$$h(t) = 1 - (1 + t/\tau) \exp(-t/\tau) \quad (103)$$

For the two-pole model, the time constant  $\tau$  is related to the 3 dB bandwidth BW by the relation shown in [Equation \(104\)](#).

$$\tau = \sqrt{\frac{\sqrt{2}-1}{2\pi \text{BW}}} \quad (104)$$

[Table 8](#) gives the worst-case error in transition duration. It also gives the ratio of  $f_s$  to BW, which helps ensure an error of 3% or less for all frequencies up to BW.

**Table 8—Worst-case aliasing error in transition duration**

| Model       | Transition duration error | $(f_s/BW)$ for 3% error |
|-------------|---------------------------|-------------------------|
| Single-pole | $230(BW/f_s)^2$           | 8.8                     |
| Two-pole    | $374(BW/f_s)^2$           | 11.2                    |

## 10. Frequency response parameters

### 10.1 Analog bandwidth

Analog bandwidth is the difference between the upper and lower frequency at which the amplitude response as seen in the data record is 0.707 (−3 dB) of the response as seen in the data record at the specified reference frequency. Usually, the upper and lower limit frequencies are specified rather than the difference between them. When only one number appears, it is taken as the upper limit. Bandwidth can be measured at any stated signal amplitude and sampling rate. When the sampling rate is not specified, bandwidth is measured at the maximum sampling rate. When amplitude is not specified, bandwidth is measured using a large signal. When the amplitude is specified only as a small signal, it is assumed to be a  $0.1 \times FSR$  signal.

#### 10.1.1 Test method for analog bandwidth

Apply a constant amplitude sine wave to the waveform recorder. See 4.3.7.1 for the general sine wave test setup. When not specified, select a reference frequency well within the passband of the recorder and not a subharmonic of the sampling rate. Acquire a sufficient number of records to establish the maximum peak-to-peak range of the recorded data. Divide the recorded peak-to-peak range by the input amplitude to establish the reference amplitude ratio. Change the frequency to another value that is not harmonically related to the sampling rate. Measure the maximum peak-to-peak range of the recorded data, and calculate the amplitude transfer ratio. Find the upper and lower frequencies closest to the reference frequency at which the amplitude transfer function is 0.707 of the reference amplitude transfer function. The difference between these two frequencies is the bandwidth of the recorder. When the bandwidth of the recorder includes dc, then the upper frequency is the bandwidth.

#### 10.1.2 Alternative method using time domain techniques

The frequency response of a waveform recorder can also be measured by taking the Fourier transform of the recorder’s impulse response, which is computed by taking the first derivative of the measured step response. This method is described in detail in 10.3.

### 10.2 Gain error (gain flatness)

Gain error is the difference between the dynamic gain  $G(f)$  of the waveform recorder at a given frequency and its gain at a specified reference frequency divided by its gain at the reference frequency. Gain error is also known as *gain flatness*. The dynamic gain of the waveform recorder under test at a frequency  $f$  is the magnitude of the frequency response at that frequency. The reference frequency is chosen to be a frequency whose gain is at or near the peak gain of the waveform recorder passband; typically it is the same frequency as the one used in the bandwidth test described in 10.1.1. For dc-coupled waveform recorders, the reference frequency is typically dc ( $f = 0$ ). To determine gain error, first determine the dynamic gain by using the sine wave-based methods of 10.1.1 or using the differentiated step response method of 10.3. The gain error at frequency  $f$  is shown in Equation (105).

$$\varepsilon_G = \frac{G(f) - G(f_{ref})}{G(f_{ref})} \times 100\% \quad (105)$$

where

- $\epsilon_G$  is the gain error
- $f_{ref}$  is the chosen reference frequency
- $G(f)$  is the dynamic gain of the waveform recorder at frequency  $f$

## 10.3 Frequency response and gain from step response

The frequency response and gain from step response are the complex gain (magnitude and phase) as a function of input frequency. The frequency response is the Fourier transform of the impulse response. The preferred method of presentation is in the form of plots of magnitude and phase versus frequency. See Souders, Flach, and Blair. [B38] for more details.

### 10.3.1 Frequency response and dynamic gain test method

Record the step response of the waveform recorder under test (see 4.8). See 4.3.7.3 for the general pulse waveform test setup. Use equivalent-time sampling if necessary (see 4.4). Determine to sufficient accuracy the step signal's input amplitude,  $s_0$  (the magnitude of the difference between the steps input base state and input high state). Select the waveform recorder's (equivalent-time) sampling rate,  $T_s$ , high enough to give negligible aliasing errors based on the waveform recorder bandwidth (see 9.6.5). If the bandwidth is unknown prior to this test, the test may have to be repeated, once the bandwidth is known, at a sufficient sample rate to make the aliasing errors negligible. Acquire a record of  $M$  samples of the step signal, with an epoch ( $MT_s$ ) long enough to enable the high state of the step to settle to within the desired accuracy. Estimate the waveform recorder's discrete-time impulse response,  $h[n]$ , by taking the discrete derivative of the step response samples,  $s[n]$ , in units of the output quantity, and dividing it by the step's input amplitude,  $s_0$ , in units of the input quantity. The discrete derivative is often estimated by the first difference of the samples in the record (see Souders and Flach [B38]) as shown in Equation (106).

$$h[n] = \frac{1}{s_0} \frac{d[s(nT_s)]}{dt} \cong \begin{cases} \frac{s[n+1] - s[n]}{s_0 T_s} & \text{for } n = 0, 1, 2, \dots, M-2 \\ \frac{s[n] - s[n-1]}{s_0 T_s} & \text{for } n = M-1 \end{cases} \quad (106)$$

Calculate the DFT of the impulse response using a non-weighted (rectangular) window. Multiply the result by the value of the sampling period,  $T_s$ . The result is an estimate,  $H(f_k)$ , of the frequency response of the converter, at the frequencies  $f_k = k/(MT_s)$  given in Equation (107).

$$H(f_k) = T_s \sum_{n=0}^{M-1} h[n] \exp\left(-\frac{-j2\pi k}{M}\right) \quad \text{for } k = 0, 1, 2, \dots, \frac{M}{2} \quad (107)$$

Note that the frequency response is estimated only at discrete frequencies  $f_k$ . To estimate the frequency response at other frequencies, linearly interpolate between the closest discrete frequencies.

For most Fourier transform calculations the phase spectrum typically is wrapped, that is, its values are modulo  $(2\pi)$ ; in other words, only the remainder after dividing by  $2\pi$  is given. The wrapping is partly due to the delay between the start of the record and the position in the record of the step transition. This delay introduces a phase term that is linearly related to frequency. The delay and the linear phase term that it induces are usually arbitrary quantities because the actual delay between the recorded signal and the time of the input step's transition is usually indeterminate. However, the portion of the phase spectrum that is not linearly related to frequency is often of interest, because this indicates effects on the phase due to the waveform recorder under test. The nonlinear phase portion of the phase response can be made more apparent by unwrapping the phase (Souders, Flach, and Blair [B38]). A simple method to do this is to create a simple program to subtract  $2\pi$

following each  $2\pi$  discontinuity. Noise will usually impose a limit on how high in frequency such an approach can be effective. The result is a plot of the nonlinear phase contribution.

This test method makes use of the natural roll-off of the waveform recorder under test as an anti-aliasing filter, attenuating the frequency components of the step that are beyond the Nyquist limit. Bounds on the magnitude and phase errors from aliasing and first differencing are given in [9.6.5](#).

Note that the digital differentiation operation accentuates high-frequency noise components, such as that due to quantization, and the equivalent noise increases as the square root of record length.

Ideally,  $H(0)$  shall equal the static gain as calculated in [Clause 6](#). This may not be the case, due to nonlinearities in the waveform recorder, incomplete settling of the step signal, and other non-ideal behavior associated with the signal used for the test. Other non-ideal behavior could include: errors due to period-to-period jitter in the test square wave, i.e., short- versus long-term jitter effect on equivalent time measures; any hysteresis error introduced as the recorder cycles periodically through its saturated and cutoff states; distortion due to bandwidth reduction architectures that translate harmonics by means of decimation filters; etc. These types of errors are all architecture dependent, so it is not possible to write general procedures to account for such effects.

### **10.3.2 Comment on aliasing errors**

Upper bounds on aliasing and first differencing errors can be estimated by assuming that the recorder's roll-off is dominated by a single pole (see Souders and Flach [\[B38\]](#)). Under these assumptions, the aliasing and first differencing errors measured in percent of full scale, in the magnitude spectrum as measured above, will be no greater than shown in [Equation \(108\)](#).

$$\varepsilon_m[f] = 400 f \frac{\text{BW}}{f_{eq}^2} \text{ percent of full scale for } f < \frac{f_{eq}}{2} \text{ and } f_{eq} \geq 2 \text{ BW} \quad (108)$$

where

|                    |   |
|--------------------|---|
| $\varepsilon_m[f]$ | is the upper bound on the aliasing and first differencing errors in the magnitude spectrum in percent of full scale |
| $f$                | is the frequency of interest  |
| BW                 | is the bandwidth of the test recorder   |
| $f_{eq}$           | is the equivalent sampling rate   |

For the phase spectrum, the aliasing and first differencing errors  $\varepsilon_\phi[f]$  will be no greater than shown in [Equation \(109\)](#).

$$\varepsilon_\phi[f] = 270 \frac{f}{f_{eq}} \text{ in degrees for } f \leq \frac{f_{eq}}{4} \text{ and } f_{eq} \geq 2 \text{ BW} \quad (109)$$

*Example:* If the expected bandwidth of the test recorder is 10 MHz and an equivalent sampling rate of 100 MHz is chosen, what is the maximum aliasing and first differencing error that can be expected at half the bandwidth (5 MHz)?

$$\varepsilon_m = \frac{400 \times 5 \times 10^6 \times 10^7}{10^{16}} = 2\%$$

$$\varepsilon_\phi = \frac{270 \times 5 \times 10^6}{10^8} = 13.5^\circ$$

**Table 9** gives the worst-case error in the calculated frequency response for the two frequency response models given in [9.6.5](#). It also gives the ratio of  $f_s$  to BW, which helps ensure an error of 3% or less for all frequencies up to BW.

**Table 9—Worst-case aliasing error in frequency response magnitude and phase**

| Model       | Frequency response magnitude error                            | ( $f_s$ /BW) for 3% error | Frequency response phase error  |
|-------------|---|---------------------------|---------------------------------|
| Single-pole | $400f \times \text{BW}/f_s^2$                                 | 11.5                      | $270f/f_s$                      |
| Two-pole    | $128f \times \text{BW}/f_s^2 + 840f \times \text{BW}^2/f_s^3$ | 8.7                       | $481f \times \text{BW}^2/f_s^3$ |

### 10.3.3 Comment on record length

The Fourier transform of the impulse response using a nonweighted (rectangular) window gives the frequency response of the recorder. The spacing of spectral components in the frequency response (and the lowest observable frequency component other than dc) equals the reciprocal of the epoch duration. If required, higher frequency resolution can be obtained by appending to the impulse response data record an appropriate estimate of the impulse response beyond the measurement epoch duration. If the step response has settled sufficiently close to its final value by the end of the data record, zero padding can serve as an adequate model. If, by the end of the measured epoch, the step response has not settled to its final value within the desired accuracy but the settling mechanism has a known analytic description, e.g., settling due to skin effect, the data record can be appended with samples fitting the analytic model. In many cases, appending zeros or modeled data will produce a better frequency response estimate than would be obtained from a longer measurement epoch. This is because increasing the record size through a longer measurement epoch increases the variance of each frequency bin in proportion to the record length and the measurement noise. It is generally best to pick a measurement epoch with a duration long enough to capture the salient aspects of the impulse response but not so long as to include noise added to the part of the system response that can be otherwise accurately estimated.

### 10.3.4 Filtering settling region of step for improved frequency response measurement

The use of a suitable digital filter to reduce noise can improve the estimation of frequency response from step response. The use of a filter is motivated by the fact that data record size can be large if high resolution in the frequency domain is required. Large data records, in turn, can lead to excessive noise because noise amplitude in the frequency domain increases in proportion to the square root of the number of points in the data record. Filtering is used to reduce noise commensurate with the uncertainty required of the frequency response measurement.

When the waveform recorder's noise level is larger than the quantization level, the noise may be presumed to be described by a Gaussian white noise process. For the case where the waveform recorder's noise level is significantly smaller than the quantization level, noise will not be described by a Gaussian white noise process because in the settled region of the step waveform, the samples do not occupy a uniform distribution of code transition levels.

In either case, the effects of noise can be reduced by applying a time-varying digital filter to the step response data. An easily implemented filter that is effective in many situations is an expanding-window moving-average filter. The window is chosen to have a duration of one sample (no averaging) before and during the region where the waveform is changing significantly, after which it expands linearly with data point index in the region where the waveform is changing slowly. The filtering operation can be written as shown in [Equation \(110\)](#).

$$y[n] = \frac{1}{2w[n]+1} \sum_{j=-w[n]}^{w[n]} x[n+j] \quad (110)$$

where

- $x[n]$  is the digitized step response
- $y[n]$  is the filtered digitized step response
- $w[n]$  is the filter window function
- $=0$  for  $1 \leq n \leq n_0$
- $=R*\text{int}(n/L)$  for  $n > n_0$

where

- $R$ ,  $L$ ,  $n_0$  are filter parameters (The filter length increases by  $R$  samples every  $L$  points after the first  $n_0$  samples.)

When such a filter is used in the measurement of frequency response, the filter parameters shall be reported along with the measurement results.

**Figure 49** shows the effect of applying an expanded-window moving-average filter on a step-like waveform with additive noise. In this case,  $n_0$  was 500, and  $L$  was 32. The effect of reducing noise in the part of the waveform beyond the transition region is the reduction of noise at all points in the frequency response.

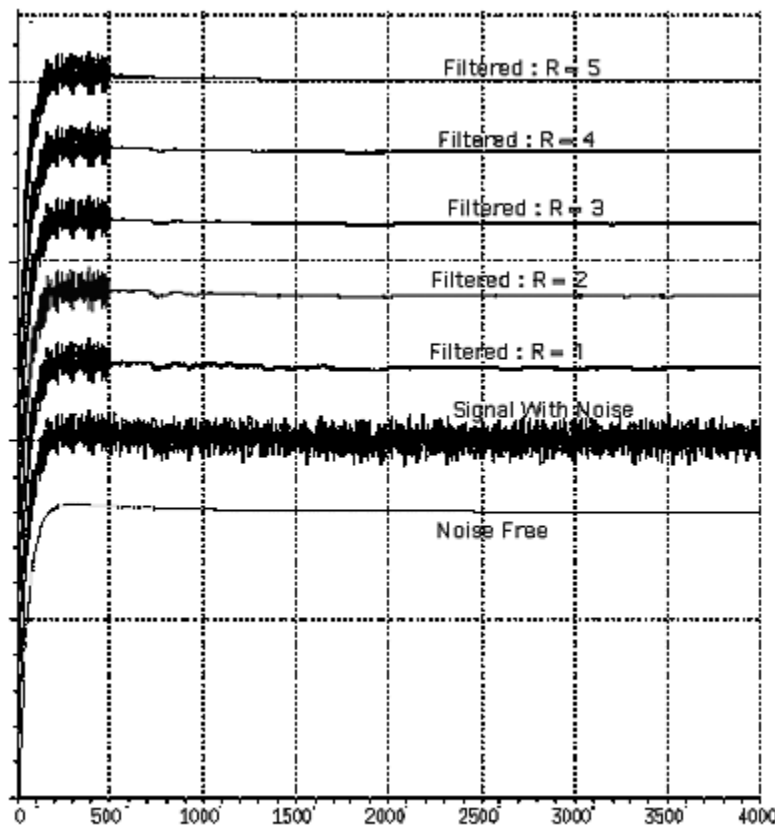


**Figure 49—Example of noise reduction using an expanding-window moving-average filter on step data for different values of  $R$  (The waveform contains two time constants separated by a factor of 10)**

Note that some caution in applying time variant filters is prudent. For example, if the window expansion is begun too early in the record, useful spectral information can be lost due to the low-pass filtering. A good rule of thumb is to begin the moving average at approximately the place in the data record where the waveform rate of change has decreased to the point that local variations in the waveform are comparable in size to the noise.

### 10.3.5 Effect of jitter on frequency response

Time jitter contributes both a systematic and a random component of error to the measurement of frequency response (see Blair [B13] and Souders et al. [B40]). The random component can be reduced with averaging, but a bias will remain. If the waveform estimates come from averaging multiple samples of the waveform, the resulting bias in the presence of jitter can be approximated in the frequency domain by a simple filter function. If  $X(f)$  is the Fourier transform of the signal  $x(t)$  averaged in the absence of jitter, then the Fourier transform of the signal averaged in the presence of jitter (with zero mean) can be approximated by Equation (111).

$$X_j(f) = X(f)H(f) \approx X(f)\{1 - [(2\pi f)^2 \sigma_t^2]/2\} \quad (111)$$

where

- $X_j(f)$  is the Fourier transform of the signal averaged in the presence of jitter
- $X(f)$  is the Fourier transform of the input signal
- $H(f)$  is the effective frequency response of the time jitter phenomenon
- $\sigma_t$  is the time jitter standard deviation

This relation applies for any jitter distribution and provides a good approximation to the bias in the frequency domain when the distribution spans a time window that is small compared to the period of the highest frequency component of interest. If the jitter distribution is Gaussian, for example, and if  $\sigma_t$  equals one-tenth the signal period  $1/f$ , the expression accounts for nearly 90% of the bias error caused by jitter. If the jitter distribution is uniform, then for the same ratio of  $\sigma_t$  to signal period, the expression accounts for nearly 95% of jitter bias error. If the jitter distribution is Gaussian or uniform, an exact expression for  $H(f)$  can be determined. For a Gaussian distribution, Equation (112) applies.

$$H(f) = e^{-(2\pi f \sigma_t)^2/2} \quad (112)$$

For a uniform distribution, Equation (113) applies.

$$H(f) = \text{sinc}(\sqrt{6\pi f \sigma_t}) \quad (113)$$

where

- sinc is the function,  $\text{sinc}(x) = \sin(x)/x$

For the specific case where the frequency response of the system being measured is described by a two-pole system with equal time constants, the standard deviation of the bias  $\sigma_s$  can be approximated by Equation (114).

$$\sigma_s = \frac{9.8}{\sqrt{K}} (f \sigma_t) \sqrt{BW \times \tau} \left( \frac{\sin(\pi f T)}{\pi f T} \right) \quad (114)$$

where

- $K$  is the number of records averaged
- $\tau$  is the time constant of the two-pole response
- $f$  is the frequency, in units inverse of  $\tau$ , at which the response is being calculated

|            |  |
|------------|--|
| $\sigma_t$ | is the rms time jitter in the same units as $\tau$             |
| BW         | is the 3 dB bandwidth of the system in units inverse of $\tau$ |
| $T$        | is the time between samples                                    |

It is worth noting that  $\sigma_s$  will be smaller for systems whose frequency response rolls off faster than that of a two-pole system.

### 10.3.6 Non-ideal step signal

The algorithms for analyzing step response data assume that the applied signal is an ideal step. Any deviation from this idealness will cause an error in any calculated results. An algorithm for computing a corrected step response is given in 9.6.1. The corrected frequency response of the recorder can be taken directly from Equation (98).

## 11. Interchannel parameters

### 11.1 Crosstalk

#### 11.1.1 Multichannel crosstalk

In waveform recorders with multiple independent recording channels, a signal in one channel can cause a spurious signal in another channel. The crosstalk (multichannel) is the ratio of the signal induced in one channel to a common signal applied to all other channels.

#### 11.1.2 Test method for multichannel crosstalk

To measure multichannel crosstalk, first terminate and shield the channel to be tested as specified (see 4.3.4). Then apply a maximum allowable amplitude sine wave of a specified frequency to all other channels. To maintain equal sine wave phasing, all inputs shall be driven from a common source using cables of equal electrical length. A resistor or transformer-coupled signal splitter that maintains proper impedances shall be used. A transformer-coupled signal splitter has less insertion loss, but typically has a lower-frequency limit of a few kilohertz. Take a record of data. The multichannel crosstalk is the ratio of rms level of the spurious signal to the rms level of the test signal. Note that this measurement can be limited by the noise and spurious effects of the channel in question.

### 11.2 Multiple input reverse coupling

#### 11.2.1 General information

In waveform recorders with multiple isolated inputs added in a single recording channel, the input to one channel can cause a spurious signal to appear at another input connector. Reverse coupling is the ratio of the spurious signal to the actual signal.

#### 11.2.2 Test method for multiple input reverse coupling

To measure input reverse coupling, apply a sine wave of full-scale amplitude and specified frequency to all but one input. Terminate this input as specified. Use a second waveform recorder to measure the signal level coming out of the input with no applied signal. The reverse coupling is the ratio of the spurious signal rms level to the test signal rms level. A null measurement shall also be made with the input cable from the unit under test to the second recorder grounded at the end normally connected to the unit under test. The null measurement is to help ensure that any measured signal is coming from the unit under test and not from stray antenna pickup. (Note that this measurement can be limited by the noise and spurious effects of the recorder used to make the measurement.)

## 12. Time base parameters

### 12.1 Fixed error in sample time

#### 12.1.1 General information

Fixed error in sample time includes nonrandom errors in the instant of sampling. They can be fixed with respect to the data samples acquired or correlated with an event that is detected by the sampling process. Examples of correlated events include subharmonics of the fundamental sampling clock itself, pickup from other logic functions within the recorder, nonlinearity in sweep circuits, and interference from external sources. Unless the recorded data accounts for these errors, an apparent amplitude error is generated. The error magnitude is the timing error times the slope of the signal recorded at that instant. Unless otherwise specified, fixed error in sample time is taken to mean the maximum fixed error that can be observed.

If the sampling is performed with multiple interleaved sampling channels, the channel number corresponding to the first sample shall be noted in the recorder's memory to correct fixed errors.

#### 12.1.2 Test method for some fixed errors in sample time

Record a large signal sine wave, triggering the recorder independently so that the starting phase of the sine wave is random. The sine wave frequency shall be as high as possible without exceeding either the analog bandwidth or one-third of the sampling rate. Perform a sine fit to the data per 4.6, and compute and store the residuals of the fit. Transform the errors into units of time by dividing the residuals by the derivative of the fitted sine wave, sample by sample. For a fitted function given by [Equation \(115\)](#):

$$x'[n] = A \cos(2\pi f t_n + \varphi) + C \quad (115)$$

The derivative is given in [Equation \(116\)](#):

$$\frac{dx'}{dt} = -2\pi f A \sin(2\pi f t_n + \varphi) \quad (116)$$

To avoid numerical instability and excessive sensitivity to NAD as the derivative approaches zero, omit this step for samples lying within 15° on either side of both (positive and negative) peaks.

Collect  $K$  (at least 10) such time records, and average them on a point-by-point basis. Averaging minimizes unwanted contributions due to amplitude noise, quantization noise, harmonic distortion, and aperture uncertainty. In addition, it provides data where they might have been omitted, by randomizing the occurrence of the sine wave peaks with respect to each record of data. When computing the averages, remember that fewer than  $K$  data points can actually be present for any given record location because of the omitted data. Compute the mean value of all the averages over the record. The mean might not be zero because of the information lost at the peaks. Fixed errors in sample time are the deviations of the averages from the mean. The maximum fixed error is the deviation that has the largest absolute value.

Because of the averaging used, this test method will detect only time-base-error patterns that are synchronous with the start of the record. It will not detect errors related to subharmonics of the clock and pickup for other logic circuits.

### 12.2 Aperture uncertainty

Aperture uncertainty is the standard deviation of the sample instant in time. As a measure of short-term stability, the time over which aperture uncertainty is measured is usually no longer than the longest single record that can be taken with the recorder. An exception occurs when the measurement method is equivalent-time sampling.

In this case, the time over which the aperture uncertainty is measured is the time required to capture a record of data, rather than the equivalent time duration represented by the record. Aperture uncertainty is also known as timing jitter, timing phase noise, or short-term timing instability. Aperture uncertainty produces a signal amplitude error whose magnitude is the timing error times the slope of the signal recorded at that instant.

### **12.2.1 General test method to determine an upper bound**

Perform the test described in [12.1.2](#) for fixed error in sample time. An upper bound for aperture uncertainty for the  $n^{\text{th}}$  sample in the record,  $\sigma_t[n]$ , is the standard deviation (from the mean) of the  $m$  values of fixed error in sample time for the  $n^{\text{th}}$  sample. An upper bound for overall aperture uncertainty,  $\sigma_t$ , is the rms value of  $\sigma_t[n]$  calculated over all  $n$ . Note that this measurement also includes error contributions from amplitude noise, quantization noise, and harmonic distortion. The relative contribution from these sources is minimized by selecting the highest test frequency consistent with bandwidth and sampling restrictions.

### **12.2.2 Alternate test method to determine an upper bound**

Apply a sine wave at frequency  $f_1$ , where  $f_1$  is a low frequency with respect to the bandwidth of the recorder, and determine the rms noise  $\eta_1$  as in [8.3](#). Then, apply a sine wave at frequency  $f_2$ , where  $f_2$  is significantly higher than  $f_1$ , as described below and determine the rms noise  $\eta_2$  as in [8.3](#). The frequency  $f_2$  shall be high enough that the rms noise is at least twice as large as measured for the low frequency  $f_1$  sine wave of the same amplitude. However,  $f_2$  shall not exceed the analog bandwidth of the recorder. An upper bound for the aperture uncertainty,  $\sigma_t$ , is then given by [Equation \(117\)](#).

$$\sigma_t = \frac{\sqrt{\eta_2^2 - \eta_1^2}}{\sqrt{2\pi f_2 A}} \quad (117)$$

where

- $A$  is the measured sine wave amplitude
- $f_2$  is the high-frequency sine wave frequency
- $\eta_2$  is the rms noise level measured at frequency  $f_2$
- $\eta_1$  is the rms noise level measured at frequency  $f_1$  and the same amplitude  $A$

This technique includes the effects of fixed pattern errors and harmonic distortion; therefore, it can provide only an upper bound for the aperture uncertainty. The error due to the harmonic distortion component can be removed by correcting both  $\eta_2$  and  $\eta_1$  for harmonic distortion. The mean squared magnitudes of the harmonics can be determined from the data records as described by Blair [\[B12\]](#).

### **12.2.3 Alternative test method for recorders that either permit external sampling clocks or port the internal sampling clock to the user**

When the internal sampling clock is available to the user and when it is compatible with the instrument's input, connect it to the input port. Alternatively, if an external sampling clock is permitted, connect a pulse or sine wave generator, as specified, to both the signal input port and the sampling clock drive port in a manner compatible with each port. The signal generator shall have subharmonic and nonharmonic content of less than  $Q/2$  of the instrument under test. Its transition duration shall lie between one and four times the minimum transition duration appropriate for the instrument under test. Vary the time delay between the signal input and sampling clock input to establish that the peak-to-peak range of the generator lies within the center 90% of the amplitude range of the recorder. When it is possible to vary the sampling rate (as with the external generator), choose a rate such that an integral cycle discrepancy does not exist between the signal path and sampler path. This action will reduce the effect of signal generator jitter on the measurement.

Adjust the time delay between the signal input and sampler to successively acquire data in four regions of interest: maximum peak (the highest amplitude, minimum slew region)  $P+$ ; minimum peak (the lowest

amplitude, minimum slew region)  $P-$ ; midpoint of the rising waveform  $R+$ ; and midpoint of falling waveform  $R-$ . Record at least 50 points in each region. Compute aperture uncertainty  $\sigma_i$  from [Equation \(118\)](#).

$$\sigma_i = \frac{1}{m} \left( \frac{\sigma_{R+}^2 + \sigma_{R-}^2}{2} - \frac{\sigma_{P+}^2 + \sigma_{P-}^2}{2} \right)^{\frac{1}{2}} \quad (118)$$

where

|                 |   |
|-----------------|---|
| $m$             | is the square root of the average of the squares of the rising and falling slopes |
| $\sigma_{R+}^2$ | is the variance in the rising region  |
| $\sigma_{R-}^2$ | is the variance in the falling region   |
| $\sigma_{P+}^2$ | is the variance in the maximum region   |
| $\sigma_{P-}^2$ | is the variance in the minimum region   |

Results from this method shall be carefully evaluated. If the internal sampling clock is ported to the signal input, it can be buffered with a noisy amplifier. Further, it is possible in this configuration for the signal and clock paths to have equal time delay and, thus, inadvertently eliminate internal sampling clock jitter. When using an external signal generator as the sampling clock, the performance might not represent the performance with the internal sampling clock. As a minimum, noise in the sampling clock itself is not included as it is in the method of [12.1.2](#). Additionally, physically different paths can link the internal and external sources to the sampler.

NOTE—A special application of this method is in testing equivalent-time sampling systems. With these systems, a variable delay circuit, triggered by the input or trigger signals, usually initiates the sample command. The equivalent aperture uncertainty can be measured for systems that permit a record of data to be taken at fixed delays. The aperture uncertainty will be a function of the delay setting, generally increasing as the delay increases.

## 12.3 Long-term stability

Long-term stability is the change in time base frequency (usually given in parts in  $10^6$ ) over a specified period of time at a specified sampling rate.

### 12.3.1 General test method

Connect the output of a sine wave generator whose frequency is known to well within the desired accuracy and stability to the input of the digitizer. The frequency shall be between 0.05 and 0.45 of the sampling rate, but shall not be the sampling frequency divided by a small integer.

Using a sine fit method such as in [4.6](#), determine the frequency of the sine wave applied to the digitizer. Because the time base of the digitizer is used in the frequency-determining process, the sampling rate accuracy is inferred from the measurement of the reference sine wave. [Equation \(120\)](#) relates the standard deviation of the digitizer's measurement of the reference sine wave frequency to the ENOB and the record length of the digitizer. The ENOB measurement of the reference sine wave establishes the bounds for the determination of the confidence interval, in accordance with standard statistical methods. For a more accurate method of estimating the sine wave frequency, which is not usually necessary, see Jenq [\[B28\]](#).

Because the frequency of the reference sine wave is known independently, the error in the sampling rate  $\epsilon_{f_s}$  is then as shown in [Equation \(119\)](#).

$$\epsilon_{f_s} = \frac{f_s}{f_{ref}} \epsilon_{f_{ref}} \quad (119)$$

where

- $\epsilon_{fref}$  is the difference between the true reference sine wave frequency and that obtained from the measurement
- $\epsilon_{fs}$  is the inferred error in the sampling rate

If the reference sine wave frequency is above the Nyquist frequency, the measured frequency shall be adjusted to the correct Nyquist band.

The above measurement is then made periodically over a specified period to establish the long-term sampling rate stability.

The sample record shall be as long as is practical. The number of reference sine wave cycles  $M_c$  in the record shall be at least 4.

The accuracy with which  $f_{ref}$  can be determined is limited by the NAD of the waveform recorder. The standard deviation is approximated by [Equation \(120\)](#).

$$\frac{\sigma_{fref}}{f_s} = \frac{0.225}{M^{3/2} 2^{ENOB-1}} \quad (120)$$

where

- $f_{ref}$  is the reference sine wave frequency as inferred by the digitizer
- $\sigma_{fref}$  is the standard deviation of measurement of reference sine wave frequency
- $f_s$  is the sampling rate
- $M$  is the number of equally spaced samples in the record
- ENOB is the effective number of bits

The ENOB measurement establishes the error bounds that can be due to NAD in the source.

### 12.3.2 Alternative test method for recorders that port the internal sampling clock to the user

Connect the recorder's clock output to a frequency counter having the required resolution and at least four times better stability than that specified for the recorder. Measure the change in sampling rate over the specified period of time at the specified sampling rate.

## 13. Out-of-range recovery

An out-of-range voltage is any voltage whose magnitude is less than the maximum safe input voltage of the recorder but is greater than the full-scale value for the selected range. An out-of-range voltage can produce changes in the characteristics of the input channel, such as saturation of an amplifier or temporary changes in component values caused by thermal effects. The out-of-range voltage recovery time is the time from the end of the overvoltage to when the input channel returns to its specified characteristics. Out-of-range voltage recovery occurs according to two different criteria. Relative recovery is achieved when the recorder's normal transfer characteristic is restored in all respects, except for signal propagation time through the recorder. Absolute recovery is achieved when the recorder's normal transfer characteristic is completely regained. Relative recovery is adequate when data before and after the out-of-range voltage need not be related in time. When the data before and after the pulse are to be related in time, then the recorder shall recover absolutely.

### 13.1 Test method for absolute out-of-range voltage recovery

Arrange a network capable of simultaneously applying both a high-purity sine wave and a specified overvoltage pulse with a flat baseline. The out-of-range voltage pulse shall be specified for amplitude, duration, polarity, and frequency. Apply a high-purity, large signal sine wave of a convenient, not harmonically related frequency (for example, 1/20th the sampling frequency). Take a record of data with the out-of-range voltage pulse occurring near the center of the record. Fit a sine wave to the data prior to the overvoltage pulse. Extrapolate the fitted sine wave to the end of the record. The measure of out-of-range voltage recovery is the deviation of recorded data from the fitted sine wave. Out-of-range voltage recovery time is measured from the last full-scale point associated with the pulse to the first point that deviates less than, and stays within, the desired tolerance of the fitted sine wave.

As a test of the method, record only the sine wave. Fit a sine wave to the portion of the record occurring prior to the point at which the out-of-range voltage pulse will be introduced. Extend the fitted sine wave in the portion of the record where the out-of-range voltage recovery is anticipated to occur. The observed deviation indicates the resolution obtainable when the pulse is applied.

### 13.2 Test method for relative out-of-range voltage recovery

When the occurrence of events before the out-of-range voltage pulse is not relevant to data acquired after the pulse, relative recovery is an appropriate criterion. Relative recovery can also be used when record length precludes the above method. To measure relative recovery, first record several records of the sine wave. Fit each record of data with a sine wave. Find the average amplitude, frequency, and dc offset of the fitted sine waves. Take a record of data in which the out-of-range voltage pulse is placed very early in the record. Align the previously fitted, average sine wave to the latter portion of the record (for example, the last 1/4 record) by varying the phase only. Extend the aligned sine wave across the entire record. Observe deviations as before.

### 13.3 Comments on test method

In a high-frequency  $50 \Omega$  system, the sine wave and the pulse shall be added using a resistive adder. An isolating reactive adder generally does not work because the top of the test pulse tilts due to the adder's limited low-frequency response. This tilt causes undershoot when the pulse returns to its initial level. The resistive adder feeds some of the pulse back to the sine wave generator, which can degrade the quality of the sine wave. This effect can be checked by applying a sine wave and pulse combination that does not go off scale on the waveform recorder. The degradation can be reduced by placing as large an attenuator as possible at the sine wave input to the resistive adder.

The out-of-range voltage test pulse shall return cleanly to its initial level. Any aberrations degrade the sine fit results.

## 14. Word error rate

Word error rate is the probability of receiving an erroneous code for an input after correction is made for gain, offset, and linearity errors and after a specified allowance is made for noise.

### 14.1 Test method for word error rate

Because the word error rate is small (usually measured in parts in  $10^6$  down to parts in  $10^{12}$ ), a great many samples are required to be collected to test for it. The number of samples required is discussed in [Annex C](#). Before starting, choose a qualified error level. This qualified error level shall be the smallest value greater than  $2Q$  that excludes from this test all other sources of error, including the noise that is associated with the input signal. Particular attention shall be paid to excluding the statistical occurrence of noise on the order of the word error rate.

Apply a large signal to the waveform recorder whose rate of change is significantly less than the equivalent of  $1Q$  per sample period. Verify that the peak-to-peak noise of the signal chosen does not exceed 10% of the error rate failure criteria. Take the largest possible record of data. Examine the differences between successive samples, and record the number of times the absolute value of this difference exceeds the qualified error level. This number corresponds to twice the number of qualified errors. Take successive records of data, and keep a running total of qualified errors until the required number of samples have been examined.

The word error rate  $\varepsilon_w$  is the number of qualified errors found through the test method and divided by the number of samples examined.

## 14.2 Comment on the number of samples required for word error rate

While the formulation given in [Annex C](#) establishes the accuracy of the word-error-rate measurement as a function of samples taken, many users are not interested in knowing an exact word error rate, but are satisfied with an upper limit. To establish only that the error rate is less than some maximum, acquire at least 10 times the number of samples for which it would be expected that a single word error would occur. For example, if the test can tolerate no more than one error per million samples, acquire 10 million samples. After acquiring and examining these samples, there are three possibilities as follows:

- A few or no errors are found. Then the error rate is certainly less than the maximum.
- The number of errors is approximately 10. A decision shall be made now if the accuracy indicated by the equations in [Annex C](#) is satisfactory or if it is necessary to acquire more data.
- The number of errors is more than 10. If it is closer to 100, then the error rate is known with greater precision. In any case, the maximum chosen is not a good estimate of the upper limit.

## 14.3 Comments on test equipment and making measurements

Although the test method does not require any particular signal shape, a triangle wave is a particularly good choice because it causes all output codes to be generated with approximately equal frequency. There is no requirement that the signal generator accurately represent its nominal shape, only that it have low noise and no sudden changes (glitches) in its output. It is important that the test setup not pick up any glitches from equipment being switched on and off because word-error-rate tests often have to be left running all night. Ground loops and long cable runs shall be avoided because they increase the chance of picking up extraneous signals. A possible but difficult solution is to use a small battery-powered signal generator connected directly to the device under test.

# 15. Differential input specifications

A waveform recorder with differential inputs produces output codes that are a function of the difference between two input signals. The two input signals are typically called positive (or plus) and negative (or minus). Such devices have a number of performance features in addition to those found in single-ended recorders. These include the impedance of each input (positive and negative) to ground, maximum common-mode signal, maximum operating common-mode signal, CMRR, and common-mode overvoltage recovery time.

## 15.1 Differential input impedance to ground

### 15.1.1 General information

Differential input impedance to ground is the impedance between either the positive input and ground or the negative input and ground. This impedance can be specified at several different frequencies. When the

frequency is not specified, the impedance given is the static value. Alternatively, the input impedance can be represented as the parallel combination of a resistance and a capacitance.

### 15.1.2 Test method for differential input impedance to ground

For each input, perform the measurement described in 5.1 or 5.2. When determining the impedance of the positive (negative) input, the negative (positive) input shall be appropriately terminated, and this termination shall be specified.

## 15.2 Common-mode rejection ratio (CMRR) and maximum common-mode signal level

### 15.2.1 General information

CMRR is the ratio of the input common-mode signal to the effect produced at the output of the recorder in units of the input.

CMRR is normally specified as a minimum value in decibels or as a ratio. CMRR shall be specified at various frequencies. The maximum common-mode signal level is the maximum level of the common-mode signal at which the CMRR is still valid. The maximum common-mode signal level shall also be specified.

### 15.2.2 Test method for common-mode rejection ratio

Arrange a network capable of simultaneously applying identical amplitude sine wave signals to both differential inputs, e.g., Figure 50. The two common-mode signal levels shall be identical to within the desired accuracy of the measurement. It is desirable that the common-mode signal level  $V_{in}$  be large enough to discern an effect in the output data; however, it shall be equal to or below the specified maximum common-mode signal level. Take a record of data. Note the recorder output  $V_{out}$  converted into input units at the common-mode sine wave frequency (using a DFT or a sine-fit algorithm). Compute CMRR in decibels from Equation (121).

$$\text{CMRR} = 20 \log_{10}(V_{in} / V_{out}) \quad (121)$$

where

$V_{in}$  is the amplitude of the input sine wave

$V_{out}$  is the amplitude of the signal in the digitized data

If no common-mode signal is detectable in the output, assign  $V_{out}$  to a value equal to the noise level of the converter. Repeat the measurement at common-mode frequencies of interest.

## 15.3 Maximum operating common-mode signal

### 15.3.1 General information

Maximum operating common-mode signal is the largest common-mode signal for which the waveform recorder will meet ENOB specifications in recording a simultaneously applied normal-mode signal.

### 15.3.2 Test method

Arrange a network capable of simultaneously applying identical amplitude sine wave common-mode signals to both differential inputs and a normal-mode, large-signal test sine wave. See Figure 50 for an example. Adjust the initial common-mode signal level to the specified maximum common-mode signal level. Take a record of data. Compute ENOB. If necessary, lower the common-mode signal amplitude to determine the

largest amplitude for which the ENOB specification is met. Repeat the measurement at common-mode and normal-mode sine wave frequencies of interest.

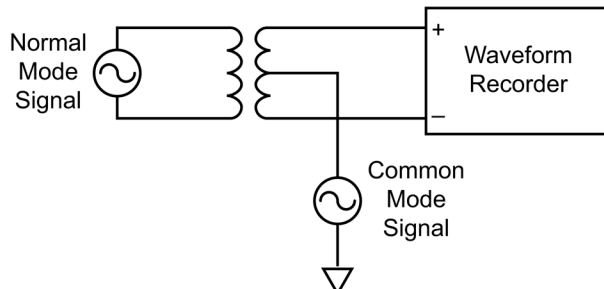


**Figure 50—Example of a network for simultaneously applying a normal-mode signal and a common-mode signal for measuring maximum operating common-mode signal level**

## 15.4 Common-mode out-of-range signal recovery time

### 15.4.1 General information

Common-mode out-of-range signal recovery time is the time required for the recorder to return to its specified characteristics after the end of a common-mode out-of-range signal pulse. A common-mode out-of-range signal is a signal level whose magnitude is less than the specified maximum safe common-mode signal but greater than the maximum operating common-mode signal.

Differential amplifiers often have poor CMRR at high frequencies, and performance will be degraded following a high-level common-mode pulse. The output will typically be driven off scale by a common-mode pulse. Comments concerning absolute and relative recovery times for normal-mode out-of-range signals in [Clause 13](#) will in general apply for common-mode overvoltage.

### 15.4.2 Test method

Arrange a network capable of simultaneously applying both a high-purity sine wave and a common-mode overvoltage pulse of specified amplitude, transition durations, and duration. For example, use the circuit shown in [Figure 50](#) with a pulse generator for the common-mode signal. Measure absolute and relative recovery times as described in [13.1](#) and [13.2](#).

## 16. Cycle time

With the recorder continually taking records of data, cycle time is real time elapsed between the start times of two records taken in succession. The length of data record and sampling rate shall be specified. Note that in addition to the internal setup time of the recorder and the experiment duration, cycle time can include the minimum time for a recorder to internally process and then transfer data to a computer and the minimum time required for a computer to send instructions to the recorder.

### 16.1 Test method

No specific general test method is suggested because the test requirements depend strongly on the particular instrument and requirements.

## 16.2 Comment

Measurements of cycle time can be limited by the computer used rather than the waveform recorder under test.

## 17. Triggering

The trigger function synchronizes the recorded waveform to an external event. The device can be triggered by either the recorded signal or by an external pulse at an independent input. Recorders can also be triggered by computer command and sometimes by a manual operation.

### 17.1 Trigger delay and trigger jitter

Trigger delay is the minimum elapsed time from the occurrence of a trigger pulse at the trigger input connector to the time at which the first or a specified data sample is recorded. The amplitude and duration of the trigger pulse shall be specified. The trigger delay can increase with decreasing trigger pulse amplitude or duration. Most modern waveform recorders have a pretrigger capability, which allows the recorder to store in the output data record a specified number of samples that occurred before the trigger event. For recorders with pretrigger capability, the trigger delay can be negative. Trigger jitter is the standard deviation in the trigger delay time over multiple records.

#### 17.1.1 General test method

A precision delayed pulse generator can be used for measuring delay and jitter. Connect the delayed pulse to the signal input and the undelayed pulse to the trigger input. Adjust the delay so the leading transition duration of the signal pulse is recorded. Adjust the recorder's trigger level to trigger at the midpoint (50% amplitude) of the trigger pulse. The pulse leading transition duration shall be at least three sample periods. Take enough records to get adequate jitter statistics. For each record, find the elapsed time from the start of the record to the occurrence of the interpolated midpoint of the pulse leading transition. If the recorder provides a measure of the time between the trigger pulse and the sample clock, use this time to adjust the elapsed times accordingly. The trigger delay is the indicated delay of the generator minus the average of the elapsed times just measured. The trigger jitter is the standard deviation of the elapsed times. The jitter of the delayed pulse generator shall be accounted for in computing the trigger jitter. Because the two are independent, the trigger jitter can be estimated as the square root of the difference of the squares of the measured jitter and the jitter of the delay generator.

#### 17.1.2 Alternate test method for recorders with pretrigger capability

Delay and jitter measurements on the external trigger of a recorder with pretrigger capability can be made without a delayed pulse generator by splitting a single pulse into two signals and routing one pulse to the signal input and the other to the trigger input. Equal electrical length cables shall be used for each leg. The pulse leading transition duration shall be at least three sample periods. Adjust the recorder's trigger level to trigger at the midpoint (50% amplitude) of the trigger pulse. Take enough records to get adequate jitter statistics. For each record, find the elapsed time from the start of the record to the occurrence of the interpolated midpoint of the pulse leading transition. If the recorder provides a measure of the time between the trigger pulse and the sample clock, use this time to adjust the elapsed times accordingly. The trigger delay is the nominal pretrigger duration minus the average of the elapsed time just measured. The standard deviation of the elapsed times is the trigger jitter.

#### 17.1.3 Comment on the inherent jitter associated with test methods

Measurements made using this test method can include an inherent jitter component due to time quantization. The rms value of the inherent jitter  $\sigma_{itrd}$  is shown in [Equation \(122\)](#).

$$\sigma_{irrd} = \frac{T}{\sqrt{12}} \quad (122)$$

where

$T$  is the sampling period

This inherent jitter can be eliminated if the trigger signal is phase locked to the recorder's sampling clock, or if the time delay between the trigger and the succeeding sampling clock pulse is measured and provided to the user.

## 17.2 Trigger sensitivity

### 17.2.1 General information

Trigger sensitivity has several components: sensitivity to the input trigger pulse level, to the rate of change of the leading transition, and to pulse duration. Trigger sensitivity is also related to hysteresis, which can be incorporated in a trigger circuit to reduce spurious triggering. A qualitative plot of the envelope of trigger voltage versus trigger delay time is shown in [Figure 51](#) for positive-going signals. Assume the input level to be initially less than  $V_{HYST}$  defined below. The minimum level that will trigger the recorder is  $V_{TH}$ . The trigger delay associated with a large input pulse is  $T_{MIN}$ . A smaller trigger level,  $V_{OD}$ , will cause a longer trigger delay,  $T_{OD}$ . The minimum pulse duration is the duration of the shortest pulse of specified amplitude that will cause triggering.  $V_{HYST}$  is the hysteresis level below which the input is required to pass before a subsequent input passing  $V_{TH}$  will trigger the recorder. The hysteresis band is the absolute value of the difference between  $V_{TH}$  and  $V_{HYST}$  and is the minimum pulse amplitude that will repetitively trigger the recorder. These parameters are illustrated graphically in [Figure 51](#).

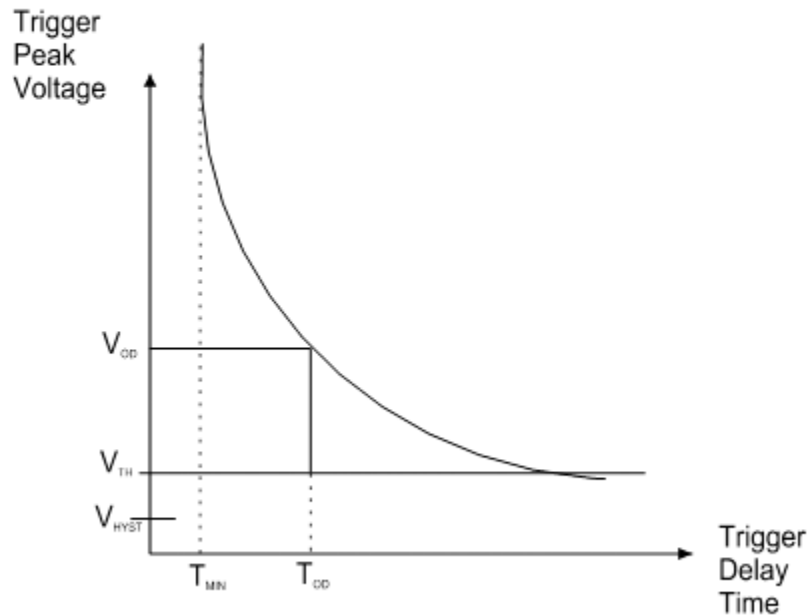


**Figure 51—Trigger sensitivity parameters**

### 17.2.2 Test methods for trigger sensitivity

To measure the minimum pulse duration, apply a pulse whose duration and amplitude can be varied and which has the proper polarity to help ensure transition duration triggering. Set the pulse amplitude to the specified level. Adjust the duration to determine the minimum that will cause triggering. (Check that the pulse amplitude does not decrease as the pulse duration is decreased.)

To measure the hysteresis band triggering on positive-going (negative-going) signals, apply a dc level below (above)  $V_{HYST}$  to the trigger input. Arm the recorder. Monotonically increase (decrease) the dc level until it is slightly below (above)  $V_{TH}$  and well above (below)  $V_{HYST}$ . Add a variable amplitude sine wave of specified frequency to the dc level. Start with a zero amplitude sine wave and increase the level until the recorder triggers. The hysteresis band is the peak-to-peak amplitude of the sine wave.

## 17.3 Trigger minimum rate of change

### 17.3.1 General information

The minimum rate of change is the slowest rate of change of the transition duration of a pulse of a specified level that will consistently trigger the recorder.

### 17.3.2 Test method for trigger minimum rate of change

To measure minimum rate of change, apply a ramp or low-frequency sine wave to the trigger input. Set the rate of change to several times faster than specified. Vary the amplitude to determine the minimum trigger

level. Again, raise the amplitude by a small but specified amount; then vary the rate of change to determine the slowest rate that will trigger the recorder.

## 17.4 Trigger coupling to signal

An external trigger signal to a recorder can cause a spurious signal to appear in the recorded data. Trigger signal coupling is the ratio of the spurious signal level to the trigger signal level.

### 17.4.1 Test method for trigger coupling to signal

To measure trigger signal coupling, first terminate and shield the input channel as specified (see 4.3.4). Apply a trigger pulse of maximum allowable operating amplitude and a leading transition duration as short as is consistent with the trigger channel bandwidth. Take a data record and determine the peak-to-peak signal level. The ratio of this signal level to the peak-to-peak trigger signal level is the trigger signal coupling.

### 17.4.2 Comment

This measurement will be limited by the noise and other spurious effects associated with the input channel itself.

## Annex A

(informative)

### Sine fitting algorithms

#### A.1 Algorithm for three-parameter (known frequency) least squares fit to sine wave data using matrix operations

This algorithm provides a least squares method for fitting digitized waveform data to a sine wave in the case where the frequency of the sine wave is known. The algorithm is presented using matrix notation.

The equation for the sine wave is shown in [Equation \(A.1\)](#).

$$x[n] = A_0 \cos(2\pi f_0 t_n) + B_0 \sin(2\pi f_0 t_n) + C_0 \quad (\text{A.1})$$

Assuming the data record contains the sequence of samples  $x[1], x[2], \dots, x[M]$  taken at times  $t_1, t_2, \dots, t_M$ , this algorithm finds the values of  $A_0$ ,  $B_0$ , and  $C_0$  that minimize the sum of squared differences shown in [Equation \(A.2\)](#).

$$\sum_{n=1}^M [x[n] - A_0 \cos(2\pi f_0 t_n) - B_0 \sin(2\pi f_0 t_n) - C_0]^2 \quad (\text{A.2})$$

where

$f_0$  is the known frequency of the sine wave applied to the waveform recorder input

Because the equation is linear, a closed form (noniterative) solution can be computed. To find the values for  $A_0$ ,  $B_0$ , and  $C_0$ , first create the matrices in [Equation \(A.3\)](#) and [Equation \(A.4\)](#).

$$D_0 = \begin{bmatrix} \cos(2\pi f_0 t_1) & \sin(2\pi f_0 t_1) & 1 \\ \cos(2\pi f_0 t_2) & \sin(2\pi f_0 t_2) & 1 \\ \vdots & \vdots & \vdots \\ \vdots & \vdots & \vdots \\ \cos(2\pi f_0 t_M) & \sin(2\pi f_0 t_M) & 1 \end{bmatrix} \quad (\text{A.3})$$

$$x = \begin{bmatrix} x[1] \\ x[2] \\ \vdots \\ \vdots \\ x[M] \end{bmatrix} \quad (\text{A.4})$$

and let [Equation \(A.5\)](#) be true.

$$s_0 = \begin{bmatrix} A_0 \\ B_0 \\ C_0 \end{bmatrix} \quad (\text{A.5})$$

In matrix notation, the sum of squared differences in [Equation \(A.2\)](#) is given by [Equation \(A.6\)](#).

$$(x - D_0 s_0)^T (x - D_0 s_0) \quad (\text{A.6})$$

where

$(*)^T$  designates the transpose of the vector or matrix (\*)

The least squares solution  $\hat{s}_0$  that minimizes [Equation \(A.6\)](#) is given by [Equation \(A.7\)](#).

$$\hat{s}_0 = (D_0^T D_0)^{-1} (D_0^T x) \quad (\text{A.7})$$

The components of  $\hat{s}_0$  can then be used in [Equation \(A.1\)](#) to compute the fitted function. Note that although the value of the least squares fit is given by [Equation \(A.7\)](#), a user might compute the value by a more numerically stable method, such as the Q-R decomposition (see Stewart [[B42](#)]).

To convert to the amplitude and phase form as shown in [Equation \(A.8\)](#):

$$x[n] = A \cos(2\pi f_0 t_n + \phi) + C \quad (\text{A.8})$$

use [Equation \(A.9\)](#) and [Equation \(A.10\)](#):

$$A = \sqrt{A_0^2 + B_0^2} \quad (\text{A.9})$$

$$\phi = -\text{ArcTan}(B_0, A_0) \quad (\text{A.10})$$

where

$\text{ArcTan}$  is the standard inverse tangent of two arguments, called ATAN2 in many programming languages, and returns a value in the range from 0 to  $2\pi$  or in the range from  $-\pi$  to  $\pi$

The residuals  $r[n]$  of the fit are given by [Equation \(A.11\)](#).

$$r[n] = x[n] - A_0 \cos(2\pi f_0 t_n) - B_0 \sin(2\pi f_0 t_n) - C_0 \quad (\text{A.11})$$

The rms error is given by [Equation \(A.12\)](#).

$$\varepsilon_{rms} = \sqrt{\frac{1}{M} \sum_{n=1}^M r[n]^2} \quad (\text{A.12})$$

## A.2 Algorithm for four-parameter (general use) least squares fit to sine wave data using matrix operations

This algorithm provides a least squares method for fitting digitized waveform data to a sine wave in the case where the frequency of the sine wave is not known. The algorithm is given in matrix notation. The equation for the sine wave is the same as that given in [Equation \(A.1\)](#) except that the input sine wave frequency  $f_0$  is not known. Because the equation is no longer linear, a closed form solution cannot be computed, and iterative techniques shall be used.

Assuming the data record contains the sequence of samples  $x[1], x[2], \dots, x[M]$ , taken at times  $t_1, t_2, \dots, t_M$ , this algorithm uses an iterative process to find the values of  $A_i, B_i, C_i$ , and  $f_i$ , which minimize the sum of squared differences shown in [Equation \(A.13\)](#).

$$\sum_{n=1}^M [x[n] - A_i \cos(2\pi f_i t_n) - B_i \sin(2\pi f_i t_n) - C_i]^2 \quad (\text{A.13})$$

where

$i$  is the iteration number

The algorithm is given as follows:

- a) Set iteration index  $i = 0$ .
- b) Make an initial estimate of the frequency  $f_0$  of the recorded data. The frequency can be estimated by using a DFT (either on the full record or a portion of it), or by taking the inverse of the average time between zero crossings, or simply by using the best measurement of the applied input frequency. A very effective general method is to use the interpolated fast Fourier transform described by Schoukens, Pintelon, and Van Hamme [[B37](#)] and Bilau et al. [[B10](#)]. This method uses an interpolation formula on the DFT coefficients of the data record and is used in the software available at the ADC Test Software website (Markos [[B30](#)]).
- c) Perform a prefit using the three-parameter matrix algorithm given in [Clause A.1](#) to determine  $A_0, B_0$ , and  $C_0$ .
- d) Set  $i = i + 1$  for the next iteration.
- e) Create the matrices shown in [Equation \(A.14\)](#), [Equation \(A.15\)](#), and [Equation \(A.16\)](#).

$$x = \begin{bmatrix} x[1] \\ x[2] \\ \vdots \\ x[M] \end{bmatrix} \quad (\text{A.14})$$

$$D_i = \begin{bmatrix} \cos(2\pi f_i t_1) & \sin(2\pi f_i t_1) & 1 & -A_{i-1} t_1 \sin(2\pi f_i t_1) + B_{i-1} t_1 \cos(2\pi f_i t_1) \\ \cos(2\pi f_i t_2) & \sin(2\pi f_i t_2) & 1 & -A_{i-1} t_2 \sin(2\pi f_i t_2) + B_{i-1} t_2 \cos(2\pi f_i t_2) \\ \vdots & \vdots & \vdots & \vdots \\ \cos(2\pi f_i t_M) & \sin(2\pi f_i t_M) & 1 & -A_{i-1} t_M \sin(2\pi f_i t_M) + B_{i-1} t_M \cos(2\pi f_i t_M) \end{bmatrix} \quad (\text{A.15})$$

$$s_i = \begin{bmatrix} A_i \\ B_i \\ C_i \\ \Delta f_i \end{bmatrix} \quad (\text{A.16})$$

- f) Compute the least squares solution  $\hat{s}_i$  using [Equation \(A.17\)](#).

$$\hat{s}_i = (D_i^T D_i)^{-1} (D_i^T x) \quad (\text{A.17})$$

- g) Note that although the value of the least squares fit is given by [Equation \(A.17\)](#), a user might compute the value by a more numerically stable method, such as the Q-R decomposition (see Stewart [[B42](#)]).
- h) Update the frequency estimate using [Equation \(A.18\)](#).

$$f_i = f_{i-1} + \Delta f_{i-1} \quad (\Delta f_{i-1} = 0 \text{ for } i = 1) \quad (\text{A.18})$$

- i) To convert to the amplitude and phase form shown in [Equation \(A.19\)](#):

$$x[n] = A \cos(2\pi f_i t_n + \varphi) + C \quad (\text{A.19})$$

use [Equation \(A.20\)](#) and [Equation \(A.21\)](#).

$$A = \sqrt{A_i^2 + B_i^2} \quad (\text{A.20})$$

$$\varphi = -\text{ArcTan}(B_i, A_i) \quad (\text{A.21})$$

where

$\text{ArcTan}$  is the standard inverse tangent of two arguments, called ATAN2 in many programming languages, and returns a value in the range from 0 to  $2\pi$  or in the range from  $-\pi$  to  $\pi$

- j) Repeat steps d) through h), recomputing the model based on the new values of  $A_i$ ,  $B_i$ , and  $f_i$  calculated from the previous iteration. It appears to be best to iterate a fixed number of times. Based on experience, six iterations have proven more than adequate. This method doubles the number of significant digits in  $f$  at each iteration and converges very rapidly.

The residuals  $r[n]$  of the fit are given by [Equation \(A.22\)](#).

$$r[n] = x[n] - A_i \cos(2\pi f_i t_n) - B_i \sin(2\pi f_i t_n) - C_i \quad (\text{A.22})$$

$$\varepsilon_{rms} = \sqrt{\frac{1}{M} \sum_{n=1}^M r[n]^2} \quad (\text{A.23})$$

## Annex B

(informative)

### Phase noise

#### B.1 What is phase noise?

A pure sinusoidal signal has the form  $x(t) = A \sin(2\pi f_c t + \varphi)$  with all of the parameters independent of time. When  $\varphi$  varies randomly with time, the oscillator is said to have phase noise. When  $A$  varies randomly with time, the oscillator is said to have amplitude noise. Amplitude noise is much easier to control in the design of oscillators; therefore, it is often the case that phase noise dominates. Amplitude noise is also much easier to measure.

If the phase error is small, the signal can be represented by the first order Taylor series as shown in [Equation \(B.1\)](#).

$$x(t) \approx A \sin(2\pi f_c t) + A(\varphi(t)) \cos(2\pi f_c t) \quad (\text{B.1})$$

Including amplitude noise yields the more general expression shown in [Equation \(B.2\)](#):

$$x(t) \approx A \sin(2\pi f_c t) + A\delta(t) \sin(2\pi f_c t) + A(\varphi(t)) \cos(2\pi f_c t) \quad (\text{B.2})$$

where the amplitude of the signal has been expressed as  $A(1+\delta(t))$ . Note that the form of the two types of distortion is the same except for a 90° phase difference. If the noise is measured on a power sensing device, such as a spectrum analyzer, the observed noise power will be the sum of that due to phase noise and that due to amplitude noise. A user shall always assume the total observed noise power is from the type that has the most deleterious effect on the measurements.

[Figure B.1](#) is a typical phase noise plot. Some typical attributes of this figure are as follows:

- The units on the vertical axis are decibels relative to the carrier per hertz. In other words, the quantity plotted is the noise power, in decibels relative to the carrier frequency power, in a 1 Hz bandwidth.
- The horizontal axis is the frequency deviation from the carrier and is plotted on a logarithmic scale.
- Both the shape and amplitude of the noise power curve depend on the carrier frequency.
- At large offsets (although not obvious in this figure), the noise usually becomes constant.

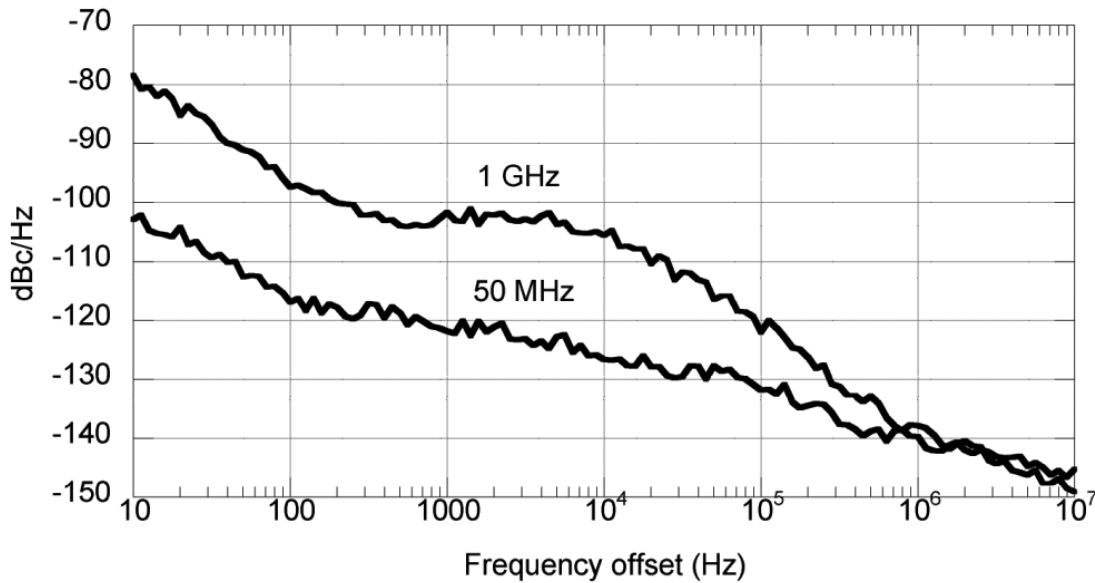


**Figure B.1—Phase noise plot**

Figure B.2 shows two phase noise displays as observed on a spectrum analyzer. The spectrum analyzer display has several differences from the previously shown phase noise plots. The horizontal scale is linear rather than logarithmic. The magnitude axis is in decibels with respect to a milliwatt rather than decibels relative to the carrier per hertz.

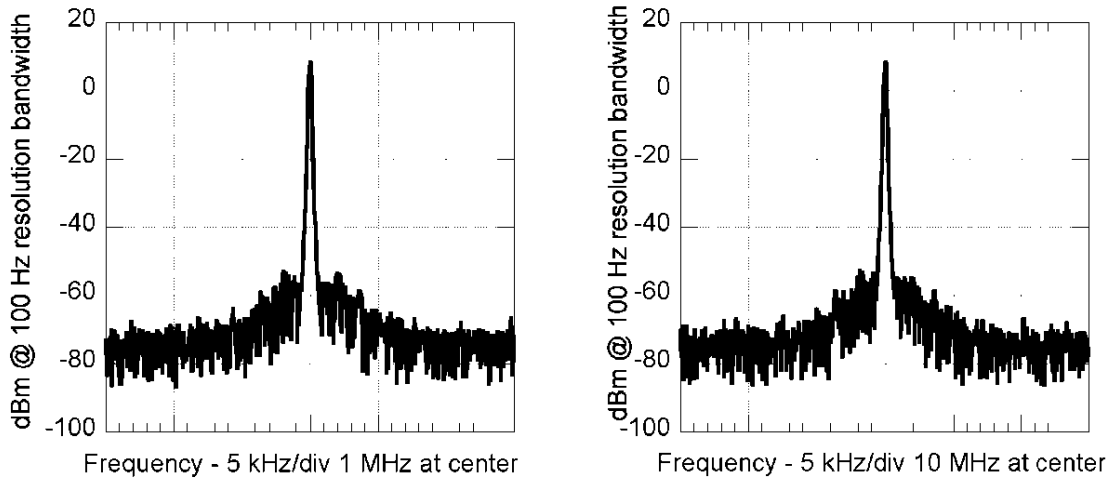


**Figure B.2—Two examples of phase noise as displayed on a spectrum analyzer**

To correct from decibels with respect to a milliwatt to decibels relative to the carrier per hertz, subtract the signal amplitude in decibels with respect to a milliwatt and subtract  $10\log(B)$ , where  $B$  is the resolution bandwidth setting of the spectrum analyzer. The display, taken with the default setting of video bandwidth equal to

resolution bandwidth, looks quite noisy; to improve this situation, set the video bandwidth significantly lower than the resolution bandwidth, and slow down the sweep rate.

The width of the central lobe is dependent on the characteristics of the resolution filter and is typically between 5 and 20 times the resolution bandwidth (this factor is called the selectivity of the filter). Phase noise measurements cannot be made with an offset frequency of less than half the width of the central lobe.

## B.2 Phase noise measurements

For the analysis given here, it is assumed that there is tabulated data of phase noise in decibels relative to the carrier per hertz versus frequency offset in hertz with at least one point for each decade of frequency.

Simple computer programs are provided to calculate the quantities of interest from this tabulated data. For “high-quality” oscillators (usually of much higher phase noise quality than required for waveform recorder testing), manufacturers often give this tabulated data for typical and worst-case behavior of their oscillators. Sometimes typical plots, such as [Figure B.1](#), are given instead of tabulated data. In this case, data can be read off of the plots.

The computer programs supplied in [B.3.1](#) and [B.3.3](#) assume that the data consists of straight line segments, on a decibels relative to the carrier versus log offset frequency plot, between the data points supplied. They also assume that, above the highest frequency for which there is a measurement, the phase noise is constant; and below the lowest frequency, the phase noise increases at 20 dB/decade as the frequency offset moves toward zero. Thus, when the manufacturer supplies only an upper limit for the phase noise at one offset frequency, the programs will still calculate a result.

Phase noise can be determined directly from spectrum analyzer data such as shown in [Figure B.2](#). It is important to follow the directions for noise measurements for a particular spectrum analyzer. For low offset frequencies, use a low-resolution bandwidth and a long sweep. To eliminate the noisy-looking trace of [Figure B.2](#), either use a video bandwidth significantly lower than the resolution bandwidth with a correspondingly long sweep time, or use an average of many sweeps if the analyzer supports this. Several sweeps with different bandwidths and sweep lengths usually are required.

An easier approach is to obtain phase noise measurement software for the spectrum analyzer. Such software automatically sets the controls of the analyzer, collects the data, and assembles the data from multiple sweeps into a phase noise plot.

## B.3 Phase noise effect on test results

The effects of phase noise are divided into three different effects: total noise, time jitter, and frequency error. In this subclause, it is shown how to calculate each error and then how each error affects various test results.

### B.3.1 Oscillator total noise

The rms noise voltage  $\eta$  is given by [Equation \(B.3\)](#).

$$\eta = V_p \sqrt{\int_{f_1}^{f_2} \eta(f) df} \quad (\text{B.3})$$

where

$V_p$  is the peak carrier voltage

$\eta(f)$  is the noise power per hertz relative to the carrier

$f_1$  and  $f_2$  are appropriately chosen lower and upper limits of integration, respectively

**Figure B.3** shows a program to calculate the square root of the integral in **Equation (B.1)**. The first argument,  $s$ , is a list of frequency-amplitude pairs, which are read directly from a phase noise plot. The frequencies are offset frequencies in hertz and the amplitudes are in decibels relative to the carrier per hertz (the amplitudes are all negative). The frequencies shall be increasing. The second and third arguments are the lower and upper frequency limits for the integral.

The limits of integration shall be selected properly. The upper limit shall be chosen large enough to capture essentially all of the noise power. If a band-pass (or low-pass) filter is going to be placed after the oscillator, the upper limit can be set to the (one-sided) bandwidth of the filter. An upper limit where the spectrum has been decreasing at 20 dB/decade for one half decade (and continues to decrease at that rate or higher) is adequate.

The lower limit is more touchy. For a real oscillator, if the lower limit were zero, the integral would be unity because the carrier energy would be captured as well as the noise. The Mathematica code below shows how to calculate the noise integral. The integral will approach infinity as the lower limit approaches zero. A practical limit for estimating the noise for waveform recorder tests is to set the lower limit at  $1/(10T_R)$ , where  $T_R$  is the record length to be acquired by the recorder and used for analysis.

```

noiseintegral[s_, f1_, f2_] := Module[{k, sp = s, v = 0, n1, n2, exp},
  sp = s; v = 0;
  If[f1 >= f2, Return[0]];
  For[k = 1, (k <= Length[s] - 1) && s[[k + 1, 1]] <= f1,
    k = k + 1, sp = Delete[sp, 1]];
  If[f1 < sp[[1, 1]],
    (*True*)
    a1 = N[sp[[1, 2]] + 20*Log[10, sp[[1, 1]]/f1]];
    sp = Prepend[sp, {f1, a1}],
    (*False*)
    If[Length[sp] > 1,
      (*True*)
      a1 = N[sp[[1, 2]] + (sp[[2, 2]] - sp[[1, 2]])*
        Log[10, f1/sp[[1, 1]]]/Log[10, sp[[2, 1]]/sp[[1, 1]]]];
      sp = Prepend[Delete[sp, 1], {f1, a1}],
      (*False*)
      sp = {{f1, sp[[1, 2]]}}];
    For[k = Length[sp], (k > 1) && (f2 <
      sp[[k - 1, 1]]), k = k - 1, sp = Delete[sp, -1]];
    If[f2 > sp[[Length[sp], 1]],
      (*True*)
      sp = Append[sp, {f2, sp[[Length[sp], 2]]}],
      (*False*)
      n2 = Length[sp]; n1 = n2 - 1;
      a2 = N[sp[[n1, 2]] + (sp[[n2, 2]] - sp[[n1, 2]])*
        Log[10, f2/sp[[n1, 1]]]/Log[10, sp[[n2, 1]]/sp[[n1, 1]]]];
      sp = Append[Delete[sp, -1], {f2, a2}];
      exp[k_] := .1*(sp[[k + 1, 2]] - sp[[k, 2]])/
        (Log[10, sp[[k + 1, 1]]] - Log[10, sp[[k, 1]]]);
      For[k = 1, k <= Length[sp] - 1, k = k + 1,
        v = v + N[Integrate[(10^(sp[[k, 2]]/10))*
          ((f/sp[[k, 1]])^exp[k]), {f, sp[[k, 1]], sp[[k + 1, 1]]}]];
      ];
    Return[Sqrt[v]];
  ]
]

```

**Figure B.3—Mathematica program to compute phase noise integral**

### B.3.2 Time jitter

The phase noise of an oscillator will cause the oscillator's zero crossings to occur at times different from those of the noiseless oscillator. The time jitter is the error in the crossing time. The rms time jitter  $\sigma_t$  due to the phase noise of the oscillator is given by [Equation \(B.4\)](#).

$$\sigma_t = \frac{1}{\sqrt{2\pi}f_0} \sqrt{\int_{f_1}^{f_2} \eta(f) df} \quad (\text{B.4})$$

where

$f_0$  is the oscillator frequency

$\eta$  is the noise power per Hertz relative to the carrier

$f_1$  and  $f_2$  are appropriately chosen upper and lower limits of integration

This is the same integral that appeared in [Equation \(B.3\)](#), and the same comments apply to selecting the limits of integration. The program of [Figure B.3](#) can be used to calculate the time jitter.

### B.3.3 Frequency error

There are several tests for which a sine wave of very accurately controlled frequency is required. The frequency of importance is the “average” frequency over one record length. The calculations use the frequency that gives the best least squares fit to the signal over one record length. The phase noise causes frequency deviations averaged over short time intervals to be larger than the frequency deviations seen with a frequency counter, which need to be measured over a time interval of a second or more to get adequate resolution. This frequency error usually goes by the name of residual frequency modulation (FM), but a user cannot use the residual FM specifications for the oscillator because they are not tied to the record length.

The rms frequency deviation over one record length,  $\Delta f_{rms}$ , is given by [Equation \(B.5\)](#):

$$\Delta f_{rms} = \sqrt{\int_0^{\infty} D(f) \eta(f) df} \quad (\text{B.5})$$

where [Equation \(B.6\)](#) is true.

$$D(f) = \frac{9}{8} \left[ \frac{\sin(\pi f T_R) - (\pi f T_R) \cos(\pi f T_R)}{T_R (\pi f T_R)^2} \right] \quad (\text{B.6})$$

where

$T_R$  is the record length in seconds

[Figure B.4](#) is a plot of the function  $D(f)$  with  $T_R = 1$ .

For  $fT_R \leq 0.3$ ,  $D(f)$  is approximated by [Equation \(B.7\)](#).

$$D(f) \approx \frac{(\pi f)^2}{8} \quad (\text{B.7})$$

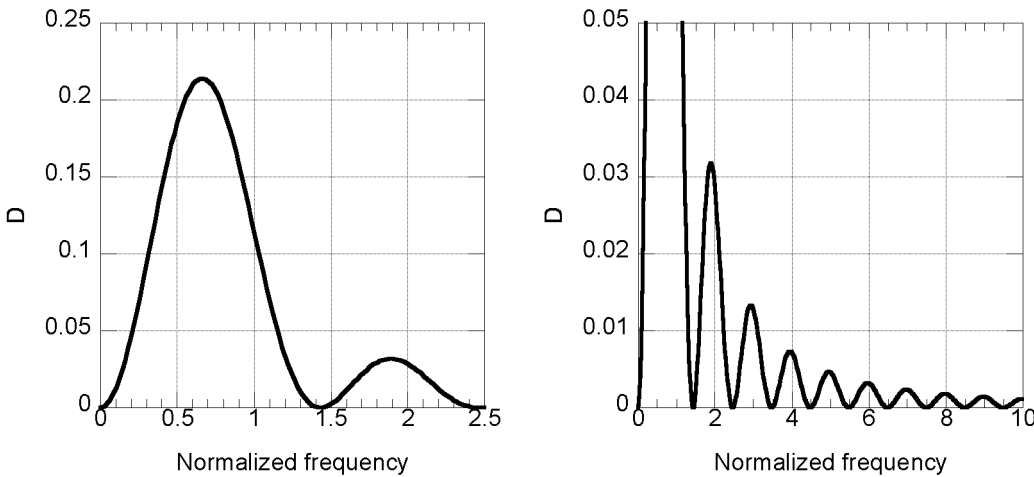


**Figure B.4—Function  $D(f)$  with record length  $T_R = 1$  s**

The integral in [Equation \(B.3\)](#) can be evaluated numerically using the Mathematica program below in [Figure B.5](#).

This program does not require a lower limit of integration because the function  $D(f)$  is proportional to  $f_2$  for  $f$  near 0. When this proportionality is combined with the assumed  $f_2$  dependence (i.e., 20 dB/decade) of  $\eta$ , the contribution from very low offset frequencies becomes small. The upper limit of integration is not very critical as long as it is chosen large enough. It shall be large enough to include the first lobe of  $D$  (see [Figure B.4](#)), which ends at about  $f = 1.5T_R$ .

The frequency deviation corresponds to an rms residual FM measured at a bandwidth of  $2/T_R$ . The typical bandwidth for specification of residual FM is 3 kHz, which corresponds to a record length of 167  $\mu$ s. For records shorter than  $2/T_R$ , the residual FM specification will underestimate the frequency deviation.

```

df[s_,T_,f2_]:=Module[{k,v=0,sp=s,wf,exp},
wf[f_,T1_]:=(9/8)((Sin[Pi f T1] -(Pi f T1)
(*Cos[Pi f T1])/((T1 (Pi f T1)^2))^2;
For[k=Length[sp],(k>1)&&(f2<=sp[[k-1,1]]),
k=k-1,sp=Delete[sp,-1]];
If[f2>sp[[Length[sp],1]],
(*True*)
sp=Append[sp,{f2,sp[[Length[sp],2]]}],
*False*)
n2=Length[sp]; n1=n2-1;
a2=N[sp[[n1,2]]+(sp[[n2,2]]-sp[[n1,2]])/
*Log[10,f2/sp[[n1,1]]]/Log[10,sp[[n2,1]]]
/ sp[[n1,1]]];
sp=Append[Delete[sp,-1],{f2,a2}];
exp[k_]:=1*(sp[[k+1,2]]-sp[[k,2]])
/(Log[10,sp[[k+1,1]]]-Log[10,sp[[k,1]]]);
For[k=1,k<=Length[sp]-1,k=k+1,
v=v+NIntegrate[(10^(sp[[k,2]]/10))
*((f/sp[[k,1]])^exp[k])
*wf[f,T],{f,sp[[k,1]],sp[[k+1,1]]},
Method->Automatic,PrecisionGoal->3]];
Return[Sqrt[v+(10^(sp[[1,2]]/10))*(Pi^2)*sp[[1,1]]/8]]]

```

**Figure B.5—Mathematica program to compute frequency deviation integral**

## B.4 Phase noise effects on specific tests

### B.4.1 Histogram tests

Phase noise affects the histogram test of 4.7.8 in two ways. Equation (24) gives a bound on the frequency error, and the phase noise of the oscillator determines the size of this error. Equation (25), Equation (26), and Equation (27) involve the noise level of the oscillator, which can be calculated from the phase noise measurements.

#### B.4.1.1 Phase noise and frequency error—histogram tests

Phase noise and frequency error are illustrated in the following example. Suppose the oscillator of Figure B.1 is to be used at a frequency of about 50 MHz to perform a histogram test on a waveform recorder with a sampling rate of 1000 MHz. As pointed out in 4.7.8.1, choosing the longest possible record length minimizes the amount of data required. However, the frequency accuracy requirements of the oscillator get tighter with longer record lengths. The phase noise data are used to determine the longest record length that can be used.

The required tolerance for oscillator frequency  $f$  is given in 4.7.8.1 in terms of  $M$ , the record length in points, and  $M_c$ , the number of cycles in a record. The tolerance can be restated in terms of  $T_R$ , the record length in seconds, by using  $M = f_s T_R$  and  $M_c = f T_R$ , where  $f_s$  is the sampling frequency ( $10^9$  in this example). Equation (24) then becomes Equation (B.8) or Equation (B.9).

$$\frac{\Delta f}{f} \leq \frac{1}{2 f T_R f_s T_R} \quad (\text{B.8})$$

$$\Delta f \leq \frac{1}{2 f_s T_R^2} \quad (\text{B.9})$$

The program of Figure B.5 can be used to calculate the rms frequency deviation. To get a good approximation to an upper bound for the frequency deviation, the rms is multiplied by value by 3. The input to the program is read from Figure B.1 at one point per decade. Table B.1 gives the tolerance from Equation (B.7) and three times the rms frequency deviation calculated by the program. An upper limit of 10 MHz was used for the integral.

**Table B.1—Frequency tolerance and deviation as a function of record length**

| $T_R$<br>(μs) | Tolerance<br>(Hz) | Deviation<br>(Hz) |
|---------------|-------------------|-------------------|
| 1             | 500               | 151               |
| 2             | 125               | 69.5              |
| 3             | 55.6              | 44.0              |
| 4             | 32.2              | 31.6              |
| 5             | 20.0              | 24.3              |

Table B.1 shows that the maximum record length is between 4 μs and 5 μs. Interpolating for  $T_R$  between 4 μs and 5 μs, a user finds that the maximum record length is 4.122 μs. This gives a record length of  $M = 4122$ .

The precise oscillator frequency to use shall be determined. By Equation (B.3), the frequency shall be of the form  $f = (M_c/M)f_s$ , where  $M_c$  and  $M$  have no common prime factors. This requirement gives  $M_c = Mf/f_s \cong 4122 \times 50/1000 = 206.1$ . By setting  $M_c = 205$ , it will have no common prime factors with 4122 because the prime factors of 4122 are 2, 3, and 229 while the prime factors of 205 are 5 and 41. This gives  $f = 1000(205/4122) = 49.73314$  MHz. Because the tolerance is less than 100 Hz, the first 6 digits of the frequency are significant. Carrying out the steps above requires the user to have the tools and skill at hand to find the prime factors of

reasonably large numbers. The user can bypass this step by setting  $M$  to a power of 2, which is smaller than the maximum value, 4096 in this case, and then any odd value for  $M_c$  will have no common factors with  $M$ . For this example,  $M_c = Mf/f_s \cong (4096)(50)/1000 = 204.8$ . So  $M_c = 205$  can be used and  $f = (205/4096)1000 = 50.04883$  MHz.

#### B.4.1.2 Amplitude noise—histogram tests

Continuing with the example of the previous subclause, the use of the 50 MHz oscillator of Figure B.1 can be used for histogram tests. The record length chosen was 1.7  $\mu$ s; therefore, the lower limit of integration is set to 50 kHz. Table B.2 gives the calculated noise level  $\eta$  for various upper limits of integration; a signal amplitude of 1 V was used for these calculations.

**Table B.2—Noise level**

| $f_2$ MHz | $\eta$ mV |
|-----------|-----------|
| 1         | 0.10      |
| 10        | 0.18      |
| 100       | 0.42      |
| 1000      | 1.26      |

#### B.4.2 Step response measurements

A precision frequency source is used for triggering step responses when the equivalent-time sampling method described in 4.4.1 is used. The phase noise of the oscillator affects the test results by introducing time jitter to the data. The effects of time jitter on the results as a function of the amount of jitter are discussed in 9.2.2.2 and 10.3.5. It is shown below how to calculate the time jitter from the phase noise data. (Also note that jitter in a step response measurement triggered by a frequency source will arise not just from phase noise in the oscillator but also from additive noise in the frequency source waveform itself. For this reason, trigger signals generally have a high dv/dt.)

As an example, assume the 50 MHz oscillator of Figure B.1 is used to perform equivalent-time sampling step response measurements using a divide by 50 rate divider (1 MHz pulse repetition rate) and a sample rate multiplication of 10. This step requires a total record length of 10  $\mu$ s; therefore, the lower limit of integration in Equation (B.4) is equal to  $1/(10T_R) = 10$  kHz. Table B.3 shows the time jitter results for various upper limits of integration. The upper limit of integration is equal to half the (two-sided) bandwidth of the filter between the oscillator and the rate divider.

**Table B.3—Step response time jitter results for various upper limits of integration**

| Upper integration limit ( $f_2$ MHz) | Time jitter ( $\sigma_t$ ps) |
|--------------------------------------|------------------------------|
| 1                                    | 0.72                         |
| 10                                   | 1.18                         |
| 100                                  | 2.68                         |
| 1000                                 | 8.06                         |

#### B.4.3 Sine wave tests

For sine wave tests (other than the histogram test), only the total noise is important. Total noise is calculated by Equation (B.9) in the same manner as for the histogram test. It is important that the total noise level be a factor of 4 below the internal noise of the waveform recorder under test.

For example, consider the use of the same 50 MHz oscillator as used in previous examples to perform sine wave tests. A 2  $\mu$ s record is assumed, which was used to calculate the results in [Table B.3](#). If the device under test has a FSR of 2 v and has up to 10 ENOB, then the internal noise level is:

$$\eta = 2 \frac{2^{-10}}{\sqrt{12}} = 5.6 \times 10^{-4} \text{ V} = 0.56 \text{ mV}$$

It is important that the oscillator noise be a factor of 4 below this value, or 0.14 mV. [Table B.3](#) shows that the oscillator shall be followed by a filter with a half bandwidth of less than 10 MHz to meet this requirement. If the ENOB of the device under test is decreased to 8, then the allowable noise increases by a factor of 4 to 0.56 mV. [Table B.3](#) shows that some filtering is still needed to meet this requirement.

## Annex C

(informative)

### Comment on errors associated with word-error-rate measurement

There are statistical errors associated with word-error-rate measurements given in Clause 14. Assuming the source of word errors is purely random, an estimate of the standard deviation  $\sigma_{\varepsilon_w}$  associated with the error rate  $\varepsilon_w$  is given in Equation (C.1).

$$\sigma_{\varepsilon_w} = \frac{\sqrt{n}}{N_s} \quad (\text{C.1})$$

where

- $n$  is the number of word errors detected
- $N_s$  is the total number of trial samples

For a given confidence level,  $\Phi$ , expressed as a fraction, the error rate  $\varepsilon_{w\Phi}$  is given by Equation (C.2).

$$\varepsilon_{w\Phi} = \varepsilon_w + k \times \sigma_{w\Phi} \quad (\text{C.2})$$

where

- $k$  is the number of standard deviations covered by confidence  $\Phi[k]$  in a Gaussian distribution and can be found in standard statistical tables (Examples of  $k$  shown in Table C.1 cover most applications.)

**Table C.1—Examples of the number of standard deviations covered by confidence  $\Phi[k]$  in a Gaussian distribution**

| $\Phi[k]$ | $k$  |
|-----------|------|
| 0.80      | 0.84 |
| 0.90      | 1.29 |
| 0.95      | 1.65 |
| 0.99      | 2.33 |

Note that one-sided confidence intervals are being used here. In other words, there is confidence level  $\Phi$  that the word error rate is equal to or less than the value given by Equation (C.4). For the more familiar two-sided confidence intervals, the values of  $k$  are larger than those in Table C.1.

For some measurements, where word error rates are very low,  $n$  can be small or even zero. The formula above is as good as any other estimate provided that  $n$  is not zero. However, even for  $n = 0$ , there is a way to estimate an upper limit on the actual word error rate.

For the case of zero observed word errors, i.e.,  $n = 0$ , a user can calculate using Equation (C.3) the probability  $p$  that not one word error would be seen.

$$p = (1 - \varepsilon_w)^{N_s} \quad (\text{C.3})$$

where

- $\varepsilon_w$  is any assumed worst-case error rate
- $N_s$  is the number of trials

When a confidence level of  $\Phi$  is desired, the worst-case estimate of the real word error rate  $\varepsilon_{wMax}$  is given in [Equation \(C.4\)](#).

$$\varepsilon_{wMax} \leq 1 - (1 - \Phi)^{1/N_s} \quad (\text{C.4})$$

where

- $\Phi$  is the desired confidence level, expressed as a fraction
- $N_s$  is the number of trials

For example, when  $n = 0$  and  $N_s = 100\,000$  for a 0.95 confidence level, according to [Equation \(C.4\)](#), the worst-case word error rate is  $3.0 \times 10^{-5}$  or less. For the same confidence level, using the sigma from [Equation \(C.1\)](#) (with the approximation that  $n = 1$ , versus 0) and solving [Equation \(C.2\)](#) with  $n = 0$  (and, therefore,  $\varepsilon_w = 0$ ), a worst-case word error rate of  $1.6 \times 10^{-5}$  is determined. This result is a reasonable correspondence to the value calculated using [Equation \(C.4\)](#).

## Annex D

(informative)

### Measurement of random noise below the quantization level

#### D.1 1 Derivation of equations

For digitizers with rms random noise greater than one quantization level, the quantization process contributes relatively little additional error and can be ignored when measuring and calculating the noise level.

For waveform recorders with rms random noise much smaller than one quantization level, however, the measurement technique and the calculation shall take into account the effects of quantization. First, the measurement shall be taken with some input signal sufficient to exercise the digitizer over several code bins to avoid understatement or overstatement of the effects of random noise as would occur if the input were centered within a code bin or on a translation level. Second, a different equation is used to calculate the rms input noise because the rms output error is not linearly related to the rms input.

If the random noise is small enough that, for any given input level, the noise will cause the output to flip between at most two adjacent codes, the noise behavior can be analyzed around each code transition level independently. Assuming the noise has a Gaussian probability distribution function, the probability of seeing output code  $k$  is as shown in [Equation \(D.1\)](#).

$$P_k(V) = \Phi(s) = \frac{1}{\sqrt{2\pi}} \int_{-\infty}^s e^{-\frac{1}{2}t^2} dt \quad (\text{D.1})$$

where

|           |  |
|-----------|--|
| $\Phi(s)$ | is the Gaussian cumulative distribution function |
| $s$       | is $V / \eta$                                    |

where

|        |  |
|--------|--|
| $V$    | is the input value relative to transition level $T[k]$     |
| $\eta$ | is the rms noise of the digitizer in the same units as $V$ |

Thus, the probability of two samples taken at the same input level near  $T[k]$  having different output codes (differing by  $\pm 1$  count) is as shown in [Equation \(D.2\)](#).

$$P_\Delta(V) = 2P_k(V)[1 - P_k(V)] \quad (\text{D.2})$$

Because this probability of different output codes repeats for every code transition level, the average probability of two samples taken at the same input level having output codes differing by  $\pm 1$  count (where the average is taken over a range of input levels for the pairs) is as shown in [Equation \(D.3\)](#).

$$\bar{P}_\Delta = \frac{1}{Q} \int_{-Q/2}^{Q/2} P_\Delta(V) dV \quad (\text{D.3})$$

Output codes differing by  $\pm 1$  count contribute a squared error of  $Q^2$ ; therefore, the mean square error  $\delta$  between two samples taken at the same input level (again, where the mean is taken over a range of input levels for the pairs) is as shown in [Equation \(D.4\)](#).

$$\delta = Q \int_{-Q/2}^{Q/2} P_\Delta(V) dV \quad (\text{D.4})$$

Assuming that the noise was small enough to not cause more than two adjacent output codes for a given input level, [Equation \(D.5\)](#) is true.

$$P_\Delta(V) \rightarrow 0 \quad \text{for } |V| > Q/2 \quad (\text{D.5})$$

Therefore, the limits of the integration can be extended to  $\pm \infty$  without any effect on the validity of [Equation \(D.4\)](#) as shown in [Equation \(D.6\)](#).

$$\delta = Q \int_{-\infty}^{\infty} P_\Delta(V) dV \quad (\text{D.6})$$

Combining [Equation \(D.1\)](#), [Equation \(D.2\)](#), and [Equation \(D.6\)](#) leads to [Equation \(D.7\)](#).

$$\delta = Q\eta \int_{-\infty}^{\infty} 2[\Phi(s)][1-\Phi(s)] ds \quad (\text{D.7})$$

The value of the integral in [Equation \(D.7\)](#) is a constant independent of any parameters of the digitizer being tested and can be evaluated by numerical integration to be approximately 1.1284 (or 1/0.886). Using this value for the integral and solving for the rms noise of the digitizer  $\eta$  yields [Equation \(D.8\)](#).

$$\eta = \frac{0.886}{Q} \delta \quad (\text{D.8})$$

[Equation \(D.8\)](#) provides an accurate estimate of a digitizer's random noise level for levels well below  $1Q$ . As mentioned earlier, for random noise levels above  $1Q$ , the quantizing effect can be ignored; and the noise level can be accurately estimated from [Equation \(87\)](#), which can be rewritten in terms of the mean square error between pairs of samples as [Equation \(D.9\)](#).

$$\eta = \left( \frac{\delta}{2} \right)^{1/2} \quad (\text{D.9})$$

Monte Carlo simulations show that [Equation \(D.8\)](#) is accurate within a few percentage points for values of  $\delta$  less than  $Q/4$  and that [Equation \(D.9\)](#) is accurate to within a few percentage points for values of  $\delta$  greater than  $Q$ . Both formulas err by almost 20% for  $\delta = Q/2$ . A heuristically derived formula that automatically crosses between [Equation \(D.8\)](#) and [Equation \(D.9\)](#) based on the value of the mean square error relative to  $Q$  is shown in [Equation \(D.10\)](#).

$$\cdot^2 = \frac{1}{\sqrt{\left(\frac{2}{\delta}\right)^2 + \left(\frac{Q}{0.886\delta}\right)^4}} \quad (\text{D.10})$$

Monte Carlo simulations show [Equation \(D.10\)](#) is accurate to within a few percentage points for any value of  $\delta$ .

### D.1.2 Alternate approach using a servo loop

An alternative approach to calculating the converter noise can be implemented by using the servo shown in [Figure 17](#).

Initially replace the logic block shown in the figure by the relationship given in [Equation \(D.11\)](#).

$$N_{DAC} = \begin{cases} N_{DAC} - N_0 & k[1] > k_n \\ N_{DAC} + 2N_0 & \text{otherwise} \end{cases} \quad (\text{D.11})$$

Change the logic block to the relationship given in [Equation \(D.12\)](#).

$$N_{DAC} = \begin{cases} N_{DAC} - 2N_0, & k[1] > k_n \\ N_{DAC} + N_0 & \text{otherwise} \end{cases} \quad (\text{D.12})$$

Measure the apparent threshold as  $T_{max}$ .

The converter noise  $\eta$  can then be expressed as shown in [Equation \(D.13\)](#).

$$\eta = 1.16(T_{max} - T_{min}) \quad (\text{D.13})$$

This method can be understood by recognizing the fact that the original relationship asked the servo to reach the value where 50% of the outputs were less than or equal to the code  $k_n$ . The new relationships described above cause the servo to search for the values of the input where the first 1/3 of the codes are less than or equal to  $k_n$ , and then 2/3 of the codes are less than or equal to  $k_n$ . These two input values define points on the cumulative probability distribution that correspond to  $\pm 0.43\eta$ . The method is fully described by Max [\[B31\]](#).

## Annex E

(informative)

### Software consideration

#### E.1 Motivation

Software is a key component of any test setup. Verifying that the computer programs are working correctly and to the required accuracy is an important step in creating a software test bench. In addition to outright bugs, software can fail because of limits in the precision of algorithms and because of loss of precision due to cumulative rounding errors in complex calculations. Precision considerations are particularly important when working with large dynamic-range or high-precision waveform recorders, e.g., those with a large number of bits.

#### E.2 Test of software to fit waveforms

The easiest way to test software that performs fits to waveforms is to computer-generate an ideal waveform and convert it to integer data with the appropriate number of bits. Apply the fitting algorithm to determine the fit parameters. Then the rms value of the differences between the data and the fit should be the ideal quantization error,  $1/\sqrt{12}$ , or 0.289. The limit of precision can be found by increasing the number of bits in the integer data until the rms residual value is no longer close to 0.289.

#### E.3 Test of DFT software

DFT algorithms can be tested in a similar way, by using ideal integer sine waves as input to the harmonic distortion test of 7.7.1. Because a pure sine wave is used, there will be no peaks at the harmonic frequencies when the software is working properly, but there will be a noise floor due to quantization noise. The decibel power ratio between the peak due to the sine wave and the quantization noise level will change by –6 dB for each bit added when the software is working properly. For example, in going from 8 bits to 10 bits in the ideal sine wave, the ratio will change by –12 dB. By increasing the number of bits in the ideal sine wave, the user can find the limit of precision for the DFT algorithm being used.

#### E.4 Software toolkit

A toolkit of software procedures for this standard is available from the ADC Test Software website (Markos [B30]).

## **Annex F**

### **(informative)**

### **Excitation with precision source with ramp verneir: determination of the test parameters**

#### **F.1 General**

The static test procedure described in [4.7.10.3](#) uses a dc source together with a triangular wave generator. It is necessary to determine, prior to the execution of the test, the triangular wave amplitude and frequency, the different dc source values to use in each step, and the number of samples to acquire.

It is assumed that the waveform recorder input range and sampling frequency are supplied and fixed. Also the maximum allowed error and the desired precision of the transition voltages estimation shall be supplied.

Also the equipment specifications shall be provided, namely the dc source error and resolution, the triangular wave generator nonlinearity, amplitude error, resolution and frequency error, and the sampling frequency error.

The levels of additive random noise and phase noise (including jitter) present in the test setup shall also be supplied beforehand.

#### **F.2 Triangular wave amplitude (A)**

In order to limit the error caused by the triangular wave nonlinearity  $\varepsilon_{NL}$  in the transition voltages estimates to  $\varepsilon_i$  in LSBs, the triangular wave amplitude has to be smaller than shown in [Equation \(F.1\)](#).

$$A \leq \frac{\varepsilon_i \times Q}{\varepsilon_{NL}} = VP \quad (F.1)$$

where

$\varepsilon_i$  is the desired error limit in the transition voltage estimates in LSBs

$\varepsilon_{NL}$  is the nonlinearity error of a triangular generator, which is defined as the maximum difference between the actual and the ideal waves, normalized to the ideal wave amplitude

VP is the maximum amplitude of the triangular wave

$Q$  is the ideal code bin width

There is the need to use overdrive, that is, to use a test signal amplitude greater than what would be strictly necessary to stimulate all the waveform recorder codes. One of the reasons is to limit the error caused by the presence of additive random noise as in the sine wave histogram test ([4.7.8](#)). The expression for the required overdrive  $V_{OD}$  in the case of a triangular signal is given in [Equation \(F.2\)](#).

$$V_{OD} = \eta \left[ \sqrt{2\pi - \ln \left( \sqrt{2\pi \frac{\varepsilon_i Q}{\eta}} \right)} - \sqrt{2\pi} \right] \quad (F.2)$$

where

$\eta$  is the additive rms random noise

$\varepsilon_i$  is the desired error limit in the transition voltage estimates in LSBs

$Q$  is the ideal code bin width

The other reason to use overdrive is to help ensure that even in the presence of errors in the triangular wave amplitude or the rounding due to finite amplitude resolution of the function generator, all the codes are stimulated, that is, the triangular waves of consecutive steps overlap.

The minimum triangle wave amplitude  $A$  is given by [Equation \(F.3\)](#).

$$A = \min\left(\frac{V'_r}{2} + V_{OD} + \epsilon_V + \frac{\epsilon_R}{2}, VP - \epsilon_V - \frac{\epsilon_R}{2}\right) \quad (\text{F.3})$$

where

$\epsilon_V$  are errors in the triangular wave amplitude

$\epsilon_R$  is the rounding error due to finite amplitude resolution of the function generator

$V'_r$  is the reduced full-scale voltage  $V_r$  enlarged to account for possible errors in gain and offset of the waveform recorder itself, i.e., as shown in [Equation \(F.4\)](#)

$$V'_r = V_r(1+G) + 2 V_{os} \quad (\text{F.4})$$

where

$G$  are errors in the gain of the waveform recorder

$V_{os}$  are errors in the offset of the waveform recorder

$V_r$  is the reduced full-scale voltage  $V_r = \text{FSR} - 2Q$

where

$\text{FSR}$  is the full-scale range of the recorder

### F.3 DC source output voltages ( $V_j$ )

The maximum value of the voltage range  $\Delta V_{max}$  stimulated by each step  $\Delta V$  is shown in [Equation \(F.5\)](#).

$$\Delta V_{max} = 2\left(VP - V_{OD} - \epsilon_v - \frac{r_v}{2}\right) \quad (\text{F.5})$$

where

$VP$  is the maximum amplitude of the triangular wave

$V_{OD}$  is the required overdrive for the case of a triangular signal

$\epsilon_v$  is the error in the dc voltage source

$r_v$  is the resolution of the dc voltage source

The total number of steps  $N_s$  to use is given in [Equation \(F.6\)](#).

$$N_s = \left\lceil \frac{V'_r}{\Delta V_{max}} \right\rceil \quad (\text{F.6})$$

where

$V'_r$  is the reduced full-scale voltage  $V_r$  enlarged to account for possible errors in gain and offset of the waveform recorder itself

$\Delta V_{max}$  is the maximum value of the voltage range

symbol  $\langle x \rangle$  denotes the smallest integer greater than  $x$

Consequently, the exact range to be stimulated in each step  $\Delta V$  is given in [Equation \(F.7\)](#).

$$\Delta V = \frac{V'_r}{N_s} \quad (\text{F.7})$$

Note that, because  $N_s$  is an integer number, the range  $\Delta V$  stimulated by each step will, generally, be smaller than the limit  $\Delta V_{max}$ .

The voltage  $V_j$  in the  $j^{\text{th}}$  step is just the middle point of the stimulated range and can be obtained from [Equation \(F.8\)](#).

$$V_j = \frac{V'_r}{2} \times \frac{1 - N_s + 2j}{N_s} \quad \text{for } j = 0, 1, \dots, N_s - 1 \quad (\text{F.8})$$

For more information, see Alegria and Cruz Serra [\[B4\]](#).

#### F.4 Number of samples ( $K$ and $M$ ) and triangular wave frequency (f)

The number of samples to acquire and the triangular wave frequency shall be chosen in order to help ensure that the acquisition samples take place during an integer number of periods of the test signal as done in [4.7.10.1.2](#).

The number of records to acquire depends on the additive random noise  $\eta$ , phase noise  $\eta_\varphi$ , and random phase difference between the stimulus signal and the sampling clock. The minimum number of records  $K_{min}$  to achieve a given uncertainty boundary  $\varepsilon_T$  on the transition levels is given by [Equation \(F.9\)](#).

$$K_{min} = \left( \frac{K_u}{\varepsilon_T} \times \frac{2A}{Q} \right) \left( \frac{\eta}{2AM\sqrt{\pi}} + \frac{\eta_\varphi}{\pi M\sqrt{\pi}} + \frac{1}{4M^2} \right) \quad (\text{F.9})$$

where

$K_u$  is the coverage factor and can be determined the same way as in 4.7.8.2

$\eta$  is the additive random noise

$\eta_\varphi$  is the phase noise

$\varepsilon_T$  is the uncertainty boundary on the transition levels

$M$  is the record length

$Q$  is the ideal code bin width

## Annex G

(informative)

### Presentation of sine wave data

#### G.1 General

This annex describes common ways of presenting and displaying the results of sine wave tests.

#### G.2 ENOB presentation

The most common specification that results for sine wave tests is the ENOB. This presentation gives an overall measure of several different sources of error. Its value will depend on the frequency and the amplitude of the test signal. [Figure G.1](#) shows an example of the presentation of the ENOB results.

Triangles: channel 1      Squares: channel 2.  
Solid: large signals      Hollow: small signals.  
Top of the symbol is data value.  
Heavy lines represent the specifications.

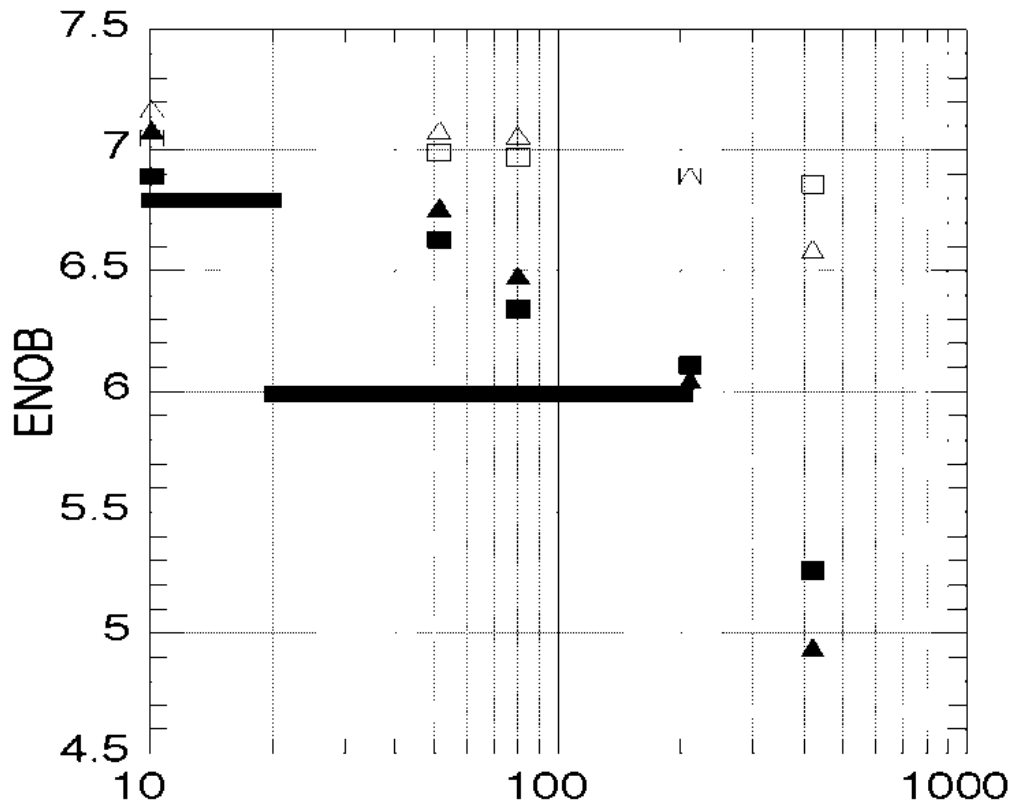


**Figure G.1—Example plot of ENOB versus frequency for a two-channel waveform recorder**

The value of ENOB is plotted as a function of frequency, with the frequency on a logarithmic scale. Different test conditions, in this case different signal amplitudes and different channels, can be represented with different symbols. In this example, the specifications of the waveform recorder are shown as a curve (a solid line). Points above the curve meet the specifications, while those below do not.

The decrease in ENOB at high frequencies is typical and is usually caused by errors in the time values of the data points. A simple method for estimating the time base errors from the ENOB plot is given by Blair [B13]. The method of 12.2.2 can also be used to estimate time base errors from the reduction of ENOB at high frequency. This method requires first converting from ENOB back to NAD using the defining formula for ENOB in 8.5.

The ENOB is based on NAD, and the NAD can be decomposed into its separate noise component and distortion component. The components can be plotted individually as above with the vertical scale in decibels.

### G.3 Presentation of residuals

Much can be learned by viewing the residuals of a particular sine wave test. In particular, a user can determine the sources of error that are responsible for an ENOB that is less than expected. The residuals can be viewed in either the time domain or the frequency domain, and it is most informative to look at both. The time and frequency domain displays that are used in software available from the ADC Test Software website (Markos [B30]) are covered in this annex. The time-domain presentation is called the modulo time plot and is described in detail by Irons and Hummel [B25]. The frequency domain presentation is called the power spectral distribution (PSD) and is described by Blair [B12]. Typical displays of each are shown in Figure G.2.

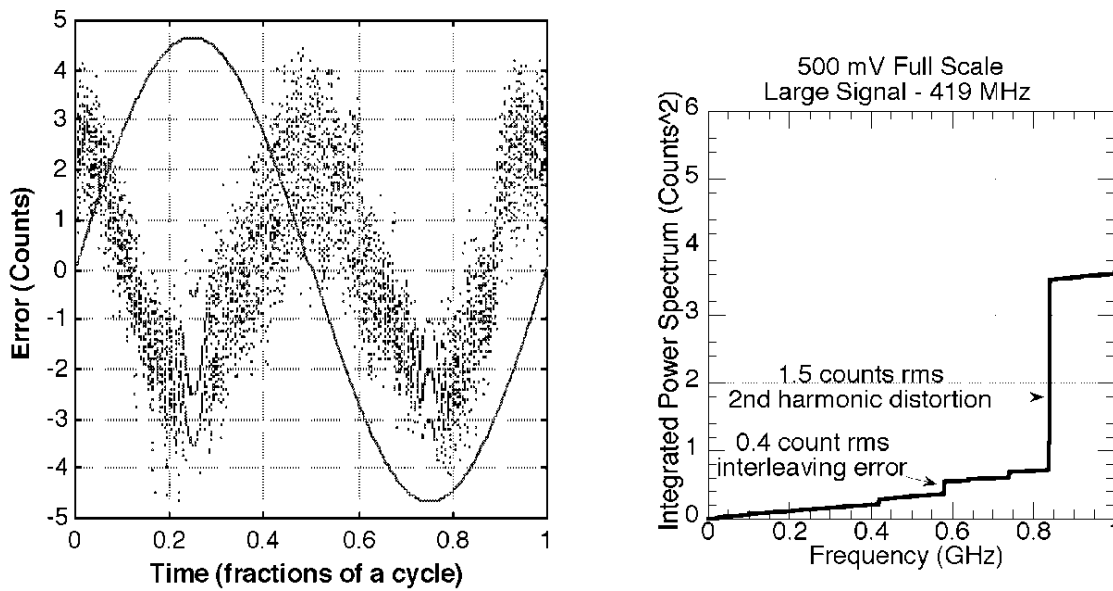


**Figure G.2—Example plots of sine fit residuals (the left side shows a modulo time plot, and the right side shows a PSD. Both represent the same data)**

To construct the modulo time plot, from the time coordinate of each data point in the record is calculated the phase value, between 0 and  $2\pi$ , relative to the input sine wave, as determined by the fit. This phase angle, divided by  $2\pi$ , is shown on the horizontal axis of the plot. The residual value is shown on the vertical axis. On this particular plot, the units are LSB, but any other units, such as volts, might be used. A scaled replica of

the fitted input signal is displayed as the continuous curve. On this plot, a user can clearly see 2nd harmonic distortion of approximately  $\pm 2.5$  LSB superimposed on random noise of about  $\pm 2$  LSB. The plot clearly displays the phase relationship of the harmonic to the input signal, having its negative peaks at the peaks of the input signal and having its positive peaks at the zero crossings.

The PSD is the integral of the power spectral density. Its units are the square of units in which a signal amplitude is measured, e.g., volts, some other physical quantity or, as in the case of [Figure G.2](#), LSBs. The value of the PSD at any frequency,  $f$ , could be obtained by filtering the residuals with a low-pass filter with cutoff frequency  $f$  and calculating the mean square value of the result. In practice it is calculated by a more efficient manner (see Blair [B12]). A jump in the PSD represents energy concentrated at a single frequency. A straight line represents white noise with density equal to the slope of the line.

The interpretation of a PSD will be illustrated using [Figure G.2](#). At 840 MHz, the 2nd harmonic of the input signal, the PSD jumps from  $0.8 \text{ LSB}^2$  to  $3.6 \text{ LSB}^2$ , an increase of  $2.8 \text{ LSB}^2$ , or (taking the square root)  $1.7 \text{ LSB}$ . This value is the rms value of the sine wave component at 840 MHz. The peak value of 2.4 is obtained by multiplying this value by  $\sqrt{2}$ . This result agrees with the 2nd harmonic observed in the modulo time plot.

These data were taken from a waveform recorder that consists of two interleaved recorders with sampling rates of 1 GSa/s, giving a combined sampling rate of 2 GSa/s. An interleaving error would occur at 581 MHz, which is the difference between the applied frequency of 419 MHz and the sampling frequency of 1 GHz. A jump of  $0.2 \text{ LSB}^2$  is seen at this frequency, which corresponds to an rms error of  $\sqrt{0.2} \cong 0.4 \text{ LSB}$ . This jump is masked by other errors in the modulo time plot. The primary sources of interleaving error are differences in gain, offset, and delay between the interleaved channels.

The PSD is well approximated by a straight line plus jumps at a few discrete frequencies. The straight-line portion corresponds to white noise, which can be approximated by extrapolating the straight-line segment of the PSD between 0 and 400 MHz. This line has an amplitude of  $0.5 \text{ LSB}^2$  or  $0.7 \text{ LSB}$  rms at the Nyquist frequency of 1 GHz. The peak-to-peak (95% probability) amplitude is expected to be 4 times the rms amplitude, or  $2.8 \text{ LSB}$ . This result agrees with the noise level observed in the modulo time plot.

[Figure G.3](#) shows the modulo time and PSD plots for another channel of the same recorder. The primary difference between the PSD here and that in [Figure G.2](#) is the much larger interleaving error component. In this case, the interleaving error is large enough to be visible in the modulo time plot. It appears as two distinct error curves, one for each of the interleaved channels.

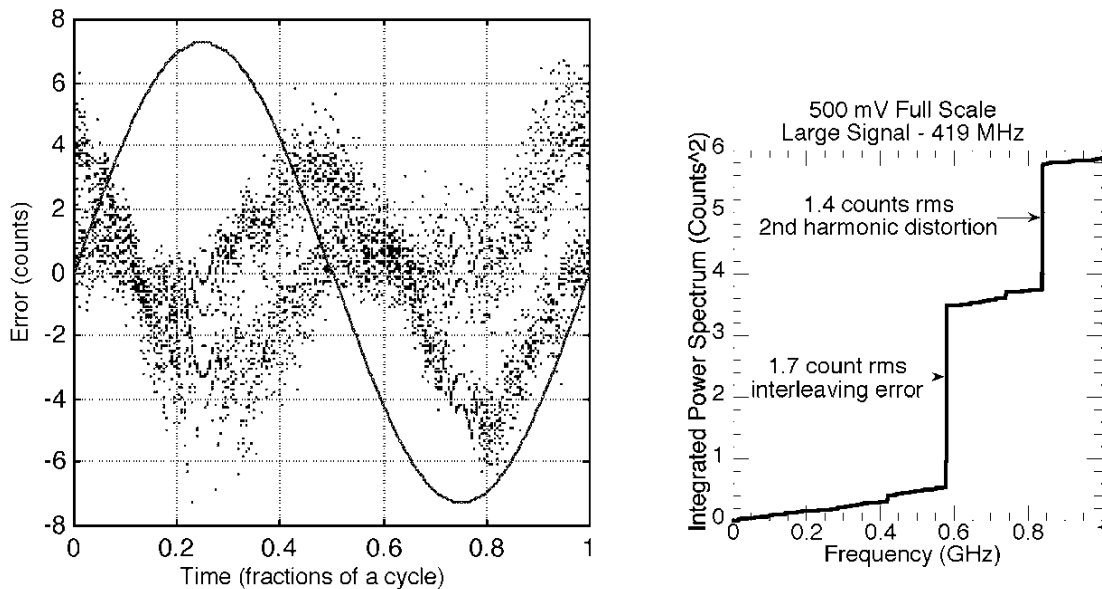


**Figure G.3—Same as Figure G.2, but for channel 1 of the recorder (this figure shows the interleaving error)**

#### G.4 Other examples of presentations of sine wave test results

There are other commonly used methods for presenting the residuals, one in the time domain and one in the frequency domain. The time domain method is simply to plot the residuals as a function of time. This method allows the user to see phenomena that change slowly over the record length. The alternate frequency domain approach is to calculate the DFT of the recorded signal (not the residuals) and plot the amplitudes of the coefficients on a decibel scale. This approach is only meaningful when using coherent sampling because otherwise the calculated magnitude of a frequency component can be as much as 6 dB below the true value. This approach allows the user to easily see the SFDR, which will be the difference between the signal component and the largest spurious component. However, if the spurious component does not have an integer number of cycles in the record, it can be shown as much as 6 dB below its true value.

A method of aiding the visualization of a data record, when coherent sampling is used, can be implemented by unwrapping the data record. When an integral number of cycles of the fundamental signal are included in the record, the unwrapping is straightforward. [Figure G.4](#) shows an example of a 1024-point data record of a 10-bit data recorder containing 7 cycles of a fundamental signal. The method used is described by Blair in “Selecting test frequencies” [\[B16\]](#).

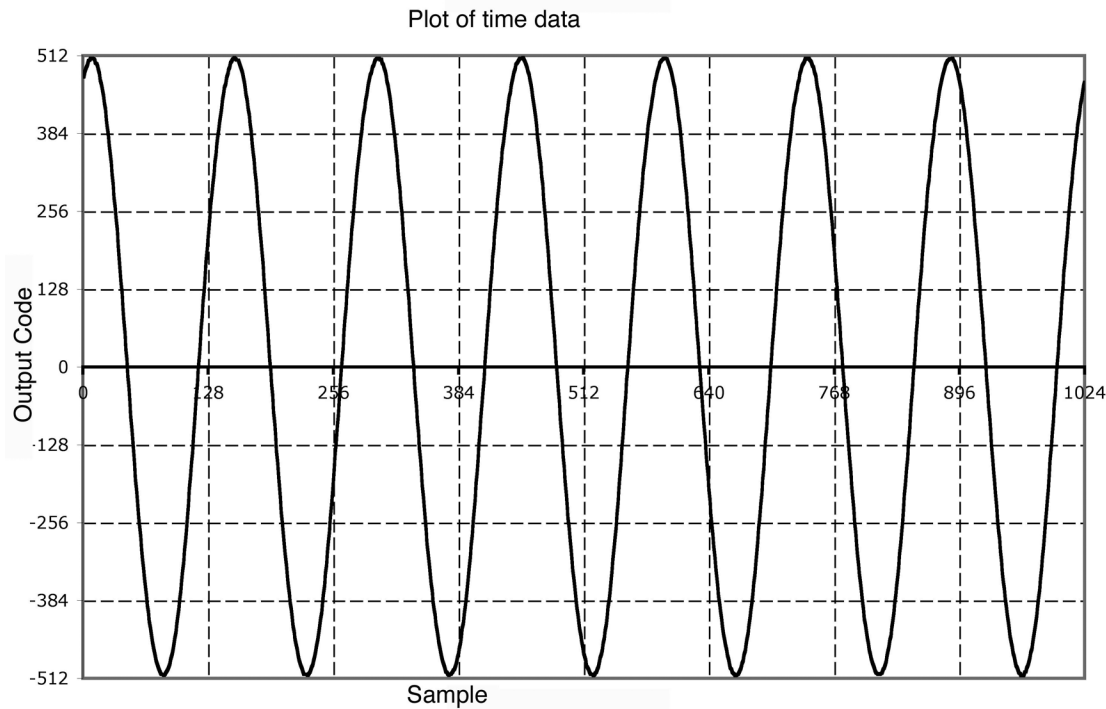


**Figure G.4—Plot of 1024-point record containing 7 cycles of the fundamental from a 10-bit data recorder**

A DFT of the record identifies that the record has a fundamental amplitude of 510.47, at a phase angle of 1.234 radians. A 2nd and a 3rd harmonic signal are also present.

The DFT-computed magnitude spectrum of the signal is shown plotted in [Figure G.5](#). The horizontal axis is in units of the inverse of the record duration. In other words, if the record duration is 10  $\mu$ s, then the first frequency on the axis would be 100 kHz, and the last frequency would be half the sample rate, or 51.2 MHz. The average of the record, the dc component, is not included in the graph. The vertical axis is given in units of decibels, where 0 dB corresponds to the amplitude of the fundamental. The plot is similar to a graph that a user would observe on a spectrum analyzer viewing the signal.

To visualize the nature of the measurement, the calculated fundamental is subtracted from the data, and a residual signal is calculated. A plot of the residual signal is shown in [Figure G.5](#).

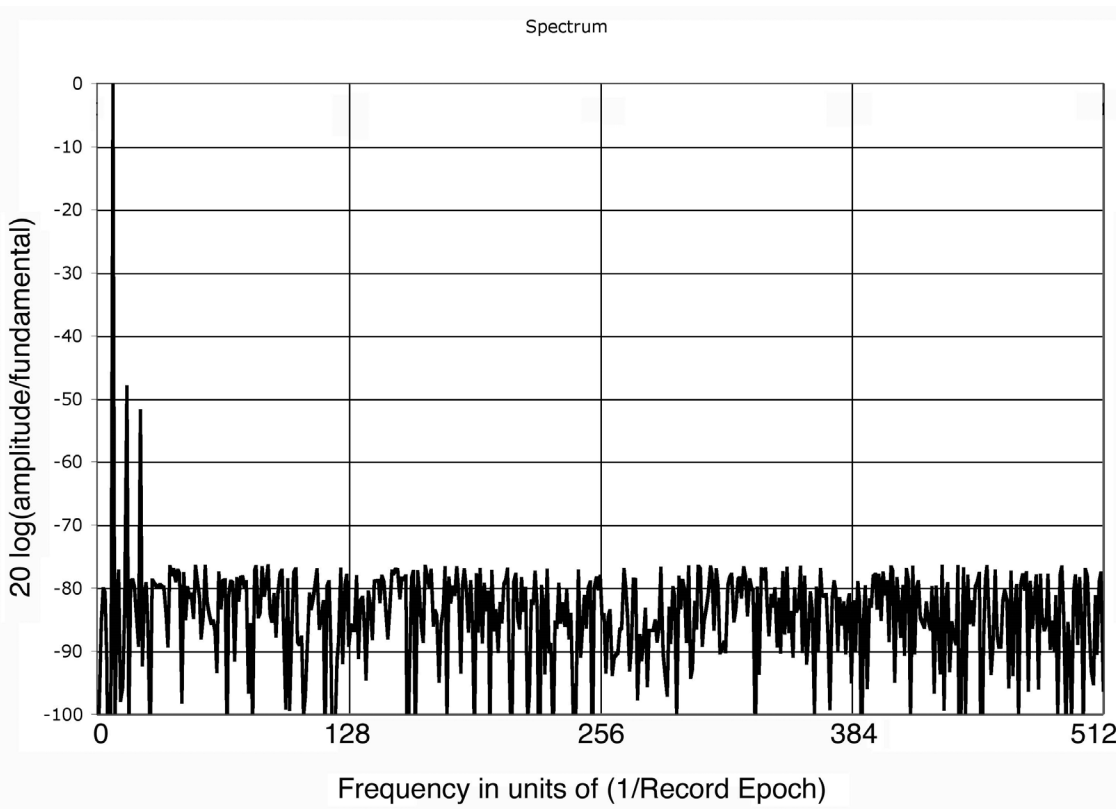


**Figure G.5—Plot of the magnitude of the spectrum of the signal shown in Figure G.4**

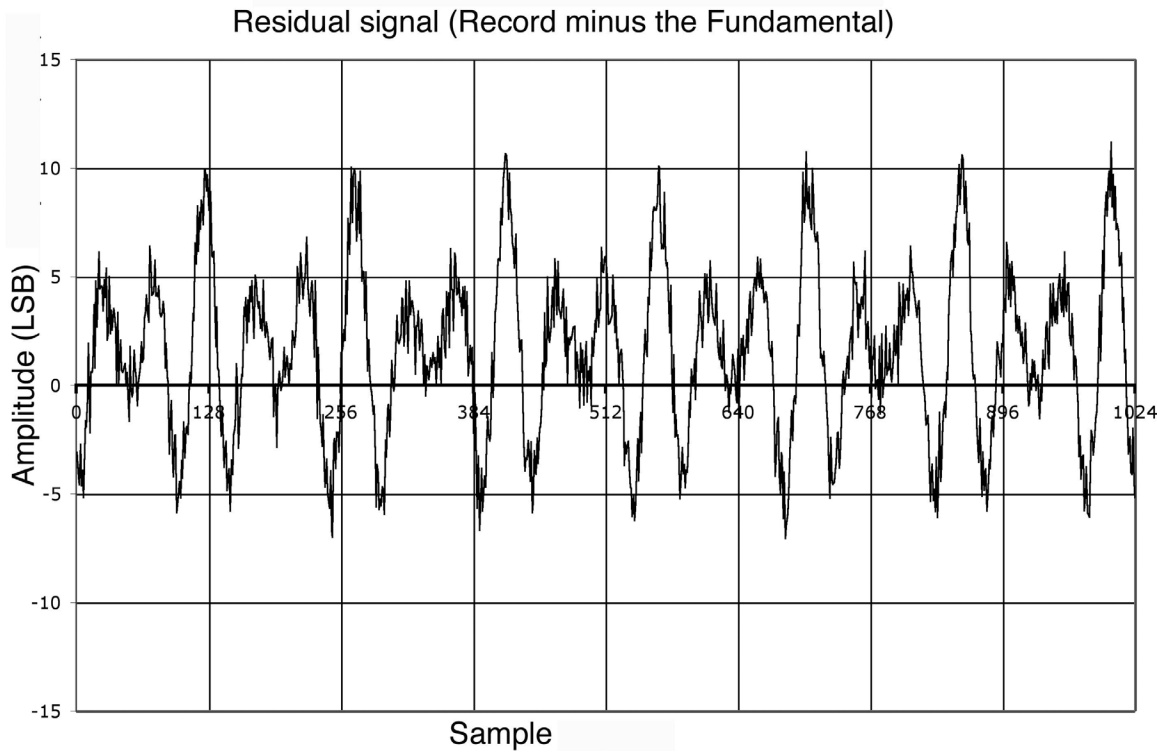


**Figure G.6—Plot of the residual signal**

**Figure G.6** can be understood better if the data are reordered. This feature can be used when an integral number of cycles of the fundamental are measured. In this example, the data contain exactly seven cycles of the fundamental. The parameter  $C$  is an integer computed from the relationship shown in Equation (G.1).

$$C = \frac{MK + 1}{m} \quad (\text{G.1})$$

where

- $M$  is the size of the data record being reordered ( $M = 1024$  in this example)
- $K$  is an integer, which is determined by trying successive integers until  $(MK+1)$  is a multiple of  $m$
- $m$  is the number of cycles of the fundamental present in the record ( $m$  is assumed to be relatively prime to  $M$  so that the data are not redundant.)

The data are then reordered by applying the algorithm described by the following pseudocode:

```

m = 7
j = 1
for i = 1 to 1024
  x'[i] = x[j] (*x'[i] contains the unfolded record)
  j = mod(j + C, 1024)
end for

```

In the example, the value of  $C$  computes to be 439. It results when  $K$  is 3. If the data in the example are reordered, the data plot shown in **Figure G.7** is generated. The value of  $C$  is computed by selecting successive values of  $K$  until  $MK + 1$  can be factored by  $m$ .

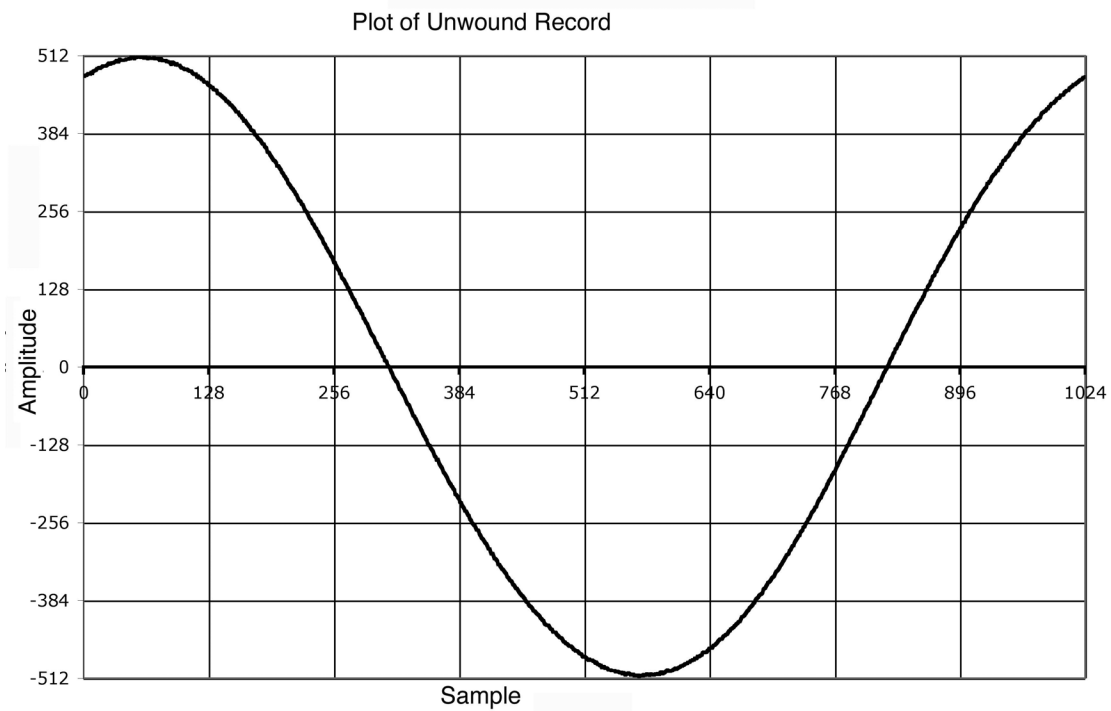


**Figure G.7—Plot of unwound data (original record is reordered)**

The residual can be similarly reordered. The resulting plot is shown in [Figure G.8](#).

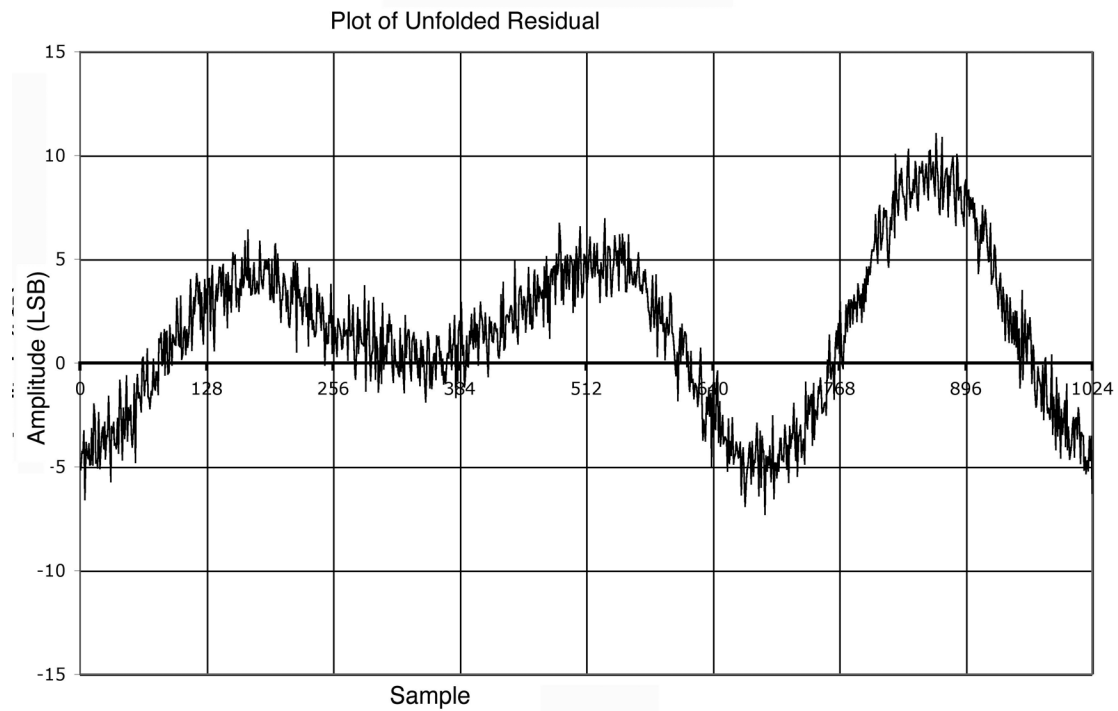


**Figure G.8—Plot of unfolded residual**

It can be noted from [Figure G.8](#) that the distortion components are more easily identified from the unfolded residual.

## Annex H

(informative)

### Bibliography

Bibliographical references are resources that provide additional or helpful material but do not need to be understood or used to implement this standard. Reference to these resources is made for informational use only.

[B1] Alegria, F., P. Arpaia, P. Daponte, and A. Cruz Serra, “An ADC Histogram Test Based on Small-Amplitude Waves,” *Measurement*, Elsevier Science, vol. 31, no. 4, pp. 271–279, June 2002.

[B2] Alegria, F., P. Arpaia, A. Cruz Serra, and P. Daponte, “Performance Analysis of an ADC Histogram Test Using Small Triangular Waves,” *IEEE Transactions on Instrumentation and Measurement*, vol. 51, no. 4, pp. 723–729, August 2002.

[B3] Alegria, F. and A. Cruz Serra, “Error in the estimation of transition voltages with the standard histogram test of ADCs,” *Measurement*, Elsevier Science, vol. 35, no. 4, pp. 389–397, June 2004.

[B4] Alegria, F. and A. Cruz Serra, “Overdrive in the Ramp Histogram Test of ADCs,” *IEEE Transactions on Instrumentation and Measurement*, vol. 54, no. 6, pp. 2305–2309, December 2005.

[B5] Alegria, F. and A. Cruz Serra, “Overdrive in the Standard Histogram test of ADCs,” *Measurement*, Elsevier Science, vol. 35, no. 4, pp. 381–387, June 2004.

[B6] Alegria, F. and A. Cruz Serra, “Precision of ADC Gain and Offset Error Estimation with the Standard Histogram Test,” *IEEE Instrumentation and Measurement Technology Conference (IMTC)*, Ottawa, Ontario, Canada, pp. 282–286, May 17–19, 2005.

[B7] Alegria, F. and A. Cruz Serra, “Uncertainty in the ADC Transition Voltages Determined with the Histogram Method,” *6th Workshop on ADC Modeling and Testing*, Lisbon, Portugal, pp. 28–32, Sept. 13–14, 2001.

[B8] Alegria, F. and A. Cruz Serra, “Uncertainty of ADC Random Noise Estimates Obtained With the IEEE 1057 Standard Test,” *IEEE Transactions on Instrumentation and Measurement*, vol. 54, no. 1, pp. 110–116, February 2005.

[B9] Alegria, F., A. Moschitta, P. Carbone, A. Cruz Serra, and D. Petri, “Effective ADC Linearity Testing Using Sine waves,” *IEEE Transactions on Circuits and Systems*, vol. 52, no. 7, pp. 1267–1275, June 2005.

[B10] Application Note 1303, “Spectrum Analyzer Measurements and Noise,” Agilent Technologies, 2003 (available from <http://www.agilent.com>).

[B11] Bilau, T., T. Mogyeri, A. Sarhegyi, J. Markus, and I. Kollar, “Four parameter fitting of sine wave testing result: Iteration and convergence,” *Computer Standards & Interfaces*, vol. 26, pp. 51–56, 2004.

[B12] Blair, J., “A Method for Characterizing Waveform Recorder Errors Using the Power Spectral Distribution,” *IEEE Transactions on Instrumentation and Measurement*, vol. IM-41, no. 5, October 1992.

[B13] Blair, J., “Error Estimates for Frequency Responses Calculated from Time-Domain Measurements,” *IEEE Transactions on Instrumentation and Measurement*, vol. 47, no. 2, April 1998.

- [B14] Blair, J., "Histogram Measurement of ADC Nonlinearities Using Sine waves," IEEE Transactions on Instrumentation and Measurement, vol. 43, no. 3, pp. 373–383, June 1994.
- [B15] Blair, J., "Method for eliminating aliasing in the measurement of the step response for a waveform recorder," *Instrumentation and Measurement Technology Conference*, vol. 1, pp. 310–313, May 2004.
- [B16] Blair, J., "Selecting test frequencies for sine wave tests of ADCs," IEEE Transactions on Instrumentation and Measurement, vol. IM-54, no. 1, February 2005.
- [B17] Carbone, P. and G. Chiorboli, "ADC sine wave histogram testing with quasi-coherent sampling," IEEE Transactions on Instrumentation and Measurement, vol. 50, no. 4, pp. 949–953, August 2001.
- [B18] Daboczi, T., "Uncertainty of Signal Reconstruction in the Case of Jittery and Noisy Measurements," IEEE Transactions on Instrumentation and Measurement, vol. 47, no. 5, p. 1062, October 1998.
- [B19] Dallet, D. and J. Machado da Silva, eds. Dynamic Characterization of Analogue-to-Digital Converters. Springer, 2005.
- [B20] Gray, R. and J. Stockham, "Dithered Quantizers," IEEE Transactions on Information Theory, vol. 39, pp. 805–812, May 1993.
- [B21] Harper, C., ed., *Handbook of Wiring Cabling and Interconnecting for Electronics*. New York: McGraw Hill, pp 4–33 to 4–51, 1972.
- [B22] Harris, F., "On the Use of Windows for Harmonic Analysis with the Discrete Fourier Transform," Proceedings of the IEEE, vol. 66, no. 1, January 1978.
- [B23] IEEE 100, *The Authoritative Dictionary of IEEE Standards Terms*, Seventh Edition.<sup>8,9</sup>
- [B24] IEEE Std 1241™-2010, Standard for Terminology and Test Methods for Analog-to-Digital Converters.
- [B25], "Irons, F., and D. Hummel, "The Modulo Time plot, A Useful Data Acquisition Diagnostic Tool," IEEE Transactions on Instrumentation and Measurement, vol. 45, no. 3, pp. 734–738, June 1996.
- [B26] Irons, F., K. Riley, and D. Hummel, "The Noise Power Ratio—Theory and ADC Testing," Proceedings of the 16th IEEE Instrumentation and Measurement Technology Conference, vol. 3, pp. 1415–1420.
- [B27] Jenkins, G. and D. Watts, Spectral Analysis and Its Applications. San Francisco: Holden-Day, 1968.
- [B28] Jenq, Y., "High-Precision Sinusoidal Frequency Estimator Based on Weighted Least Square Method," IEEE Transactions on Instrumentation and Measurement, vol. 36, no. 1, pp. 124–127, March 1987.
- [B29] Linnenbrink, T., "Effective Bits: Is That All There Is?" IEEE Transactions on Instrumentation and Measurement, vol. IM-33, no. 3, September 1984.
- [B30] Markos, J., "ADC Test Software for Matlab," Verson 3.1, June 2004, Web site address: <http://www.mit.bme.hu/projects/adctest/>.
- [B31] Max, S., "Fast Accurate and Complete ADC Testing," Paper 5.1, *Proceedings of the 1989 International Test Conference*, pp. 111–117.

<sup>8</sup>The IEEE standards or products referred to in Annex H are trademarks owned by the Institute of Electrical and Electronics Engineers, Incorporated.

<sup>9</sup>IEEE publications are available from the Institute of Electrical and Electronics Engineers (<http://standards.ieee.org/>).

- [B32] Max, S., "Optimum Measurement of ADC Code Transitions Using a Feedback Loop," Proceedings of the 16th IEEE Instrumentation and Measurement Technology Conference, vol. 3, pp. 1415–1420.
- [B33] Morrison, R., Grounding and Shielding Techniques in Instrumentation, 3rd Ed. New York: John Wiley & Sons, 1985.
- [B34] Nuttall, A., "Some Windows with Very Good Side Lobe Behavior," IEEE Transactions on Acoustics, Speech, and Signal Processing, vol. ASSP-29, no. 1, February 1981.
- [B35] Oppenheim, A. and A. Willsky, Signals and Systems. Englewood Cliffs, NJ: Prentice-Hall, 1983.
- [B36] Papoulis, A., Probability and Statistics. Englewood Cliffs, NJ: Prentice-Hall, 1990.
- [B37] Schoukens, J., R. Pintelon, and H. Van Hamme, "The interpolated fast Fourier transform: A comparative study," IEEE Transactions on Instrumentation and Measurement, vol. 41, no. 2, pp. 226–232, February 1992.
- [B38] Souders, T. and D. Flach, "Accurate Frequency Response Determinations from Discrete Step Response Data," IEEE Transactions on Instrumentation and Measurement, vol. IM-36, no. 2, June 1987.
- [B39] Souders, T., D. Flach, and J. Blair, "Step and Frequency Response Testing of Waveform Recorders," IEEE Instrumentation and Measurement Technology Conference, pp. 214–220, Feb. 1990.
- [B40] Souders, T., D. Flach, C. Hagwood, and G. Yang, "The Effects of Timing Jitter in Sampling Systems," IEEE Transactions on Instrumentation and Measurement, vol. 39, no. 1, February 1990.
- [B41] Stearns, S. and D. Hush, Digital Signal Analysis, 2nd Ed. Englewood Cliffs: Prentice-Hall, 1990.
- [B42] Stewart, G., An Introduction to Matrix Computations. New York: Academic Press, 1973, pp. 208–249.
- [B43] Strickland, J., Time-Domain Reflectometry Measurements. Beaverton, OR: Tektronix Inc., 1970.
- [B44] Vanden Bossche, M., J. Schoukens, and J. Renneboog, "Dynamic Testing and Diagnostics of ADCs," IEEE Transactions on Circuits and Systems, vol. CAS-33, no. 8, August 1986.
- [B45] Wiggington, R. and N. Nahman, "Transient Analysis of Coaxial Cables Considering Skin Effect," Proceedings of the IRE, Feb. 1957.

# Consensus

WE BUILD IT.

Connect with us on:

-  **Facebook:** <https://www.facebook.com/ieeesa>
-  **Twitter:** @ieeesa
-  **LinkedIn:** <http://www.linkedin.com/groups/IEEESA-Official-IEEE-Standards-Association-1791118>
-  **IEEE-SA Standards Insight blog:** <http://standardsinsight.com>
-  **YouTube:** IEEE-SA Channel

---

IEEE

[standards.ieee.org](http://standards.ieee.org)

Phone: +1 732 981 0060 Fax: +1 732 562 1571

© IEEE